


T 109

T 109
26/02/13
41911



STUDY AND DEVELOPMENT OF AUTOMATIC DETECTION AND DIAGNOSIS TOOLS FOR MEDICAL APPLICATIONS

A Thesis Submitted in partial fulfillment of the requirements
For the degree of
Doctor of Philosophy
(Faculty of Engineering)

Swapna Devi

Registration No. 002 of 2008



**School of Engineering
Computer Science & Engineering Department
Tezpur University
Assam, India
January, 2008.**

*To my dearest Ma
Bapin, Shyam & kids*

Preface

The technological revolution has opened up a new dimension for medi-care or health care system. Information Communication Technology (ICT) revolution has facilitated the medical science to do wonders or at least to explore the wonders. The future is more promising. With the advent of 4G communication, microwave imaging, high speed computation, hardware efficient systems, the medical science is going to see a transformation to fight against the known and unknown. The expertise will not be confined to only urban or developed region bit also to the remote region to provide services to masses. Today's dream of one expert to many patient and many regions will be a reality.

This thesis is an attempt to achieve some of the parameters to meet the dream, so that an integration of technological development with medical science will be able to provide a better health care system not only in urban areas but also in rural areas. The thesis has addressed automated detection, accuracy, computational efficiency and image quality by using artificial neural networks and optimization technique like bacterial foraging to contribute towards the endeavor of technology driven healthcare systems. Chapter 4 to chapter 9 of the thesis present the various methods proposed, their implementation and the results achieved to meet the objectives where as chapter 1 to chapter 3 discuss the background and need for automated systems including the present status. The issues have been clearly stated and attempts have been made to provide efficient solutions to these issues.

Although the thesis is primarily focuses on presenting the outcomes of the objectives but the quest to be a part of the technologically driven medi-care or health care system to serve to the masses has ignited a strong motivation on me to go further and contribute in high tech automatic diagnosis process in years to come.

Abstract of the Dissertation

Key Words: Arrhythmias, Single Photon Emission Computed Tomography (SPECT) imaging, mammography, automatic detection, artificial neural networks, bacterial foraging, denoising, lesion, peak signal to noise ratio.

The principal contributions of the thesis aim at developing automatic detection and diagnosis tools to add to the developments taking place in the computer aided Medicare system. Soft computing approaches such as Fast neural networks, back propagation algorithm based artificial neural networks, median filters, bacterial foraging are used by different researchers and are integrated to devise various novel soft tools to detect, denoise, restore and enhance medical images for diagnosis. The findings of this thesis will go a long way in meeting the automatic detection and diagnosis techniques required to meet urban and more so the rural patient where the experienced and expert doctors are scanty in numbers. Medical imaging for detection and diagnosis is an important and complex task that should be performed in less time with efficiency and accurately to provide proper patient care system. However, the limiting factors for medical imaging are (i) cost (ii) processing time (iii) accuracy i.e., reduction of false detection (iv) effect of Noise (v) resolution i.e. capability to detect small object through enhancement (vi) absence of true original image data (vii) and more so the dependency an experience and expertise of medical specialist. The dependency on human expertise and experience makes the detection and diagnosis more error prone in the absence of required expertise. Therefore, automated detection and diagnosis techniques have drawn the attentions of many researchers and industries for development. There have been continuous developments in this direction and these are well noticeable in advanced sophisticated hospitals equipments.

The advancement of the high performance computing techniques both software and hardware have contributed significantly in the recent time towards the development of efficient and accurate tools for detection and diagnosis of diseases. Motivated with the potential requirements of automated detection and diagnosis tools for Medicare system, attempts are made to provide solutions to arrhythmias detection, denoising, fast and accurate lesion detection and localization, image enhancement in terms of peak signal to noise ratio (PSNR), blind detection for mammography and Single Photon Emission Computed Tomography (SPECT) images. The organizations of the works have been divided into ten (10) major sections leading to ten (10) major chapters of the thesis. The rationale, problem statement, organization of thesis is presented in 1st section called chapter 1 in the thesis.

Chapter 2 presents for detailed review of artificial neural networks, its chronological developments and their application in Medicare system. Evolutionary optimization technique has been discussed in Chapter 3 of the thesis where the algorithm of Bacterial foraging technique, have been discussed in detail elaborating the merits and demerits of the technique. More than 200 research papers have been referred to bring out these two chapters a few of which have been presented as reference in respective chapters. After acquiring a good insight from these three chapters, the knowledge has been implemented in Chapter- 4 to Chapter 8 to provide solutions to the addressed problems. Last but not the least, Chapter 9 presents conclusions, future scope.

The following sections present the abstracts of Chapters 4 to Chapter 8.

Section I: In the first phase of the work, attempt is made to design and develop artificial neural network to detect arrhythmias accurately in a less computational time. Arrhythmias are defined as any deviation from the normal sinus rhythm and heart rate. As there are numerous arrhythmias and the existing systems do not have any provisions for detections of arrhythmias, therefore, the need for automatic detection of arrhythmia is felt. The application of signal processing technique on ECG wave was reported in the late 90s. However, only in 2000, the detection of arrhythmia

through computational techniques saw the light of the day. U R Acharya *et.al.* in 2004, used an artificial neural network ANN and Fuzzy classifier to classify the cardiac abnormalities based on heart rate with an accuracy level of 80-85%. Hoai, L Tran *et. al.* in 2005, integrated multiple neural classifier for the heart beat recognition. But all these methods could present solutions for maximum of three arrhythmias. Using wavelet and Fourier transformation for ECG beat classification. Z. Doker *et. al.*, could address the problem of 10 arrhythmias with an accuracy of 89.40%. In this thesis, an artificial neural network is developed using back propagation algorithm to solve 16 arrhythmias and an average accuracy of 98.63% is achieved. Provisions are made to process either digital data from data set or converting image into graph to automatically detect and diagnose the arrhythmias. The ECG wave is segmented into its P, Q, R, S, T and U waves and their intervals and complexes have been calculated. A comparison is drawn among the different published methods and the proposed method as regards the detection accuracy. The proposed method seems to be computationally simple, efficient and accurate technique for arrhythmias detection.

Section II: The second phase of the work deals with techniques to remove noise, mainly impulse or salt and pepper noise from the SPECT images. Images are often corrupted by impulse noise due to noisy sensors or channel transmission error. The basic principle of noise removal is to detect impulse pixel and replace them with their estimated value while leaving the other pixel unchanged. The progressive switching median filter, SDRM and CSAM filter, adaptive median filter, standard median filter and two state SD-ROM and CSAM filters are used by researchers for noise removal. Filtration of impulse noise is also accomplished by the use of ANN. In the proposed method, a gradient descent algorithm is used for training the neural network. 512x512 Lena image is corrupted with different noise densities and fed to the trained network for testing. A comparison of the proposed method with others methods like 3x3 Median filter, 5x5 Median filter, Fuzzy Filter, SD-ROM filter, MMEM filter at noise densities ranging from 10% to 70% is made. It is observed that the proposed technique gives better performance by 0.1db to 1db for different cases

of noise densities. The outcome of the proposed method proves it to be a better denoising approach and can find potential applications in medical imaging.

Section III: Among all forms of illness, Coronary artery diseases (CAD) is the single greatest cause of morbidity and mortality in the world. Early detection of any lesions in cardiac is an effective method to reduce the number of death caused by coronary artery disease. Current diagnostic modalities such as SPECT, PET, CT, MRI have advantages and disadvantages. Myocardial PET, Cardiac Vascular MRI remain expensive and are less accessible than SPECT. Ability to perform attenuation correction and the lesion to background contrast is higher in SPECT. But it suffers from prolonged steady time because of relatively low detection efficiency. Therefore, in the third phase of the thesis work, a fast neural network in conjunction with back propagation neural network is proposed to detect with localization of lesion in SPECT image. The proposed method is computationally efficient, accurate and takes less time. The large data content increases training time in neural network. Therefore, in the proposed method, preprocessing of data is done before feeding them to fast neural network. A Lesion is defined as a window having size of 3x3, 2x3, 3x2 pixel or more with a defined intensity level. Output layer of the network consists of five neurons viz., one to indicate absence or presence of lesion, two to give x- and y- position of lesion and two more to give distance in the x and y directions. The activation function used is a log sigmoid, a threshold is used to give a binary output of 0 or 1 to indicate the presence or absence of the lesion. The output of the FNN may have a false positive or false negative. So, to ensure the accuracy of the detection, the output of the FNN is fed as input to an error back propagation neural network. The network is trained to achieve an error limit of 0.0001. Data collected from MIRL, University of Utah and from the Internet have used. 450 slices of emission images of SPECT are used for training, out of which 300 are without lesion. 105 images out of which 36 are with lesion are tested in the proposed method. An accuracy of 96.2% is achieved. The rate of false positive detection is found to be 0.95% and that of false negative is

2.87%. The computation time due to Fast Neural Network reduces by 5 folds. The method seems to be promising time efficient accurate detection method.

Section IV: Breast cancer is the fifth most common cause of cancer related deaths. In 2005, breast cancer caused 502,000 deaths i.e. 1% of all deaths worldwide. Breast cancer can occur in female and male. However, females are more prone. One of the best ways to reduce fatal rate is to detect cancer in the early stage. If the cancer is detected when the size is less than 2cm, then the survival rate is more than 95%. The early detection requires the detection of small size object, which is possible with enhanced peak signal to noise ratio (PSNR) value. Therefore in the fifth phase of the thesis work, recently developed bacterial foraging technique, a recently developed algorithm, is used with median filter to achieve very high value of PSNR. Bacterial foraging is applied to minimize the error that arises due to difference of image parameters between the true image and image obtained from the output of median filter. The method is validated with standard Lena image and subsequently applied to mammography and SPECT images. The images are tested after corrupting them with varied noise density (10% to 90%) to see the performance in critical situations. PSNR and Mean Absolute Error (MAE) have been studied. The findings are compared with reported methods. The peak signal to noise ratio (PSNR) of the existing methods range from 26.21 db to 31.36 db (for a noise density of 40%) but the PSNR found using the proposed method is 54.90 db. Other performance metrics like mean absolute error, structural contents, image fidelity, normalized correlation quantity have also been computed. The achievement of high PSNR and low MAE makes the proposed method more promising and suitable for medical imaging detection and diagnosis more specifically the mammography.

Section V: Image enhancement algorithm leading to enhancement of PSNR values relies on the true image data. But at times getting original image or accurate data representing true image is quite difficult or may be impossible. Therefore, the need is felt to restore image with high PSNR to meet the detection and


diagnosis in medical science in absence of true image. In the fifth phase of the thesis work, a novel technique is devised using bacterial foraging with median filter to achieve high PSNR value while restoring image corrupted with impulse noise in the absence of the true image. Here, in the proposed method the difference between the output of the median filter and the noisy image is minimized using bacterial foraging technique and an enhanced PSNR ranging from 61.91db to 55.99 db is achieved even for a noise density of 10% to 50% respectively. The method is validated using standard Lena image and then is applied to SPECT and mammography images. Image quality measures such as PSNR, structural contents, image fidelity, normalize correlation quantity are found out for varied noise density. The results show potentiality of the method to be used in detection and diagnosis in the absence of original image.

Medical imaging and computer aided detection and diagnosis are continually growing field of research. In this dissertation, artificial neural networks and bacterial foraging soft computing tools have been used to develop tools or techniques that achieve better accuracy, show time reduction and are computationally efficient to be used in intelligent Medicare system. The outcomes of the work pave ways to integrate fuzzy logic, neural networks and bacterial foraging to further improve on accuracy, cost, efficiency, time to develop intelligent or smart medical imaging tools for detection and diagnosis.

DECLARATION

I hereby declare that the thesis entitled “**STUDY AND DEVELOPMENT OF AUTOMATIC DETECTION AND DIAGNOSIS TOOLS FOR MEDICAL APPLICATIONS**” submitted by me in partial fulfillment of the requirements for the degree of **Doctor of Philosophy (Faculty of Engineering)** is a record of my bonafide research work carried out under the guidance of *Professor. (Dr.) Malayananda Dutta*, Computer Science & Engineering Department, Tezpur University, India.

The research work included in the thesis has not been submitted to any other university or institute for the award of any other degree.


(Swapna Devi)



TEZPUR UNIVERSITY

(A Central University established by an act of Parliament)
NAPAAM, TEZPUR - 7840028
DISTRICT : SONITPUR :: ASSAM, INDIA.

Ph : 03712 67004, 67005
67006, 67007
67008, 67009
Fax : 03712 -67006
03712 -67005


e-mail : adm@agnigarth.tezu.ernet.in

This is to certify that the thesis entitled “**STUDY AND DEVELOPMENT OF AUTOMATIC DETECTION AND DIAGNOSIS TOOLS FOR MEDICAL APPLICATIONS**” submitted to the Tezpur University under the School of Engineering in partial fulfillment for the award of the degree of **Doctor of Philosophy (Engineering)** is a record of research work carried out by Mrs. Swapna Devi under my personal supervision and guidance.

All the helps received by her from various sources have been duly acknowledged.

No part of this thesis has been reproduced elsewhere to award of any other degree.

Date : 31.1.08
Place: Tezpur University
INDIA


Dr. Malayananda Dutta
(Supervisor)
Professor
Computer Science & Engineering Department.

Acknowledgements

“Guru Govind dou khare, kaku lago paye; Guru balihari apne jin Govind diyo milaye” Meaning....

Guru & God standing in front,

Prostration on to thee -

As you showed me the path,

Which ought to be!

So, in my endeavor for quenching the thirst of knowledge and a degree, I put on record my deepest salutations for my Supervisor *Professor (Dr.) Malayananda Dutta*. His positive attitude and enthusiasm are contagious. I am particularly indebted to him for his relentless support, valuable guidance and endless patience he generously provided during the thesis work. He has tremendously motivated me.

Numerous people have contributed to my being here and finishing this dissertation. My thanks goes to all of them. I'm specifically mentioning a few of them here.

Prof. D Bhattacharya, Head of Department has been instrumental in my development as a scholar. I express my sincere gratitude for all that he has done and sincerely thank him.

Thanks are due to Prof. D K Saikia, Professor of Computer Science and Engineering Department for extending all the support during my endeavour.

The professors of my research doctoral committee have contributed much to my accomplishments through their constructive criticism on my work. My felicitations are all due to them for this effort of theirs.

The completion of a PhD takes many years and a lot of dedications not only from the scholar but also from family, friends, and all the near and dear ones. My parents had left no stones unturned to see this day. I thank them for their blessings, the sacrifices made for me, for being a constant emotional support and providing an unconditional safety net.

I'm thankful to the love of my life, husband Dr. S S Pattnaik for his unending emotional support during this tenure and also providing much needed proof reading of my written work. It was indeed a difficult and a long road but his understanding of the importance of this endeavor in my life kept me going during the toughest periods. His knowledge and experience has helped me in this work and carried me through the times when nothing seemed to work.

Thanks to my angel kids – Zadjiya and Shubransu, while they don't totally understand why I should still study, they have always been supportive and tolerated me through the most tumultuous years of my life. I'm indebted to my little kids for sacrificing their precious tender age time for these years to see their mother meet the goal.

My siblings – Sujit, Subrata continue to provide me all the love and support. Thanks to them for being so wonderful and just being a phone call or an email away. May the Almighty, the uncaused cause of all being shower peace and mercy to my sister who left this world in between my work.

In the five years it took to complete this work, I have made friends and built relationships. I thank Dr. R K Ratho, Mrs. Saila Misra, Dr. O P Bajpai, Dr. B K Kanungo and their families for being so supportive. Their encouragement and assistance is beyond any appreciation limited in a paper.

This work would not have been interesting and rewarding without the interactions with the research group members – Dhruva, Deepak, Pradumna, Sastry, Vidya, Bakwad and my energetic students – Kriti, Anjali, Rashmi, Shilpa.

I thankfully acknowledge the support of my dear students and colleague Rajesh, Vineyji, Shantanuda. Last but not the least I would like to thank one and all who have helped me directly or indirectly in getting this dissertation work see the light of the day.

Table of Contents		Page
A. Title Page		
B. Preface.....		i
C. Abstract.....		ii
D. Declaration		viii
E. Certificate of Supervisor		ix
F. Acknowledgement.....		x
G. Table of Contents.....		xii
H. List of Tables		xvi
I. List of Figures.....		xvii
J. List of Abbreviations		xxii
K. List of common symbols used.....		xxiv
CHAPTER 1: Introduction		1-9
1.1 Automatic Detection of Diseases		1
1.2 Problem Statement		3
1.3 Organization of the thesis		4
1.4 References.....		4
CHAPTER 2: A brief review of Artificial Neural Networks		10-32
2.1 Introduction		10
2.2 Biological Motivation of Neural Networks		11
2.3 Model of a Neuron		12
2.4 Activation Function and Characteristics		13
2.5 Learning Rules.....		15
2.6 Multilayer Neural Networks.....		17
2.7 Implementation Procedures and Issues Involved in Neural Network Training		19

2.8	Error Back Propagation Neural Networks.....	20
2.9	Backpropagation Algorithm	21
2.10	References	29
CHAPTER 3: Soft Computing; Optimization Techniques		33-56
3.1	Evolutionary Algorithms.....	33
3.2	Swarm Intelligence.....	34
3.3	Particle Swarm Optimization Algorithm	36
3.4	Genetic Algorithm.....	36
3.5	Bacterial Foraging Algorithm.....	37
3.6	Critical Analysis of these techniques	38
3.7	Details of Bacterial Foraging theory	39
3.7.1	Concepts of Bacterial Foraging theory.....	39
3.7.2	Searching techniques for foraging.....	40
3.7.3	E. Coli Bacteria's foraging	41
3.7.4	Bacterial Foraging Optimization	43
3.7.5	BFO Algorithm	49
3.8	References	51
CHAPTER 4: Detection of Arrhythmia from ECG		57-89
4.1	Introduction	57
4.1.1	Electrocardiogram	58
4.1.2	Arrhythmia	65
4.2	Detection techniques - a literature survey	72
4.3	Proposed method; Objective – 1	73
4.3.1	Conversion of an image into a graph	75
4.3.2	Segmentation of the ECG wave	77
4.3.3	Detection by Neural Network	77
4.3.4	Results	79
4.4	Conclusion	84
4.5	References	85

CHAPTER 5: ANN for Denoising Images; Objective – II	90-123
5.1 Introduction	90
5.2 Techniques for Noise Removal	93
5.3 Critical Analysis of Some Filters	96
5.4 Image Metrics	97
5.5 The Problem Statement	99
5.6 Preprocessing of the images	99
5.7 Development of the Model	104
5.8 Results	105
5.9 Performance Evaluation	113
5.10 References	117
CHAPTER 6: Lesion Detection in SPECT Cardiac images; Objective –III	124-141
6.1 Introduction	124
6.2 Literature survey	126
6.3 Fast Neural Networks	127
6.4 Proposed & Developed Method.....	128
6.5 Results	130
6.6 Conclusion	136
6.7 References	136
CHAPTER 7: PSNR Enhancement using Bacterial Foraging (BFG) Optimization Technique; Objective – IV & V	142-180
7.1 Introduction to breast cancer detection	142
7.2 Limitations of the present techniques	145
7.2.1 Effect of noise	145
7.2.2 Denoising: Present status	146
7.2.3 Performance Metrics	148

7.3	Proposed BFG optimization	149
7.3.1	Results of proposed method	150
7.3.2	Result with Lena test image & performance evaluation ..	154
7.3.3	Results with Mammogram Images, SPECT Images	155
7.3.4	Discussion on the results	158
7.4	Proposed Median-BFG hybrid method	158
7.4.1	Median-BFG hybrid method (MED-BFO)	158
7.4.2	Result of the Median-BFG code	161
7.4.3	Results with Lena test image & performance evaluation .	162
7.4.4	Results with Bridge test image	167
7.4.5	Results with Mammogram image	171
7.5	References	175
CHAPTER 8: Noise Removal from a single image; Objective – VI		181-191
8.1	Introduction to breast cancer detection	181
8.2	Proposed Median BFO Filter from a single image.....	181
8.3	Results	182
8.4	Conclusion	191
8.5	Reference	191
CHAPTER 9: Conclusion		193-197
9.1	Conclusion	193
9.2	Future Scope	197

Appendix – A : List of publications out of this thesis work

LIST OF TABLES		Page
Table 4.1.	Different arrhythmias with its respective percentage of errors using first neural network	82
Table 4.2.	Different arrhythmias with its respective percentage of errors using second neural network	83
Table 4.3.	Comparison of different ECG classifiers	84
Table 5.1	Network Parameters	104
Table 5.2	Comparison of the different methods	113
Table 5.3	PSNR of the proposed method at different noise densities	114
Table7.1	Comparison of proposed BFO Technique with other existing methods with a noise density of 40%.	151
Table7.2	Values of different performance metrics of proposed method	152
Table 7.3	Result of denoising using BFO Technique	158
Table 7.4	Comparison of Proposed method and other existing methods with noise density of 70% on Lena image	164
Table 7.5	Comparison of Proposed method with other existing methods for noise density of 40% on Lena image	166
Table 7.6	Result of Median-BFO method as applied on Lena image (512x512) corrupted with different noise densities	167
Table 7.7	Result of Median-BFO method as applied on Bridge test image corrupted with different noise densities	170
Table 7.8	Result of Median-BFO method as applied on mammogram image (305X259) corrupted with different noise densities	171
Table 7.9	Comparison of the proposed method with other existing methods for Lena image in terms of computational time	175
Table 8.1	Results of the proposed method as applied on Lena image	184
Table 8.2	Results of the proposed method as applied on mammography image	188

LISTS OF FIGURES

Page

- Figure 2.1 Structure of Biological Neuron
- Figure 2.2 Model of Biological Neuron
- Figure 2.3 Model of Artificial Neuron
- Figure 2.4 Activation Functions
- Figure 2.5 Generalized Learning Rule
- Figure 2.6 Multilayer Neural Network Structure
- Figure 2.7 Flow Chart of Backpropagation Algorithm
- Figure 3.1 Flocking of birds
- Figure 2.2 Different types of Search for foraging
- Figure 3.3 An E. Coli bacterium
- Figure 3.4 Foraging of E. coli with Reproduction, Elimination and Dispersion: Contour Plot
- Figure 3.5 Foraging of E. Coli with Reproduction, Elimination and Dispersion: contour plot after Elimination and Dispersion
- Figure 3.6 Foraging of E. Coli in a noisy environment: Bacteria positions at different Chemotactic steps (without cell-to-cell attractant)
- Figure 3.7 Foraging of E.coli in a noisy environment: Bacteria positions at different chemotactic steps(with cell to cell attractant)
- Figure 4.1 ECG machine.
- Figure 4.2 Leads showing the waves
- Figure 4.3 Location of chest electrodes in 4th and 5th intercostal spaces
- Figure 4.4 Electrocardiographic view of heart.
- Figure 4.5 Inside of the heart
- Figure 4.6 PQRST wave
- Figure 4.7 Different components of the PQRST wave
- Figure 4.8 U wave
- Figure. 4.9 The generation of PQRST wave

-
- Figure 4.10 A Normal Sinus Rhythm
- Figure 4.11 Complete Heart Block
- Figure 4.12 Atrial Fibrillation
- Figure 4.13 Atrial Fibrillation
- Figure 4.14 Ventricular Fibrillation
- Figure 4.15 Atrial Flutter
- Figure 4.16 Sinus Tachycardia
- Figure 4.17 Ventricular Tachycardia
- Figure 4.18 Sinus Bradycardia
- Figure 4.19 Atrial premature beat
- Figure 4.20 Sick Sinus Syndrome
- Figure 4.21 Right and Left Bundle Branch Block
- Figure 4.22 Left Bundle Branch Block characteristics
- Figure 4.23 Flow diagram of the detection process
- Figure 4.24 Conversion flow chart
- Figure 4.25 Architecture of the proposed neural network
- Figure. 4.25 Scanned ECG graph which has been converted from a colored image to a gray level image
- Figure 4.26 Scanned image (one cycle).
- Figure,4.27 ECG data as read and plotted in MATLAB
- Figure 4.27 A Plot of data (1 cycle only) obtained after converting it into 1D
- Figure. 4.28 Isolated P wave
- Figure.4.29 QRS Complex
- Figure. 4.30 QT interval
- Figure 5.1 (a): Gaussian distribution, (b): a true image, (c): corrupted with Gaussian noise
- Figure 5.2 True image, its impulse noise corrupted image with $p=0.1$.
- Figure. 5.3 Some texture images and their noisy counterparts that formed the input – output pair of the training database.

-
- Figure 5.4 (a) some of the SPECT images that formed the part of the training / testing database, (b) their noisy images with densities of 10%, 20%, 30% 40% and 50% respectively
- Figure. 5.5 Architecture of the error back propagation neural network
- Figure: 5.6 Original Lena image
- Figure. 5.7 Lena image corrupted with Salt and Pepper impulse noise of densities 10%, 20%, 30%, 40%, 50% and 60% respectively
- Figure 5.8 Plot of the error versus the iteration of the neural network
- Figure 5.9 Effect of the network performance with variation of neuron variation
- Figure 5.10 Effect of the network performance with Learning rate
- Figure 5.11 Effect of the network performance with Learning increment
- Figure 5.13 Matlab window showing the true image, noisy image and the denoised image
- Figure 5.14 (a) Original images, (b) noisy images (with densities of 10%, 20%, 30% and 40%), and (c) the denoised images
- Figure 5.15 Comparison of the proposed technique with other methods
- Figure 5.16 Performance of the neural network at different noise densities in percentage
- Figure 6.2 (a): Some of the original images that have been considered for our work
- Figure 6.2 (b): Some of the original images considered for the work
- Figure 6.3 Images resized after converting them to their grey level; (a) grey level conversion (b) resized to 50x40 image matrix
- Figure 6.4 Graph for different values of Eta
- Figure 6.5 Graph showing the convergence of the network
- Figure 6.6 Images after the post processing
- Figure 6.7 Comparison between Artificial Neural Network and Fast Neural Network

-
- Figure 7.1 A mammogram image
- Figure 7.2 A mammography equipment
- Figure 7.3 A Mammogram image showing a mass
- Figure 7.4 Block diagram of the proposed BFO method
- Figure 7.5 (a) Lena image cropped into 80x80 size (b) Corrupted with 40 % noise, (c) Output Image after using the proposed BFO on (b).
- Figure 7.6 (a) Lena image corrupted with noise density of 20%, 30%, 40% and 50% respectively (b) denoised image from (a).
- Figure 7.7 Mammogram image showing a mass
- Figure 7.8 (a) : Original mammogram image cropped into 80x80 pixels, (b) Corrupted with 20 % noise, (c) with 30% noise, (d) with 40% noise, (e) with 50% noise, (f) – (i) Output Image after using BFO on (b) - (e) respectively
- Figure 7.9 (a) : Original SPECT image cropped into 60x60 pixels, (b) Corrupted with 20 % noise, (c) with 30% noise, (d) with 40% noise, (e) with 50% noise, (f) – (i) Output Image after using BFO on (b) - (e).
- Figure 7:10 Proposed Median-BFG filter
- Figure 7.11 (a) Original 512 X 512 Lena Image cropped into 80X80 size, (b) Original Image of (a) corrupted with noise density of 10%, 20 %, 30%,40%, and 50% respectively, (c) Image after median filtering of mask 3x3, (d) Restored image using proposed MED-BFO technique
- Figure 7.12 (a) Lena and Mammography images, (b) Images with 70% noise density , (c) Median filter output, (d) Restored images using BFG&MF
- Figure 7.13 (a) Lena and Mammography images, (b) Images with 40% noise density, (c) Median filter output, (d) Restored images using BFG&MF.
- Figure 7.14 From left to right, respectively, (a) Original Bridge Image (b) Image corrupted with noise (c) denoising after using Median Filter (d) denoising result after using developed method
- Figure 7.15 (a) Original Mammography (305X259) image cropped into 80x80 size; (b) corrupted with noise density of 40%; (c) Median filter output image corresponding to (c); (d) Restored image using MED-BFO
- Figure 7.16 (a) & (b) Comparison in PNSR and MAE for the Lena Image at noise density with various algorithms and developed method
- Figure 7.17 (a) & (b) PSNR & MAE of Lena restored image for noise densities 10% to 90%.

-
- Figure 7.18 (a) & (b) PSNR & MAE of Mammography restored image for noise densities 10% to 90%.
- Figure 8.1 Proposed Median-BFG filter
- Figure 8.2 : (a) Original 512 x512 Lena Image cropped into 80x80 size (b) Original image is corrupted with noise density of 10%-50% resp. (c) Image after median filtering of mask 3x3 (d) Restored image corresponding to (c).
- Figure 8.3 Mean and Variance of Noisy Lena Image
- Figure 8.4 Mean and Variance of restored Image
- Figure 8.5 (a) Plot of PSNR against the noise density and (b) plots SC, IF, NCQ against the noise density (for Lena image).
- Figure 8.6 (a) Original 305x259 mammography image cropped to 80x80 size (b) Original image corrupted with noise density of 10%-50% resp. (c) Image after median filtering of mask 3X3 (d) Restored image corresponding to (c)
- Figure 8.7 (a) Plot of PSNR against the noise density and (b) plots SC, IF, NCQ against the noise density (mammography).

LIST OF ABBREVIATIONS

ANN	Artificial Neural Network
LV	Left Ventricle
ACO	Ant Colony Optimization
AWGN	Additive White Gaussian Noise
BFO	Bacterial Foraging Optimization
BPM	Beats per minute
CAD	Coronary Artery Disease
CHD	Coronary Heart Disease
CT	Computed Tomography
EA	Evolutionary Algorithms
E_{abs}	Absolute Error
EBPA	Error Backpropagation Algorithm
ECG	Electrocardiogram
E_{rms}	Root Mean Square Error
FNN	Fast Neural Network
GA	Genetic Algorithm
HR	Heart Rate
IF	Image Fidelity
LMS	Least Mean Square Error
MAE	Mean Absolute Error
MLP	Multilayer Perceptron
MRI	Magnetic Resonance Imaging
MSE	Mean Square Error
NK	Normalized Correlation Quality
PET	Positron Emission Tomography
PSD	Power Spectral Density
PSNR	Peak Signal to Noise Ratio

PSO	Particle Swarm Optimization
RVIN	Random Valued Impulse Noise
SC	Structural Content
SI	Swarm Intelligence
SNR	Signal to Noise Ratio
SPECT	Single Photon Emission Computed Tomography
SPN	Salt and Pepper Noise

LIST OF COMMON SYMBOLS USED

φ	Activation Function
α	Momentum factor
η	Learning Constant
ρ	Strength of learning
$J(\theta)$	Cost Function
N_{re}	Number of Reproduction steps
N_s	Swimming length
N_c	Number of steps in a Chemotactic loop
N_{ed}	Number of Elimination and Dispersion steps
P_{ed}	Probability of Elimination and Dispersal
$f(x, y)$	Image
$\eta(x, y)$	Noise in an image
$\hat{f}(x, y)$	Restored image

Chapter 1

Introduction

- 1.1 Automatic Detection of Diseases
- 1.2 Problem Statement
- 1.3 Organization of the thesis
- 1.4 References

1. Introduction

1.1 Automatic Detection of Diseases

Recent technological advancements have significantly expanded the use of Computer Engineering, Information Technology and Signal Processing in Health Care, as manifested by wide array of applications developed for supporting clinical activities. This has made physician and specialists dependent or accustomed to the use of different technologies and computing techniques in their clinical decision making and patient management. Of particular relevance is radiology, nuclear medical imaging that has greatly evolved with and benefited from vast technological innovations and advancements. Radiology has become increasingly critical in clinical patient care and its practice has progressively changed from conventional film based settings to a technology-ended digital paradigm.

Diagnoses missed on imaging are a common problem [1]. Of all medical malpractice lawsuits filed against medical imaging professionals, close to 70% are related to the miss of a diagnosis [2]. Errors, which occurs when abnormalities that are readily detectable in retrospect are simply “not seen”, is one of the most common reason why diagnosis are missed and account for around 60% of cases [3]. This risk of “not seeing” lesions is found maximum in the diagnosis of cancer. Studies [4] have shown that the rates for this type of error are up to 75%. However, a recent study reported by *New England Journal of Medicine* shows that the estimated cumulative risk of having at least one false positive result after screening was about 50% from mammograms, 25% from clinical breast examinations, and 19% from biopsy [5]. Such false positives not only cause substantial stress in those women but cost money in follow-up studies to verify the results [6]. So, the risk of incorrect diagnosis can be mitigated to some extent if computer aided detection (CAD) is used as an additional safety tool. Different from a human observer, the CAD system is not affected by distraction or fatigue and always operates at the same performance level. Besides, a human eye can only discern among some shades of gray whereas a computer can differentiate the least changes (Least Significant Bit) in the images as it reads an image as a data.

Therefore, the consistency of a CAD system combined with the knowledge and experience of the doctor can have a positive impact on detection accuracy. **Thus, it is desirable to develop new techniques for accurate detection of diseases and to reduce false positive rates.**

Various research communities are involved in machine learning research, areas such as computational, learning theory, artificial neural networks (Rumelhart et al., 1986)[7], statistics, stochastic modeling, probabilistic models (Weiss and Kulikowski, 1991)[8], genetic algorithms (Goldberg, 1989; Wnek and Michalski, 1994) [9-10], reinforcement learning (Cichosz, 1995) [11] and pattern recognition. Medical diagnostic reasoning and techniques is also very important application area of computer systems [12-14]. Here, a set of clinical cases are taken as examples to make an intelligent system or code to learn and produce a logical description of the clinical features that uniquely model the clinical conditions. A classic example of this type of system is KARDIO which was developed to do the interpretation of ECGs [15].

Biomedical Signal Processing as reported in papers [16-23] and computer based medical image interpretation systems [24-33] proves their significant assistance to medical diagnosis. In most of these cited cases, they have tried to emulate a doctor's expertise in the identification of malignant regions in minimally invasive imaging procedures (like computed tomography, ultrasonography, endoscopy, confocal microscopy, computed radiography or magnetic resonance imaging, single photon emission computed tomography or positron emission tomography) [34].

There are several difficulties that are encountered while developing a model for such a system – missing parameter values, incorrectness (systematic or random noise in the data), sparseness of patient record (few or non-representable record) and inappropriate selection of parameters. The generalization capability of neural network and its robustness makes it a very useful tool for improved medical decision making [35-39].

1.2 Problem Statement

Motivated with the potential requirements of automated detection and diagnostics techniques for Medicare system, attempts are made to overcome impairments that limits the present automatic detection and diagnosis. The works presented in the thesis are basically novel techniques or tools developed as a part of this thesis work use artificial neural networks and evolutionary optimization techniques i.e., Bacterial foraging. Looking into the alarming situation of cardiac related functional disorder, a sincere effort is made to address the problem of detection of arrhythmias using artificial neural networks. The arrhythmia problem is formulated and solutions are provided to automatically detect the charges in various wave shapes i.e., P, Q, R, S, T, U etc. including the rate of heart beats.

Noise is a strong limitation to medical imaging in terms of detection and diagnosis. The automatic noise removal is felt as a needed solution towards automatic detection and diagnosis. Therefore, artificial neural networks are used to remove noise from medical images.

Detecting lesion and locating it is a challenging cardiac imaging problem. A wrong approach may lead to false detection adding treatment cost to patient. Therefore, to address the problem in a machine intelligent way, fast neural network is used to detect the lesion along with its location in a cardiac image. Image enhancement is one of the preferred methods to counter false detection. A method or technique that provides denoising and enhancement is most wanted in the medical imaging to give new dimensions to automatic detection and diagnosis technique. In an attempt to meet the requirement, in this thesis bacterial foraging technique is used in conjunction with median filter to denoise the images while improving the peak signal to noise ratio (PSNR) considerably. The proposed hybrid method is a finding of the search for denoising with image enhancement and may go a long way in automatic detection in medial images including mammography images.

1.3 Organization of the thesis

The following is a brief presentation on organization of the thesis.

The rationale of the thesis is presented in Chapter One. Chapter Two describes the different medical imaging modalities in use. Chapter Three introduces the concept of artificial neural network. It also illustrates backpropagation algorithm in detail. Recent soft-computing optimization techniques are all listed and discussed in Chapter Four. A critical analysis of these methods clearly brings out their advantages and disadvantages. Following this is Chapter Five that deals with the detection of arrhythmia and gives the proposed network with its subsequent results. Chapter Six discusses the technique of noise removal from medical image using a neural network. It also gives a current literature survey of the methods used for noise removal. Lesion detection in SPECT cardiac image is a work that is described in Chapter Seven, where in a method, FNN (Fast Neural Network), is used to detect the lesion along with its location. In Chapter Eight, new methods are proposed to enhance a mammogram image by removing noise. In this chapter, bacterial foraging algorithm is used to denoise an image and its performance metrics are evaluated with a standard Lena image. In the next part of the chapter, a cascade Median Filter and Bacterial Foraging Optimization method is used to enhance the PSNR of an image. The performance metrics show a considerable rise in the enhancement quality of the proposed methods. Lastly, Chapter Nine concludes with critical analysis and summarization of the whole work and also proposing the future scope.

1.4 References

- [1]. Peldschus Kersten, Herzog Peter, Wood Susan A, Cheema Jugesh I, COSTELLO Philip, SCHOEPF U. Joseph, "Computer-aided diagnosis as a second reader : Spectrum of findings in CT studies of the chest interpreted as normal", The Journal of CHEST Foundation: The Critical Care Family Assistance Program, vol. 128, no. 3 (30 ref.), pp. 1517-1523, 2005.

-
- [2]. Berlin, L, Berlin, J, "Malpractice and radiologists in Cook County, IL: trends in 20 years of litigation", *AJR Am Journal Roentgenol*, vol. 165, pp. 781-788, 1995.
 - [3]. Abe, H, MacMohan, H, Engelmann, R, *et. al*, "Computer aided diagnosis in chest radiography: results of large scale observer tests at the 1196-2001 RNSA Scientific Assemblies", *Radiographics*, vol. 23, pp. 255-265, 2003.
 - [4]. Berlin, L, "Malpractice issues in radiology: perceptual errors", *AJR Am Journal Roentgenol*, vol. 167, pp. 587-590, 1996.
 - [5]. J G Elmore, M B Barton, V M Mocerri, S Polk, PJ Arena and S W Fletcher, "Ten-year risk of false positive screening mammograms and clinical breast examination", *New Englands J. Med.*, vol. 338, pp. 1089-1096, 1998.
 - [6]. H Liu, C L Matson, K Lau, R R Mapakshi, "Experimental validation of a backpropagation algorithm for three-dimensional breast tumor localization", *IEEE Journal of selected topics in Quantum Electronics*, vol. 5, no. 4, pp. 1049-1057, July/August 1999.
 - [7]. Rumelhart, D.E. and McClelland, J.L. (eds.) *Parallel Distributed Processing, Vol. 1: Foundations*, MIT Press, Cambridge, MA: MIT Press, 1986.
 - [8]. Weiss, S. and Kulikowski, C. *Computer Systems that Learn-Classification and Prediction Methods from Statistics, Neural Nets, Machine Learning and Expert Systems*, Morgan-Kaufmann, 1991.
 - [9]. Goldberg, D., *Genetic Algorithms in Search, Optimization, and Machine Learning*. Addison-Wesley, 1989.
 - [10]. Wnek, J. and Michalski, R. "Comparing symbolic and subsymbolic learning: three studies", *Machine Learning: a multistrategy approach.*, Michalski, R and Tecuci, G. (eds.), 4, Morgan-Kaufmann, 1994.
 - [11]. Cichosz, P. "Truncating temporal differences: on the efficient implementation of the TD for reinforcement learning", *Journal of AI Research*, vol. 2, pp. 287-318, 1995.
 - [12]. Kralj, K. and Kuka, M. "Using machine learning to analyze attributes in the diagnosis of coronary artery disease", *Proceedings of Intelligent Data Analysis in Medicine and Pharmacology-IDAMAP98*, Brighton, UK, 1998.

-
- [13]. Strausberg, J. and Person, M. "A process model of diagnostic reasoning in medicine", *International Journal of Medical Informatics*, vol. 54, pp. 9-23, 1999.
- [14]. Zupan, B., Halter, J.A., and Bohanec, M. "Qualitative model approach to computer assisted reasoning in physiology", *Proceedings of Intelligent Data Analysis in Medicine and Pharmacology-IDAMAP98*, Brighton, UK, 1998.
- [15]. Bratko, I., Mozetic, I., and Lavrac, N., *KARDIO: A study in deep and qualitative knowledge for expert systems*, Cambridge, Massachusetts: MIT Press, 1989.
- [16]. Dawant, B.M., Ozkan, M., Sprenkels, H., Aramata, H., Kawamura, K., and Margolin, R.A. "A neural network approach to magnetic resonance imaging tissue characterization", *Communication, Control, and Signal Processing*, Arıkan E., (ed.), 2, Bilkent University, Ankara, Turkey. Elsevier, Amsterdam, pp. 1803-1809, 1990.
- [17]. Gindi, G.R., Darken, C.J., O'Brien, K.M., Sterz, M.L., and Deckelbaum, L.I. "Neural network and conventional classifiers for fluorescence-guided laser angioplasty", *IEEE Transactions on Biomedical Engineering*, vol. 38, no. 3, pp. 246-252, 1991.
- [18]. Guo, Z., Durant, L.G., Lee, H.C., Allard, L., Grenier, M.C., and Stein, P.D. "Artificial neural networks in computer-assisted classification of heart sound in patients with porcine bioprosthetic valves", *Medical, Biological Engineering and Computing*, vol. 32, pp. 311-316, 1994.
- [19]. Kennedy, L.R., Harrison, R.F., Burton, A.M., Fraser, H.S., Hamer, W.G., MacArthur, D., McAllum, R., and Steedman, D.J. "An artificial neural network system for diagnosis of acute myocardial infarction (AMI) in the accident and emergency department: evaluation and comparison with serum myoglobin measurements", *Computer Methods and Programs in Biomedicine*, vol. 52, pp. 93-103, 1997.
- [20]. Nekovei, R. and Sun, Y. "Back-propagation network and its configuration for blood vessel detection in angiograms", *IEEE Transactions on Neural Networks*, vol. 6, no. 1, 64-72, 1995.

-
- [21]. Prentza, A. and Wesseling, K.H. "Catheter-manometer system damped blood pressures detected by neural nets", *Medical and Biological Engineering and Computing*, vol. 33, pp. 589-595, 1995.
- [22]. Rayburn, D.B., Klimasauskas, C.C., Januszkiewicz, A.J., Lee, J.M., Ripple, G.R., and Snapper, J.R. "The use of back propagation neural networks to identify mediator-specific cardiovascular waveforms" *Proceedings of the International Joint Conference on Neural Networks*, vol. 2, pp. 105-110, 1990.
- [23]. Yeap, T.H., Johnson, F., and Rachniowski, M. "ECG beat classification by a neural network", *Proceedings of the 12th Annual International Conference of the IEEE Engineering in Medicine and Biology Society*, Philadelphia, Pennsylvania, USA, vol. 3, pp.1457-1458, 1990.
- [24]. Coppini, G., Poli, R., and Valli, G. "Recovery of the 3-D shape of the left ventricle from echocardiographic images", *IEEE Transactions on Medical Imaging*, vol. 14, pp. 301-317, 1995.
- [25]. Hanka, R., Harte, T.P., Dixon, A.K., Lomas, D.J., and Britton, P.D. "Neural networks in the interpretation of contrast-enhanced magnetic resonance images of the breast", *Proceedings of Healthcare Computing*, Harrogate, UK, pp. 275-283, 1996.
- [26]. E. Riddington, E. Ifeachor, E. Allen, N. Hudson, D. Mapps. "A Fuzzy Expert System for EEG Interpretation" *Proc. of Conference on Neural Networks and Expert Systems in Medicine and Healthcare, NNESMED'94*, Plymouth, England, University of Plymouth, pp. 291-302, 1994.
- [27]. Innocent, P.R., Barnes, M., and John, R. "Application of the fuzzy ART/MAP and MinMax/MAP neural network models to radiographic image classification", *Artificial Intelligence in Medicine*, vol. 11, pp. 241-263, 1997.
- [28]. Karkanis, S., Magoulas, G.D., Grigoriadou, M., and Schurr, M. "Detecting abnormalities in colonoscopic images by textural description and neural networks" *Proceedings of Workshop on Machine Learning in Medical Applications, Advance Course in Artificial Intelligence-ACAI99*, Chania, Greece, pp. 59-62, 1999.
- [29]. Lo, S.-C. B., Lou, S.-L. A., Lin, J.-S., Freedman, M.T., Chien, M.V., and Mun, S.K. "Artificial convolution neural network techniques and

-
- applications for lung nodule detection", *IEEE Transactions on Medical Imaging*, vol. 14, pp.711-718, 1995.
- [30]. Miller, A.S., Blott, B.H., and Hames, T.K. "Review of neural network applications in medical imaging and signal processing", *Medical and Biological Engineering and Computing*, vol. 30, pp. 449-464, 1992.
- [31]. Phee, S.J., Ng, W.S., Chen, I.M., Seow-Choen, F., and Davies, B.L. "Automation of colonoscopy part II: visual-control aspects", *IEEE Engineering in Medicine and Biology*, pp. 81-88, May/June, 1998.
- [32]. Veropoulos, K., Campbell, C., and Learmonth, G. "Image processing and neural computing used in the diagnosis of tuberculosis", *Colloquium on Intelligent Methods in Healthcare and Medical Applications*, York, UK, 1998.
- [33]. Zhu, Y. and Yan, H. "Computerized tumor boundary detection using a Hopfield neural network". *IEEE Transactions on Medical Imaging*, 16, 55-67, 1997.
- [34]. George D. Magoulas and Andriana Prentza, "Machine learning in medical applications" presented at the Workshop on Machine Learning in Medical Applications, hosted by the ECCAI Advanced Course on Artificial Intelligence for 1999 (ACAI-99).
- [35]. Akay, Y.M., Akay, M., Welkowitz, W., and Kostis, J.B. "Noninvasive detection of coronary artery disease using wavelet-based fuzzy neural networks", *IEEE Engineering in Medicine and Biology*, pp. 761-764, 1994).
- [36]. Lim, C.P., Harrison, R.F., and Kennedy, R.L. "Application of autonomous neural network systems to medical pattern classification tasks", *Artificial Intelligence in Medicine*, vol. 11, pp. 215-239, 1997.
- [37]. Micheli-Tzanakou, E., Yi, C., Kostis, W.J., Shindler, D.M., and Kostis, J.B. "Myocardial infarction: Diagnosis and vital status prediction using neural networks", *IEEE Computers in Cardiology*, pp. 229-232, 1993.
- [38]. Pattichis, C., Schizas, C., and Middleton, L. "Neural network models in EMG diagnosis", *IEEE Transactions on Biomedical Engineering*, vol. 42, no. 5, pp. 486-496, 1995.
-

-
- [39]. Reategui, E.B., Campbell, J.A., and Leao, B.F. "Combining a neural network with case-based reasoning in a diagnostic system", *Artificial Intelligence in Medicine*, vol. 9, pp.5-27, 1996.

Chapter 2

A brief review of Artificial Neural Networks

2.1 Introduction

2.2 Biological Motivation of Neural Networks

2.3 Model of a Neuron

2.4 Activation Function and Characteristics

2.5 Learning Rules

2.6 Multilayer Neural Networks

**2.7 Implementation Procedures and Issues Involved in
Neural Network Training**

2.8 Error Back Propagation in Neural Networks

2.9 Backpropagation Algorithm

2.10 References

2. A brief review of artificial neural networks

2.1 Introduction

Neural networks are powerful techniques to solve many real world problems. A most fascinating aspect of Artificial Neural Networks (ANN) is its potential to modeling of large complex systems. Neural networks, with their remarkable ability to derive meaning from complicated or imprecise data, can be used to extract patterns and detect trends that are too complex to be noticed by either human beings or other computer techniques. They learn from experience in order to improve their performances and to adapt themselves to changes in the environment. In addition to this, they can deal with incomplete information or noisy data and can be very effective especially in situations where it is not possible to define the rules or steps that lead to the solution of a problem. Due to these reasons, ANNs have drawn the attentions of scientists and technologists from large number of disciplines [1]. They functions as massive parallel distributed computing networks. Their performances in terms of Fault tolerance, Self-organization, Generalization ability, Continuous adaptively have made them prominent as softcomputing tools [2-6]. Large number of neural models exists. Applications determine the type of neural network to be selected [7-13]. In order to perform a particular task, a neural network required to be trained. They learn new associations, new patterns, and new functional dependencies. One of the distinct strengths of neural networks is their ability to generalize well while sensibly interpolating input pattern that are new to the network. The parallel distribution structure and generalization capability make neural network to solve complex problems easily. Neural networks have a built in capability to adapt their synaptic weights with changes in the surrounding environment. A neural network trained to operate in a specific environment can be easily retrained to deal with the changes in the operating environmental conditions.

2.2 Biological Motivation of Neural Network

An Artificial Neural Network can be defined as “a system composed of many simple processing elements operating in parallel whose function is determined by network structure, connection strength, and processing performed at computing elements or nodes”. Much of the inspiration for neural network came from the desire to produce artificial system capable of sophisticated and intelligent computations similar to that performed by human brain.

Biological neurons are the basic building blocks of human brain. The brain consists of huge number of neurons(of the order of 10^{10}) and interconnecting synapses between them(of the order of 60×10^{12}). The neurons perform pattern recognition, perception and motor control. Neuron, as shown in the figure2.1, consists of synapses, dendrites, cell body and axon.

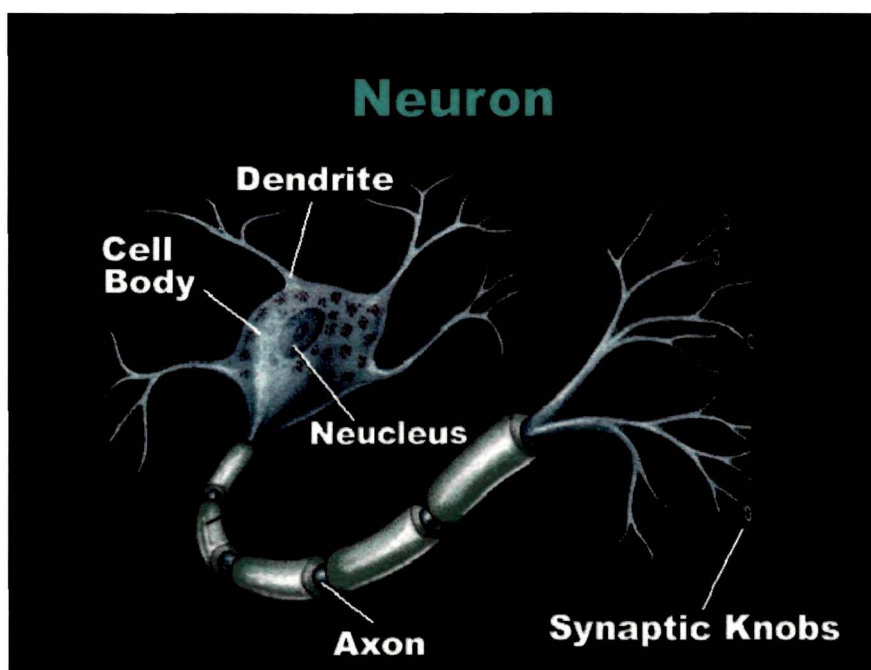


Figure 2.1: Structure of Biological Neuron

The synapse converts a pre-synaptic electrical signal into a chemical signal and then back into a post-synaptic electric signal. The post-synaptic signals are aggregated and transferred along the dendrites to the neuron cell body. If the cumulative inputs raise the electrical potential of the cell body, then the neuron fires

by propagating the action potential down the axon to excite or inhibit other neurons. The frequency of firing of a neuron is proportional to the total synaptic weights.

2.3 Model of a Neuron

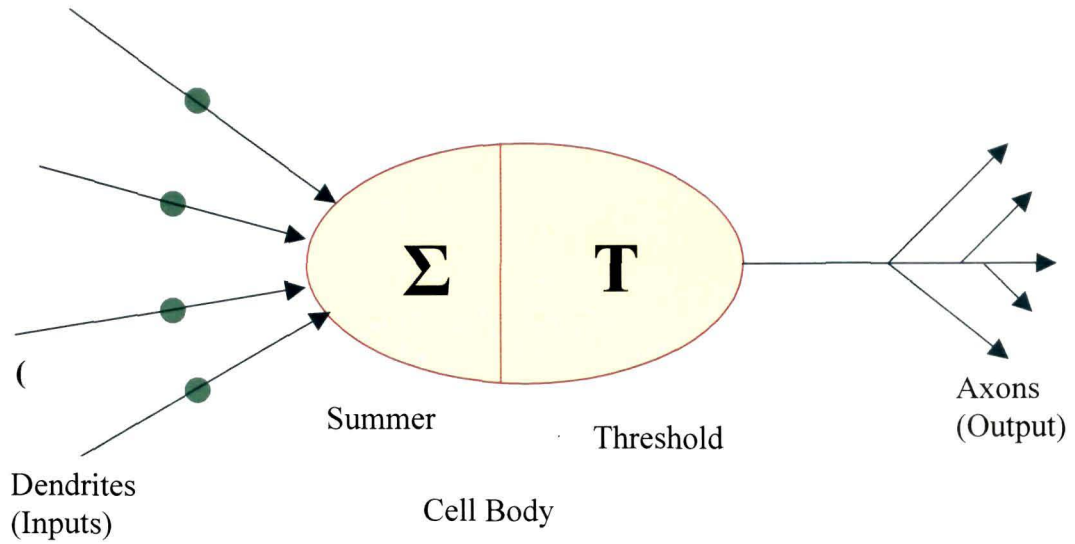
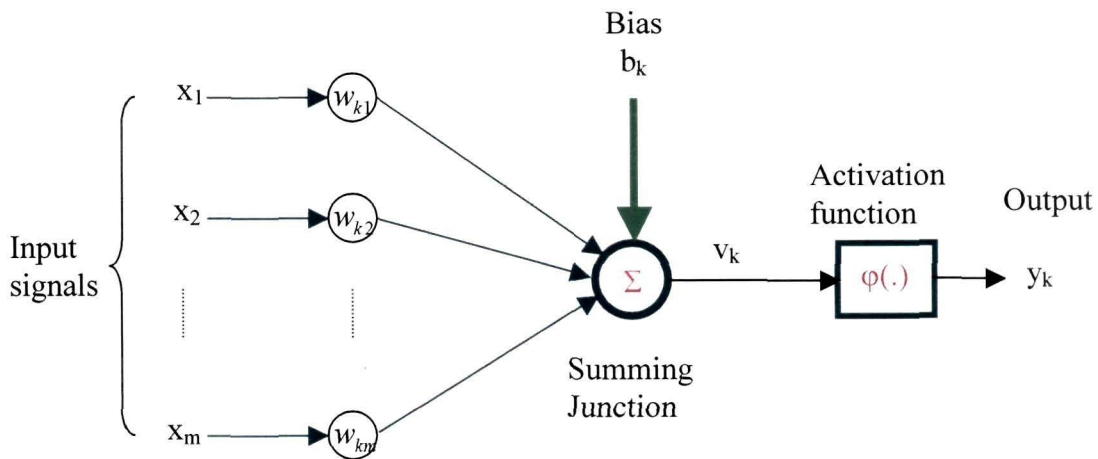


Figure 2.2 Model of Biological Neuron



(c)

Figure 2.3 Model of Artificial Neuron

The behavior of a biological neuron can be represented as a simple model as shown in figure 2.2. The analogous model shown in figure 2.3 is called artificial neuron. This model forms the basis of what is known as artificial neural network. All the information processing operations of neural network occur at the neuron. The four basic elements of a neuron are synapses or connecting weights, summing junction, activation function, and bias. It has a set of synapses or connecting weights, each of which are characterized by a weight or strength of its own. Specifically, a signal x_j at the input of synapse j connected to neuron k is multiplied by the synaptic weight w_{kj} . The synaptic weight of an artificial neuron may lie in a range that includes negative as well as positive values. At the summing junction, the input signals, weighted by the respective synapses of the neuron, get added up. The activation function or squashing function limits the amplitude of output of neuron. The range of normalized amplitude of the output of a neuron lies between 0 and 1 or -1 and 1. The bias, with fixed input $+1$ or -1 , has the effect of increasing or decreasing the net input of the activation function, depending on whether it is positive or negative, respectively.

The output of a neuron k can be written as,

$$y_k = \varphi(v_k) \quad 2.1$$

where,

$$v_k = \sum_{j=1}^m w_{kj} x_j + b_k \quad 2.2$$

x_1, x_2, \dots, x_m are input signals, $w_{k1}, w_{k2}, \dots, w_{km}$ are the synaptic weights of neuron k , b_k is the bias, $\varphi(\cdot)$ is the activation function and y_k is the output signal of neuron.

2.4 Activation Function and their Characteristics

The activation function defines the output of a neuron with in a defined range. Various types of activation functions are used in neural networks [14-15]. Broadly the activation function can be put into three categories.

Threshold Function

$$\varphi(v) = \begin{cases} 1 & \text{if } v \geq 0 \\ 0 & \text{if } v < 0 \end{cases} \quad 2.3$$

In this case, the output of a neuron takes on the value of 1 if the induced local field of that neuron is nonnegative and 0 otherwise.

Piecewise-Linear Function

The piecewise-linear function can be described as

$$\varphi(v) = \begin{cases} 1 & \text{if } v \geq +1/2 \\ 1 & \text{if } +1/2 > v > -1/2 \\ 0 & \text{if } v \leq -1/2 \end{cases} \quad 2.4$$

The function, though consists of linear segments, is nonlinear

Sigmoid Activation Function

The sigmoid is most common form of activation function in construction of neural network. A sigmoid function limits an input with very large values to a range of +1 to -1.

Mathematically,

$$\varphi(v) = \frac{1}{1 + \exp(-\lambda v)} \quad 2.5$$

$$\varphi(v) = \frac{2}{1 + \exp(-\lambda v)} - 1 \quad 2.6$$

where λ is called activation constant and is the slope controlling parameter of the sigmoid. Figure 2.2 shows the input-output shape of various activation functions. The range of unipolar sigmoid, expressed in eqn. 2.5, lies between 0 and 1. Where as the sigmoid, expressed in eqn. 2.6, is bipolar and its range lies between -1 and 1.

An alternative form of the sigmoid function is the hyperbolic tangent. It is represented as,

$$\varphi(v) = \tanh(v) \quad 2.7$$

The choice of activation function for a neural network may influence the learning speed and convergence. Neural networks with sigmoid activation functions are capable of approximating unknown mappings well [16].

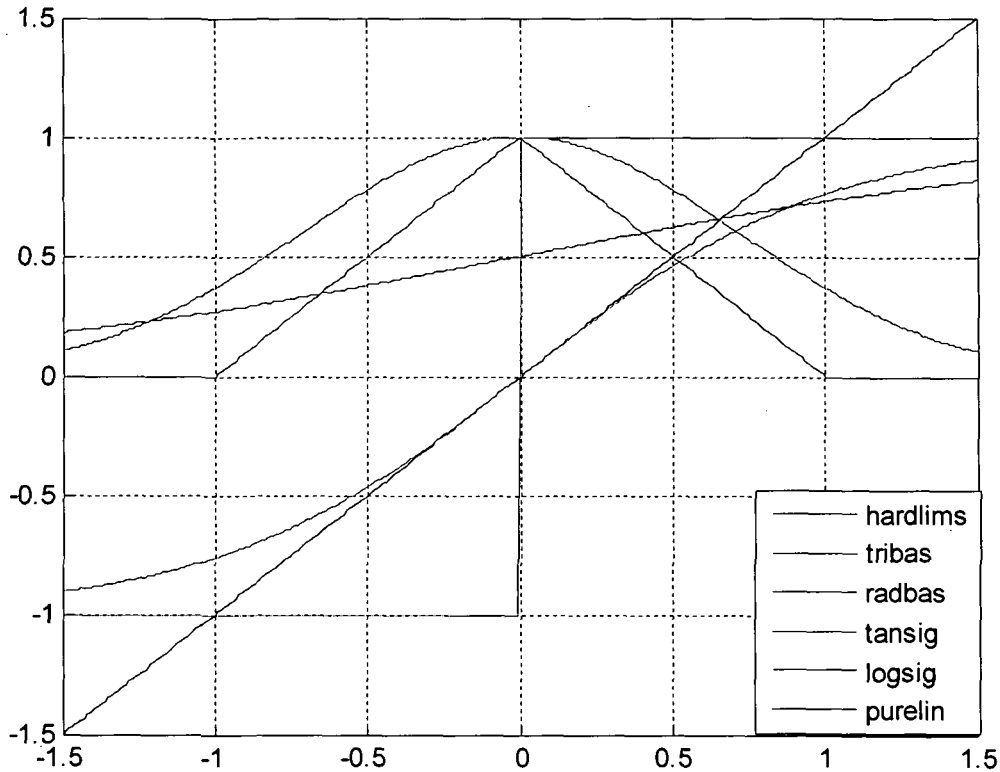


Figure 2.4 Activation Functions

2.5 Learning Rules

Neural networks follow a similar pattern of decision making as followed by human brain. Like human being, which learn from its environment, neural networks also need to be trained. While training, care has to be taken to distinguish the learning from memorization. In fact, training of neural network is done on a case-to-case basis. In some cases, the memorization may be important than the learning.

Training a neural network in input-output mapping, involves modification of the synaptic weights by applying a set of training samples called patterns. Each pattern consists of one or more input signal and its/their corresponding desired response. The synaptic weights are modified to minimise the difference between the desired response and the actual response of the network produced by the input signal in accordance with an appropriate statistical criterion. The training of the network is repeated for many examples in the set until the network reaches a steady state, where there are no further significant changes in the synaptic weights. Thus, the network learns from the examples by constructing an input-output mapping for the problem at hand.

Neural Networks does not have a unique learning algorithm, as one would expect. There is a saga of neural networks, each of which offers advantage of its own. The selection of a particular network depends on the type of application. Depending upon the type of neural network, there is a learning rule. To name a few, following are the learning rules, (i) Hebbian learning rule, (ii) Perceptron learning rule, (iii) Delta learning rule, (iv) Widrow-Hoff learning rule, (v) Correlation learning rule, (vi) Winner-Take-All learning rule and (vii) Outstar learning rule (viii) Stochastic learning rule ix) Boltzmann learning rule [17-21].

However, as shown in figure 2.5, following general learning procedure is adopted for training neural network [22]. The weight vector increases in proportion to the product of inputs x and learning signal 'r'. The learning signal 'r' is in general a function of w_i , x and the testing signal d_i and can be expressed as,

$$r = r(w(t), x, d_i) \quad 2.8$$

Where, $w_i = [w_{i1}, w_{i2}, \dots, w_{ij}, w_{in}]^T$ are the weights connecting i^{th} neuron.

w_{in} stands for the bias weight. The input x_n of input vector x is the fixed input of bias with a value of -1 .

The increment of the weight vector w_i produced by the learning step at time t according to the general learning rule is,

$$\Delta w_i(t) = cr[w_i(t), x(t), d_i(t)]x(t) \tag{2.9}$$

where, c is a positive number called the learning constant that determines the rate of learning. The weight vector adapted at time ‘ t ’ becomes

$$w_i^{k-1} = w_i^k(t) + cr[w_i^k, x^k, d_i^k]x^k \tag{2.10}$$

in the next step.

The learning in 3.9 is in the form of a sequence of discrete-time weight modifications. Continuous-time learning can be expressed as $\frac{dw_i(t)}{dt} = crx(t)$

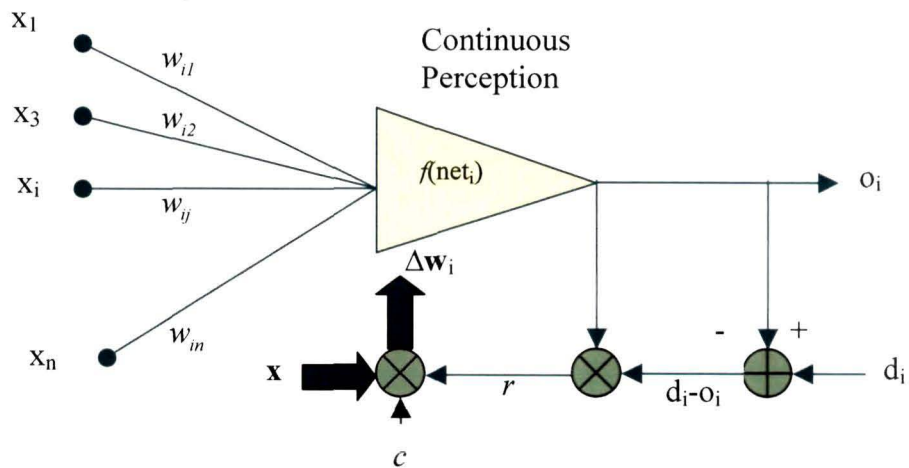


Figure 2.5 Generalized Learning Rule

2.6 Multilayer Neural Network

The most important attribute of multilayer feed forward network, as shown in figure 2.6, is that it can learn a mapping of any complexity. The network learning is based on repeated presentations of the training samples. A three layer neural network, in principle, is sufficient to model a problem [23,24]. The nodes in the input layer

supply input vector to the second layer or first hidden layer. The output of second layer or first hidden layer flows to the second hidden layer, and so on for the rest of the network. The set of output signals of the neurons in the output layer or final layer constitutes the response of the network for the input pattern in the input layer. Figure 2.6 shows a three layers *i.e.*, one input layer, one hidden layer and one output layer, feed forward neural network.

From the point of view of active phase, ANNs can be classified as feedforward (static) and feed back(dynamic) systems. Based on their learning phase, it can be classified into supervised and unsupervised systems. Feedforward supervised networks are typically used for function approximation tasks. Linear recursive least-mean-square (LMS) networks, Backpropagation networks and radial basis networks belong to this category. Feedforward unsupervised networks are used to extract important properties of the input data and map input data into representation domain. Hebbian

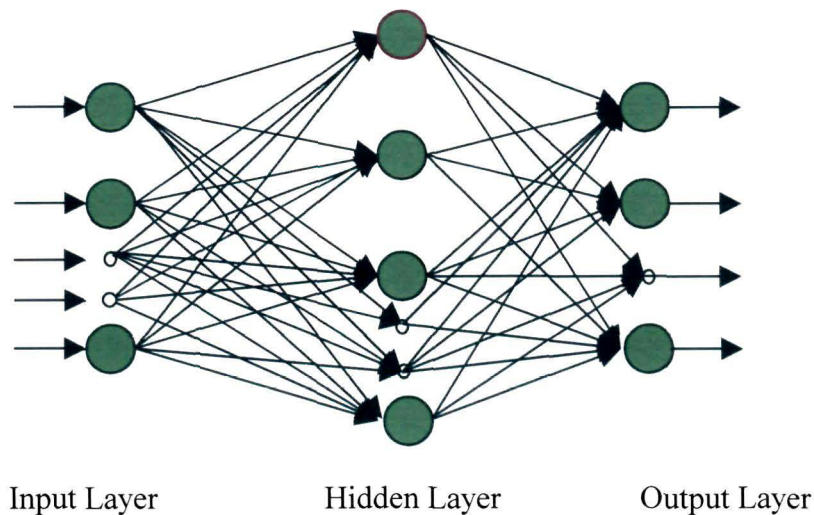


Figure 2.6 Multilayer Neural Network Structure

networks and competitive network belong to this category. Feedback networks are used to learn temporal features of the input data and their internal state evolve with time.

2.7 Implementation Procedures and Issues Involved in Neural Network Training

To begin with, a neural network is ignorant about the system. In order to represent the system, the neural network has to be trained with its behaviour i.e a set of input-output patterns. The key steps involved in modeling a system with neural network comprises data generation/collection, data scaling, choice of neural network and its structure and finally training.

The preliminary step in neural model development for a particular problem is identification of model inputs on which the output depends on. In general, data generation means, collection of a set of output vector for a set of input vector. The total number of patterns to be collected for a given problem is chosen such that the developed model suitably represents the original problem. The choice of data generator depends on the application, availability of data generator and accuracy concerned. Data collected from measurements is always regarded as the best choice.

While presenting input-output patterns to a neural network, the values of the patterns need to be suitably scaled between 0 to 1 or -1 to 1 depending upon a unipolar or bipolar activation function used respectively. The necessity arises due to the fact that the activation function transforms the input signals to the above stated range. It is worth noting that the data scaling restricts application of neural network trained for a particular problem to a specific range of input and output parameters only. Commonly a linear scaling or a log scaling is used for data scaling. An intelligent choice of scaling can enlarge the range of operation. In general, the input-output scaling makes the problem better conditioned for training and facilitates better training.

The accuracy of neural network based model may very dramatically depend on many features, including the network topology and learning technique. For learning in error backpropagation algorithm, the choice of initial synaptic weights may

significantly affect the convergence of learning [25-27]. The best network chosen is often not the best. A common practice is to carve out a small set of data from test data set and use it for cross validation after training. Sometimes, a neural network becomes an unstable predictor. A small change in data set may yield a different configuration and consequently different performance on unseen data [28-29].

Hidden units allow a network to learn nonlinear functions and allow the network to represent combinations of input features. Given too many hidden units, a neural network will simply memorize the input patterns. Given too few hidden units, the network may not be able to represent all of the necessary generalization.

Learning rate limits the change of weight for each iteration. Ideally, the learning rate should be small but then learning becomes very slow. If the learning rate is too high then the system can suffer from severe oscillations. Over training leads a network into memorization.

2.8 Error Back Propagation Neural Network

For many years, there was no theoretically sound algorithm for training multilayer artificial neural networks. The resurgence of interest in artificial neural network began after the invention of error back propagation algorithm. Rumelhart *et al.* [1] presented a clear and concise description of the backpropagation algorithm. It is a systematic method of training multilayer artificial neural networks with sigmoid as activation function. As the name suggests, neuron activation propagates forward and error calculated at the output layer are back propagated to the hidden layers and weights are modified according to these changes. Although a Backpropagation can be applied to networks with any number of layers, it has been shown that one hidden layer suffices to approximate any function with finitely many discontinuities to arbitrary precision, provided the activation functions of the hidden units are non-linear [30-36]. Coding of the algorithms in the present thesis work are done using a MATLAB [37-40] in Windows XP platform.

2.9 Backpropagation Algorithm

The generalized Backpropagation algorithm can be best explained with a three layers neural network (one input layer, one hidden layer and one output layer).

The activation function (which is differentiable) of the total input is, given by

$$y_k^p = \varphi(s_k^p) \quad 2.11$$

$$\text{where, } s_k^p = \sum_j w_{jk} y_j^p + \theta_k \quad 2.12$$

$$\Delta_p w_{jk} = -\eta \frac{\partial E^p}{\partial w_{jk}} \quad 2.13$$

The error measure, E^p is the total quadratic error for pattern p at the output units

$$\text{Thus, } E^p = \frac{1}{2} \sum_{o=1}^{N_o} (d_o^p - y_o^p)^2 \quad 2.14$$

where d_o^p is the desired output for units o when pattern p is clamped.

Further $E = \sum_P E^p$ is the summed squared error

One can write

$$\frac{\partial E^p}{\partial w_{jk}} = \frac{\partial E^p}{\partial s_{jk}^p} \frac{\partial s_{jk}^p}{\partial w_{jk}} \quad 2.15$$

Using equation 2.12, the second term of equation 2.15 can be expressed as

$$\frac{\partial s_{jk}^p}{\partial w_{jk}} = y_j^p \quad 2.16$$

The error signal δ_k^p produced by k^{th} neuron is defined as

$$\delta_k^p = -\frac{\partial E^p}{\partial s_{jk}^p} \quad 2.17$$

Therefore, equation 2.15 can be rewritten as

$$\frac{\partial E^p}{\partial w_{jk}} = \delta_k^p y_j^p \quad 2.15a$$

which is further modified to

$$\Delta_p w_{jk} = \eta \delta_k^p y_j^p \quad 2.18$$

Expression 2.18 represents the general formula for weight adjustments for a single layer network in delta training/learning. It can be noted that $\Delta_p w_{jk}$ in equation 2.18 does not depend on the form of activation function. It also follows from 2.18 that the adjustment of weight w_{jk} is proportional to the input activation y_j and to the error signal value δ_{ok} at k^{th} neuron's output.

To compute δ_k^p , we apply the chain rule to write this partial derivative as the product of two factors, one factor reflecting the change in error as function of the output unit and one reflecting the change in the output as a function of the input,

Thus,

$$\delta_k^p = -\frac{\partial E^p}{\partial s_{jk}^p} = -\frac{\partial E^p}{\partial y_k^p} \frac{\partial y_k^p}{\partial s_k^p} \quad 2.19$$

The second term can be computed as

$$\frac{\partial y_k^p}{\partial s_k^p} = \varphi'(s_k^p) \quad 2.20$$

Which is a simple derivative of the squashing function φ for the k^{th} unit evaluated at the net input s_k^p .

To compute the first factor of equation 2.19, two cases are considered. First, k is assumed as an output unit ' $k=0$ ' of the network. In this case, it follows from the definition of E^p that

$$\frac{\partial E^p}{\partial y_o^p} = -(d_o^p - y_o^p) \quad 2.21$$

Substituting 2.21 and 2.20 in equation 2.19, the equation reduces to:

$$\delta_o^p = (d_o^p - y_o^p)\phi'(s_o^p) \quad 2.22$$

for any output unit o .

Secondly, if k is not an output unit but a hidden unit $k=h$, one does not readily know the contribution of the unit to the output error of the network. However, the error measure can be written as a function of the net inputs from hidden to output layer.

$E^p = E^p(s_1^p, s_2^p, \dots, s_j^p, \dots)$ and we use the chain rule to write

$$\begin{aligned} \frac{\partial E^p}{\partial y_h^p} &= \sum_{o=1}^{N_o} \frac{\partial E^p}{\partial s_o^p} \frac{\partial s_o^p}{\partial y_h^p} \\ &= \sum_{o=1}^{N_o} \frac{\partial E^p}{\partial s_o^p} \frac{\partial}{\partial y_h^p} \sum_{j=1}^{N_h} w_{ko} y_j^p \\ &= \sum_{o=1}^{N_o} \frac{\partial E^p}{\partial s_o^p} w_{ho} = - \sum_{o=1}^{N_o} \delta_o^p w_{ho} \end{aligned} \quad 2.23$$

Substituting this in equation 2.9 yields

$$\delta_h^p = \phi(s_h^p) \sum_{o=1}^{N_o} \delta_o^p w_{ho} \quad 2.24$$

Equation 2.12 and 2.14 give a recursive procedure for computing the δ 's for all units in the network, which are then used to compute the weight changes according to equation 2.8. This procedure constitutes the generalized delta rule for feed forward network of non-linear units.

Working with Backpropagation Algorithm

The application of the generalized delta rule thus, involves two phases: During the first phase, the input \mathbf{X} is presented and propagated forward through the network to compute the output values y_o^p for each output unit. This output is compared with its

desired value d_o , resulting in an error signal δ_o^p for each output unit. The second phase, involves a backward pass through the network during which the error signal is passed to each unit in the network and appropriate weight changes are calculated.

Weight adjustments with sigmoid activation function

The Backpropagation algorithm can be summarized in following three equations:

➤ The weight of a connection is adjusted by an amount proportional to the product of an error signal δ_k on the unit k receiving the input and the output of the unit j sending this signal along the connection:

$$\Delta_p w_{jk} = \eta \delta_k^p y_j^p \quad 2.26$$

➤ If the unit is an output unit, the error signal is given by

$$\delta_o^p = (d_o^p - y_o^p) \varphi'(s_o^p) \quad 2.27$$

It takes as the activation function φ the ‘sigmoid’ function.

$$y^p = \varphi(s^p) = \frac{1}{1 + e^{-sp}} \quad 2.28$$

In this case the derivative is equal to

$$\begin{aligned} \varphi'(s^p) &= \frac{\partial}{\partial s^p} \frac{1}{1 + e^{-sp}} \\ &= \frac{1}{(1 + e^{-sp})^2} (-e^{-sp}) \\ &= \frac{1}{(1 + e^{-sp})} \frac{(-e^{-sp})}{(1 + e^{-sp})} \\ &= y^p(1 - y^p) \end{aligned} \quad 2.29$$

The error signal for an output unit can be written as:

$$\delta_o^p = (d_o^p - y_o^p) y_o^p (1 - y_o^p) \quad 2.30$$

➤ The error signal for a hidden unit is determined recursively in terms of error signals of the units to which it directly connects and the weights of those connections. For the sigmoid activation function:

$$\begin{aligned}\delta_o^p &= \varphi'(s_h^p) \sum_{o=1}^{N_o} \delta_o^p w_{ho} \\ &= y_h^p (1 - y_h^p) \sum_{o=1}^{N_o} \delta_o^p w_{ho}\end{aligned}\quad 2.31$$

In a Backpropagation algorithm, when a learning pattern is clamped, the activation values are propagated to the output units, and the actual network outputs is compared with the desired output values, which usually ends up with an error in each of the output units. This error, e_o (say) for a particular output unit o is to be minimized to zero.

One strives to change the connections in the neural network in such a way that, next time, the error e_o will be zero for this particular pattern. From the delta rule, in order to reduce an error, the incoming weights is adapted according to,

$$\Delta w_{ho} = (d_o - y_o) y_h \quad 2.32$$

But, when this rule is applied, the weights from input to hidden units are never changed, and the full representation power of the feed-forward network is not seen as promised by the universal approximation theorem. In order to adapt the weights from input to hidden units, we again apply the delta rule. The value for δ for the hidden units is obtained by the chain rule which is : Distribute the error of an output unit o to all the hidden units that it is connected to, weighted by this connection. Differently put, a hidden unit h receives a delta from each output unit o equal to the delta of the output unit weighted with(= multiplied by) the weight of the connection between those units. In symbols: $\delta_h = \sum_o \delta_o w_{ho}$. The activation function of the hidden unit; 'φ' has to be applied to the delta, before the backpropagation process can continue. The flow chart of the algorithm is presented in the following figure :

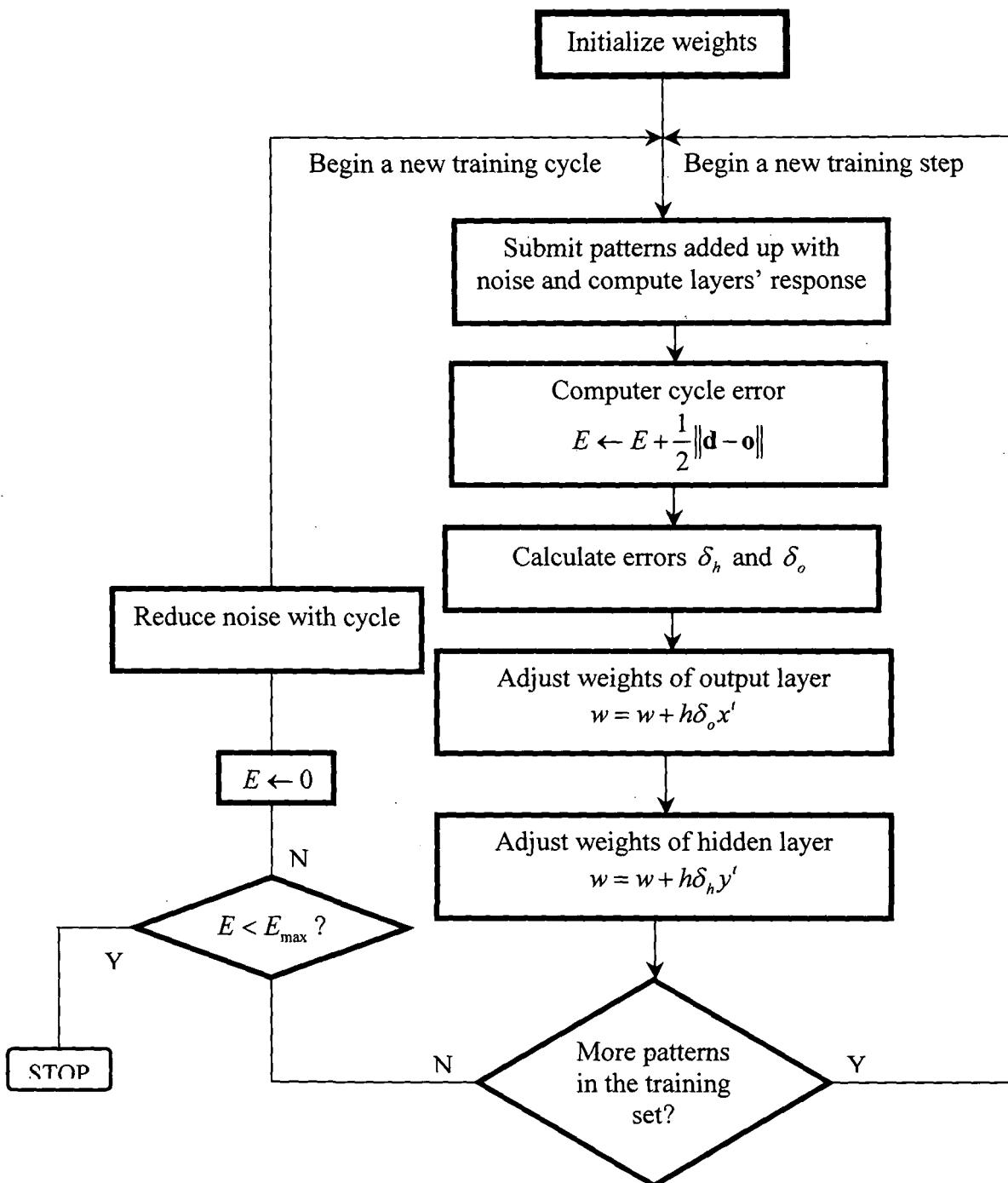


Figure 2.7 Flow Chart of Backpropagation Algorithm [15]

Momentum Method

The learning procedure requires that the change in weight is proportional to $\frac{\partial E^p}{\partial w}$. True gradient descent requires infinitesimal incremental /decremental steps. Practically, the learning rate is chosen as large as possible, to conserve time, without leading to oscillation. One way to avoid to oscillation at large learning constant ' η ', is to make the change in weight dependent on the past weight change by adding a momentum term, expressed as,

$$\Delta w_{jk}(t+1) = \eta \delta_k^p y_j^p + \alpha \Delta w_{jk}(t) \quad 2.33$$

where ' t ' indexes the presentation number and ' α ' is moment factor which determines the effect of the previous weight change. Typically ' α ' is chosen between 0.1 and 0.8.

When momentum term is not used, it takes a long time before the minimum is reached with a low learning rate, whereas for high learning rates the minimum is never reached because of the oscillations.

Learning Constant

The effectiveness and convergence of the error Backpropagation learning algorithm depend significantly on the value of the learning constant η . In general, however, the optimum value of η depends on the problem being solved. There is no single learning constant suitable for different training cases. When a broad minima yield small gradient values, then a large value of η results in a more rapid convergence. However, for problems with steep and narrow minima, a small value of η should be chosen so that overshooting of the solution is avoided. Learning constant ' η ' should be chosen experimentally for each problem. It is seen that only small learning constants guarantee a true gradient descent. The price of this guarantee is an increased total number of learning steps that need to be made to reach the satisfactory solution. Though the choice of the learning constant depends strongly on the class of

the learning problem and on the network architecture, the values ranging from 10^{-3} to 10 have been, successfully applied for many computational Backpropagation experiments, as reported in literature.

Noise Factor

Adding noise factor helps in jumping out of local minima. It enhances generalization ability of the network [22]. Another reason for using noise is to prevent memorization by the network. Since, one effectively presents a different input pattern with each cycle, so it becomes hard for the network to memorize patterns. A random number is added to each input component of the input vector as it is applied to the network. This is scaled by an overall noise factor which has range 0 to 1 range. The noise factor is gradually decreased to zero with the increase in the number of iteration.

Steepness of the Activation Function

The neuron's continuous activation function $\phi(\text{net}, \lambda)$ is characterized by its steepness factor, λ . Also, the derivative of $\phi'(\text{net})$ of the activation function serves as a multiplying factor in building components of the error signals. Thus, both choice and shape of the activation function would strongly affect the speed of network learning.

2.10 References

- [1]. B. Yegnanarayana. Artificial Neural Networks, Prentice-Hall of India Pvt. Ltd. New Delhi, Ch.8, 2001.
- [2]. Simpson PK. Artificial Neural Systems Foundation, Paradigms, Application and Implementation, Permagnon Press, ISBN -08-037895-1, 1990.
- [3]. Haykin S. Neural Networks: A Comprehensive Foundation. 2nd edition. Prentice Hall, 1999.
- [4]. Neural Ware Handbook, Neural Computing, A Technology Handbook for Professional II/PLUS and Neural Works Explorer, Pittsburg, USA, 1996.
- [5]. Ripley BD. Pattern Recognition and Neural Networks, Cambridge University Press. ISBN 0-521 46086-7, Jan. 1996.
- [6]. Demuth H, Beale M. Neural Toolbox User's Guide, The Math Works Inc., 1998.
- [7]. A.Lorenzi,L.C.P Silva Filho, and J.L.Copmpagnalo, "Using a Backpropagation algorithm to create a neural Network for interpreting ultrasonic reading of concrete", International Journal of Materials and Product Technology (IJMPT), vol. 26, Issue 1/2, 2006.
- [8]. Paik JK and Katsaggelos AK. "Image restoration using a modified Hopfield network", IEEE Trans. Image Processing, vol. 1, no.1, pp. 49-63, 1992.
- [9]. Wong HS and Guan L. "Adaptive Regularization in Image –Restoration Using A Model –Based Neural Network", Optical Engineering, vol. 36, no. 12, pp. 3297-3308, 1997.
- [10]. Celebi M.E. and Guzelis, C. "Image restoration using cellular neural network", Electronics Letter, vol. 33 no. 1, pp. 43-45, 1997.
- [11]. Jianye Zhao, Daoheng Yu, "A new approach for Medical Image Restoration based on CNN", International Journal of Circuit Theory and Applications, vol. 27, no. 3, pp. 339-346, 1999.
- [12]. Steriti RJ and Fiddy MA. "Regularized image reconstruction using SVD and a neural network method for matrix inversion", IEEE Trans. Signal. Proc., vol. 41, no. 10, pp. 3074-3077, 1993.

-
- [13]. Egmont-Petersen M, Ridder D and Handels H, "Image processing with neural networks – a review", *Pattern Recognition*, vol. 35, pp. 2279-2301, 2002.
- [14]. R J Schalkoff. *Artificial Neural Networks*, McGraw-Hill Comp. Inc., 1997.
- [15]. Jacek M Zurada. *Introduction to Artificial Neural Systems*, PWS Publishing Company, 1992.
- [16]. B. L. Kalam and S. C. Kwasny, "Why tanh: Choosing a Sigmoidal function," *IEEE Int. Conf on Neural Networks*, vol. IV, pp.578-581, 1992.
- [17]. P. Baldi, "Gradient descent learning algorithm overview: A general dynamical systems perspective", *IEEE Transactions on Neural Networks*, vol. 6, no. 1, pp. 182-195, Jan. 1995.
- [18]. Pierre Baldi "Computing with arrays of Bell-shaped and Sigmoid functions", *IEEE Transactions on Neural Networks*, vol. 5, pp. 735-742, 1994.
- [19]. D. Randall Wilson, Tony R. Martinez, "The need for small Learning Rates on large problems", *IEEE Trans. on Neural Networks*, vol. 1, pp. 115 - 119, 1991.
- [20]. Jacobs, R. A., "Increased Rates of Convergence through Learning Rate Adaptation", *Neural Networks*, vol. 1, issue 4, pp. 295-307, 1988.
- [21]. Zhang, Z.; Sarhadi, "Performance aspects of a novel neuron activation function in multi-layer feed-forward networks", *IEEE Transactions on Neural Networks*, vol. 3, pp. 2727 - 2730, Oct. 1993.
- [22]. S. I. Amari, "Mathematical foundation of Neurocomputing," *IEEE Proceedings*, vol. 78, no.9, pp.1443-1463, 1990.
- [23]. K. Hornik, M. Stinchcombe, and H. White, "Multilayered Feed-Forward Networks are Universal Approximators," *IEEE Trans. Neural Networks*, vol.2, pp.359-366, 1989.
- [24]. T. Chen, H. Chen, and R. Liu, "Approximation Capability in $C(\mathbb{R}^n)$ by Multilayer Feedforward Networks and Related Problems," *IEEE Transaction on Neural Networks*, vol.6, no.1, pp.25-30, Jan.1995.
- [25]. Y. Lee, S. H. Oh, and M. W. Kim, "The effect of initial weights on premature saturation in Backpropagation Learning," *IEEE Proceedings, International Joint Conference on Neural Networks*, vol. I, pp. 765-770, 1991.

-
- [26]. H. Lari-Najafi, M. Nasiruddin, and T. Samad, "Effect of initial weights on Backpropagation and its variations," *IEEE International Conference on Systems, Man and Cybernetics*, pp. 218-219, 1989.
- [27]. G. P. Drago and S. Ridella, "Spastically controlled activation weight initialization SCAWI," *IEEE Transaction on Neural Networks*, vol.3, no.4, pp. 627-631, 1992.
- [28]. L. Breiman, "Bagging Predictors," *Machine Learning*, vol. 24, pp. 123-140, 1996.
- [29]. L. Breiman, "Combining Predictors, in Combining Artificial Neural Nets: Ensemble and Modular Multi-Net Systems," A.J.C. Sharkey (ed.), pp. 31-50, Springer, London, 1999.
- [30]. I. Rechenberg, "Cybernetic Solution Path of an Experimental Problem," *Royal Aircraft Establishment Translation*, no. 1122, 1965.
- [31]. J. H. Holland, "Adaptation in Natural and Artificial Systems," University of Michigan Press, 1975.
- [32]. D. E. Rumelhart, G. E. Hinton, and R. J. Williams, "Learning Internal Representations by Error Propagation," *Parallel Distributed Processing*, Cambridge, MA, MIT Press, vol. I, pp. 318-362, 1986.
- [33]. P. J. Werbos, "Beyond Regression: New Tools for Prediction and Analysis in the Behavioural Sciences," PhD Thesis, Havard University.
- [34]. K. Hornik, M. Stinchcombe, H. White, "Multilayer Feed Forward Networks are Universal Approximators," *Neural Networks*, vol. 2, no. 5, pp. 359-366, 1989.
- [35]. G. Cybenko, "Approximation by Superpositions of a Sigmoidal Function. Mathematics of Control," *Signals, and Systems*, vol. 2, no. 4, pp.303-314, 1989.
- [36]. E. J. Hartman, J. D. Keeler, and J. M. Kowalski, "Layered Neural Networks with Gaussian Hidden Units as Universal Approximations," *Neural Computation*, vol. 2, no. 2, pp.210-215, 1990.
- [37]. Swapna Devi, "MATLAB Module 1: Basics of MATLAB", NITTTR, Chandigarh.
- [38]. Swapna Devi, "Image Processing with MATLAB", NITTTR, Chandigarh.
-

- [39]. Swapna Devi, “Digital Signal Processing using MATLAB”, NITTTR, Chandigarh.
- [40]. MATAB: The Language of Technical Computing: www.mathworks.com.
- [41]. Bogdan M Wilamowski. “Neural Network Architectures and Learning”, IEEE, TU1-TU12, 2003.

Chapter 3

Soft Computing; Optimization Techniques

- 3.1 Evolutionary Algorithms
- 3.2 Swarm Intelligence
- 3.3 Particle Swarm Optimization Algorithm
- 3.4 Genetic Algorithm
- 3.5 Bacterial Foraging Algorithm
- 3.6 Critical Analysis of these techniques
- 3.7 Details of Bacterial Foraging theory
 - 3.7.1 Concepts of Bacterial Foraging theory
 - 3.7.2 Searching techniques for foraging
 - 3.7.3 Bacterial foraging of E. Coli
 - 3.7.4 E. Coli Bacterial Foraging for Optimization
 - 3.7.5 BFO Algorithm
- 3.8 References

3. Soft Computing Optimization Techniques

3.1 Evolutionary Algorithms (EA)

Nature has inspired researchers in many ways. Airplanes have been designed based on the structures of birds' wings. Movements of insects have been imitated and modeled to design robots. Resistant materials have been synthesized based on spider webs. It is interesting to learn how these tiny insects can find the shortest path, for instance between two locations without any knowledge about distance, linearity, etc. After millions of years of evolution all these species have developed incredible solutions for a wide range of problems. Genetic Algorithm, Simulated Annealing Algorithm, Evolution Strategy, Ant Colony optimization, Particle Swarm Optimization, Bacterial Foraging Algorithm are some of the bio-inspired algorithms. Biologically inspired systems have been gaining importance and it is clear that many other ideas can be developed by taking advantages of the examples that nature offers.

These evolutionary algorithms (EA) are randomized search procedures that mimic the process of natural evolution to solve optimization problems [1]. The representation of a solution is defined by the user and may be as simple as string of zeroes and ones or as complex as a computer program. The initial population may be created entirely at random or using some domain knowledge. The algorithm evaluates the individuals to determine how well they solve the problem at hand with an objective function. This objective function is unique to each problem and is defined by the programmer. The process of optimization is to search the values for a set of parameters that maximize or minimize a given objective function subject to certain constraints [2]. This thesis aims at the minimization of the objective function. The minimization of an objective function is defined as:

Given $f: S \rightarrow \mathbb{R}$ where $S \subseteq \mathbb{R}^{N_d}$ and N_d is the dimension of the search space S , we need to find

$$x^* \in S \text{ such that } f(x^*) \leq f(x), \forall x \in S.$$

The variable x^* is called the global minimizer of f and $f(x^*)$ is called the global minimum value of f . The process of finding the global optimal solution is known as global optimization.

The individuals with better performance are selected into a mating pool to serve as parents of the next generation of individuals. EAs create new individuals using simple randomized operators that are inspired by recombination (crossover) and mutation in natural organisms. The new solutions are evaluated, and the cycle of selection and creation of new individuals is repeated until a satisfactory solution is found or a predetermined time limit elapses.

3.2 Swarm Intelligence (SI)

Swarm Intelligence (SI) is the property of a system whereby the collective behaviors of entities interacting locally with their environment cause functional global patterns to emerge. SI provides a basis with which it is possible to explore collective (or distributed) problem solving without centralized control or the provision of a global model. The famous bio-inspired computational algorithms known as ACO (*Ant Colony Optimization* algorithm [3-11]), and PSO (*Particle Swarm Optimization* [12-15]), BFO (*Bacterial Foraging Optimization* [16]) are just some among many successful examples. Flocks of migrating birds and schools of fish are similar examples of spatial self organized patterns formed by living organisms through social foraging. Such aggregation patterns are observed not only in colonies of organisms as simple as single-cell bacteria, as interesting as social insects like ants and termites as well as in colonies of multi-cellular vertebrates as complex as birds and fish but also in human societies [17]. Wasps, bees, ants and termites all make effective use of their environment and resources by displaying collective “swarm” intelligence. For example, termite colonies build nests with a complexity far beyond the comprehension of the individual termite, while ant colonies dynamically allocate labor to various vital tasks such as foraging or defense without any central decision-making ability [18, 19]. Slime mould is another example. These are very simple cellular organisms with limited

motile and sensory capabilities, but in times of food shortage they aggregate to form a mobile slug capable of transporting the assembled individuals to a new feeding area. If food shortage persists, they then form a fruiting body that disperses their spores using the wind, thus, ensuring the survival of the colony [19, 20, 21]. New research suggests that microbial life can be even richer, highly social, intricately networked, and with more interactions [22]. Bassler [23] and other researchers have determined that bacteria communicate using molecules comparable to pheromones. By tapping into this cell-to-cell network, microbes are able to collectively track changes in their environment, communicate with their own species, build mutually beneficial alliances with other types of bacteria, gain advantages over competitors, and communicate with their hosts. Eshel Ben-Jacob [24] indicate that bacteria have developed intricate communication capabilities to cooperatively self-organize into highly structured colonies with elevated environmental adaptability, proposing that they maintain linguistic communication. Eshel [25,26] argues that colonies of bacteria are able to communicate and even alter their genetic makeup in response to environmental challenges, asserting that the lowly bacteria colony is capable of computing better than the best computers, and attributes them properties of creativity, intelligence, and even self-awareness. Wilson [27] showed that ants emit specific pheromones and identified the chemicals, the glands that emitted them and even the fixed action responses to each of the various pheromones. The pheromone signals that each ant sends out to other ants enable the ant community [28] as a whole to find the most abundant food sources. Some other authors also defend this self-organizing realm into brain function [29, 30].

All these above mentioned aspects show that the study of social foraging is vital for the development of distributed search algorithms, and the construction of social cognitive maps, with interesting properties in collective memory, collective decision-making and swarm pattern detection.

3.3 Particle Swarm Optimization Algorithm (PSO)

PSO [35 - 39] is an exciting new methodology in evolutionary computation. This population based stochastic optimization technique has been developed by Dr. Russel C Eberhart & Dr. James Kennedy in 1995, and is inspired by social behavior of bird flocking or fish schooling [40]. This is an adaptive algorithm where the population of individuals (particles) adapts by returning stochastically towards previously successful regions [41]. In this algorithm, an objective function is optimized by undertaking a population based search. It suffers from the problem of premature convergence. Usually, the quality of the solutions can not be improved even if the number of iterations is increased.

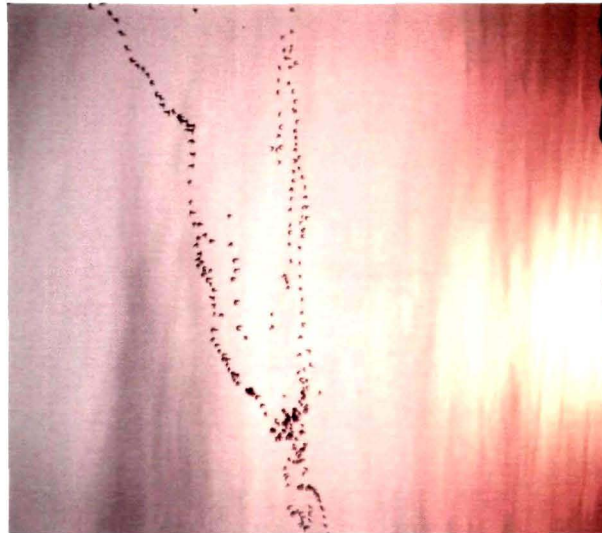


Figure 3.1. Flocking of birds.

3.4 Genetic Algorithm (GA)

It is a search algorithm based on the conjuncture of natural selection and genetics [31]. It is in the early 1970's that Holland and his student presented the first work [32] on Genetic Algorithm but it is only in 1980s that the real coded GA came up [33] into light. The characteristics of GA are different from other techniques. Firstly, this algorithm follows a multi-path to search many peaks in parallel and hence reduces the possibility of local minimum trapping. Secondly,

GA works with a coding of parameters instead of the parameters themselves. The coding of the parameter in turn helps the genetic operator to evolve the current state into the next state with minimum computations [34]. Thirdly, GA evaluates the fitness of each string to guide its search instead of the optimization function. GA only needs to evaluate objective function to guide its search and doesn't need any derivative or other auxiliary knowledge. GA have been very popular in academia and the industry mainly because of its intuitiveness, ease of implementation, and the ability to effectively solve highly nonlinear, mixed integer optimization problems that are typical of complex engineering systems

3.5 Bacterial Foraging Algorithm (BFO)

Social foraging capabilities have also been a source of inspiration to some authors in the area of distributed Optimization and Control. Based on the biology and physics underlying the foraging behavior of *E. coli* bacteria, Passino and Liu [42-44] exploit a variety of bacterial swarming and social foraging behaviors, discussing how the control system on the *E. Coli* dictates foraging should proceed.

By parallel search, BFO can check various regions of search space at a time. So, BFO is less sensitive to local minima. Yet another important aspect of BFO is its manipulation of representation of potential solution rather than the solution itself. BFO does not require a complete understanding of the system or the model.

Foraging strategies are methods for locating, handling and ingesting food by an organism. Animals with a poor foraging strategy are eliminated in due course of time and animals with better foraging strategies are naturally selected to propagate their genes for their next generation success [45-48]. Since a foraging organism/animal takes actions to maximize the energy utilized per unit time spent foraging, considering all the constraints presented by its own physiology, such as sensing and cognitive capabilities and environmental parameters (e.g., density of prey, risks from predators. physical characteristics of the search area), natural evolution could lead to optimization. It is essentially this idea that could be applied to complex optimization problems. The optimization problem search space could be modeled as a social

foraging environment where groups of parameters communicate cooperatively for finding solutions to difficult engineering problems [49].

3.6 Critical Analysis of these techniques

The Genetic algorithm [50] is an optimization process based on recent evolutionary search technique. This method has attracted researches in the recent past. The main advantage of Genetic algorithm lies in the fact that it does not depend on methods like Newton's gradient-descent algorithm, sparing the programmer from the need for calculation of derivatives. As real life problems are not only multi-modal but also distorted due to the superimposed noise, Genetic algorithm is quite effective. Genetic algorithm can explore many regions of search space simultaneously and find out global minima. Yet another important aspect of Genetic algorithm is their manipulation of the representation of a potential solution, rather than the solution itself.

Though GA offers good solution to various problems, it suffers from its limitations. It has the problem of getting trapped in local minimum. In Genetic algorithm [51], local minima are avoided by operations like crossover and mutation between the chromosomes. Since there are only two parameters to operate on, there is still possibility of getting trapped in local minima. Its convergence time is rather slow [47]. Besides, it needs random creation of initial population and also randomness of exploration. The quality of solution is dictated by the choice of initial population which limits the generalization capability of GA. Another drawback of GA is its expensive computational cost.

The main difference between the PSO approaches as compared to GA is that PSO does not have genetic operators such as crossover and mutation [52]. Particles update themselves with internal velocity; they also have a memory that is important to the algorithm. The information sharing mechanism in PSO is significantly different [53], as compared to other evolutionary programming. In PSO the best particle gives out the information to others. As compared to GA,

PSO is easy to implement and there are few parameters to adjust [54]. The PSO has the same effectiveness (for finding the true global optimal solution) as GA but with significantly better computational efficiency (less function evaluations). In paper [55], a performance comparison between GA and PSO is shown based on a set of benchmark test problems as well as two space systems design optimization problems. The search efficiency in PSO increases due to the computation of two stage transformation of the objective function. This eliminates the local minima and elevates the neighbourhood of the local minima [50].

Bacterial Foraging Optimization that has been proposed recently [51] uses more parameters for searching as compared to Genetic algorithm. The BFO is a useful alternative to GA. In addition BFO is also derivative free optimization technique [56]. The number of parameters that are used for searching the total solution space are much higher in BFO compared to those in GA. Searching for an optimal solution through more parameters in the search domain reduces the chances of getting trapped in local minima. This search and optimal foraging of bacteria have been used for solving optimization problems [57]. Bacterial Foraging Optimization does not focus on single high quality solution [58]. Its convergence is fast as compared to the other two. Its focus is mainly on cost function. However, many researchers have tried to use a combination code of GA-BFO for their optimization problems [49, 63]. So, in this thesis work, the problem of image enhancement by the optimization of signal quality is solved by using Bacterial Foraging Theory.

3.7 Details of Bacterial foraging theory

3.7.1 Concepts of Bacterial foraging theory

Foraging theory is based upon the assumption that organizational animals search and gather those nutrients such that it maximizes their intake of energy per unit time. So, if E is the long term average energy intake, then, bacteria aims at maximizing the function E/T .

This foraging strategy is different for different species of animals. Herbivores find food easily and in abundance. But they need to eat a lot of food to gain the required energy level. Carnivores, on the other hand, have difficulty in finding their food but as their food has high energy content, a little food gives them their required energy intake.

The environmental factors like distance between two pieces of food impose several constraints on obtaining the food. The prey may be mobile which indicates that it needs to be chased. Added to this, are the risks factors due to predators, psychological characteristics of the animal or organism that makes the foraging process a complex one. So, the optimal foraging theory mainly finds a solution subject to the constraints like physiological (eg. sensing and cognitive capabilities) and environment (eg. the density of prey, risks from predators, the physical characteristics of the search area).

Usually, if a bacterium finds a region that has less nutrient than if it expects a better region (nutrient rich) then the bacteria considers all the risks and efforts to find another region. Again, if a bacterium has extracted nutrient for some time in a particular region, it can start to deplete its own resources. So, there should be a time to leave the nutrient region and venture out to find a new richer region. On one hand, a bacterium does not want to waste the readily available resources but on the other hand, it does not want to waste time in extracting the nutrients with diminishing energy returns. This foraging theory is modeled for optimal solution using dynamic programming.

3.7.2 Searching techniques for foraging

The process of search and optimal foraging decision-making of animals can be broken into three basic types :

- A. Cruise (eg., tuna fish, hawks),
- B. Saltatory (eg. , birds, fish, lizards, and insects)
- C. Ambush (eg., rattle snakes, lions)

In a cruise search, the animal searches the perimeter of a region; in an ambush it halts and waits for a suitable moment; and in saltatory search, an animal moves in

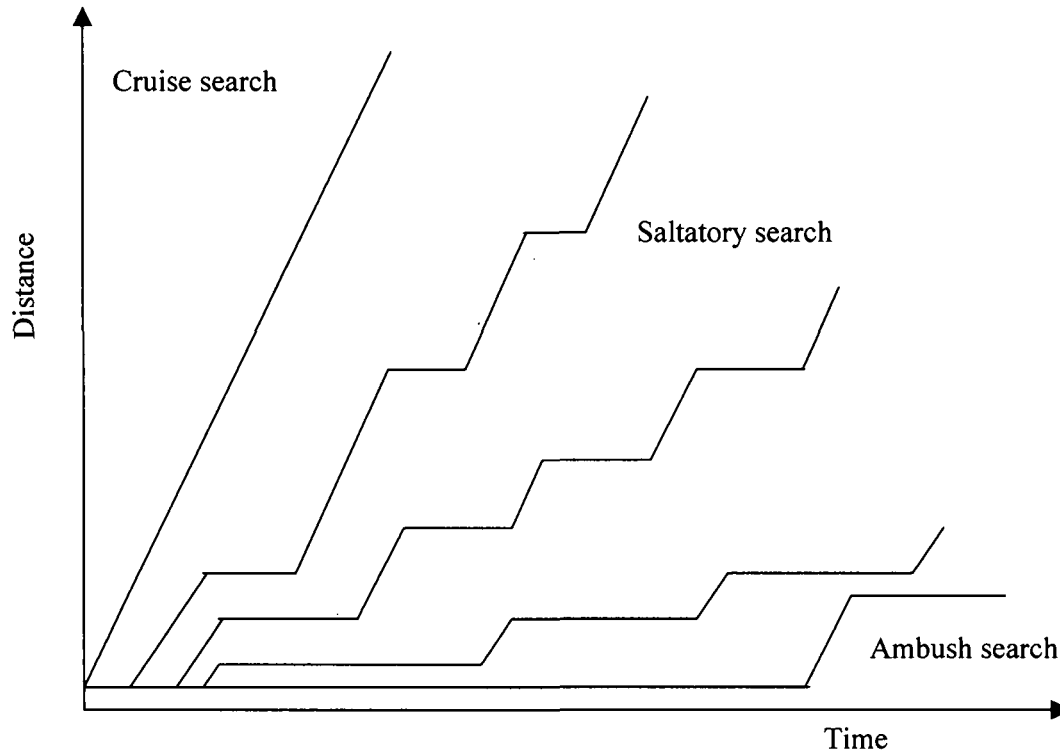


Figure 3.2. Different types of Search for foraging (figure drawn from [2]).

one direction, stops or slows looks around, and then changes direction. These strategies are illustrated by the above figure, fig2.2.

3.7.3 E. Coli Bacteria's foraging

In this work, the foraging of Escherichia coli (E.Coli) bacterium is considered. The E. Coli bacterium is a very common and probably the best understood microorganism. It lives in the gut of human intestine and has a plasma membrane, cell wall, and a capsule that contains the cytoplasm and nucleoid. With a diameter of $1\mu\text{m}$, and a length of around $2\mu\text{m}$, it can reproduce in 20 min. It moves with the help of its

flagella. It has a set of upto six flagella that spins at a rate of 100-200 rps, each driven by a biological motor.

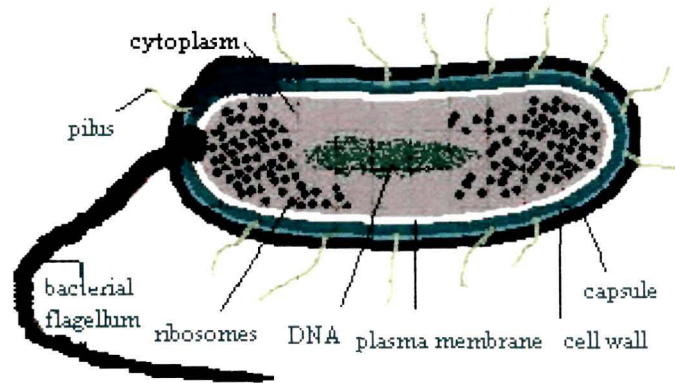


Figure 3.3. An E. Coli bacterium.

Chemotaxis, Swarming, Reproduction, Elimination & Dispersal

Bacteria move with the help of its relatively rigid flagella. An E. coli bacterium alternates between running (at 10-20 $\mu\text{m}/\text{sec}$, they cannot swim straight) and tumbling (changing direction). Each flagellum is a left-handed helix configured so that as the base of the flagellum (ie., where it is connected to cell) rotates counterclockwise (as viewed from the end of the flagellum to the cell), it produces a force against the bacterium so it pushes the cell. So, rotation of the flagella in clockwise or counterclockwise direction acts as propellers and hence an E.coli runs or tumbles.

Following are the chemotactic actions:

- i) if the medium is neutral, the bacteria alternates between tumbles and runs. its action could be similar to search.
- ii) If it swims up a nutrient gradient or is out of noxious substance, it swims longer. That is it climbs up the nutrient gradient or down noxious gradient. Its behavior seeks increasingly favorable environments.

iii) If it swims down a nutrient gradient or climbs up to a noxious substance gradient, then it searches. The search action is like avoiding an unfavorable environment.

Therefore, it follows that the bacterium can climb up nutrient hills and at the same time avoids noxious substances. The sensors it needs for optimal resolution are receptor proteins, which are very sensitive and possess high gain. That is, a small change in the concentration of nutrients can cause a significant change in behavior. This is probably the best-understood sensory and decision-making system in biology [59].

Bacteria are often killed and dispersed and this can be viewed as part of their motility. Mutations in *E. Coli* affect, e.g., the reproductive efficiency different temperatures, and occur at a rate of about 10^{-7} per gene and per generation. *E. Coli* occasionally engages in a type of sex called conjugation that affects the characteristics of a population of bacteria [60]. There are many types of taxes that are used by bacteria. For instance, some bacteria are attracted to oxygen (aerotaxis), light (phototaxis), temperature (thermotaxis), or magnetic lines of flux (magnetotaxis). Some bacteria can change their shape and number of flagella based on the medium to reconfigure so as to ensure efficient foraging in a variety of media. *E. Coli* can form intricate stable spatio-temporal patterns in certain semisolid nutrient media [60]. Under certain conditions, they will secrete cell-to-cell attractant signals so that they will group and protect each other. These bacteria can swarm and bring favorable results.

3.7.4 Bacterial foraging optimization.

Here, the basic goal is to find the minimum of $J(\theta)$, $\theta \in R^P$, where $J(\theta)$ is the cost function.

When we do not have the gradient $J(\theta)$ suppose that is the position of a bacterium, and $J^{icc}(\theta)$ represents an attractant-repellant profile [60, 51] i.e., it represents where nutrients, noxious substances are located, so $JF0$, $JG0$, $JH0$

represent the presence of nutrients, a neutral medium, and the presence of noxious substances, respectively [61].

$$\text{Let } P(j, k, l) = \{\theta^i(j, k, l) / i = 1, 2 \dots S\} \dots \dots \dots \quad 3.1$$

represent the positions of each member in the population of the S bacteria at the j th chemo tactic step, k th reproduction step, and l th elimination-dispersal event [47].

Let $J(i, j, k, l)$ denote the cost at the location of the i th bacterium $J(\theta), \theta \in R^P$

Let N_c be the length of the lifetime of the bacteria as measured by the number of chemotactic steps. To represent a tumble, a unit length random direction, say $\phi(j)$, is generated; then, we let

$$\theta^i(j+1, k, l) = \theta^i(j, k, l) + C(i)\phi(j) \dots \dots \dots \quad 3.2$$

so that $C(i) > 0$ is the size of the step taken in the random direction specified by the tumble. If at $\theta^i(j+1, k, l)$, the cost $J(i, j+1, k, l)$ is better (lower) than at $\theta^i(j, k, l)$, then another Chemotactic step of size $C(i)$ in this same direction [51] will be taken and repeated up to a maximum number of steps N_s . Let d_{attract} be the depth of the attractant released by the cell, and let w_{attract} be a measure of the width of the attractant signal [47]. Cell repels another one via local consumption, and cells are not food for each other. Let

$$h_{\text{repellant}} = d_{\text{attract}}$$

be the height of the repellant effect (magnitude), and let $w_{\text{repellant}}$ be a measure of the width of the repellant [48]. Then, we may use functions, $J^{icc}(\theta)$, $i=1, 2 \dots S$, to model the cell-to-cell signaling via an attractant and a repellant.

Let

$$J_{cc}(\theta) = \sum_{i=1}^S J^{icc} = \sum_{i=1}^S [-d_{\text{attract}} \exp(-w_{\text{attract}} \sum_{j=1}^p (\theta_j - \theta_j^i)^2)] \quad 3.3$$

where

$$\theta = [\theta_1 \dots \dots \dots \theta_p]^T, \text{ is a point on the optimization domain.}$$

The expression of $J_{cc}(\theta)$ implies that its value does not depend on the nutrient

concentration at position θ , actually, it is reasonable to assume that the depth of the chemical secreted by a bacterium is affected by environment i.e., a bacterium with high nutrient concentration will secrete stronger attractant than one with low nutrient concentration [62]. Let the function $J_{ar}(\theta)$ represent the environment-dependent cell-to-cell signaling [60].

Let

$$J_{ar}(\theta) = \exp(M - J(\theta)J_{cc}(\theta)) \dots 3.4$$

where M is a tunable parameter. Then, swarming needs minimization of

$$J(i, j, k, l) + J_{ar}(\theta)(\theta^i(j, k, l)) \dots 3.5$$

so that the cells try to find nutrients, avoid noxious substances, and at the same time try to move toward other cells, but not too close to them [60]. The function

$J_{ar}(\theta)(\theta^i(j, k, l))$ implies that, with M being constant, the smaller $J(\theta)$, the larger $J_{ar}(\theta)$ and thus the stronger attraction. In tuning the parameter M , it is normally found that [60], when M is very large, $J_{ar}(\theta)$ is much larger than $J(\theta)$ and thus the profile of the search space is dominated by the chemical attractant secreted by E. Coli. On the other hand, if M is very small, $J_{ar}(\theta)$ is much smaller than $J(\theta)$ and it is the effect of the nutrients that dominates. After N_c chemotactic steps, a reproduction step is taken. Suppose there are N_r reproduction steps. For reproduction, the healthiest bacteria (the ones that have the lowest accumulated cost over their lifetime) split, and the same number of unhealthy ones are killed (hence, we get a constant population size). Let N_{ed} be the number of elimination-dispersal events and, for each elimination-dispersal event [62], each bacterium in the population is subjected to elimination-dispersal (death, then random placement of a new bacterium at a random location on the optimization domain) with probability ped [60, 62].

Bacterial Patterns

The nutrient map is constructed by summing up several gaussian functions with different magnitude and variance [60]. The contour plots of the map are shown in fig 3.4. Nutrient concentration function in the contour map (shown on Fig. 3.4), has a zero value at $[15,15]^T$ and decreases to successively more negative values as we move away from that point; hence, the cells tend to swim away from the peak.

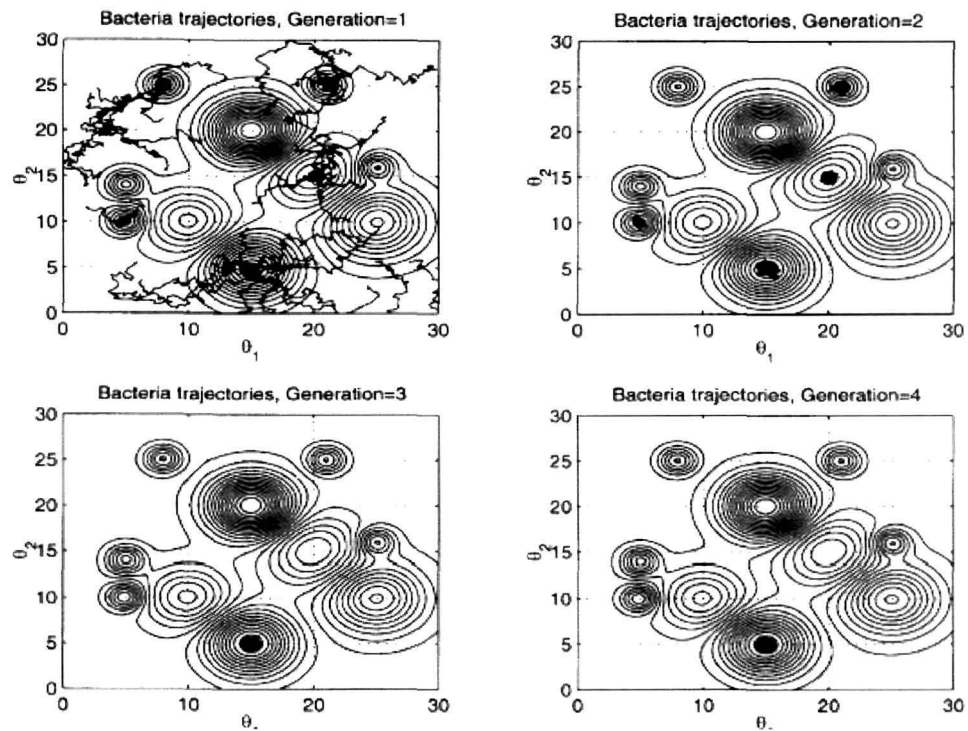


Figure 3.4 Foraging of E. coli with Reproduction, Elimination and Dispersion: Contour Plot [16].

In this example, reproduction, elimination, and dispersal of E. Coli is included and the roles which these processes play in the E. Coli evolution is demonstrated [43]. In the simulation, we choose $N_{re}=4$ and $N_{ed}=2$, which means that, during the simulation, E.Coli evolve four generations and experience elimination and dispersal event once, respectively. Initially, the bacteria are distributed randomly over the nutrient map.

In Fig.3.4, the first generations of *E. coli* are moving around to search for places with a better nutrient concentration, as shown by those curvy trajectories on the contour plot. In the second generation, almost all the bacteria have found such places, though all of them are not global optimal points [60]. With evolution, all in the third generation find the position on the map with the best nutrient concentration, and the fourth generation stays there firmly. Simulation results in Fig. 3.5 are a continuation of Fig. 3.4, but an elimination and dispersal process happens in between. In Fig. 3.5, some bacteria of the first generation appear in some bad positions. But after

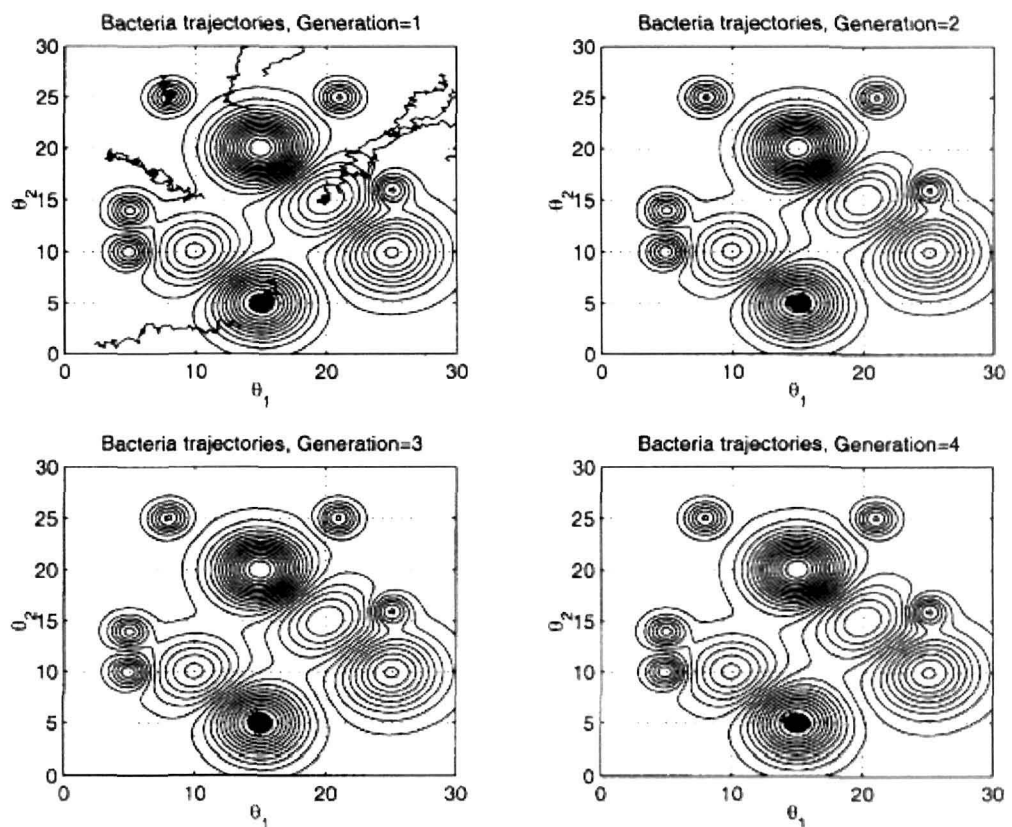


Figure 3.5 Foraging of *E. Coli* with Reproduction, Elimination and Dispersion: contour plot after Elimination and Dispersion[16].

reproduction, almost all of the *E. Coli* locates the global optimal position quickly and stays there from the second generation. In the above example, it is assumed that the nutrient map is noise-free [60]. But in reality, the environment is always noisy, which generally will prevent the individual bacterium from finding the optimal position. In next, by secreting chemicals, *E. Coli* may swarm and

perform social foraging. As a result, the bacteria may overcome the noise trap and pull each other into the optimal position [60]. In this case, a simple noise-contaminated quadratic nutrient profile with contour map shown on Fig.3.4. The profile has the best nutrient concentration at $[15, 15]^T$. The Bacterial pattern is seen 300 steps. Figure 3.6 demonstrates the results when no chemical-attractant-induced swarming is present. Specifically, it shows the positions of the bacteria on certain chemotactic steps, where each + in the plots represents a bacterium.

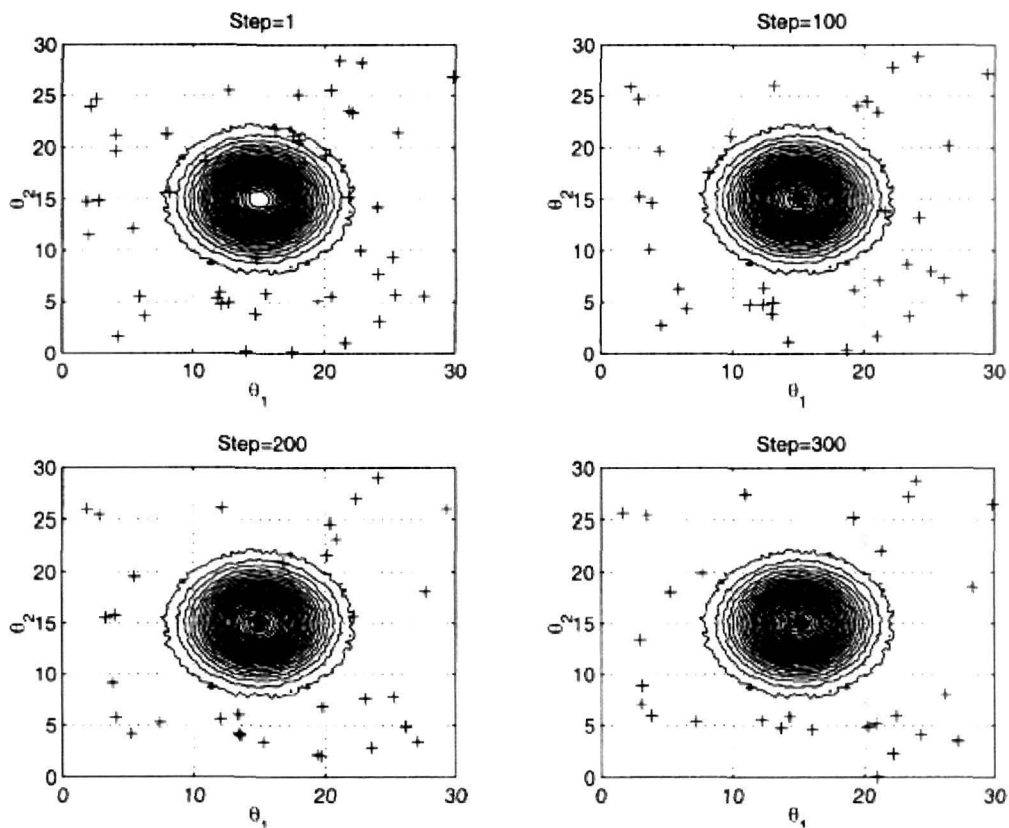


Figure 3.6 Foraging of E. Coli in a noisy environment: Bacteria positions at different Chemotactic steps (without cell-to-cell attractant)[16].

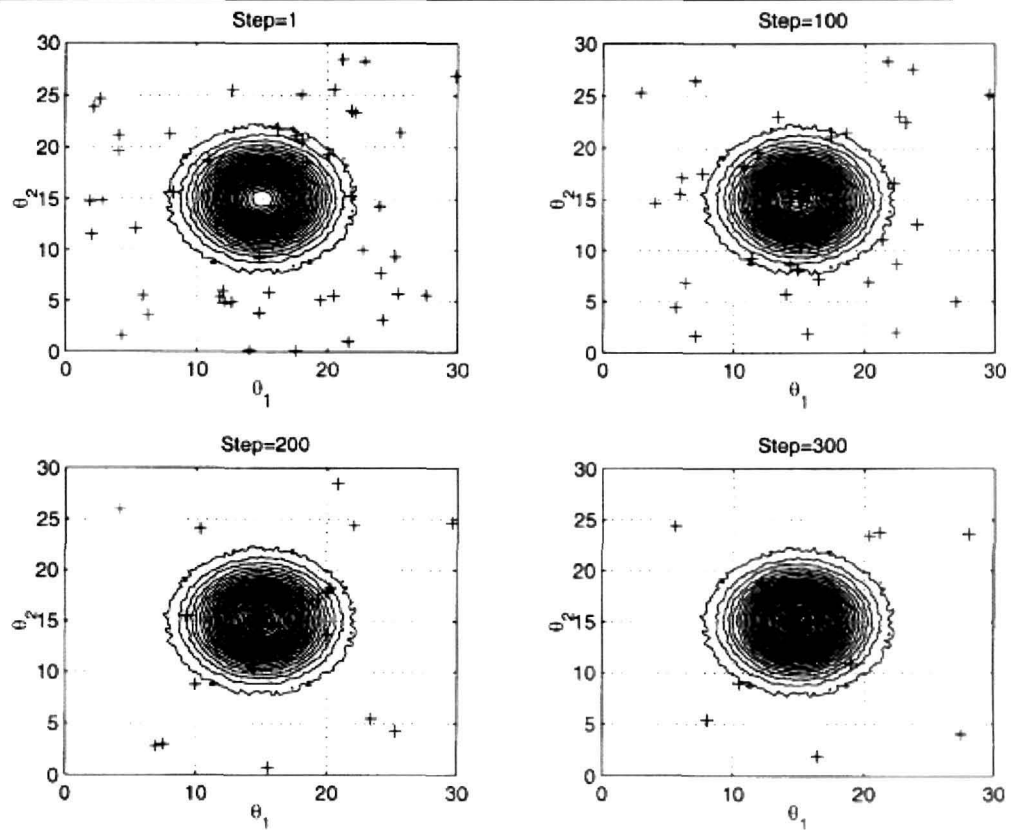


Figure 3.7. Foraging of E.coli in a noisy environment: Bacteria positions at different chemotactic steps(with cell to cell attractant).

bacteria fail to find the optimal point even at step 300. Figure 3.7 demonstrates the results when attractant exists. It is clear that, by performing social foraging, E. Coli have better chance in locating the optimal point in a noisy environment

3.7.5 BFO Algorithm

In the first step of the BFO algorithm, p , S , N_c , N_s , N_{re} , N_{ed} , P_{ed} and the $C(i)$, $i=1,2,\dots,N$ are initialized. Swarming includes cell-to-cell attractant function; the parameters chosen above can be used to define the function. θ_i , for $i=1,2,\dots,S$ are also chosen. It is to be noted that any changes to θ_i automatically changes P .

1. Elimination and dispersal loop: $l=l+1$.

2. Reproduction loop: $k=k+1$.

3. Chemotaxis loop: $j=j+1$.

i) for $i=1,2,\dots,S$, a chemotactic step for bacterium i is taken as follows:

ii) Compute $J(i,j,k,l)$. Let $J(i,j,k,l) = J(i,j,k,l) + J_{cc}(\theta_i(j,k,l), P(j,k,l))$

[effect of cell to cell attractant to the nutrient concentration is added]

iii) Let $J_{last}=J(i,j,k,l)$ [this value is saved as we expect to find a better cost via a run].

iv) **Tumble** : A random vector $\Delta(i) \in \mathfrak{R}^p$ with each element $\Delta_m(i)$, $m=1,2,\dots,p$, a random number on $[-1,1]$.

v) **Move**: Let $\theta_i(j+1,k,l) = \theta_i(j,k,l) + C(i) \frac{\Delta(i)}{\sqrt{\Delta^T(i)\Delta(i)}}$

This moves the bacterium with a step size $C(i)$ in the direction of the tumble.

vi) Compute $J(i, j+1, k, l)$ and then find $J(i, j+1, k, l) = J(i, j+1, k, l) + J_{cc}(\theta_i(j,k,l), P(j,k,l))$.

vii) **Swim** : (here, some approximation is used)

A. Let $m=0$ [this is the counter for swim length].

B. While $m < N_c$,

a. let $m=m+1$.

b. If $J(i,j+1,k,l) < J_{last}$ [if it is doing better]. Let $J_{last} = J(i,j+1,k,l)$ and let

$\theta_i(j+1,k,l) = \theta_i(j+1,k,l) + C(i) \frac{\Delta(i)}{\sqrt{\Delta^T(i)\Delta(i)}}$

This $\theta_i(j+1,k,l)$ is used to compute the new $J(i,j+1,k,l)$.

c. Else, let $m=N_s$. While statement ends here.

viii) Try the next bacterium $(i+1)$ if $i \neq S$. [this implies, go to ii)].

4. If $j < N_c$, go to step 3. Here, chemotaxis is continued as the life of the bacteria is not over.

5. Reproduction:

i) For the given k and l , and for each $i=1,2,\dots,S$, let

$$J_{health}^i = \sum_{j=1}^{N_c+1} J(i,j,k,l)$$

be the health of bacterium i (a quantitative measure of the total nutrient collected over the entire lifetime and to what extent it could avoid the noxious substances). The bacteria and the chemotactic $C(i)$ parameters are sorted in order of ascending cost J_{health} [higher cost indicates lower health].

ii) The bacteria with the highest J_{health} values die and the bacteria with the best values are split into two and are placed in the same location as that of the parent bacteria.

6. If $k < N_{\text{re}}$, go to step 2. The next generation chemotactic step is started and this continues till all the generations are completed.

7. **Elimination-dispersal:** For $i=1,2,\dots,S$ with probability p_{ed} , eliminate and disperse each bacteria to keep each bacteria in the population constant.

8. If $l < N_{\text{ed}}$, then go to step 1; otherwise end.

3.8 References

- [1]. Erick Cant'ú-Paz and Chandrika Kamath "An Empirical Comparison of Combinations of Evolutionary Algorithms and Neural Networks for Classification Problems", IEEE Transaction on system, man and cybernetics, Part-B, Cybernetics, pp. 915-927, 2005.
- [2]. VOSE MICHAEL D. The Simple Genetic Algorithm — Foundations And Theory, Prentice Hall of India.
- [3]. Dorigo M, Blum C, "Ant colony optimization theory: A survey", Theoretical Computer Science, vol. 344, pp. 243-278, 2005.
- [4]. Dorigo M, Gambardella LM, "Ant Colonies for the Traveling Salesman Problem" BioSystems, vol. 43, pp. 73-81, 1997.
- [5]. Dorigo M, Bonaneau E, Theraulaz G, "Ant algorithms and stigmergy", Future Generation Computer Systems, vol. 16, pp. 851-871, 2000.
- [6]. Caro GD, Dorigo M, "Ant Net Distributed stigmergetic control for communications networks", Journal of Artificial Intelligence Research, vol. 9, pp. 317-365, 1998.
- [7]. Dorigo M, Caro GD, Gambardella LM, "Ant algorithms for discrete optimization", Artificial Life, vol. 5, no. 2, 137-172, 1999.

-
- [8]. Dorigo M, Bonabeau E, Theraulaz G, "Ant algorithms and stigmergy" Future Generation Computer Systems, vol. 16, no. 8, pp. 851-871, 2000.
- [9]. Dorigo M, Caro GD, "The ant colony optimization metaheuristic, New Ideas in Optimization, D. Corne, M. Dorigo, and F. Glover, Eds. New York: McGraw-Hill, Springer Annals of operations Research, col. 140, No. 1, pp. 189-213, November, 2005.
- [10]. Dorigo M, Stutzle T. The ant colony optimization metaheuristic: Algorithms, applications, and advances, Handbook of Metaheuristics, F. Glover and G. Kochenberger, Eds. Norwell, MA: Kluwer, 2002.
- [11]. Dorigo M, Maniezzo V, Colomi "A Positive Feedback as a Search Strategy, Dipartimento Elettronica, Politecnico Milano", Italy, Tech. Rep. 91-016, 1991.
- [12]. Eberhart RC, Kennedy J, "A new optimizer using particle swarm theory", Proceedings of the Sixth International Symposium on Micromachine and Human Science, Nagoya, Japan, pp. 39-43, 1995.
- [13]. Eberhart RC, Shi Y, "Particle swarm optimization: developments, applications and resources" Proceedings of the IEEE Congress on Evolutionary Computation (CEC), Seoul, Korea, vol.1, pp. 81-86, 2001.
- [14]. Eberhart RC, Simpson PK, Dobbins RW. Computational Intelligence PC Tools, Boston, MA: Academic Press Professional, First Edition, 1996.
- [15]. Kennedy, J. Eberhart, Russel C. and Shi, Y., *Swarm Intelligence*, Academic Press, Morgan Kaufmann Publ., San Diego, London, 2001.
- [16]. Passino KM, *Biomimicry for Optimization, Control, and Automation*, Springer-Verlag, London, UK, 2005.
- [17]. Farmer, J.D., "A Rosetta Stone for Connectionism", in S. Forrest (Ed.), *Emergent Computation*, Cambridge, MA: The MIT Press, 1991.
- [18]. Bonabeau, E., Dorigo, M., Theraulaz, G., *Swarm Intelligence: From Natural to Artificial Systems*, Santa Fe Institute in the Sciences of Complexity, Oxford Univ. Press, New York, Oxford, 1999.
- [19]. Williams, H., *Spatial Organisation of a Homogeneous Agent Population using Diffusive Signalling and Role Differentiation*, MSc Evolutionary & Adaptive Systems Thesis, COGS, Univ. of Sussex, UK, Sept. 2002.
-

-
- [20]. Maree, A.F.M., Hogeweg, P., "How Amoeboids Self-Organize into a Fruiting Body: Multicellular Coordination in *Dictyostelium discoideum*", PNAS, vol. 98, no. 7, pp. 3879-3883, 2001.
- [21]. Savill, N.J., Hogeweg, P., "Modelling Morphogenesis: From Single Cells to Crawling Slugs", J. Theor. Biology, vol. 184, pp. 229-235, 1997.
- [22]. Silberman, S., "The Bacteria Whisperer", *Wired*, 11-04, pp. 104-108, April 2003.
- [23]. Bassler, B.L., "Small Talk: Cell-to-Cell Communication in Bacteria", *Cell*, vol. 109, pp. 421-424, May 2002.
- [24]. Ben-Jacob, E., Becker, I., Shapira, Y., Levine, H., "Bacterial Linguistic Communication and Social Intelligence", *Trends in Microbiology*, vol. 12, no.8, pp. 366-372, 2004.
- [25]. Ben-Jacob, E., Shochet, O., Tenenbaum, A., Cohen, I., Czirók, A., Vicsek, T., "Generic Modelling of Cooperative Growth in Bacterial Colonies", *Nature*, 368, pp. 46-49, 1994.
- [26]. Ben-Jacob, E., "Bacterial Wisdom, Gödel's Theorem and Creative Genomic Webs", *Physica A*, 248, pp. 57-76, 1998.
- [27]. Wilson, E.O., *The Insect Societies*, Cambridge, MA., Belknap Press, 1971.
- [28]. Chialvo, D.R., Millonas, M.M., "How Swarms build Cognitive Maps", In Steels, L. (Ed.): *The Biology and Technology of Intelligent Autonomous Agents*, 144, NATO ASI Series, pp. 439-450, 1995.
- [29]. Hofstadter, D.R., *Gödel, Escher, Bach: An Eternal Golden Braid*, New York: Basic Books, 1979.
- [30]. Kennedy, J. Eberhart, Russel C. and Shi, Y., *Swarm Intelligence*, Academic Press, Morgan Kaufmann Publ., San Diego, London, 2001.
- [31]. Gen, M. and Chang, R., *Genetic Algorithms and Engineering Optimization*, John Willey and Sons, New York, 2000.
- [32]. Holland H J., *Adaptation in Natural and Artificial Systems, an introductory analysis with applications to Biology, Control and Artificial Intelligence*, The University of Michigan Press, Ann Arbor, USA, 1975.
- [33]. Anders Angantyr, "Rotordynamic Optimizations of Large Turbo Systems using Genetic Algorithms", Doctoral Thesis, March 2006.
- [34]. Goldberg DE., *Genetic Algorithm in search, optimization and Machine Learning in Addison Wesley*, 1989.
-

-
- [35]. Kennedy J, Eberhart RC., "Particle Swarm Optimization" Proceedings of IEEE International Conference on Neural Networks, Perth, Australia, IEEE Service Center, Piscataway, NJ, vol. IV, pp. 1942-1948, 1995.
- [36]. Kennedy J "The Behavior of Particles", Proceedings of 7th Annual Conference on Evolutionary Programming, San Diego, USA, 1998.
- [37]. Kennedy J, "The Particle Swarm: Social Adaptation of Knowledge", Proceedings of IEEE International Conference on Evolutionary Computation, Indianapolis, Indiana, IEEE Service Center, Piscataway, NJ, pp. 303-308, 1997.
- [38]. Kennedy J. "Thinking is social: Experiments with the adaptive culture model", *Journal of Conflict Resolution*, vol. 42, pp. 56-76, 1992.
- [39]. Kennedy J, Eberhart R, *Swarm Intelligence*, Morgan Kaufmann Academic Press, 2001.
- [40]. Kennedy, J., and Eberhart, R. C. "Particle swarm optimization", *Proc. of IEEE International Conference on Neural Networks (ICNN)*, vol. IV, pp.1942-1948, Perth, Australia, 1995.
- [41]. Eberhart, R. C., and Kennedy, J. "A new optimizer using particle swarm theory" *Proceedings of the Sixth International Symposium on Micro Machine and Human Science*, Nagoya, Japan, 39-43, 1995.
- [42]. Y. Liu and K. M Passino "Biomimicry of social foraging bacteria for Distributed Optimization: models, principles, and emergent behavior," *Journal of optimization theory and applications*, vol.115, no. 3, pp. 603-628, December 2002.
- [43]. Kevin M. Passino "Distributed optimization and control using only a germ of intelligence", *Proceedings of the IEEE International Symposium on Intelligent Control*, pp.5-13, 2000.
- [44]. K.M. Passino, *Biomimicry of Bacterial foraging for Distributed Optimization*, University Press, Princeton, New Jersey, 2001.
- [45]. T.K.Das and G.K.Venayagamooorthy "Bio inspired algorithm for design of multiple optimal power system stabilizers: SPPSO and BFA," 41st IAS Annual Meeting. *Conference Record of the IEEE*, vol.2, pp. 635-641, Oct. 2006
-

-
- [46]. W.J.Tang and Q.H.Wu "Bacterial foraging for dynamic environments," IEEE Congress on Evolutionary Computation, Canada, pp. 1320-1330, July 16-21, 2006.
- [47]. S. Mishra "Hybrid least square-fuzzy bacterial foraging strategy for harmonic estimation", IEEE transactions on evolutionary computation, pp. 61-73, vol. 9, no. 1, February 2005.
- [48]. S. Mishra, B, K, Panigrahi, M. Tripathy "A hybrid adaptive-bacterial-foraging and feedback linearization scheme based d-statcom," International Conference on Power System Technology, vol. 1, Issue , 21-24, pp. 275-280, Nov.2004
- [49]. D.H. Kim, J.H. Cho, "Intelligent control of AVR system using GA-BF", Proceeding of KES 2005, Melbourne, Australia, Lecture Notes in Computer Science, vol. 3684/2005, pp. 854-860, 2005.
- [50]. R.S.Ramakrishana, Chang Wook Ahn "A genetic algorithm for shortest path routing and sizing of population," IEEE Transaction on Evolutionary Computation, pp. 566-578, vol-6, no.6, December 2002.
- [51]. S.Mishra, "Hybrid least-square adaptive bacterial foraging strategy for harmonic estimation" IEEE Proc.-Gener. Transm. Distribution, vol. 152, no. 3, pp. 379 - 389, May 2005.
- [52]. <http://www.ece.osu.edu/~passino/swarms.pdf>
- [53]. Eberhart, R. C. and Shi, Y. " Comparison between Genetic Algorithms and Particle swarm optimization" Evolutionary Programming VII: Proceedings of the Seventh Annual Conference on Evolutionary Programming, San Diego, CA, 1998.
- [54]. C R Mouser, S A Dunn "Comparing Genetic Algorithm and Particle swarm optimization for an inverse problem exercise", Journal of Austrian and New Zealand Industrial and Applied Mathematics Journal, vol. 46(E), pp. 89-101, 2005.
- [55]. Jakob Vesterstrom and Jacques Riget, "Particle Swarm Extensions for improved local, multimodel, and dynamic search in numerical optimization" A Master's Thesis, May 2002.
- [56]. Babita Majhi and G. Panda "Recovery of Digital Information Using Bacterial Foraging Optimization Based Nonlinear Channel Equalizers", 1st

-
- International Conference on Digital Information Management, pp. 367-372, Dec.2006.
- [57]. Vitorino Ramos, Carlos Fernandes, Agostinho C. Rosa “Social cognitive maps, swarm collective perception and distributed search on dynamic landscapes,” Journal of New Media in Neural and Cognitive Science, NRW, Germany, March 2005.
- [58]. S. Mishra, B, K, Panigrahi, M. Tripathy “A hybrid adaptive-bacterial-foraging and feedback linearization scheme based d-statcom,” International Conference on Power System Technology, vol. 1, Issue , 21-24 pp. 275-280, Nov.2004.
- [59]. Crina Grosan and Ajith Abraham “Stigmergic optimization: inspiration technologies and perspective”, Department of Computer Science Babes,-Bolyai University, Cluj Napoca, 3400, Romania 2IITA Professorship Program, School of Computer Science and Engineering Chung-Ang University, Seoul 156-756, Korea.
- [60]. K.M. Passino, “Biomimicry of bacterial foraging for distributed optimization and control”, IEEE Control Systems Magazine, pp. 52–67, 2002.
- [61]. Enrique Alba, J.Francisco Chicano “Evolutionary algorithm in the telecom” Evolutionary Computation, IEEE Trans. on vol.5, Issue4, pp.309–322, Aug 2001.
- [62]. Ahmed Jan, Masahito Yamamoto, Azuma Ohuchi “Evolutionary algorithm for nurse scheduling problem” Proceedings of the 2000 Congress on Evolutionary Computation, vol. 1, pp.196 – 203, 2000.
- [63]. Dong Hwa Kim , Ajith Abraham, Jae Hoon Cho, “A hybrid genetic algorithm and bacterial foraging approach for global optimization”, Elseviour International Journal of Information Sciences, vol. 177, pp. 3918–3937, 2007.

Chapter 4

Detection of Arrhythmia from ECG

4.1 Introduction

4.1.1 Electrocardiogram

4.1.2 Arrhythmia

4.2 Detection techniques - a literature survey

4.3 Proposed method

4.3.1 Conversion of an image into a graph

4.3.2 Segmentation of the ECG wave

4.3.3 Detection by Artificial Neural Network

4.3.4 Results

4.4 Conclusion

4.5 References

4. Detection of Arrhythmia from ECG

4.1 Introduction

The heart has four chambers called the left atrium, the left ventricle, the right atrium, and the right ventricle. After blood travels throughout the circulatory system it runs out of oxygen and must return to the heart through the right atrium. Then the blood moves to the right ventricle, where it is pumped to the lungs so it can be re-oxygenated. Once the blood is oxygenated, it goes to the left ventricle. The left ventricle then gives the blood a forceful push into the arteries. That powerful push stems from a high-pressure contraction of the heart.

There are dozens of risk factors for heart disease. Those cited most often by medical orthodoxy include high blood cholesterol, smoking, lack of exercise, stress and overweight. A high level of cholesterol in the blood is a mild risk factor for individuals with familial hyper-cholesterolemia (cholesterol levels chronically above 350 mg/dl) but for most of us, there is no greater risk of heart disease between cholesterol levels that are "high" (over 300 mg/dl) and those that are "low" (under 200 mg/dl) [1].

What Is Heart Disease?

Coronary Heart Disease (CHD) is not a single disease, but a complex of diseases of varied etiology [2]. Some of the recognized causes of heart disease include damage to the heart muscle or valves due to a congenital defect; or to inflammation and damage associated with various viral, bacterial, fungal, rickettsial or parasitic diseases. Rheumatic fever or syphilis can lead to heart disease, as can genetic or autoimmune disorders in which cellular proteins in the heart muscle are deranged or which disrupt enzymes affecting cardiac function. Inflammation may also cause blockages. The health and integrity of the blood vessel walls is another factor that must be considered.

A heart attack, which is also referred to by medical professionals as a myocardial infarction, is the deterioration and eventual death of heart muscle usually resulting from a blood clot suddenly blocking the coronary arteries [3]. When the coronary arteries are blocked, the heart can't get the blood it needs to

survive, nor can it get the oxygen that the blood normally carries to it from the lungs. If the flow of blood to the heart is not restored within about one half an hour, irreversible damage to the heart in the form of muscle death may begin to occur. Myocardial infarction (MI) was almost nonexistent in 1910 and caused no more than 3,000 deaths per year in 1930 in USA. Dr. Paul Dudley White, who introduced the electrocardiograph machine to America, stated the following during a 1956 American Heart Association televised fund-raiser: "I began my practice as a cardiologist in 1921 and I never saw an MI patient until 1928." By 1960, there were at least 500,000 MI deaths per year in the US. Rates of stroke have also increased and the cause is similar—blockage in the large arteries supplying the brain with blood [4]. In India, heart disease is the single largest cause of death in the country with heart attacks being responsible for one third of all deaths caused by heart diseases. According to a projection by the World Health Organization (WHO) and the Indian Council of Medical Research (ICMR), India will be the heart attack capital by 2020. Arrhythmias—abnormalities in the rhythm of the heart's pumping mechanism—can lead to interrupted blood flow, oxygen starvation of the heart muscle or complete shut down of the heart—the so-called cardiac arrest. Regulation of the nervous impulses that govern the heart depends on a large number of factors—from mineral status to the integrity of the myelin sheath.

4.1.1 Electrocardiogram (ECG)

The electrocardiogram (ECG) is a machine most widely used in the investigations in contemporary medicine. It is essential for the identification of disorders of the cardiac rhythm, extremely useful for the diagnosis of abnormalities of the heart (such as myocardial infarction), and a helpful clue to the presence of generalized disorders that affect the rest of the body too (such as electrolyte disturbances).



Figure.4.1. ECG machine.

ECG machine records the bioelectrical activity of the heart versus time. This machine also picks up the activity of other muscles, such as skeletal muscle, but it filters this out as much as possible. By convention, the main waves on the ECG are given the names P, Q, R, S, T and U (Fig. 4.6). Each wave represents depolarization (electrical discharging) or repolarization (electrical recharging) of a certain region of the heart. The ECG paper moves through the machine at a constant rate of 25 mm/s.

An ECG machine uses the information it collects via its four limb and six chest electrodes to compile a comprehensive picture of the electrical activity in the heart as observed from 12 different viewpoints. This set of 12 views, otherwise called 'leads' gives the 12-lead ECG its name. Each lead is given a name (I, II, III, aVR, aVL, aVF, V₁, V₂, V₃, V₄, V₅, and V₆) [44] and its position on a 12 lead ECG is usually standardized to make pattern recognition easier.

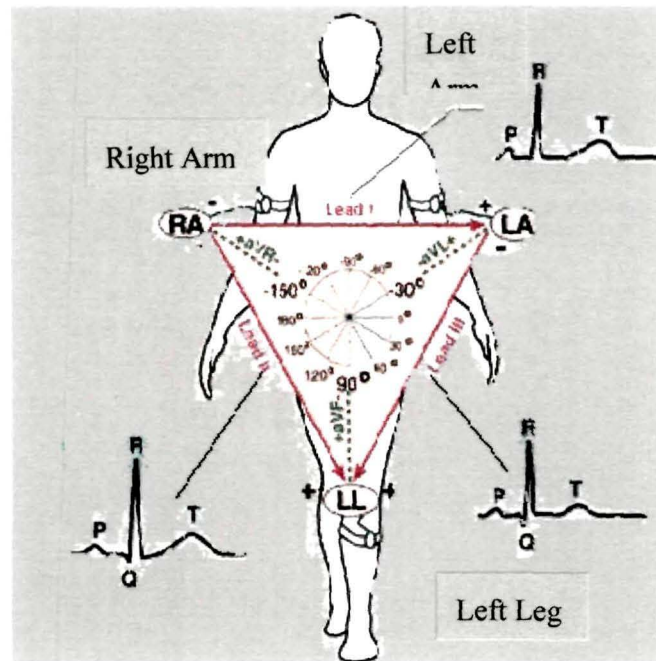


Figure 4.2. Leads showing the waves.

Fig. 4.3 shows the Einthoven's Triangle. Each of the 6 frontal plane leads has a negative and positive orientation (as indicated by the '+' and '-' signs).

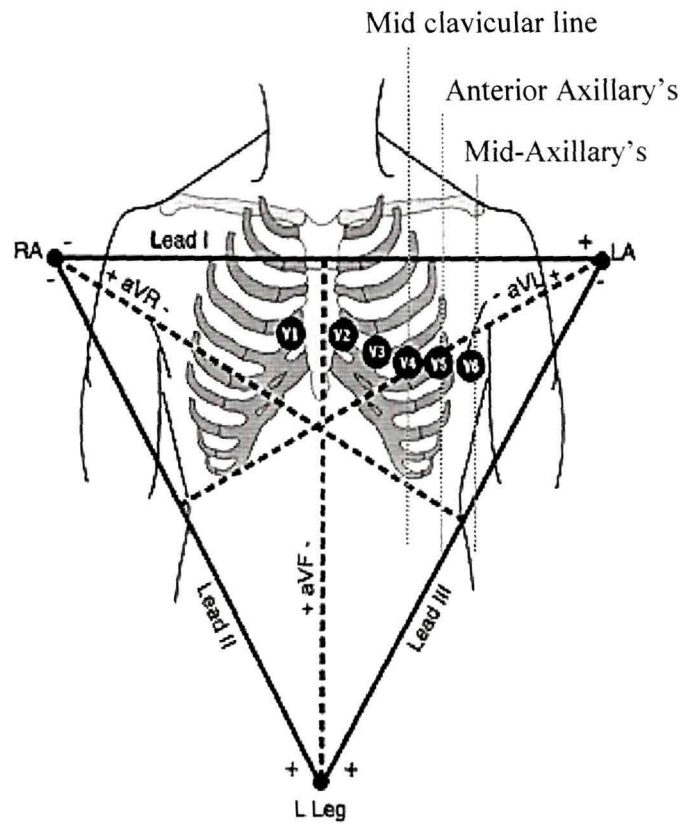


Figure 4.3. Location of chest electrodes in 4th and 5th

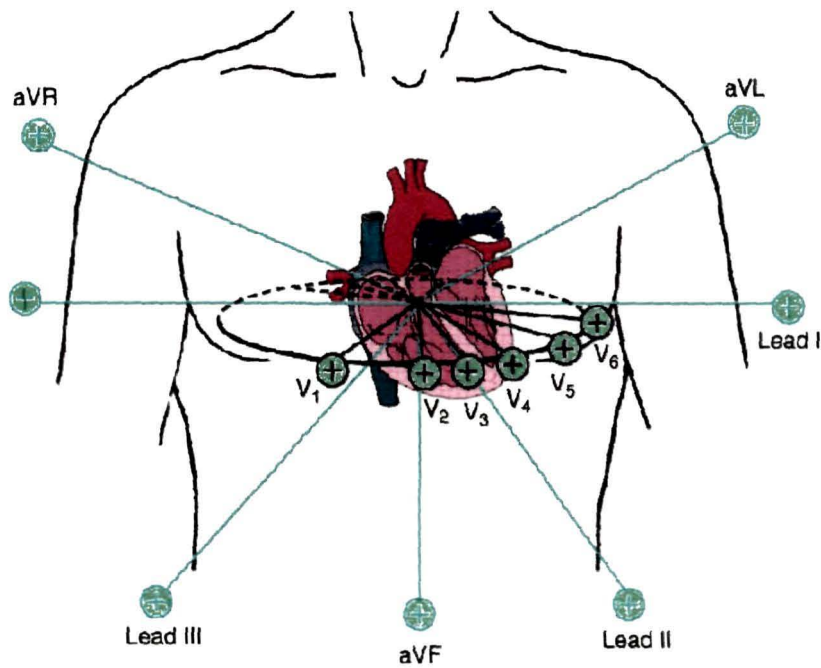


Figure 4.4. Electrocardiographic view of heart.

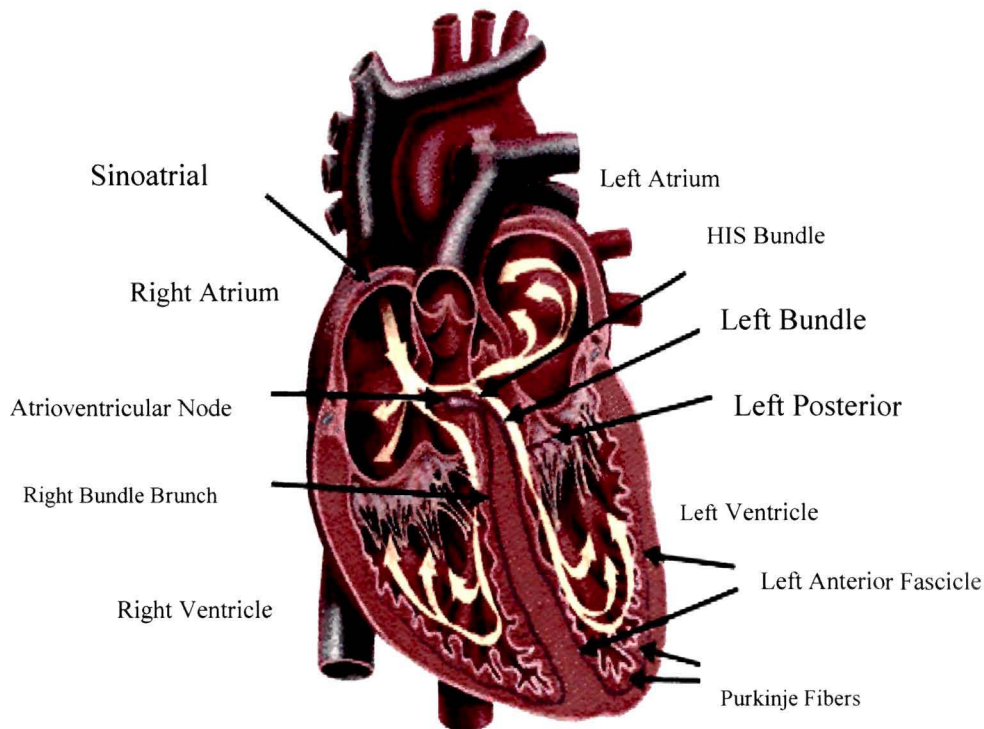


Figure 4.5 Inside of the heart.

In the normal heart, each beat begins with the discharge (‘depolarization’) of the sinoatrial (SA) node, high up in the right atrium [5]. The normal heart beat ranges between 60 to 100 beats per minute.

Depolarization of the SA node does not cause any noticeable wave on the ECG. The first detectable wave appears when the impulse spreads from the SA node to depolarize the atria. This produces the **P wave**. Different electrodes give different views of these waves- the wave below is typical for lead II (lead II has the same direction as the axis of the normal heart).

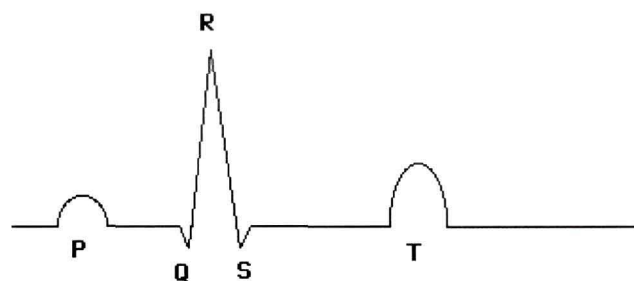


Figure 4.6. PQRST wave

The atria contain relatively little muscle, and so the voltage generated by atrial depolarization is relatively small. From the viewpoint of most leads, the electricity appears to flow towards them and the P wave will be a positive (upward) deflection. The exception is lead aVR, where the electricity appears to flow away, and so the P wave is negative in that lead. After flowing through the atria, the impulse reaches the atrioventricular (AV) node located low in the right atrium. The AV node is normally the only route by which an electrical impulse can reach the ventricles. Activation of the AV node does not produce an obvious wave on the ECG, but it does contribute to the time interval between the P wave and the subsequent Q or R wave. It does this by delaying conduction, and in doing so acts as a safety mechanism, preventing rapid atrial impulses from spreading to the ventricles at the same rate. The time taken for the depolarization wave to pass from its origin in the SA node, across the atria, and through the AV node into ventricular muscle is called the **PR interval**. This is measured from the beginning of the P wave to the beginning of the R wave, and is normally between 0.12 and 0.20s, or 3-5 small squares.

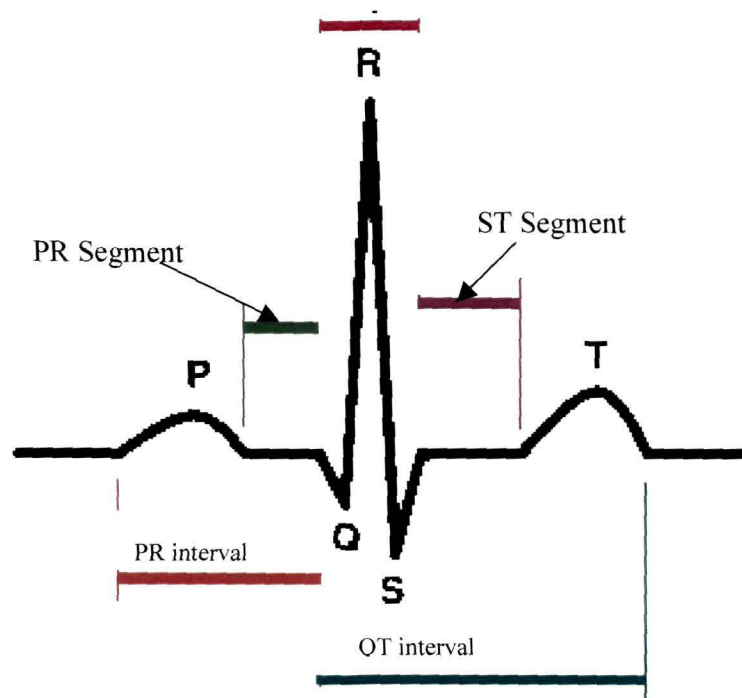


Figure 4.7: Different components of the PQRST wave.

Once the impulse has traversed the AV node, it enters the bundle of His, a specialized conducting pathway that passes into the interventricular septum and divides into the left and right bundle branches.

Current normally flows between the bundle branches in the interventricular septum, from left to right, and is responsible for the first deflection of the **QRS complex**. Whether this is a downward deflection or an upward deflection depends upon which side of the septum a lead is 'looking' from. If the first deflection of the QRS complex is downward, it is called a **Q wave** [45]. The first upwards deflection is called **R wave**. A downward deflection after R wave is called **S wave**.

The right bundle branch conducts the wave of depolarization to the right ventricle. The depolarization of the ventricles, represented by the QRS complex, is normally complete within 0.12s. QRS complexes are 'positive' or 'negative' depending on whether the R wave or the S wave is bigger. This, in turn, will depend upon the view each lead has of the heart. The left ventricle contains considerably more myocardium than the right, and so the voltage generated by its depolarization will tend to dominate the shape of the QRS complex. The **ST segment** is the transient period when no further electrical current can be passed through the myocardium. It is measured from the end of the S wave to the beginning of the T wave. The ST segment is of particular interest in the diagnosis of myocardial infarction and ischemia. The T wave represents repolarization ('recharging') of the ventricular myocardium to its resting electrical state. The **QT interval** measures the total time for activation of the ventricles and recovery to the normal resting state.

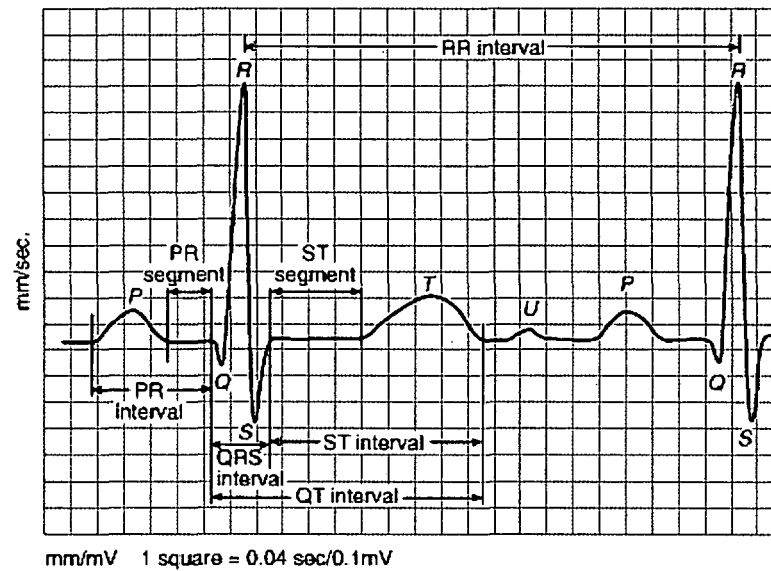


Figure 4.8: U wave.

The origin of the **U Wave** is uncertain, but it may represent repolarization of the interventricular septum or slow repolarization of the ventricles. U waves can be difficult to identify. Pictorially the whole phenomena is shown graphically as below:

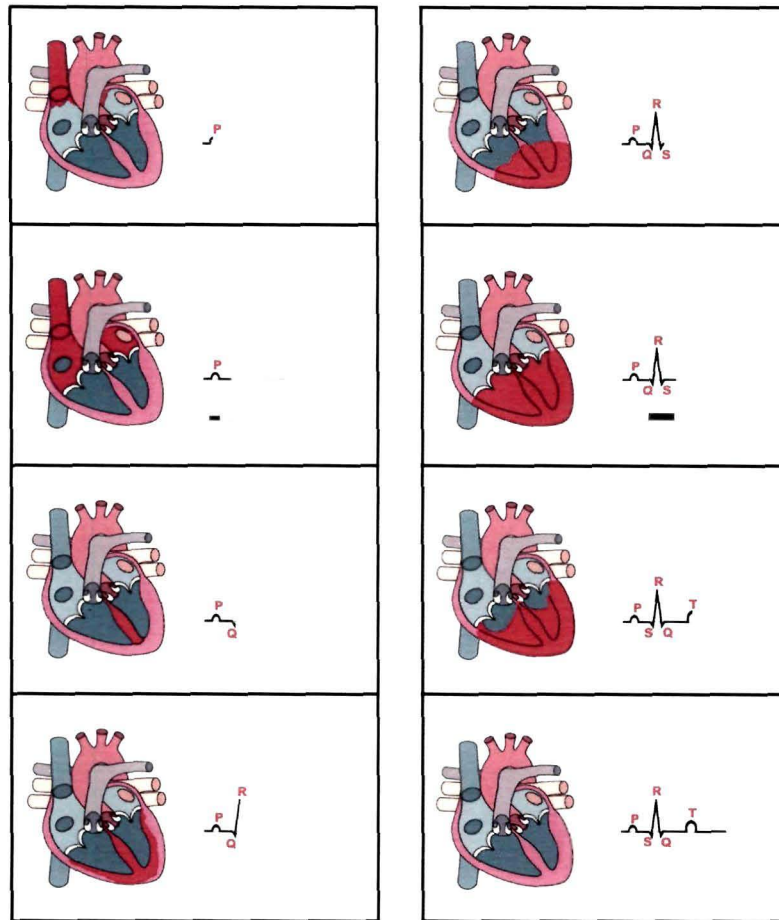


Figure. 4.9: The generation of PQRST wave.

4.1.2 Arrhythmia

The sinus node creates spontaneous electrical impulses at a rate of 60-100 per minute at rest. It can increase or decrease its rate in relation to various needs such as reduction in the rate during sleep to as low as 40 per minute, and increase to as high as 150 per minute during physical activities. The sinus node thus, regulates the pumping of the heart in a rhythmic fashion and this is the normal rhythm of the heart. An arrhythmia is an abnormal rhythm outside of the normal variations mentioned above. In essence, an arrhythmia [46] is an abnormal rhythm or beating of the heart. It can be due to abnormal function of the sinus node or it can arise from other areas which normally do not initiate electrical impulses. The

arrhythmia can be manifested as rapid and regular heart beats (tachycardia), rapid and irregular heartbeats (fibrillation), slow heart beats (bradycardia), and abnormal extra beats occurring before the anticipated normal beats in a periodic fashion (premature contractions). Arrhythmias originating from the upper chambers (above the ventricles) of the heart are called supraventricular arrhythmias. Those originating in the lower chambers (ventricles) are called ventricular arrhythmias.

Some of the arrhythmias [47] are described as follows:

1. Normal Sinus Rhythm: An ECG in normal sinus rhythm, p-waves are followed after a brief pause by a QRS complex, then a T-wave.



Figure 4.10: A Normal Sinus Rhythm.

2. Complete Heart Block : Complete heart block (complete AV block) means that the heart's electrical signal doesn't pass from the upper to the lower chambers. When this occurs, an independent pacemaker in the lower chambers takes over. The ventricles can contract and pump blood, but at a slower rate than that of the atrial pacemaker. On the ECG, there's no normal relationship between the P and the QRS waves.

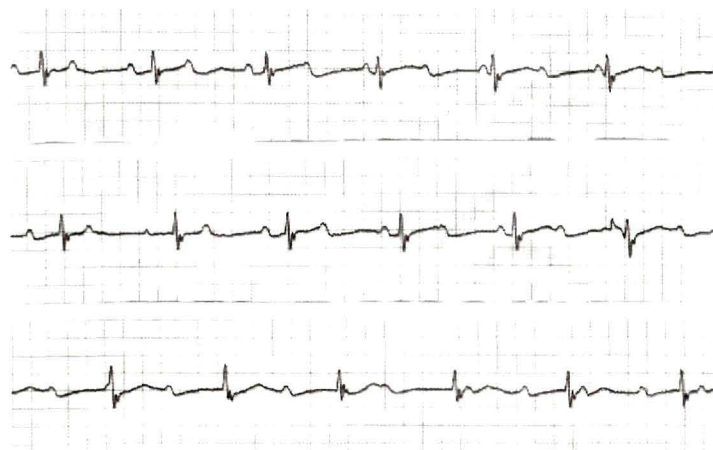


Figure 4.11: Complete Heart Block.

3. Atrial Fibrillation:

Atrial fibrillation occurs when the atria depolarize repeatedly and in an irregular uncontrolled manner usually at atrial rate greater than 350 beats per minute. No P-waves are observed in the EKG due to the chaotic atrial depolarization. The chaotic atrial depolarization waves penetrate the AV node in an irregular manner, resulting in irregular ventricular contractions. The QRS complexes have normal shape, due to normal ventricular conduction. However the RR intervals vary from beat to beat as shown in figure 4.12.

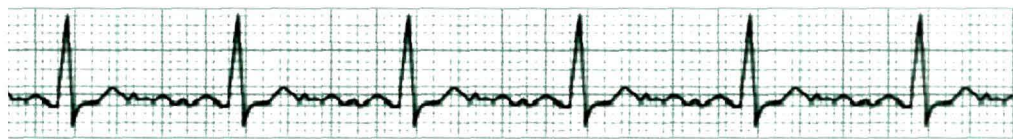


Figure 4.12: Atrial Fibrillation.

During atrial fibrillation, the heart's two upper chambers (the atria) beat chaotically and irregularly — out of coordination with the two lower chambers (the ventricles) of the heart. The heart rate in atrial fibrillation may range from 100 to 175 beats per min which is presented in figure 4.13.

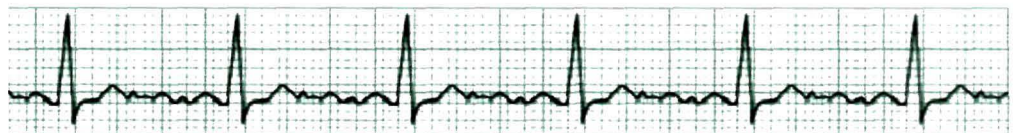


Figure 4.13: Atrial Fibrillation

4. Ventricular Fibrillation : Ventricular fibrillation occurs when parts of the ventricles depolarize repeatedly in an erratic, uncoordinated manner. The EKG in ventricular fibrillation shows random, apparently unrelated waves. Ventricular Fibrillation, a cardiac condition that is almost invariably fatal, does not have a recognizable QRS complex.

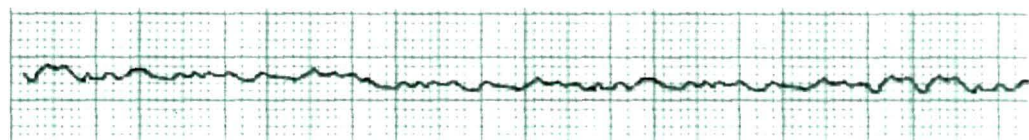


Figure 4.14: Ventricular Fibrillation.

5. Atrial Flutter: Atrial flutter, is characterized by the absence of a P wave. Instead, a wavy base line is observed in the waveform. The typical ECG during atrial flutter shows a narrow QRS complex with a ventricular rate of approximately 150 beats/min. Atrial activity during atrial flutter causes a specific alteration in the surface ECG, giving the baseline a characteristic sawtooth appearance. The atrial rates in atrial flutter range from 250 to 350 beats/min, but they are remarkably close to 300 beats/min in most patients, with very little beat-to-beat variation (usually less than 20 msec).

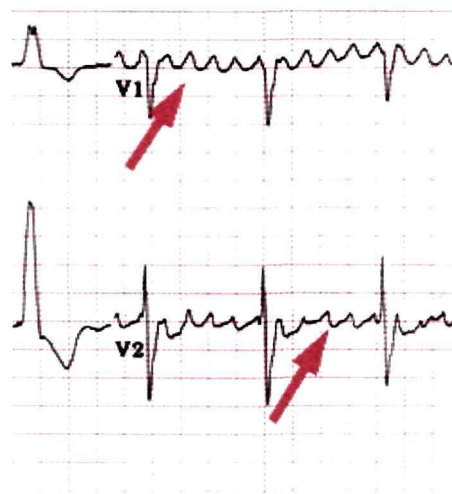


Figure 4.15: Atrial Flutter

6. Sinus Tachycardia: A rate faster than 100 beats a minute in an adult is called tachycardia. The two main types of tachycardia are abnormal supraventricular tachycardias (which originate in the upper chambers of the heart, the atria) and ventricular tachycardias (which originate in the lower chambers of the heart, the ventricles). The rhythm in sinus tachycardia is similar to normal sinus rhythm with the exception that the RR interval is shorter, less than 0.6 seconds. P waves are present and regular and each P-wave is followed by a QRS complex in a ratio of 1:1. At very rapid rates, the P-waves might become superimposed on the preceding T waves such that the P waves are obscured by T waves.

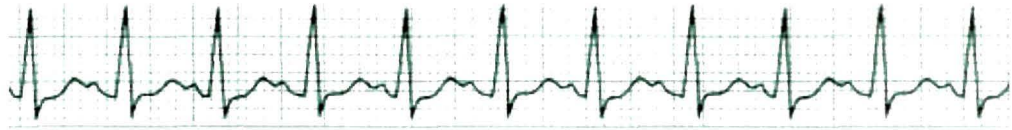


Figure 4.16: Sinus Tachycardia.

7. Ventricular Tachycardia: Ventricular tachycardia, a very serious arrhythmia initiated in the ventricles, in which the heart rate is usually between 150 and 250. Since the impulse originates from the ventricles, the QRS complexes are wide and bizarre. Ventricular impulses can be sometimes conducted backwards to the atria, in which case, P-waves may be inverted. Otherwise, regular normal P waves (60-100 beats per minute) may be present but not associated with QRS complexes (AV dissociation). The RR intervals are usually regular.

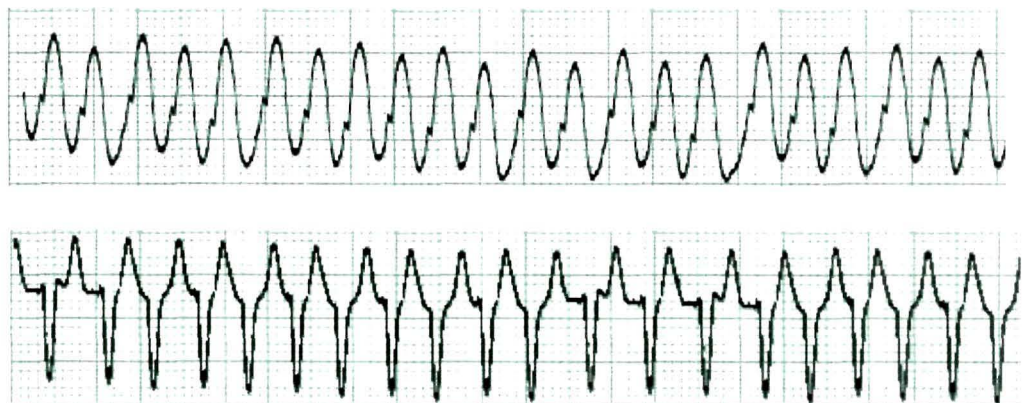


Figure 4.17: Ventricular Tachycardia.

8. Sinus Bradycardia: The sinus bradycardia rhythm is almost like a normal sinus rhythm except for the fact that R-R interval is longer. It is characterized by the following

- Rate: 40-59 bpm
- P wave: sinus
- QRS : normal (.06-.12)

- Conduction : P-R normal or slightly prolonged at slower rates
- Rhythm: regular or slightly irregular

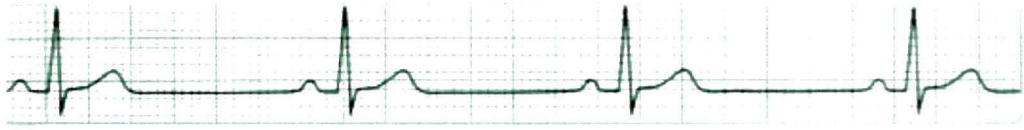


Figure 4.18: Sinus Bradycardia

9. Premature Ventricular contraction: Also known as **ventricular premature beat (VPB)** or **extrasystole**, is a form of irregular heartbeat in which the ventricle contracts prematurely. This results in a "skipped beat" followed by a stronger beat. Individuals with the condition may report feeling that his or her heart "stops" after an attack. PVCs are also called **heart palpitations**. The depolarization begins in the ventricle instead of the usual place, the sinus node.

PVCs are diagnosed by: **1. prematurity 2. wide QRS 3. the presence (usually) of a compensatory pause.**

10. Atrial premature beat: The impulse is discharged prematurely giving rise to a distorted P wave (wide, narrow, notched, inverted or superimposed on the preceding T wave). PR interval may be normal or slightly prolonged. Premature P is followed by QRS less than 0.11 sec except when a very premature P is not conducted. The RR interval between two QRS enclosing APB is less than twice the normal RR interval.

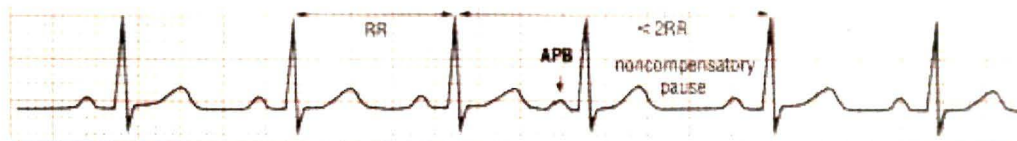


Figure 4.19: Atrial premature beat.

11. Sick Sinus Syndrome: is a type of bradycardia in which the sinoatrial (SA), or sinus node is not working as it should.

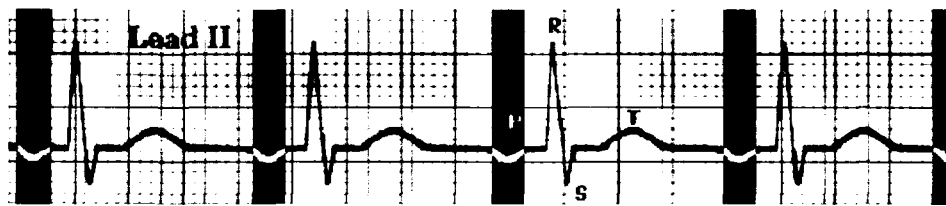


Figure 4.20: Sick Sinus Syndrome.

The sinoatrial exit block that occurs in patients with sick sinus syndrome may demonstrate a Mobitz type I block (Wenckebach block) and a Mobitz type II block. The ECG may reveal a long pause following cardioversion of atrial tachyarrhythmias, and a greater-than three-second pause following carotid massage.

12. Right Bundle Branch Block: the top image shows a normal QRS complex. The middle figure shows RBBB, and the bottom figure shows LBBB. With both kinds of bundle branch block, the QRS is wide and misshapen. The characteristic shapes of the QRS complex allow doctors to determine whether the right or the left bundle branch is blocked. Diagnostic criteria for right bundle branch are:

- Tall R' in V1
- QRS duration 0.12s or greater.
- In addition to this, there is usually a prominent S in the lateral leads (I, V5, V6).

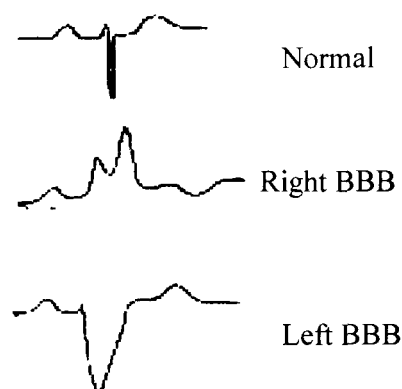


Figure 4.21: Right and Left Bundle Branch Block.

13. Left Bundle Branch Block: The criteria to diagnose a left bundle branch block on the electrocardiogram.

- The heart rhythm must be supraventricular in origin.
- The QRS duration must be = or > 120 ms.
- There should be a QS or rS complex in lead V1.
- There should be a monophasic R wave in leads I and V6.
- The T wave should be deflected opposite the terminal deflection of the QRS complex.

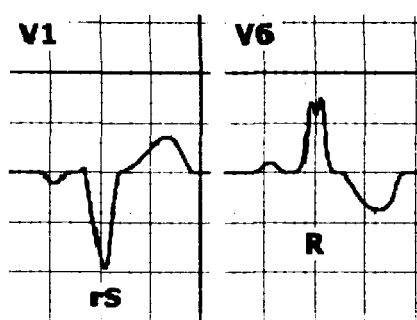


Figure 4.22. Left Bundle Branch Block characteristics

4.2 Detection techniques - a literature survey

Detection of abnormal ECG signals is a critical step in administering aid to patients. Usually patients with heart conditions are continuously hooked up to cardiac monitors in hospital. Due to large number of patient in intensive care units and the need for continuous observation of them, several methods for automated arrhythmia detection have developed in the past few decades in an attempt to simplify the monitoring task. Various techniques have been utilized to classify arrhythmias. Generally, these techniques classify two or three arrhythmias or have significantly large processing times [6]. Most of the techniques uses: signal preprocessing, QRS detection, feature extraction and neural network for signal classification [7]. Many signal processing techniques have been proposed in the literature for the classification of ECG beats, such as frequency analysis [8, 9], template matching [10, 11], hidden Markov field [12-14], Bayesian [15], heuristic

approaches [16], expert systems [17], self organizing maps[18] and artificial neural networks [19- 27, 41-43] or by other recognition systems[28 - 30].

Since ECG is a nonlinear signal generated by a nonlinear system, the body, neural networks provide a powerful and flexible non linear modeling tool for time series analysis. They are also utilized for classification. Guvenir et. al [31] developed a supervised machine learning algorithm for arrhythmia analysis based on a technique called features interval for the UCI "Arrhythmia" dataset [32] with missing features and unlabeled classes to address this problems and achieved an accuracy of 62%. Such a performance is not sufficiently good for clinical use. It is required to develop detection schemes which give a high accuracy, or equivalent, low false-positive and false-negative statistics, so that they can be useful in a practical deployment. Rahat Abbas et. al [33], presented a neuro-wavelet approach to predict ventricular tachyarrhythmia with a confidence of 74%. Belgacem et. al [34] showed that he could achieve 91.55% correct classification in detecting premature ventricular contraction (PVC). George Q Gao [35] could detect five cardiac conditions with a recognition rate of 91.8%; with an average accuracy of 84.93%. Wei Jiang [36-38] showed that using evolvable block based neural networks, detection accuracies of 98.1% and 96.6% could be achieved for ventricular ectopic bears and supraventricular ectopic beats respectively. In their paper [39], Prasad et at. reported that using multi-resolution analysis and neural networks, they could classify sinus rhythm and 12 different arrhythmias with an accuracy of 96.77%.

4.3 Proposed method

Different cardiac arrhythmias are analyzed and diagnosed based on the ECG trace as recorded by ECG machine. Here, a complete process is proposed wherein an ECG trace is scanned; the scanned image converted into a graphical form, and then entire wave is partitioned into its sub waves. The shape, interval and the width of these individual sub waves govern the occurrence of an arrhythmia. So, a MATLAB based code is developed to read the ECG waveform and then

synthesize it to yield P, R, Q, T waves, QRS complex, along with their respective intervals. Regularity of heartbeat, otherwise known as cardio-intervals, is a quantitative measurement of heart rate and is equal to the time elapsed between successive heartbeats. This regularity is checked from the R-R intervals by a self developed code. These factors have direct implication on the diagnosis of arrhythmia. These are then processed through an error back propagation neural network to detect the kind of arrhythmia. The base line wander and noise in the signal is taken care of while processing the waves. The proposed method is simple and detect 16 types of arrhythmias with accuracy.

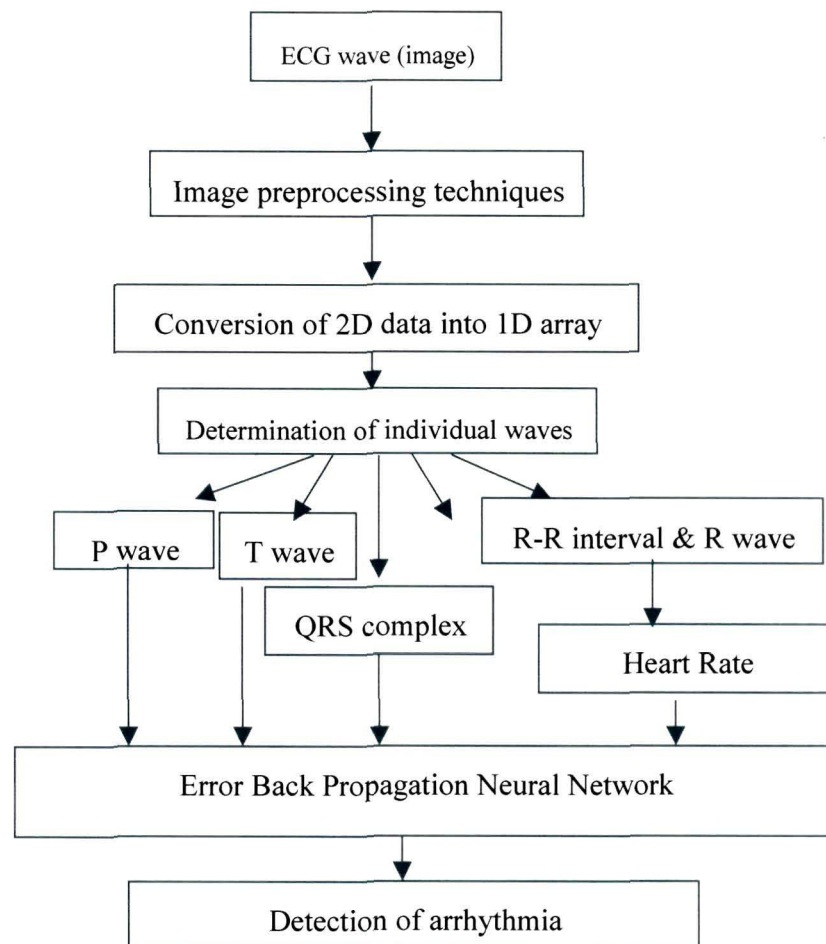
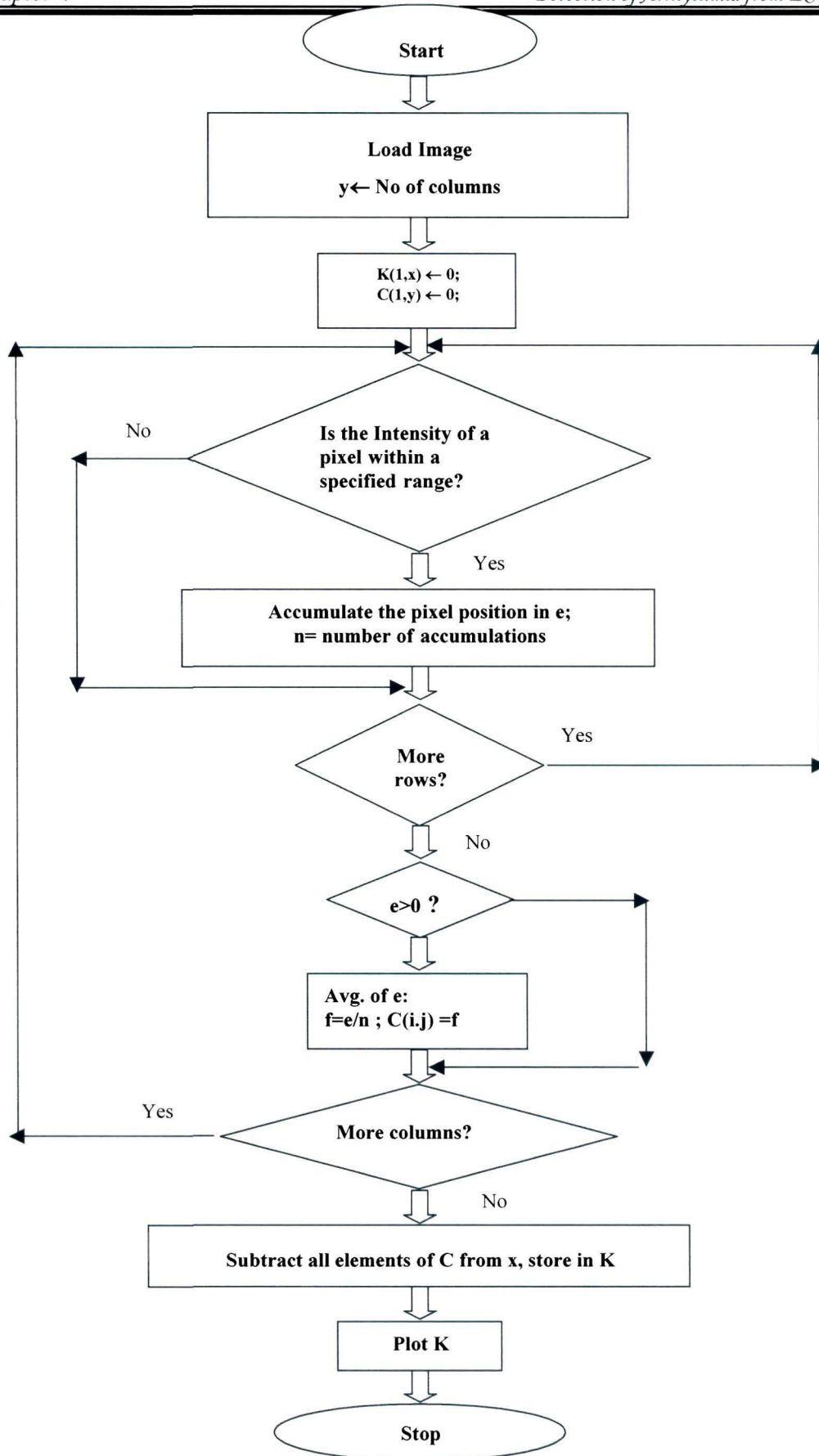


Figure 4.23: Flow diagram of the detection process.

4.3.1 Conversion of an image into a graph

Data acquisition from medical equipments has always posed problem, especially in those cases, where the equipment does not have the flexibility of data conversion from one format to another, data storage and data transfer. So, in the present approach, a code based on MATLAB [40] has been developed to read an ECG graph and store it as an image data file as shown in **fig. 4.4**. An image is defined by three attributes viz., spatial coordinates like x-, y- coordinates and the intensity of the picture elements at these coordinate points. Further, an algorithm is developed that reads the intensity of each of the pixels corresponding to its spatial coordinates and then translates the total pixel information as one dimensional vector. When plotted, this vector gives the same ECG waveform shown in **fig. 4.5**.

Database: The ECG data for the analysis is taken from the MIT-BIH (Massachusetts Institute of Technology-Beth Israel Hospital Arrhythmia Laboratory) ECG arrhythmia database [48], Government Multi-specialty Hospital, and nursing homes in Chandigarh, India.



4.3.2 Segmentation of the ECG wave

The ECG signal is filtered using a high pass filter to remove the DC component. Then from this ECG vector, the base line wander corrections have been made. This is done by a simple short code. The maxima of the ECG vector denote the peaks of the R wave. The interval between the two adjacent R-R peaks is used to evaluate the heart rate. But simultaneously, it is also checked if all the RR intervals are same or not. If the time interval of subsequent RR intervals is same, then the heart rate is regular otherwise it is irregular. A derivative method compounded with a 'threshold' condition is used to evaluate the base line of the plot. Any deviation of values of adjacent array elements bigger than the 'threshold' implies a wave. The start and the terminating point of the wave is tracked by a counter and the difference between these values defines the interval of a wave by the code. This way, all the required information about the interval and the amplitude are obtained.

4.3.3 Detection by Artificial Neural Network (ANN)

This is an algorithm that learns the patterns or rules from the given input – output signal combination. Cardiac arrhythmia can be detected if proper information on different parameters of the ECG waveform is known. Hence, the neural network is trained in a way similar to how doctors would make a diagnosis. The key point is to judiciously choose the wave components from the waveform to feed to the input layer of the neural network. The normal components of the ECG waveform considered for the purpose of diagnosis are the P interval, P amplitude, R height, QRS interval, PR interval, QT interval, T interval, regular or irregular RR interval, and the heart rate. The R-R interval mainly decides the heart rate. A number of conditional checks have been imposed to check if any of the waves are absent or abnormal. We use a three level structure. The architecture of the neural network is 9x13x7x4. If noise in the signal is non-Gaussian with a mean other than zero, then the model then, a bias may be included towards the noise [49]. So, both the input layer and the hidden layers have a bias each to take

care of the noise in the signal. Different combinations of the output give the occurrence of different arrhythmia. Neurons between two adjacent layers are fully connected. In the training, the weights are adjusted by rules (Widrow-Hoff rule) and theories of inhibition and excitation. A standard sigmoid function is chosen for the forward signal flow to the output layer and a pure linear function as the activation function for the output layer. In order to have a fast convergence, the network is trained with a momentum factor. A noise factor has also been added to the network for a better result.

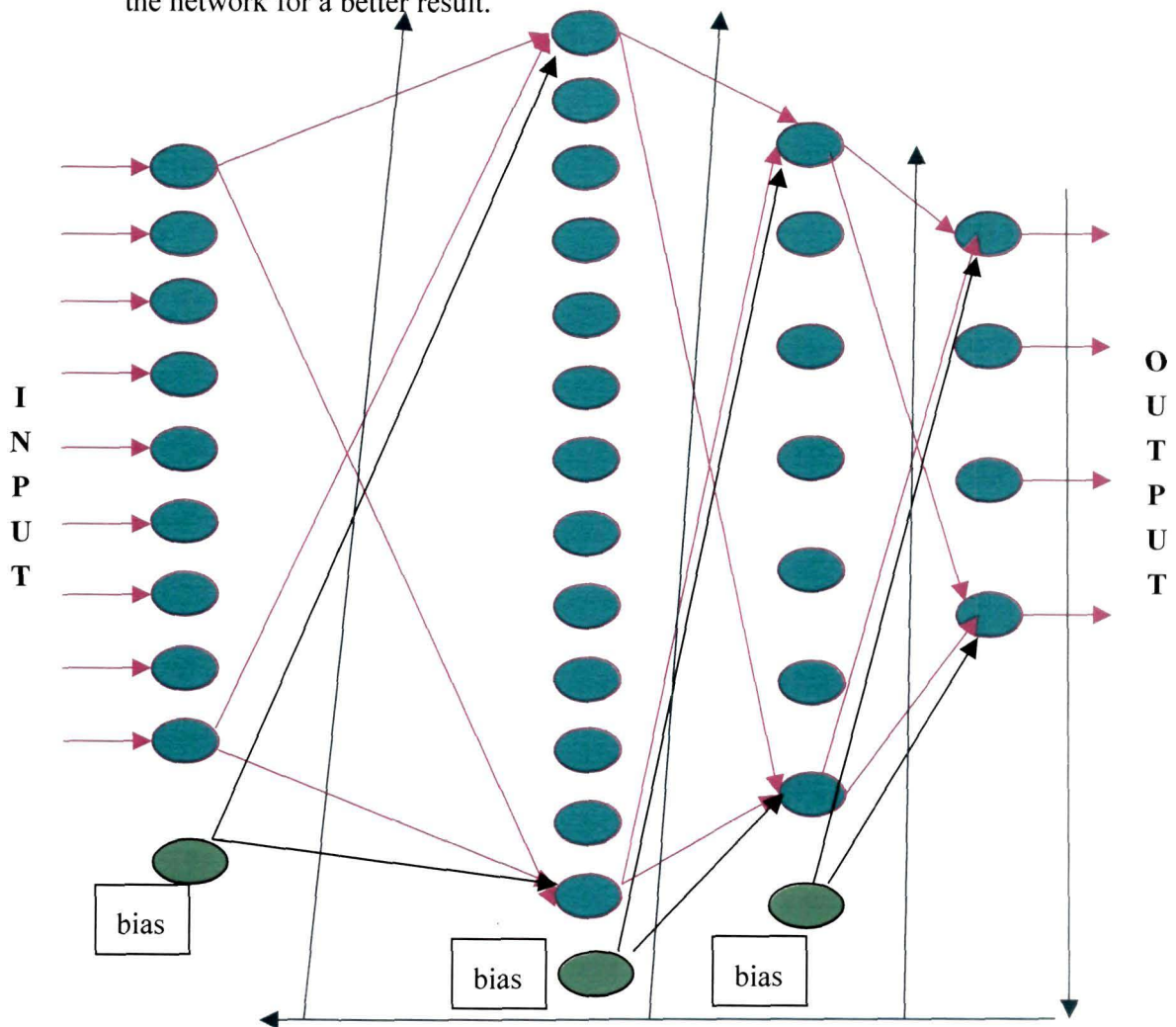


Figure 4.25. Architecture of the proposed neural network.

4.4 Results

539 ECG graphs of patients from different Government Hospitals and nursing homes were collected for testing the conversion code. These graphs were scanned and stored its spatial coordinates were read by the MATAB code and then translated the total pixel information as an one dimensional vector which when plotted gave the same ECG waveform(fig. 4.27) shown by fig.4.25. In the plot of fig.4.25, only one complete wave (fig. 4.26) from fig. 4.27 have been considered for conversion. The figures in fig 4.26 and fig. 4.27 are in good agreement with each other. From this waveform or the data vector obtained from it, the different wave segments have been identified and plotted. Fig. 4.28 shows an isolated P wave with its time interval in ms, fig.4.29 shows the total QRS complex with its time duration being shown in the time axis, while fig. 4.30 shows the QT wave and its interval. The maxima of the vector denote the peak value of R. The R-R repetition rates, as calculated from the total waveform i.e., the converted waveform of the total figure of fig. 4.25 containing many cycles, are used to find out the normal or abnormal behavior of the heart. The heart rate is then calculated by the code. Heart rates evaluated by the code have been compared with the ECG machine's value and validated by a physician. An error of 0.23% was observed between these two.

ECG signal of a real patient has been picked up randomly for the result shown above. The PR interval of 0.1938s, QT interval of 0.7025s, 0.2423s in the case of QRS interval and 1.1565s as RR interval have been found out by the code.

ECG data for the analysis and the implementation of the neural network model are obtained from MIT, BIH arrhythmia database and from different hospitals. Two neural network models are developed. The first network has 3 outputs to detect 9 arrhythmias and the second network has 4 output nodes and detects 16 arrhythmias. Table 4.1 gives the percentage of errors in each case of the diseases for the first network while table 4.2 gives the percentage of errors in each of the cases for the second network.

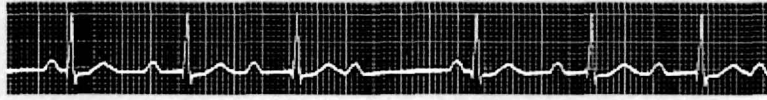


Figure. 4.25. Scanned ECG graph which has been converted from a colored image to a gray level image.



Figure 4.26 : Scanned image (one cycle).

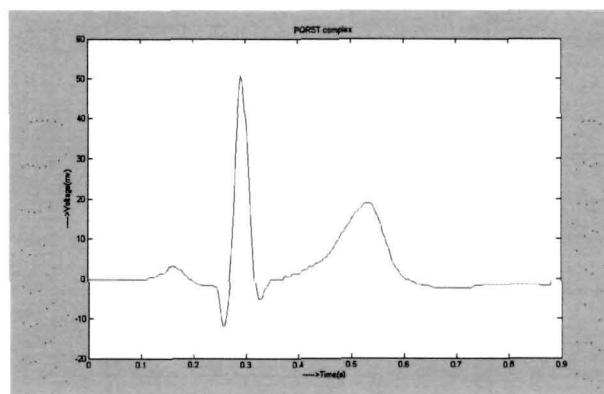


Figure 4.27 : ECG data as read and plotted in MATLAB from Fig. 4.26.

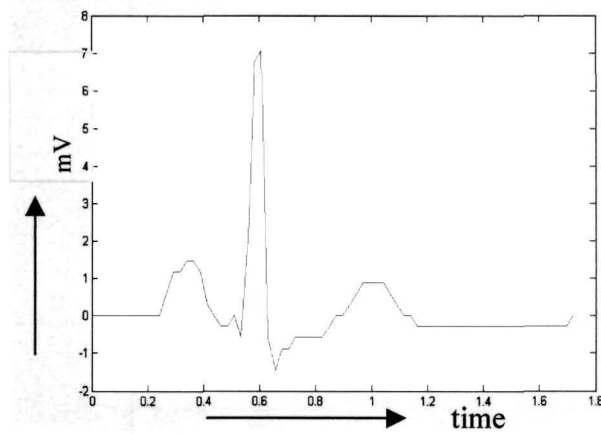


Figure 4.27. A Plot of data (1 cycle only) obtained after converting it into 1D

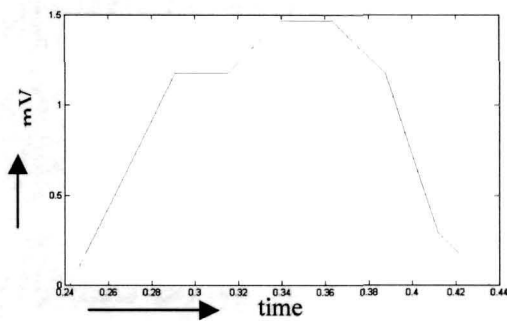


Figure. 4.28. Isolated P wave

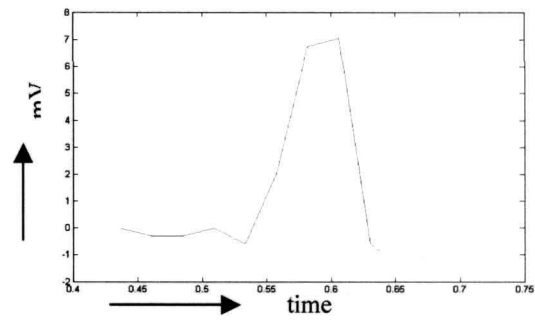


Figure.4.29. QRS Complex

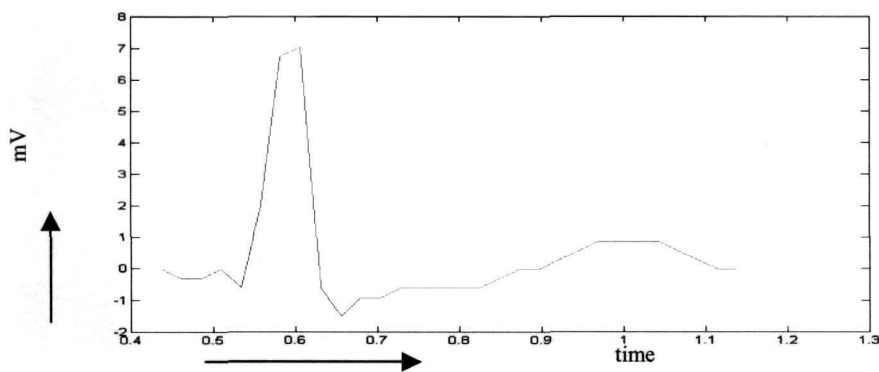


Figure. 4.30. QT interval

Table 4.1. Different arrhythmias with its respective percentage of errors using first neural network.

Sl.No.	Disease	Percentage of errors
1	Atrial Fibrillation	0.39
2	Ventricular Fibrillation	0.57
3	Normal Sinus Rhythm	0.14
4	Complete Heart Block	0.33
5	Sinus Tachycardia	0.13
6	Sinus Bradycardia	0.12
7	Pre Ventricular contraction	0.28
8	Sick Sinus Syndrome	0.35
9	Left Bundle Branch Block	0.61

Table 4.2. Different arrhythmias with its respective percentage of errors using second neural network.

Sl. No.	Disease	% of errors
1	Atrial Fibrillation	1.3
2	Ventricular Fibrillation	0.8
3	Normal Sinus Rhythm	0.5
4	First degree Heart Block	1.7
5	Sinus Tachycardia	0.6
6	Sinus Bradycardia	0.8
7	Pre Ventricular contraction	1.6
8	Sick Sinus Syndrome	1.5
9	Left Bundle Branch Block	1.9
10	Right Bundle Branch Block	1.2
11	Atrial premature beat	1.1
12	Ventricular Tachycardia	2.1
13	Atrial Flutter	2.5
14	Hypercalcemia	1.9
15	Asystole	0.3
16	Idioventricular rhythm	2.1

Table 4.3. Comparison of different ECG classifiers

Method	Arrhythmia types	Accuracy (%)
Proposed Neural Network (second)	16 (average)	98.63
Proposed Neural Network (first)	09	99.68
DWT approach[39]	13	96.77
USCL[50]	5	98.02
MOE[51]	4	94.00
FHhd-HOSA[23]	7	96.06
FTNN[26]	3	98.00
DFT1[52]	10	89.40
DWT1[52]	10	97.00

4.3 Conclusion

In actual clinical environment, the ECG is generally corrupted with powerline interference, muscle noise, and base line wanders. The code takes care of the base line wander by comparing the signal with a reference line and then by drawing a new reference line. In order to handle the powerline interference and other noise

due to the other organs, proper biasing has been incorporated in the neural network. This way, the network proves its robustness in the presence of these disturbances.

4.4 References

- [1]. <http://www.causesofheartdisease.com/>
- [2]. Winslow R. Heart-Disease Sleuths Identify Prime Suspect: Inflammation of Artery, *Wall Street Journal*, October 7, 1999.
- [3]. Malhotra SL, "Epidemiology of ischemic heart disease in India with special reference to causation", *British Heart Journal*, vol. 29, pp. 895-905, 1967
- [4]. Spake A. "The Valley of Death: Researchers probe a mysterious plague of heart disease", *US News & World Report*, pp. 53-54, December 21, 1998.
- [5]. http://library.med.utah.edu/kw/ecg/image_index/index.html#Diagrams
- [6]. Dingfei G E, N Srinivasan, S M Krishnan, "Cardiac arrhythmia classification using autoregressive modeling" Biomedical Engineering OnLine, 2002.
- [7]. George Qi Gao, "Computerized detection and classification of five conditions"
- [8]. B.H. Hung, Y. S. Tsai and T. H. Chu, "FFT algorithm for PVC detection using IBM PC", Proc. IEEE Eng. Med. Biol. Soc. 8th annual International conf., pp.292-295, 1986.
- [9]. M.A. Chikh, N.Belgacem, F. Breksi-Reguig "A PVC beat recognition with Fourier analysis and neural network", Séminaire National sur l'Automatique et les Signaux SNAS'02, Annaba : pp. 27-28, October 2002.
- [10]. S.A. Caswel, K.S Kluge and CM Chiang, "Pattern recognition of cardiac arrhythmias using two intracardiac channels", *Computer in Cardiology*, pp. 549-554, 1993.
- [11]. L. Sornmo, P. O. Borjesson, M. E. Nygards, and O. Pahlm, "A method for evaluation of QRS shape features using a mathematical model for the ECG," *IEEE Trans. Biomed. Eng.*, vol. 28, pp. 713-717, Aug 1981.

- [12]. D. A. Coast, R. M. Stern, and G. G. Cano, "An approach to cardiac arrhythmia analysis using hidden Markov models", *IEEE Tran. Biom. Eng.*, vol. 37; no. 9, pp. 826-836, September 1990.
- [13]. N .V. Thakor and Y. S. Zhu, "Application of cardiac filtering to ECG analysis: Noise cancellation and arrhythmia detection", *IEEE Tran. Biom. Eng.*, vol. 39; no. 8, pp. 785-794, August 1991.
- [14]. W. H. Chang, K.P. Lin and S. Y. Tseng, "ECG analysis based on Hilbert transform in ECG diagnosis", *Proc. IEEE Eng. Med. Biol. Soc.*, 10th annual International conf. pp.36-37, 1988.
- [15]. J L Willems and E Lesafre, "Comparision of multigroup logistic and linear discriminant ECG and VCG classification", *Journal of Electrocardiol.*, vol. 20, pp. 83-92, 1987.
- [16]. J L Talmon, "Pattern Recognition of the ECG", Berlin, Germany: Akademisch Proefschrift, 1983.
- [17]. Y H Hu, S Palreddy and W J Tompkins, "A patient-adaptable ECG beat classifier using a mixture of experts approach", *IEEE Trans. On Biomedical Engg.* vol. 37, pp. 826-835, 1990.
- [18]. M. Lagerholm, C Peterson, G Braccini, L Edebrandt, and L Sornmo, "Clustering ECG complexes using hermite functions and self-organizing maps", *IEEE Trans. Biomedical Engg.*, vol. 47, pp. 838-848, 2000.
- [19]. R Silipo and C Marchesi, "Artificial Neural Networks for Automatic ECG Analysis", *IEEE Trans. Signal Processing*, vol. 46, no. 5, pp. 1417-1425, 1998.
- [20]. Dayong Gao, Michael Madden, Michael Schukat, "Arrhythmia Identification from ECG Signals with a Neural Network. Classifier Based on a Bayesian Framework." Twenty-fourth SGAI International Conference on Innovative Techniques and Applications of Artificial Intelligence, December 2004.
- [21]. Yang Wang, Yi-Sheng Zhu, Nitish V. Thakor, and Yu-Hong Xu, "A Short Time Multifractal Approach for Arrhythmia Detection Based on Fuzzy Neural Network," *IEEE Trans Biomed. Eng.*, vol. 48, no. 9, pp. 989-995, 2001.

- [22]. Y. H. Hu, S. Palreddy, and W. Tompkins, "A patient adaptable ECG beat classifier using a mixture of experts approach," *IEEE Trans. Biomed. Eng.*, vol. 44, pp. 891–900, Sept 1997.
- [23]. S. Osowski and T. H. Linh, "ECG beat recognition using fuzzy hybrid neural network," *IEEE Trans. Biomed. Eng.*, vol. 48, pp. 1265–1271, Nov 2001.
- [24]. Y. Sun, "Arrhythmia recognition from electrocardiogram using non-linear analysis and unsupervised clustering techniques," Ph.D. dissertation, Nanyang Technological University, 2001.
- [25]. K. Minami, Y. Ohkuma, H. Nakajima, and T. Toyoshima, "Arrhythmia diagnosis system which can distinguish atrial arrhythmias from ventricular rhythms," *18th Annual International Conference of the IEEE Engineering in Medicine and Biology Society*, Amsterdam, pp. 1640–1641, 1996.
- [26]. K. Ichiro Minami, H. Nakajima, and T. Toyoshima, "Real-time discrimination of ventricular tachyarrhythmia with fourier-transform neural network," *IEEE Trans. Biomed. Eng.*, vol. 46, no. 2, Feb 1999.
- [27]. P. Chazal and R. B. Reilly, "A comparison of the use of different wavelet coefficients for the classification of the electrocardiogram," *15th International Conference on Pattern Recognition*, vol. 2, pp. 255–258, 2000.
- [28]. Z. Dokur, T. Olmez, and E. Yazgan, "Comparision of discrete wavelet and fourier transform for ECG beat classification," in *Electronics Letters*, vol. 35, pp. 1502–1504, Sep 1999.
- [29]. Akhavan, S. and Calva, G., "Automatic Anomaly Detection in ECG Signal by Fuzzy Decision Making", Proceedings of 6th International Conference on Fuzzy Theory and Technology: Association for Intelligent Machinery, Research Triangle Park, North Carolina, pp. 96-98, 23-28 October 1998.
- [30]. Dayong Gao, Michael Madden, Des Chambers, and Gerard Lyons "Bayesian ANN Classifier for ECG Arrhythmia Diagnostic System: A Comparison Study", International Joint Conference on Neural Networks, Montreal, July 2005.

- [31]. H. A. Guvenir, B. Acar, G. Demiroz, A. Cekin, "A Supervised Machine Learning Algorithm for Arrhythmia Analysis," *In: Proc. Computers in Cardiology Conference*, Lund, Sweden, vol. 24, pp. 433-436, 1997.
- [32]. C. L. Blake, C. J. Merz, "UCI Repository of machine learning databases", [<http://www.ics.uci.edu/~mlearn/MLRepository.html>], Irvine, CA: University of California, Department of Information and Computer Science, 1998.
- [33]. Rahat Abbas, Wajid Aziz, Md. Arif, "Prediction of ventricular tachyarrhythmia in Electrocardiograph signal using neuro-wavelet approach", National Conference on Emerging Technologies, pp. 82-84, 2004.
- [34]. N Belgacem, M A Chikh, F Bereksi Reguig, "Supervised classification of ECG using Neural Networks", Website : <http://www.univ-tlemcen.dz/manifest/CISTEMA2003/cistema2003/articles/Articles%20-%20GBM/GBM8.pdf>
- [35]. George Qi Gao, "Computerized detection and classification of five cardiac conditions"
- [36]. W. Jiang and S. G. Kong, "Block-based Neural Networks for Personalized ECG Signal Classification," accepted, *IEEE Transactions on Neural Networks*, 2007.
- [37]. W. Jiang, S. G. Kong, and G. D. Peterson, "Continuous Heartbeat Monitoring using Evolvable Block-based Neural Networks," *Proc. Int'l. Joint Conf. Neural Networks*, Vancouver, Canada, July 2006.
- [38]. Wei Jiang, "Personalized ECG Heartbeat Classification Using Evolvable Block-based Neural Networks" accepted, *IEEE Transactions on Neural Networks*, 2007.
- [39]. G. Krishna Prasad , J. S. Sahambi, "Classification of ECG Arrhythmias using Multi-Resolution Analysis and Neural Networks". Website: <http://www.ewh.ieee.org/ecc/r10/Tencon2003/Articles/739.pdf>
- [40]. MATLAB version: 7.4: Mathworks
- [41]. K Papik, B Molnar, R Schaefer, Z Dombovari, Z Tulassay, J Faher "Application of neural networks in medicine - A review", *Diagnostics & Medical Technology*, pp.538-546, 1997.

- [42]. R Acharya U, A Kumar, P S Bhat, C M Lim, S S Iyengar, N Kannathal, S M Krishnan, "Classification of cardiac abnormalities using heart rate signals" *Medical & Biological Engineering & Computing*, vol.42, 2004.
- [43]. Hoai, L Tran, Osowski, Stanislaw, "Integration of multiple neural classifiers for hear beat recognition", *Int. J for computation and Maths in Electrical & Electronics Eng.*, vol. 24, no.2, Feb. 2005.
- [44]. The standard 12 Lead ECG : <http://www.medstat.utha.edu/kw/ecg>
- [45]. How to read an EKG strip : <http://www.rnceus.com/ekg>
- [46]. Arrhythmia: a problem with your heart beat : <http://www.familydoctor.org>
- [47]. Normal Cardiac Rhythm : <http://www.arrythmia.org>
- [48]. MIT-BIH Database: <http://ecg.mit.edu>.
- [49]. T. Kärkkäinen and E. Heikkola "Robust formulations for training multilayer Perceptrons", *Neural Computation*, 2003.
- [50]. Y. Sun, "Arrhythmia recognition from electrocardiogram using non-linear analysis and unsupervised clustering techniques," Ph.D. dissertation, Nanyang Technological University, 2001.
- [51]. Y. H. Hu, S. Palreddy, and W. Tompkins, "A patient adaptable ECG beat classifier using a mixture of experts approach," *IEEE Trans. Biomed. Eng.*, vol. 44, pp. 891–900, Sept 1997.
- [52]. Z. Dokur, T. Olmez, and E. Yazgan, "Comparision of discrete wavelet and fourier transform for ECG beat classification," in *Electronics Letters*, vol. 35, pp. 1502–1504, Sep 1999.
-

Chapter 5

ANN for Denoising Images

5.1 Introduction

5.2 Techniques for Noise Removal

5.3 Critical Analysis of Some Filters

5.4 Image Metrics

5.5 The Problem Statement

5.6 Preprocessing of the images

5.7 Development of the Model

5.8 Results

5.9 Performance Evaluation

5.10 References

5. ANN for Denoising Images

5.1 Introduction

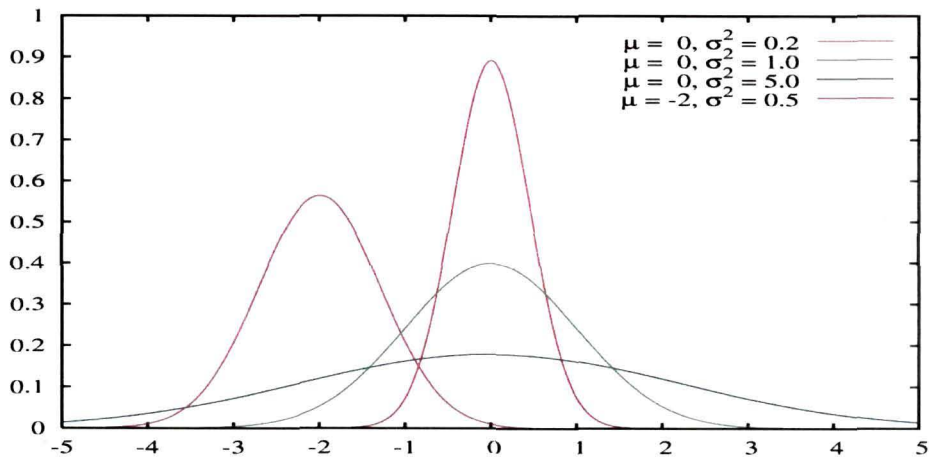
The imperfections of an image acquisition system and the transmission channels often corrupt a digital image with noise. Besides, malfunctioning pixel elements in the camera sensors, faulty memory locations and timing errors in analog to digital conversion result in the corruption of the image by impulse noise [1]. This degradation significantly reduces the quality of the image which makes it more difficult to perform high level vision tasks like recognition, 3-D reconstruction, or image interpretation [2]. An important characteristic of this type of noise is that only a part of the pixels of an image is corrupt and rest of them is noise free. A digital image, $f(x,y)$ containing random noise η , superimposed on the pixel intensity values, is given by the formula :

$$g(x, y) = f(x, y) + \eta(x, y) \quad 5.1$$

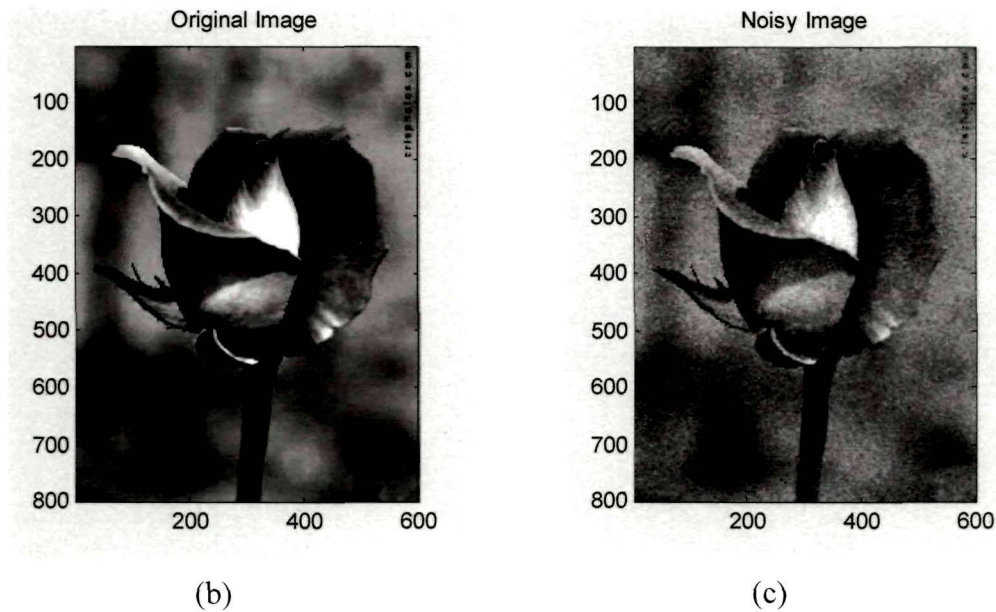
Noise in image always causes serious problem. This noise could be Additive White Gaussian Noise (AWGN), Salt and Pepper Noise (SPN), Random Valued Impulse Noise (RVIN), or a mixed noise. Proper suppression of this noise in an image is a very important issue. Denoising finds extensive applications in many fields of image processing, not to mention its special importance in medical image processing. Conventional techniques of image denoising using linear and nonlinear techniques have already been reported and sufficient literatures are available in this area. Recently, various nonlinear and adaptive filters have been suggested for the purpose. The objectives of these techniques are not only to reduce noise but also to retain the edges and fine details of the original image in the restored image. But, both these objectives conflict each other and these reported techniques are not able to perform satisfactorily in both aspects. Hence, researches are still working on to develop better filtering method that can denoise effectively maintaining the image details. In the present thesis work, efforts have been made to develop a neural network driven filter to denoise an image effectively.

Impulse Noise:

An image signal can be corrupted with noise superimposed during acquisition, transmission, storage and retrieval processes. Acquisition noise is usually additive white Gaussian noise (AWGN) with very low variance.



(a)



(b)

(c)

Figure 5.1: (a): Gaussian distribution, (b): a true image, (c): corrupted with Gaussian noise.

In many medical imaging applications, the acquisition noise is quite negligible. This is mainly due to very high quality sensors used in the imaging cameras. But in some sensing or biomedical instrumentation, the total acquisition noise may be quite high. It is due to the fact that the **image acquisition system itself comprises of**

transmission channel. So in such cases, noises are due to the transmission noise. And acquisition noise is considered to be negligible. The acquisition noise is considered negligible due to another fact that the human visual system (HVS) can't recognize a large dynamic range of image. That is why, an image is usually quantized at 256 levels. Thus, each pixel is represented by 8 bits (1 byte). The present-day technology offers very high quality sensors that don't have noise level greater than half of the resolution of the analog-to-digital converter (ADC), i.e., noise magnitude in time domain is:

$$n(t) < \frac{1}{2} \cdot \frac{A}{2^8} \quad 5.2$$

where $n(t)$ is the noise amplitude at any arbitrary instant of time t , and A is the maximum output of the sensor and is also equal to the maximum allowed input voltage level for the ADC. That is, for $A = 3.3 \text{ volts}$, the noise amplitude should be less than $\sim 6.5 \text{ mV}$. In many practical applications, the acquisition noise level is much below this margin. Thus, the effect of acquisition noise is not considered in this thesis work. However, as a word of caution, it must be considered for instruments that are quite old and have not been calibrated for quite long time.

Therefore, most of the research works are concerned with the noise in a transmission system. Usually, the transmission channel is linear, but dispersive due to a limited band width. The image signal may be transmitted either in analog form or in digital form. If an analog image signal is transmitted through a linear dispersive channel, then the image edges (step-like or pulse like signal) get blurred and the image signal gets contaminated with AWGN since no practical channel is noise free. If the channel is so poor that the noise variance is high enough to make the signal excursion to very high positive or high negative value, then the threshold operation done at the front end of the receiver will contribute to saturated max and min values. Such noisy pixels are seen as white and black dots. Therefore, this type of noise is referred to as salt and pepper noise (SPN). This salt and pepper noise is also known as bipolar fixed-valued impulse noise. The following figures demonstrate the effect of a random valued impulse noise on a standard image of a clown.

Let a digital image $f(x,y)$, after being corrupted with salt and pepper noise of density d , be represented by $f_{im}(x,y)$. Then, the noisy image $f_{im}(x,y)$ is given mathematically as:

$$f_{im}(x,y) = \begin{cases} f(x,y) & \text{with probability } p=1-d \\ 0 & p=d/2 \\ 1 & p=d/2 \end{cases} \quad 5.3$$

Impulse noise corrupts an image at random pixel locations, with a probability of d . Both

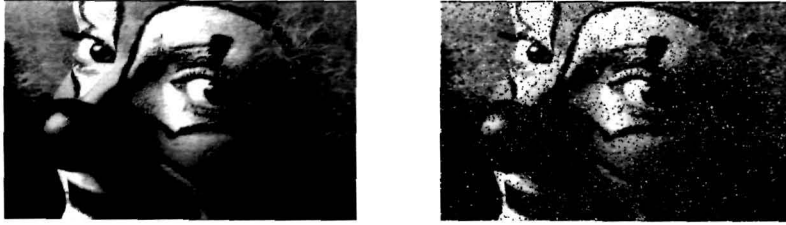


Figure 5.2: True image, its impulse noise corrupted image with $p=0.1$.

the salt and pepper noise and the random valued impulse noise are substitutive in nature. A random valued impulse noise of density d , is mathematically represented as:

$$f_{rim}(x,y) = \begin{cases} f(x,y) & \text{with probability } p=1-d \\ \eta(x,y) & p=d \end{cases} \quad 5.4$$

where, $\eta(m,n)$ is a uniformly distributed random variable, ranging from 0 to 1.

5.2 Techniques of Noise Removal

There are linear filters to remove the impulse noise but they tend to blur edges, at times, do not remove impulse noise effectively. In the presence of signal dependent noise, they do not perform well [3-6]. For all these reasons, various nonlinear filters have been proposed and have been developed by the researchers.

The most popular type of filter in this category is the median (MED) filter. It is computationally efficient, but results in blurred and distorted outputs. Huang *et al.* [7] proposed a 2-D median filtering that is based on sorting and updating gray level histogram of the picture elements in the window. Subsequently, a fast real-time algorithm has been reported for median filtering of signals and images [8]. In this method, noise filtering is done based on their local mean and variance. It has been shown that the use of local statistics works better for removal of additive white and multiplicative noise [9]. However, it is not suitable for the removal of impulse noise as it employs optimal linear approximations.

A novel class of nonlinear filter for image processing known as order statistics (OS) filter has been reported in [10]. This filter reduces white noise, signal-dependent noise, and impulse noise. Another filter, signal adaptive median filter has been developed [11] that performs better than other nonlinear adaptive filters for different kinds of noise. The adaptive averaging filter proposed in [12] shows poor performance in the presence of impulsive noise and does not remove noise close to the edges. The filtering scheme proposed in [13] cannot suppress the impulsive noise sufficiently, but can preserve the edge better than the mean filter. It is reported that decision-based order statistics filters reduces both impulsive and non-impulsive noise and also enhances blurred edges better than many other OS filters [14]. An adaptive filtering algorithm for the class of stack filters has been proposed in [15,16]. In [17], adaptive neural filter removes both Gaussian and impulse noise. Adaptive median filters have also been proposed for removing impulse noise and preserving the image sharpness [18]. Two such filters are: the rank-order based adaptive median filter (RAMF), and the size based adaptive median filter (SAMF). A fuzzy operator has also been suggested in [19] for enhancement of blurred and noisy images. In paper [20], a novel algorithm has been suggested in which the nature of filtering operation is conditioned on a state variable. A reliable and efficient computational algorithm for restoring blurred and noisy images has been proposed by Li and Santosa in [21]. By using inverse filtering technique blurred images can be restored. In their publication [22], Malladi and Sethian have suggested a unified approach for noise removal, image

enhancement, and shape recovery. This approach relies on the level of set formulation of curves and surface motion, which leads to a class of PDE-based algorithm. Enhancement of medical images can be successfully achieved by this technique. Several adaptive Least Mean Square (LMS) filters have also been proposed [23] for noise suppression from images. An adaptive order statistics filter [24] is proposed for gamma corrupted image sequence. This technique estimates the weights of an adaptive order statistics estimator that adapts to the probability density function of the noise. This approach performs well in handling the signal dependent noise. Higher order statistics removes impulse noise but this method needs computation of higher order statistical terms, which are computationally expensive [25]. Filtering of impulse noise is also performed using Artificial Neural Network (ANN). It has been reported that a single layer neural network accurately detects the impulse noise of fixed amplitude [26], their accuracy decreases with random valued impulse noise. To further improve the performance, various generalized and modified median based filters such as multi-stage median (MSM) filter [27], center weighted median (CWM) filter [28], and stack filter [29] have been proposed. These methods produce good results at low noise conditions, but their performance deteriorates as the noise density increases. One possible solution is to use a filter that is capable of identifying the pixels contaminated by noise prior to filtering and leave noise-free pixels unaltered. Such decision-based median filters realized by threshold operations have been suggested in literature [30-37]. Some of them perform at par with the median filter, whereas, others perform even better. But as the noise density increases, their performance too becomes inferior.

The concept of fuzzy logic by Zadeh [38, 39] has revolutionized the research and development in the areas of signal processing, control, instrumentation, etc. [40-43]. Many researchers have used fuzzy logic to develop efficient image filters [44 -55].

Neural network is another important tool used in signal processing [56-58]. Many neural network based noise detectors and noise filters have been proposed [17,26, 44,46,59]. Panda *et al.* in [60] have proposed a novel impulse detection scheme.

Discrete Wavelet Transform (DWT) [61, 62] is also a very powerful signal analysis tool. DWT has been used by many researchers to design efficient digital image filters [63-67]. But they are highly computational intensive algorithms.

5.3 Critical Analysis of Some Filters

The SD-ROM filter of Abreu, *et al.* [36] and the MMEM filter of Han and Lin [68] are some of the landmarks in the image filtering. The authors claim that it gives a very good performance in suppressing SPN of high density. But despite the claim by the authors, it shows slightly poorer performance at low SPN density as compared to the SD-ROM filter. T. Chan, *et al* [31] have developed a tri-state median (TSM) filter, for preserving image details while effectively suppressing impulse noise.

H-L Eng and K-K Ma have proposed a noise adaptive soft-switching median (NASM) filter [69]. A soft-switching noise-detection scheme classifies each pixel into a corrupted or uncorrupted pixel, isolates impulse noise, non-isolated impulse noise or image object's edge pixel. 'No filtering', a standard median (MED) filter or the proposed fuzzy weighted median (FWM) filter is then employed according to respective characteristic type identified. The scheme changes the scrolling window size depending on the impulse noise density. For a 'Lena' image corrupted with 10% impulse noise, NASM filter shows a PSNR of 42 dB. Its performance is very good as compared to fixed filters but it suffers from the disadvantage of being a highly computational intensive algorithm.

T. Chen and H. R. Wu have designed a space variant median filter [70] for filtering impulse noise from corrupted images. At 10% impulse noise density, it yields a PSNR of 28 dB against 22.5 dB for the MED filter. M. Ma, *et al*, have developed a fuzzy hybrid filter (FHF) [71] for removal of impulse noise from highly impulse corrupted images. This filter achieves a PSNR of 30.87 dB for removing

SPN (under mixed noise condition) from the ‘Lena’ image, while a MED 3×3 filter achieves 28.10 dB.

Aizenberg and Butakoff have developed a novel impulse detector based on rank-order criteria [72]. The scheme is called a differential rank impulse detector (DRID). At 1%, 5% and 20 % of SPN, this DRID plus median filtering scheme gives a PSNR of 49.4 dB, 43.84 dB and 36.64 dB respectively. This may be categorized as a very good filter. Its performance is very good at low noise density. Further, the computational complexity involved is also not very high.

Another impulse detection scheme, based on pixel-wise MAD (Median of Absolute Deviation from median), has been proposed by Crnojevic, *et al* [73]. This algorithm does not have any varying parameters, does not require previous training or optimization, and removes all types of impulse noise. For ‘Lena’ image corrupted with 20% SPN, this scheme achieves a PSNR of 33.20 dB (slightly poorer than SD-ROM of Abreu, *et al.*). For the same test image corrupted with 20% RVIN, it achieves a PSNR of 32.82 dB (slightly better than SD-ROM). It can be said that this scheme is better than the SDRM only if the impulse noise is random-valued.

In their paper [1], Dong *et. al.*, suggested a two-stage method for denoising random valued impulse noise for a noise level as high as 60%. This method first identifies the noisy pixels and then combines it with edge preserving regularization. Their method achieved a PSNR of 29.03dB against 22.96 dB by Iterative Median Filter for a Lena image corrupted with 60% random valued impulse noise.

5.4 Image Metrics

The quality of an image is determined by objective as well as subjective evaluation. The pleasing aspect of an eye decides its subjective evaluation, but the human visual system (HVS) is so complicated that at times, it fails in a comparative

evaluation. Therefore, objective evaluation forms the basis of evaluation to judge its quality.

There are various metrics used for objective evaluation of an image. Some of them are mean squared error (MSE)[74], Signal to Noise ratio (SNR), root mean squared error (RMSE), mean absolute error (MAE) and peak signal to noise ratio (PSNR).

Let the original noise-free image, noisy image, and the filtered image be represented by $f(x, y)$, $g(x, y)$, and $f'(x, y)$, respectively. Here, x and y represent the discrete spatial coordinates of the digital images. Let the images be of size $M \times N$ pixels, i.e. $m=1,2,\dots,M$, and $n=1,2,\dots,N$. Then, MSE is defined as:

$$MSE = \frac{\sum_{m=1}^M \sum_{n=1}^N [f'(x, y) - f(x, y)]^2}{M \times N} \quad 5.5$$

The Root mean squared error is :

$$RMSE = \sqrt{MSE} \quad 5.6$$

Among the various image quality measures, the most widely used is the peak signal-to-noise ratio (PSNR) [75-76]. The PSNR is defined in logarithmic scale, in dB. It is a ratio of peak signal power to noise power. Since the MSE represents the noise power and the peak signal power is unity in case of normalized image signal, the image metric PSNR in decibels (dB) is computed by using

$$PSNR = 10 \log_{10} \frac{255^2}{\frac{1}{MN} \sum_{m=1}^M \sum_{n=1}^N [f'(x, y) - f(x, y)]^2} \text{ (dB)}$$

or,

$$PSNR = 10 \times \log_{10} \frac{255^2}{MSE} \text{ dB} \quad 5.7$$

The MPEG committee used an informal threshold of 0.5 dB PSNR to decide whether to incorporate a coding optimization because they believed that an improvement of that magnitude would be visible. Higher PSNR represents better image quality. In general, PSNR above 30 is considered acceptable. Reconstructed images with higher metrics are judged better.

5.5 The Problem Statement

In this section of work, efforts are made to develop a scheme to filter impulse noise that deteriorates the medical image. In today's medical imaging systems, doctors use various scans (e.g. cardiograms, CAT scans, ultrasonic scans, Magnetic Resonance Imaging, Single Photon Emission Computed Tomography (SPECT), Positron Emission Tomography (PET) etc.) for recognizing diseases. But the scanned images are corrupted with noises of various kinds. With the present day state-of-the-art technology, we get high quality gamma cameras, high quality electronic circuitry, e.g., system on chip (SOC) etc. the scope of other noises like AWGN, Speckle noise, mixed noise etc. is very negligible. Hence, an improvement in the filtration of impulse noise will yield the best overall performance. Therefore, it is very important to design and develop a highly efficient image filter that can suppress impulse noise quite effectively. Moreover, if the computational complexity could be kept at very low value, it would be an added advantage to get the filtering operation performed in a short time for online and real-time applications. Since linear filters don't perform well, nonlinear filtering schemes, viz., artificial neural network filter is developed for achieving better performance.

5.6 Preprocessing of the images

Neural net requires that the input data be in the range $[0, 1]$. So, all the image data is normalized before feeding to the neural network. The images have been normalized using the formula:

$$\tilde{x} = \frac{x - x_{\min}}{x_{\max} - x_{\min}} \quad 5.8$$

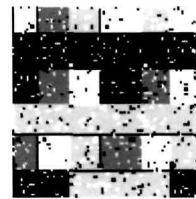
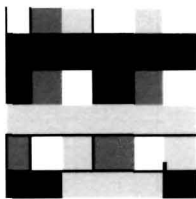
where, x – initial value of the image,

\tilde{x} – normalized value

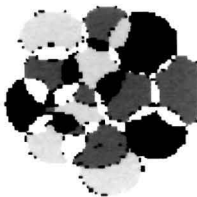
x_{\min} = minimum value of the image data

x_{\max} = maximum value of the image data.

The total database for the images consists of some self created texture images and SPECT images of cardiac showing the left ventricle. The SPECT data used for both training and testing have been obtained from Medical Imaging Research Laboratory, Dept, of Radiology, University of Utah, USA and from internet. Next, all the images are resized to a uniform size of 80x80. In the next step of preprocessing, it is ascertained that all the images have the same data types, *i.e.*, double class. Hence, the images with class **uint8** are converted to class double using MATLAB function. Out of the 300 images in the database, 200 images are used for training and 100 for testing. These 100 images are images of lena image and SPECT images. The testing images consists of 50 texture images and the rest SPECT images. A set of true image along with its impulse corrupted noisy image constitutes the input-output data pair for training the network. Some of the texture and SPECT images are shown below.



P=0.1



P=0.5

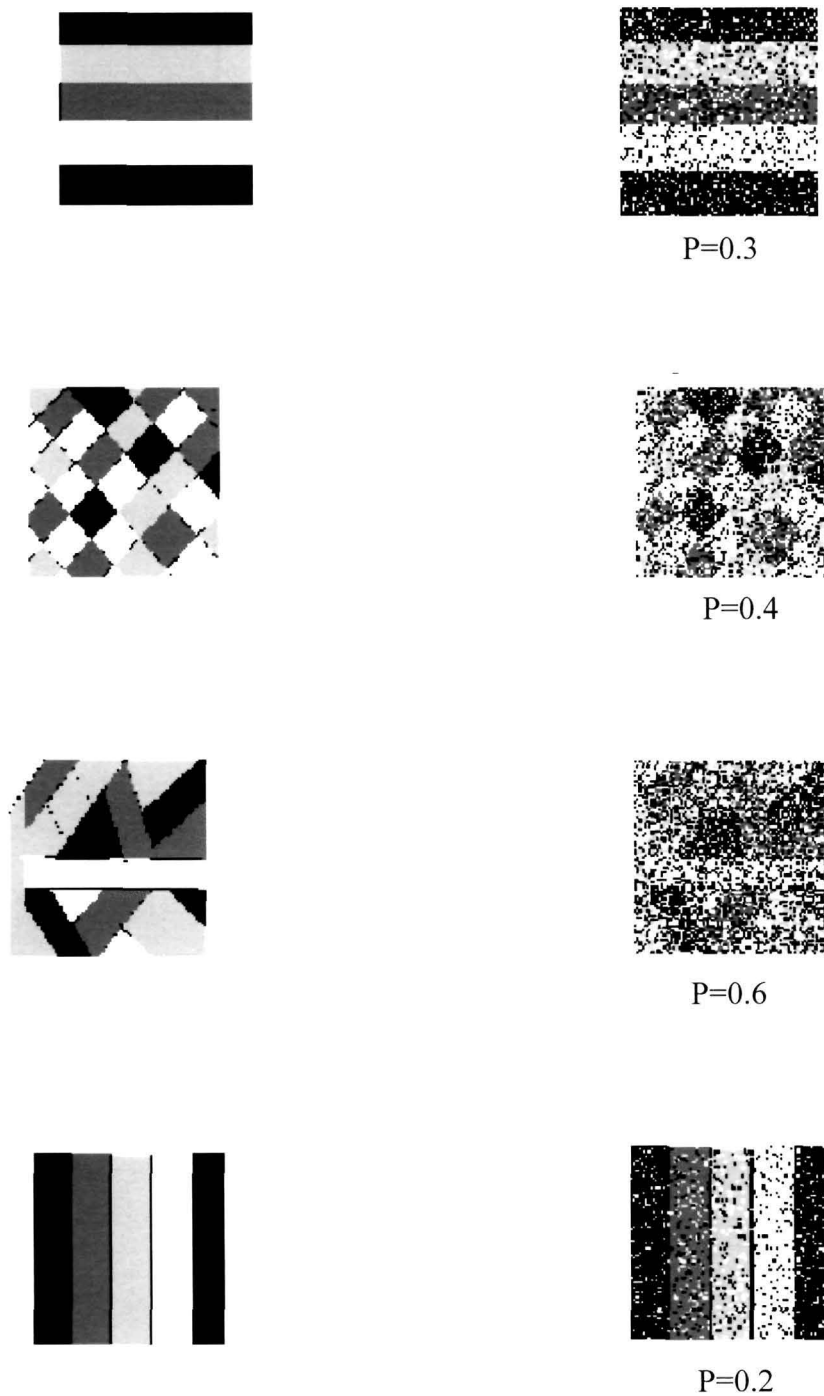
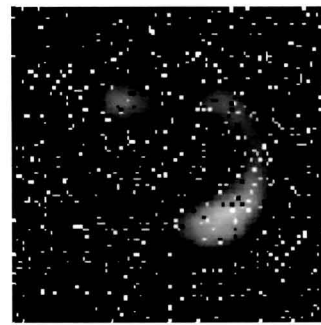
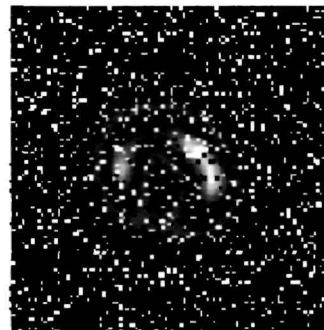
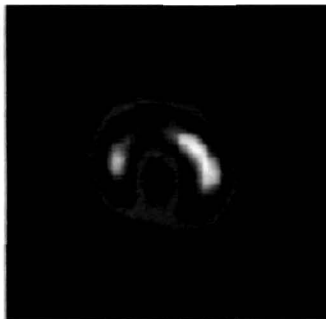


Figure 5.3: Texture images and their noisy counterparts that formed the input – output pair of the training database.

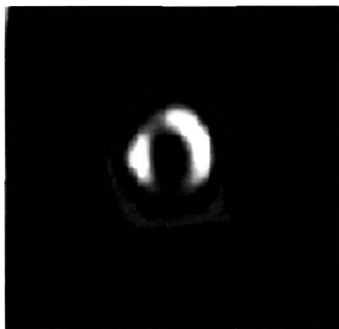
10 % impulse noise



20 % impulse noise



30 % impulse noise



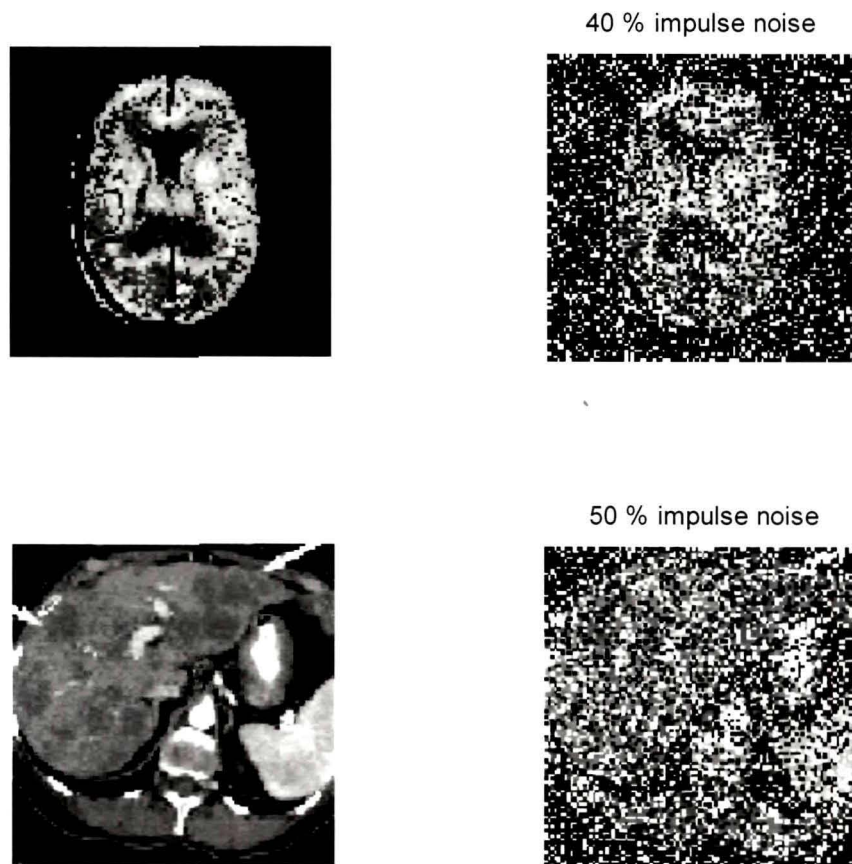


Figure 5.4: (a) some of the SPECT images that formed the part of the training / testing database, (b) their noisy images with densities of 10%, 20%, 30% 40% and 50% respectively.

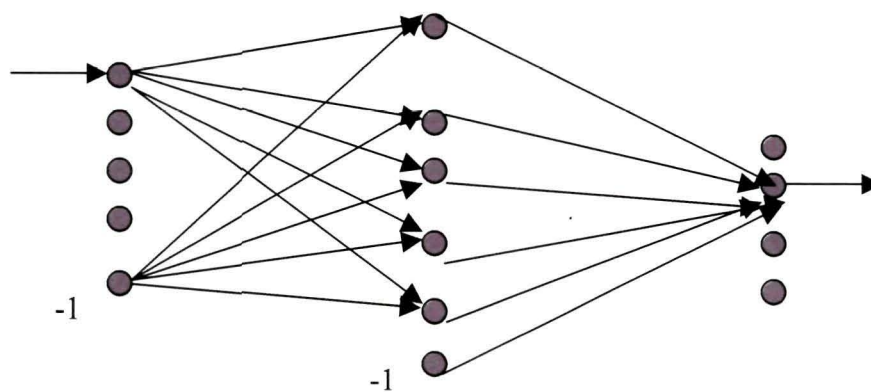


Figure. 5.5: Architecture of the error back propagation neural network

5.7 Development of the Model

The back propagation algorithm, a gradient descent algorithm is used for training the network in a supervised manner. Three layers neural networks have been used for the network. Tan sigmoid is chosen as activation function for the hidden layer. The training parameters of the network are shown in Table 5.1.

Noise parameters	0.0005
Learning Constant(parameter)	0.05
Learning Increment	1.05
Momentum factor	0.2

The addition of a little noise to each of the training patterns helps the structure generalizing rather than memorizing [77]. Figure 5.5 shows the networks structure used.

5.8 Results



Figure: 5.6 Original Lena image



Figure. 5.7: Lena image corrupted with Salt and Pepper impulse noise of densities 10%, 20%, 30%, 40%, 50% and 60% respectively.

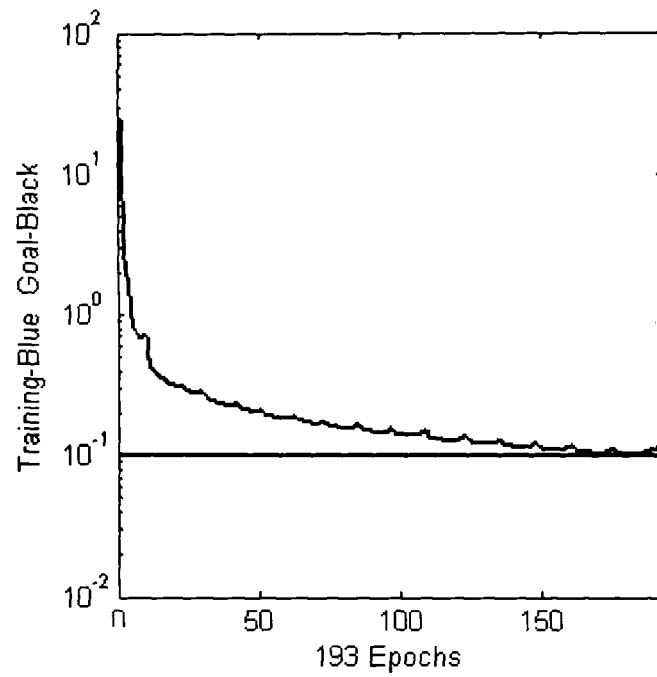


Figure 5.8. Plot of the error versus the iteration of the neural network.

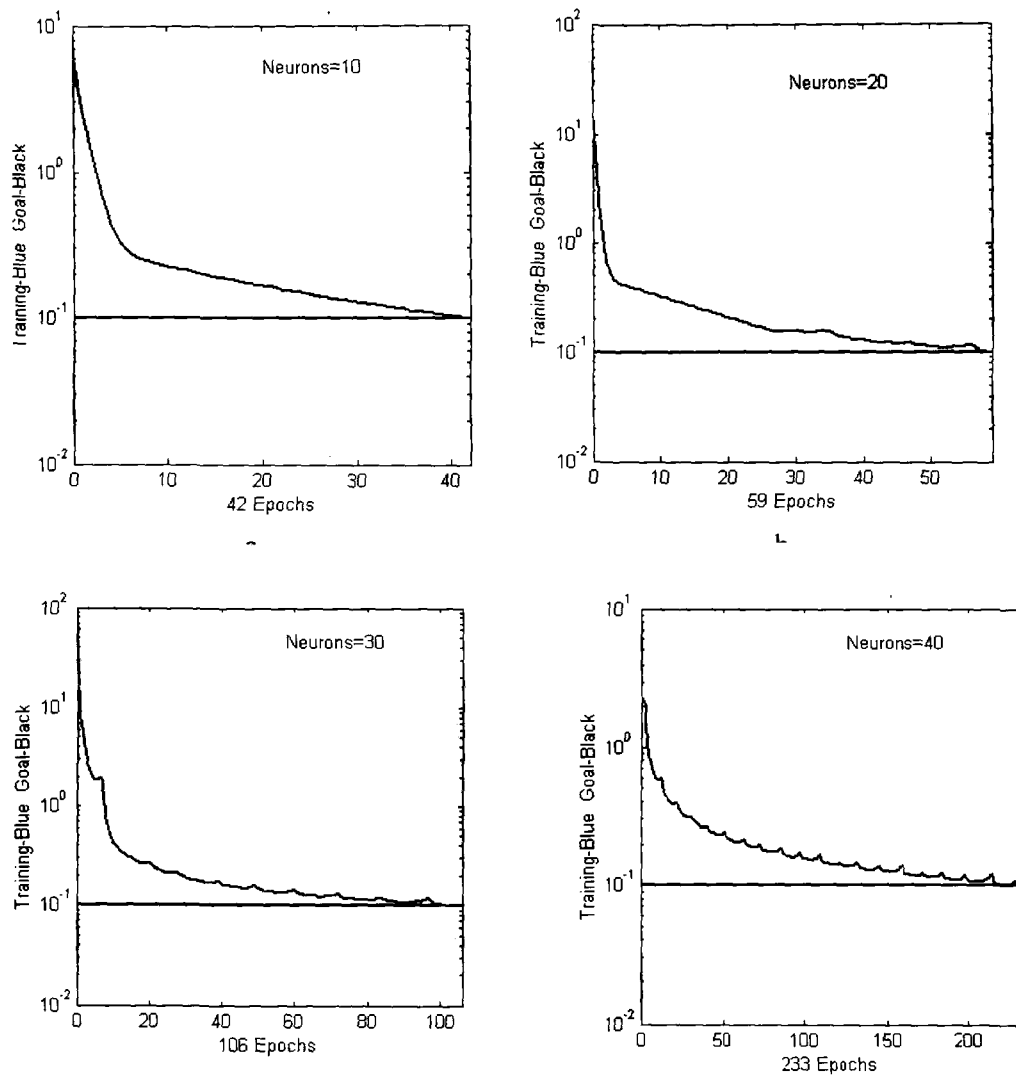
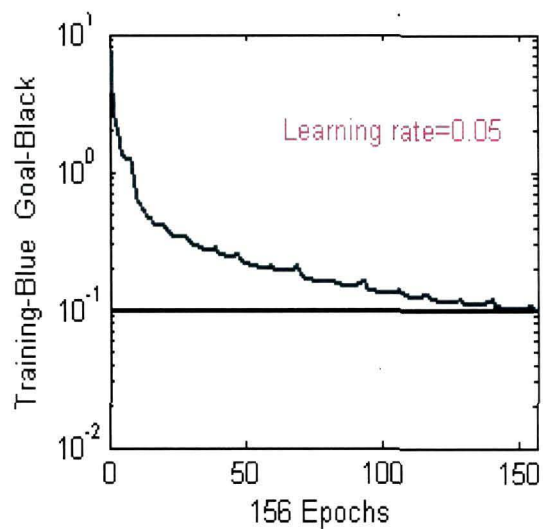
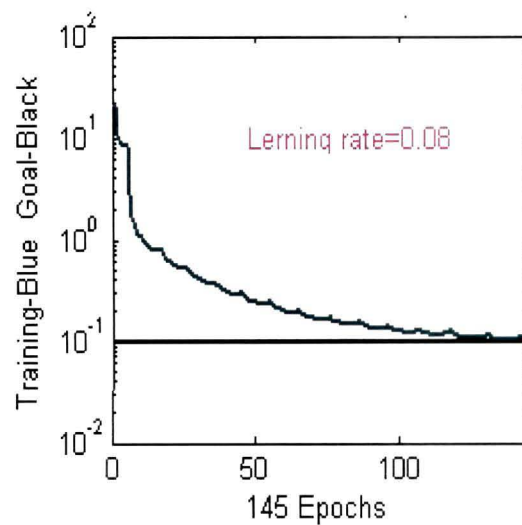
Effect of Hidden neuron

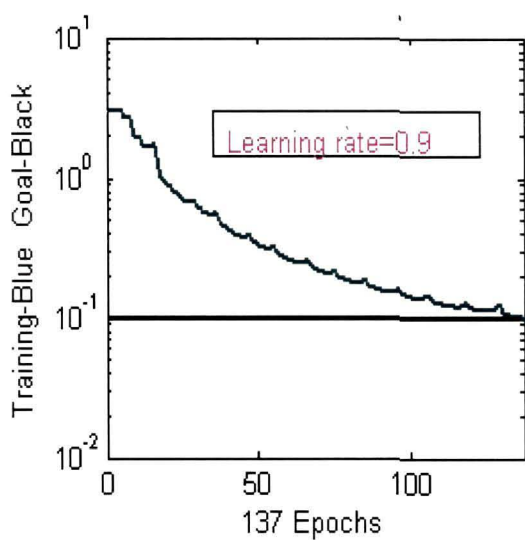
Figure 5.9 Effect of the network performance with variation of neuron
(Momentum=0.02, learning rate=0.05, goal error=0.01)



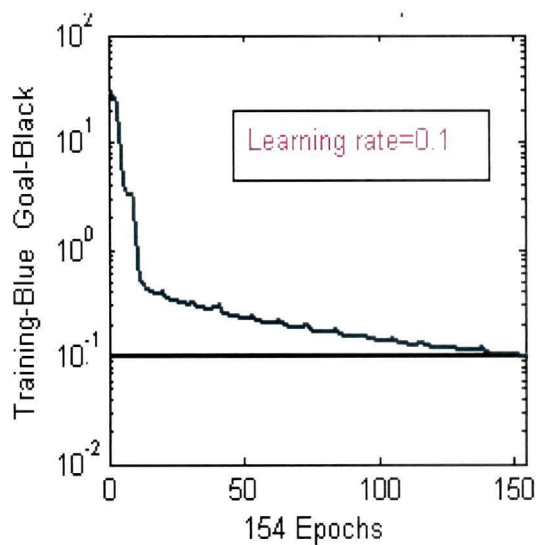
(a)



(b)



(c)



(d)

Figure 5.10 Effect of the network performance with learning rate
(Learning increment=1.05, Learning momentum=0.2, goal=0.01)

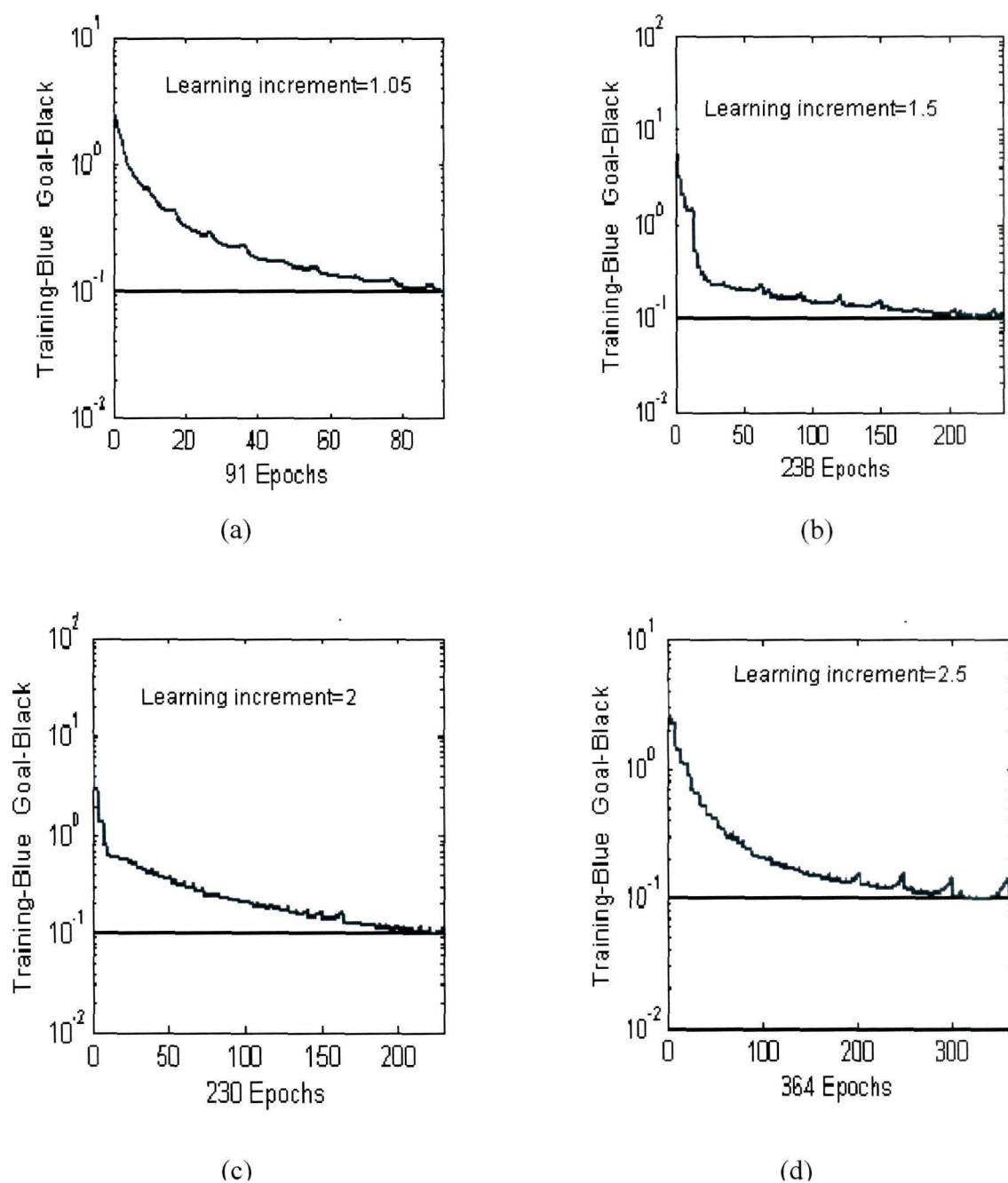
Effect of Learning increment variation

Figure 5.11 Effect of the network performance with learning increment
(Learning rate=0.05, Learning momentum=0.2, goal=0.01)

Output Images

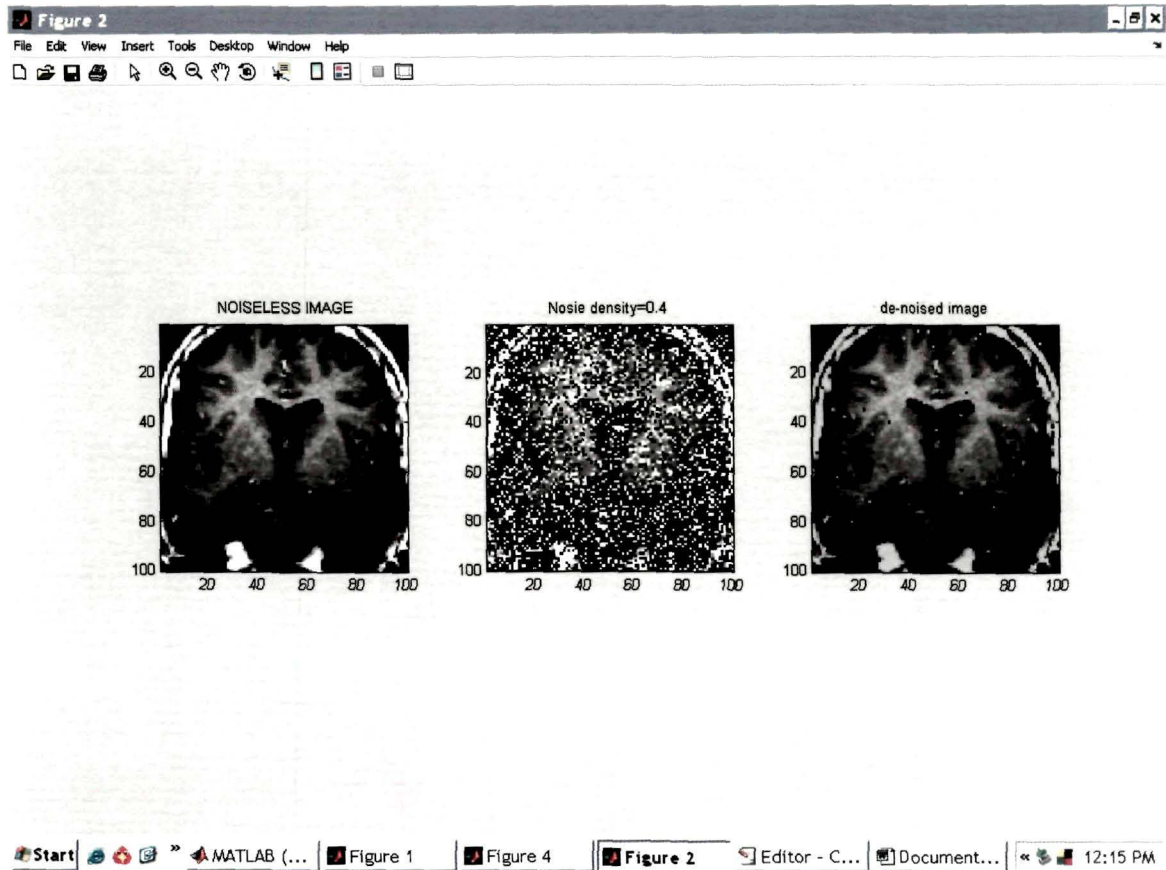
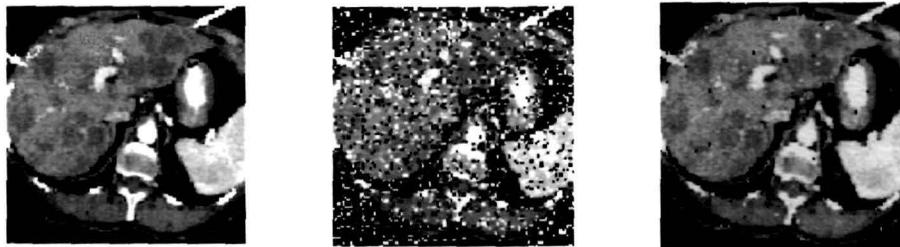


Figure 5.12: Matlab window showing the true image, noisy image and the denoised image.



Figure 5.13: (a) Original images, (b) noisy images (with densities of 10%), and (c) the denoised SPECT image.



(a)

(b)

(c)

Figure 5.14: (a) Original images, (b) noisy images (with densities 20%, 30% and 40%), and (c) the denoised images.

5.9 Performance Evaluation

To test the performance of the developed ANN, the network has been tested with a standard Lena image [78]. This Lena image is corrupted with noise with different densities and fed to the neural network. Once the output of the network is obtained, its PSNR is calculated. This PSNR is then compared with the PSNR obtained by different filters for Salt and Pepper Noise (SPN) corrupted image 'Lena'. The comparison is shown in the following table 6.2.

Table 5.2 : Comparison of the different methods

SPN Density %	MED 3*3 [dB]	MED 3*5 [dB]	Fuzzy [79] (dB)	SD-ROM [20] (dB)	MMEM [68] (dB)	Proposed ANN (dB)
10	34.25	31.23	37.88	38.98	38.60	39.6794
20	29.25	30.60	34.19	36.55	36.76	37.47
30	23.85	29.72	31.19	33.43	35.41	35.7448
40	19.18	28.21	28.00	29.88	34.32	34.49446
50	15.28	24.44	24.97	26.04	32.97	33.0319
60	12.31	19.09	21.66	21.97	31.76	31.8060
70	9.95	14.16	18.27	18.12	30.29	30.8145

The PSNR at other noise densities have been found out to be:

Table 5.3 : PSNR of the proposed method at different noise densities

SPN Density %	Calculated using ANN
5	40.8577
15	38.3983
25	36.3983
35	34.9141
45	33.4713
55	32.4871
65	31.1330
75	30.2133

The following graph demonstrates the performance of the respective filters and the developed neural network :

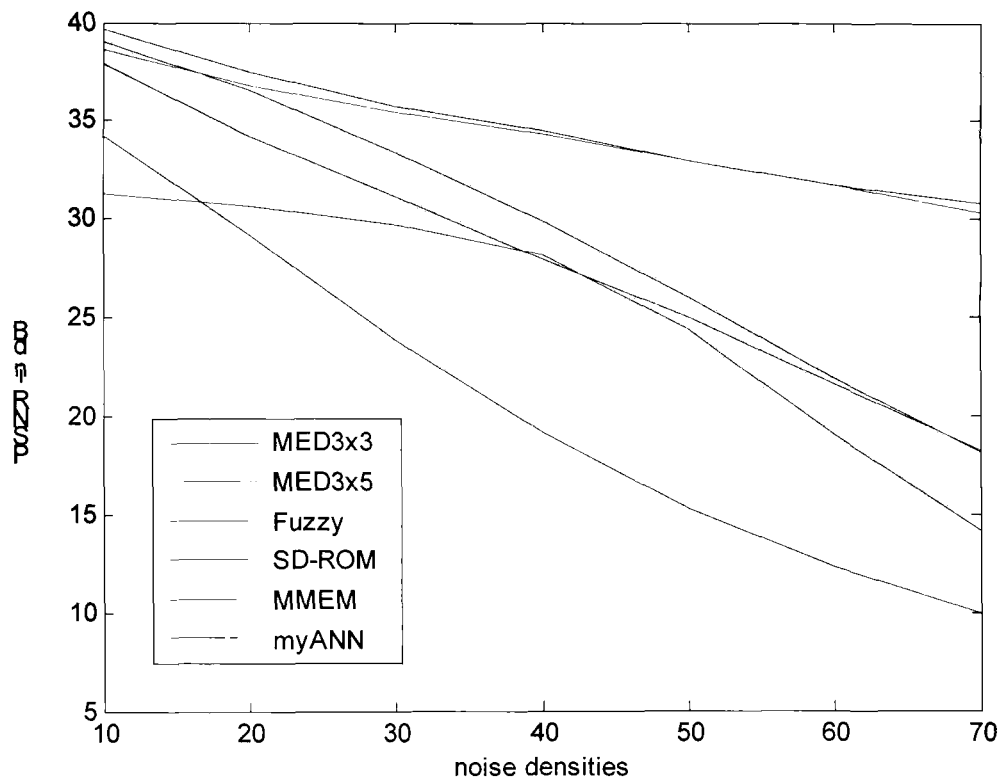


Figure 5.15. : Comparison of the proposed technique with other methods.

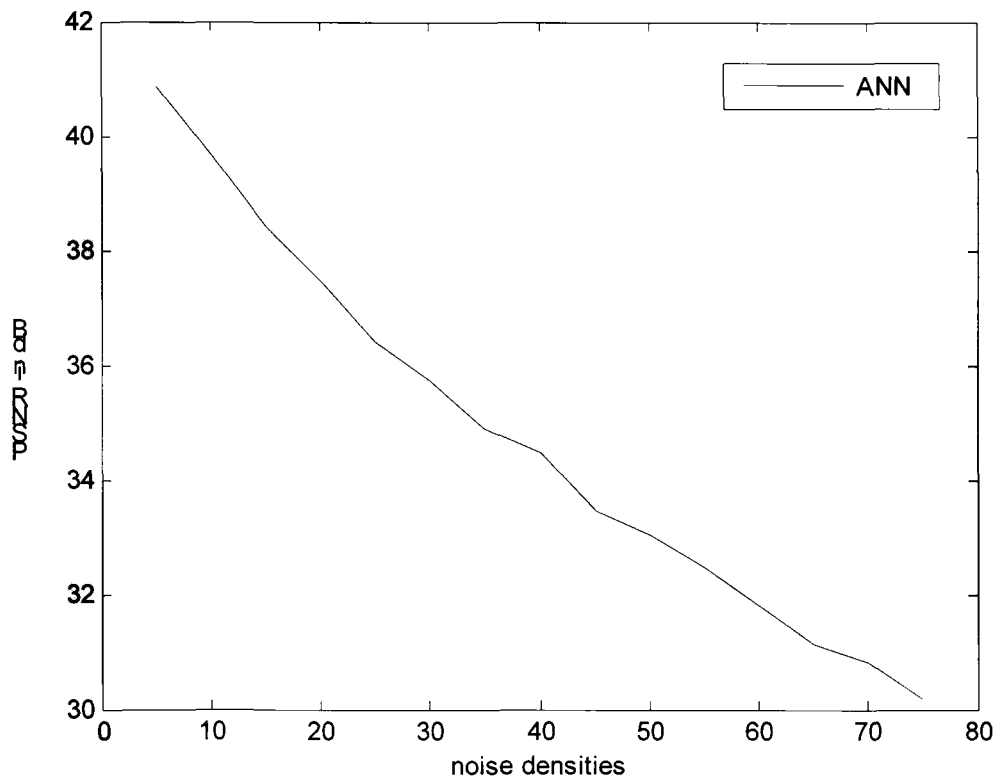


Figure 5.16: Performance of the neural network at different noise densities in percentage.

5.10 References

- [1]. Yiqui Dong, Raymond H Chang, and Shufang Xu, "A detection statistic for random-valued impulse noise" *IEEE Transactions on Image Processing*, vol. 16, No. 4, pp. 1112-1119, April 2007.
- [2]. Max Mignotte, "Image denoising by Averaging of Piecewise constant simulations of Image partitions", *IEEE Transactions on Image Processing*, vol. 16, No. 2, pp. 523-533, February 2007.
- [3]. A. K. Jain, *Fundamentals of digital Image Processing*, Englewood Cliff, N.J.: Prentice Hall, 1989.
- [4]. R. C. Gonzalez and R.E. Woods, *Digital Image Processing*, Addison-Wesley Longman Inc., 2000.
- [5]. W. K. Pratt, *Digital Image Processing*, NY: John Wiley & Sons, 2001.
- [6]. Pitas and A. N. Venetsanopolous, *Nonlinear Digital Filters: Principles and applications*, Norwell, M. A., Kluwer, USA, 1990
- [7]. T. S. Huang, G. J. Yang, and G. Y. Tang, "A Fast Two Dimensional Median Filtering Algorithm", *IEEE Trans on Acoustics, Speech, Signal Processing*, vol. ASSP-27, no.1, February, 1979.
- [8]. E. Ataman , V. K. Aatre, and K. W. Wong , "A Fast Method For Real Time Median Filtering", *IEEE Trans. on Acoustics, Speech, Signal Processing*, vol. ASSP -28 , no.4 , August, 1980.
- [9]. J. S. Lee, "Digital Image Enhancement And Noise Filtering By Use Of Local Statistics", *IEEE Trans. on Pattern Analysis and Machine Intelligence*, vol. PAMI-2, no.2, March, 1980.
- [10]. Pitas and A. N. Venetsanopoulos, "Nonlinear Order Statistics Filters For Image Filtering and Edge Detection", *IEEE Signal Processing*, vol.10, no.4, June, 1986.
- [11]. R. Bernstein, "Adaptive Nonlinear Filter for Simultaneous Removal of Different Kinds of Noise in Images", *IEEE Trans. on Circuits and Systems*, vol.35, no.1, January, 1988.

-
- [12]. Y. H. Lee and S. A. Kassam, "Generalized Median Filtering and Related nonlinear Filtering Techniques", *IEEE Trans. on Acoustics, Speech, Signal processing*, vol. ASSP-33, no.3, June, 1985.
- [13]. X. Z. Sun and A. N. Venetsanopoulos, "Adaptive Schemes for Noise Filtering and Edge Detection by Use of Local Statistics", *IEEE trans. On Circuits and Systems*, vol.35, no.1, January, 1988.
- [14]. Y-Hwan Lee and S. Tantaratana, "Decision –Based Order statistics filters", *IEEE Trans. on Acoustics, Speech, Signal Processing*, vol.38, no.3, March, 1990.
- [15]. J. H. Lin and E. J. Coyle, "Minimum Mean Absolute Error Estimates over the class of Generalized Stack Filters", *IEEE Trans. on Acoustics, Speech, Signal Processing*, vol.-38, no.4, April, 1990.
- [16]. J. H. Lin, T. M. Sellke, and E. J. Coyle, "Adaptive Stack Filtering under the Mean Absolute error Criterion", *IEEE Trans. on Acoustics, Speech, Signal Processing*, vol.38, no.6, June, 1990.
- [17]. Lin Yin, J. Astola, and Y. Neuvo, "A New Class of Nonlinear filters- Neural Filters", *IEEE Trans.on Signal Processing*, vol.41, no.3, March, 1993.
- [18]. H. Hwang and R. A. Haddad, "Adaptive Median Filters: New Algorithms and Results", *IEEE Trans. on Image Processing*, vol. 4, no.4, April 1995.
- [19]. F. Russo and G. Ramponi, "A Fuzzy Operator for the Enhancement of Blurred and Noisy Images", *IEEE Trans. on Image Processing*, vol.4, no.8, August, 1995.
- [20]. E. A. Michael Lightstone, S.K. Mitra, and K. Arakawa, "A New Efficient Approach for the Removal of Impulse Noise from Highly Corrupted Images", *IEEE Trans. on Image Processing*, vol.5, no.6, June, 1996.
- [21]. Y. Li and F. Santosa , "A Computational Algorithm for Minimising Total Variation in Image Restoration", *IEEE Trans. on Image Processing*, vol.5, no.6, June, 1996.
- [22]. R. Malladi and J. A. Sethian, "A unified approach to Noise Removal, Image Enhancement and Shape Recovery", *IEEE Trans. on Image Processing*, vol.5, no.11, November, 1996.

-
- [23]. Kotropoulos and I. Pitas, "Adaptive LMS L-Filters for Noise suppression in images, *IEEE Trans. on Image Processing*", vol.5, no.12, December, 1996.
- [24]. R .P. Kleihorst , R .L.Lagendijk and Jan Biemond , "An Adaptive Order Statistic Noise Filter For Gamma Corrected Image Sequence", *IEEE Trans. on Image Processing*, vol.6, no.10, October, 1997.
- [25]. W. H. Lau, F.L. Hui, S.H. Leung and A. Luk, "Blind Separation of Impulsive Noise from Corrupted Audio Signal", *Electronics Letter*, vol.32, no.3, pp.166-168, Feb., 1996.
- [26]. Ralph Sucher, "A New Adaptive nonlinear filtering Algorithm", *Proceedings of IEEE, International Conference on Signal Processing, Circuits & Systems*, pp. 1-4, Singapore, July 1995.
- [27]. Neirman, P.Heinonen and Y. Neuvo, "A New Class of Detail Preserving Filters for Image Processing", *IEEE Trans. on Pattern Analysis, Machine Intelligence*, vol. PAMI-9, pp. 74-90, January,1987.
- [28]. S. J. Ko, Y.H. Lee, "Centre weighted Median Filters and their Applications to Image Enhancement", *IEEE Trans. on Circuits and Systems*, vol. 38, pp. 984-983, September 1991.
- [29]. E. J. Coyle, J. H. Cin and M. Gabbouj, "Optimal stack filtering and the estimation of structural approaches to Image Processing", *IEEE Trans. On Signal Processing*, vol. 37, pp. 2037-2066, December,1989.
- [30]. T. Chen, H. R. Wu, "Space variant Median Filters for restoration of Impulse Noise Corrupted images", *IEEE Trans. on Circuits and Systems – II, Analog and Digital Signal Processing*, vol. 48, no. 8, pp. 784-789, August, 2001.
- [31]. T. Chen, K. K. Ma and L. H. Chen, "Tri-state Median filter for Image Denoising", *IEEE Trans. on Image Processing*, vol. 8, pp.1834-1838, December, 1999.
- [32]. P. S. Windyga, "Fast Impulsive Noise Removal", *IEEE Trans. on image Processing*, vol.10, no. 1, pp.173-179, January, 2001.
- [33]. S. R. Kim and A. Effron, "Adaptive robust impulse noise Filtering", *IEEE Trans. on Signal Processing*, vol.43, no.8, pp.1855-1866, August, 1995.

-
- [34]. R. Sucher, "Removal of impulse noise by selective filtering", *Proceedings of IEEE International Conference on Image Processing*, vol.2, pp.502-506, Austin, November,1994.
- [35]. T. Chen and H. R. Wu, "Adaptive Impulse Detection Using Centre-Weighted Median Filters", *IEEE Signal processing Letter*, vol.8, no.1, January, 2001.
- [36]. E. Abreu, M. Lightstone, S. K. Mitra, K. Arakawa, "A new Efficient approach for Removal of impulse noise from highly corrupted images", *IEEE Trans. on Image Processing*, vol.5, no.6, pp. 1012-1025, June,1996.
- [37]. B. Hazma and H. Krim, "Image Denoising: A nonlinear robust statistical approach", *IEEE Trans. on Image processing*, vol.49, no.12, pp. 3045-3054, Dec, 2001.
- [38]. L. A. Zadeh, "Fuzzy Sets", *Information and control*, vol.8, pp. 338-353, 1965.
- [39]. L. A. Zadeh, "Fuzzy Logic", *IEEE Computer Magazine*, pp. 83-93, April, 1988.
- [40]. M. Janshidi, N. Vedic, T. Ross, *Fuzzy Logic & Control: software and hardware Applications*, Prentice Hall Inc., 1993
- [41]. J. Klir, B. Yuan, *Fuzzy Sets and Fuzzy Logic: Theory and Applications*, Prentice Hall Inc., 1995.
- [42]. J. Yen, R. Langari, *Fuzzy Logic: Intelligence, Control and Information*, Prentice Hall Inc., 1999.
- [43]. J. Mendel, *Uncertain Rule-Based Fuzzy Logic Systems: Introduction and New Directions*, Prentice Hall Inc., 2001.
- [44]. F. Russo, "Evolutionary Neural Fuzzy System for Noise Cancellation in Image Processing", *IEEE Trans. Inst & Meas.*, vol. 48, no. 5, pp. 915-920, Oct. 1999.
- [45]. F. Farbiz, M. B. Menhaj, S.A. Motamedi and M.T. Hagan, "A new Fuzzy logic Filter for Image Enhancement", *IEEE Trans. on Syst. Man, Cybern.B*, vol. 30, pp. 110-119, Feb. 2000.
- [46]. *Cybernetics – Part B: Cybernetro*, vol.30, no.1, pp. 110-119, Feb 2000.
- [47]. F. Russo, "Noise Removal from Image data using recursive Neuro-fuzzy filters", *IEEE trans on Inst & Meas*, vol. 49, no.2, pp.307-314, April 2000.

-
- [48]. F. Russo, "An Image Enhancement Technique Combining Sharpening and Noise Reduction", *IEEE Trans on Int & Meas*, vol. 51, no.4, pp.824-828, Aug 2002.
- [49]. H. K. Kwan and Y. Cai, "Fuzzy Filters for Image Filtering", *Proc. Of Circuits and Systems, MWSCAS-2002, The 2002 45th Midwest Symposium*, vol.3, pp. III-672-675, August 2002.
- [50]. M. Ma, X. Jiao and X. Tan, "Fuzzy Hybrid filter for Removal of Impulsive Noise from Highly Corrupted Images", *Proceeding of IEEE Conf. TENCON'02* pp.885-888, 2002.
- [51]. Y. Hawwar and Ali Reza." Spatially Adaptive Multiplicative Noise Image Denoising Technique", *IEEE Trans. on Image Processing*, vol. 11, no.12, pp. 1397-1404, Dec 2002.
- [52]. D.V.D. Ville, M. Nacetegael, D.V. Wekan, E.E. Kere, W. Philips, I. Lemahiev, "Noise Reduction by Fuzzy Image Processing", *IEEE Trans. On Fuzzy systems*, vol.11, no.4, pp. 429-436, Aug 2003.
- [53]. F. Russo and A. Lazzari, "A robust approach based on hybrid Fuzzy Networks for Removing Impulse noise from Images", *Proceedings of IEEE Conf. on Inst & Meas Technology IMTC-2003*, Vail, CO, USA, pp. 545-550., 20-22 May 2003.
- [54]. F. Russo, " A Method for Estimation of Filtering of Gaussian Noise in Images", *IEEE Trans. on Inst & Meas*, vol 52, no.4, pp. 1148-1154, Aug 2003.
- [55]. Russo F., and Ramponi G., "A Fuzzy Filter for Images corrupted by Impulse Noise", *IEEE Signal Processing Letters*, vol-3, no. 6, pp. 168-170, June 1996.
- [56]. J. C. Patra, G. Panda, R. N. Pal, and B. N. Chatterjee, "Neural Networks for signal Processing Applications", *Journal of Computer Science and Informatics*, India, vol.27, no.3, pp.24-34, September, 1997.
- [57]. Simon Haykin, *Neural Networks, A Comprehensive Foundation*, Prentice Hall International Inc., 1999.
- [58]. B. Widrow , "Adaptive Filters" in *Aspects of Neural Network and System Theory*, ed. R.E. Kalman and N.Declaris, Holt, Rinehart and Winston, New York.

-
- [59]. X. P. Zhang, "Thresholding Neural Network for Adaptive Noise Reduction", *IEEE Trans. Neural Network*, vol. 12, no. 3, pp. 567-584, May. 2001.
- [60]. G. Panda, B. Majhi, and P. K. Dash, "A Novel Impulse Filtering Scheme for Corrupted Image using ANN Detector", *Proceedings, Int. Conf. on Communications, Computers, & Devices (ICCCD-2000)*, IIT, Kharagpur, pp. 603-606, December, 14-16, 2000.
- [61]. D. L. Donoho and I. M. Johnstone, "Ideal Spatial Adaptation by Wavelet Shrinkage", *Biometrika*, vol. 81, pp. 425-455, 1995.
- [62]. Daubechies, "The Wavelet Transform, Time-Frequency Localization and Signal Analysis", *IEEE Trans. on Information Theory*, vol. 36, pp.961-1005, 1990.
- [63]. N. Weyrich and G. T. Warhula, "Wavelet Shrinkage and Generalized Cross Validation for Image Denoising", *IEEE Transaction, Image Processing*, vol. 7, no. 1, pp. 82-90, Jan. 1998.
- [64]. M. L. Hilton and R. T. Ogten, "Data Analytic Wavelet Threshold Selection in 2-D Signal Denoising", *IEEE Transaction, Signal Processing*, vol. 45, no. 2, pp. 496-500, Feb. 1997.
- [65]. S. G. Chang, B. Yu, and M. Vetterli, "Adaptive Wavelet Thresholding for Image denoising and Compression", *IEEE Transaction, Image Processing*, vol. 9, no. 9, pp. 1532-1546, 2000.
- [66]. D. L. Donoho, "Denoising by soft-thresholding", *IEEE Trans. On Information Theory*, vol.41, pp. 613-627, May,1995.
- [67]. S. G. Chang, B. Yu, and M. Vetterli, "Spatially Adaptive Wavelet Thresholding with Context Modeling for Image Denoising", *IEEE Transaction, Image Processing*, vol. 9, no. 9, pp. 1522-1531, Sept. 2000.
- [68]. W-Y. Han and J-C. Lin, "Minimum-maximum exclusive mean (MMEM) filter to remove impulse noise from highly corrupted images", *IEE Electronics Letters*, vol. 33, no. 2, pp 124-125, Jan 1997.
- [69]. H-L Eng and K-K Ma, " Noise Adaptive Soft switching Median Filter", *IEEE Trans. on Image Processing*, vol.10, no.2, pp. 242-251, Feb 2001.

- [70]. T. Chen and H. R. Wu, "Space Variant Median Filters for Restoration of Impulse Noise Corrupted Images", *IEEE Trans. on CAS-II, A & D SP*, vol.48, no.8, pp.784-789, Aug 2001.
- [71]. M. Ma, X. Jiao and X. Tan, "Fuzzy Hybrid filter for Removal of Impulsive Noise from Highly Corrupted Images", *Proceeding of IEEE Conf. TENCON'02*, pp.885-888, 2002.
- [72]. Aizenberg and C. Butakoff, "Effective Impulse Based on Rank Order Criteria", *IEEE Signal Processing Letters*, vol.11, no.3, pp.363-366, Mar 2004.
- [73]. V. Crnojevic, V. Senk and Z. Trpovski, "Advanced Impulse Detection Based on Pixel-Wise MAD", *IEEE Signal Proc. Lett.*, vol.-11, No.-7, pp. 589-592, July 2004.
- [74]. Max Mignotte, "Image Denoising by Averaging of Piecewise Constant Simulations of Image Partitions", *IEEE Transactions on Image Processing*, vol. 16, No. 2, pp. 523-533, Feb 2007.
- [75]. A.N. Netravali and B.G. Haskell, *Digital Pictures: Representation, Compression, and Standards (2nd Ed)*, Plenum Press, New York, pp. 602, 1995.
- [76]. K. K. Parhi, F. H. Wu , K. Genesan, "Sequential and Parallel Neural Network Vector Quantizers", *IEEE Transactions on Computers*, vol. 43 no.1, pp.104-109, Jan. 1994.
- [77]. V Rao and H Rao , *C++ Neural Networks and Fuzzy Logic*, BPB, New Delhi, pp. 336, 1996.
- [78]. Lena image :: <http://giga.cps.unizar.es/~spd/pub/img/lena/Lena.png>
- [79]. Russo F., and Ramponi G., "A Fuzzy Filter for Images corrupted by Impulse Noise", *IEEE Signal Processing Letters*, vol-3, no. 6, pp. 168-170, June 1996.

Chapter 6

Lesion Detection in SPECT Cardiac images

- 6.1 Introduction
- 6.2 Literature survey
- 6.3 Fast Neural Networks
- 6.4 Proposed & Developed Method
- 6.5 Results
- 6.6 Conclusion
- 6.7 References

6. Lesion Detection in SPECT Cardiac images

6.1 Introduction

Among all forms of illness, coronary artery disease (CAD) is the single greatest cause of morbidity and mortality in the world at large [1, 2]. Early detection of any lesions in cardiac is effective to reduce the number of death caused by coronary artery disease. Current diagnostic methods include Single Photon Emission Computed Tomography (SPECT), echocardiography, Positron Emission Tomography (PET), Computed Tomography (CT), and Magnetic Resonance Imaging (MRI). Each of these modalities has its advantages and limitations [3]. In recent years, MRI has been found useful to assess myocardial perfusion, but it is compromised in the presence of pacemakers, defibrillators and other metallic devices [4, 5]. In addition to this, like myocardial PET, cardiovascular MRI remains expensive and is less accessible than SPECT [6]. Myocardial perfusion imaging with SPECT, in which the gamma camera or the scintillation camera rotates around the entire torso, remains critically important tool for diagnosing, assessing and evaluating treatment of coronary artery disease[7]. Further, because of SPECT's ability to perform attenuation correction, the lesion-to-background contrast is higher in SPECT [8]. However, it suffers from prolonged study times because of relatively low detection efficiency.

Computer-aided interpretation of diagnostic images has gained much interest in the fields of radiology, nuclear medicine and magnetic resonance imaging [9, 10]. Development of these kinds of systems leads to valuable diagnostic tools that may largely assist physicians in the identification of lesions in an image. Computer technology can also be used to support non-experts with a preliminary interpretation in those situations in which experts are not present. These systems improve expert's ability to identify abnormal regions in cardiac image while decreasing the need for aggressive intervention and enhancing the capability to make accurate diagnosis [11, 12].

Interpretation of diagnostic images is a pattern-recognition task, the result of which generally cannot be encapsulated in a set of criteria. Specially, in nuclear medicine, clinical assessment and diagnosis are generally based on qualitative assessment of the distribution pattern of radiotracers used [13]. Consequently,

conventional rule-based expert systems have achieved only limited success in this area. Artificial neural networks represent a computer-based decision method that has proved to be of special value in pattern recognition tasks [14, 15, 35, 36, 37]. It is, therefore, of interest to evaluate the feasibility of using artificial neural networks for interpretation of medical images.

Problem Statement :

The current research focuses on the detection of a cold lesion from a cardiac SPECT image using fast neural network (FNN). Hence, the task is to detect a cold lesion of 1.0 cm in radius at any unknown location of the image. So, if a lesion is present, the out put of the FNN should be 1 or else 0 (in the absence of a lesion). The output of the FNN should be able to specify the location of the lesion in the image. To take care of the false detection (a false positive or a false negative), a simple conventional error back propagation is used. A post processing algorithm is used to reconstruct the image after the detection algorithm is run.

The detection scheme consists of two different parts: detection of lesion and false detection elimination processing.

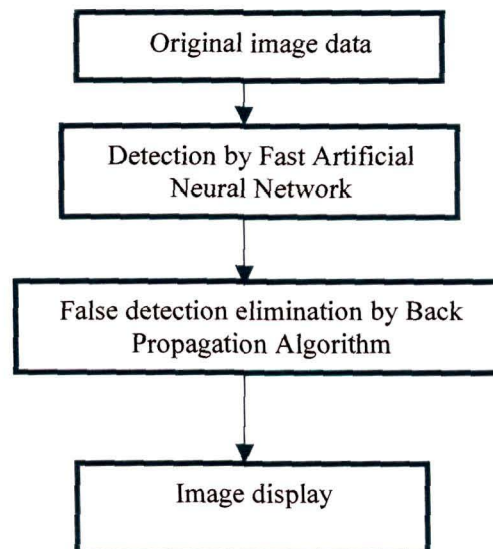


Figure. 6.1 Overview of the work to be done.

6.2 Literature survey

Algorithms and the construction of social cognitive maps, with interesting properties in collective memory, collective decision-making and swarm pattern detection have inspired many researchers to use these techniques for their research problems [17-20]. David Hamilton *et al.* [21] have tried to use a feed forward neural network to extract patterns from bull's eye data to predict lesion presence. They used this technique to classify patterns from bull's eye myocardial perfusion images and detect the presence of hypoperfused areas. In their work, [22] lesion were indicated by two detection process by GA template matching and ANN technique which yielded 77% sensitivity and 2.6% False Positive per image.

In a slightly different study, Metin Akay in his paper [23] has reported his results of detecting coronary artery disease noninvasively using neural networks. He used feature set based on poles and power spectral density function (PSD) of Autoregressive (AR) method after Adaptive Line Enhancement (ALE) method and his method correctly identified 84% of the subjects with CAD and 89% of the normal subjects. In yet another paper [24], Constantin Tranulis *et al.*, estimated pulmonary arterial pressure using an neural network. He claimed to achieve accuracy as high as 97%.

Most of the object detection problems have been solved with proper choice of the algorithm and a proper selection of features. In [25], GA has been used for selecting good subsets of features that leads to improved detection rates. Of late a convolutional neural network has been used for face detection [26]. But the problem with neural networks is that the computational complexity is very high because the networks have to process many small local windows in the images [38, 39]. Some authors have tried to speed up the detection process of the neural networks [20, 40, 41]. To reduce the computational time, Bakry combined both fast and cooperative modular networks to enhance the performance of the detection process [27] and he identified faces in cluttered scenes. In their paper [28], Zuo and deWith used successive face detectors in cascade and got an average of 92% detection rate. A fast neural network has been used for face detection [29- 32], but up till now no work that uses Fast neural network has been

reported for the detection of a lesion in cardiac SPECT image. In this thesis, a fast neural network combined with conventional error back propagation network for the elimination of false detection is proposed. This method accurately detects any cold lesion (along with its position) present in the left ventricle of the images acquired from Single Photon Emission Computed Tomography (SPECT) scanner.

6.3 Fast Neural Networks

Fast neural network is used here to detect any positive detection including false detection. This FNN is developed on two dimensional cross- correlation between the whole image of left ventricle (LV) and a sliding window with a defined size. Elements of this window may be thought of as the neural network situated between the input/output & the hidden layer. This cross correlation is nothing but product in frequency domain.

For detection, a sliding window, or a mask γ of size $N \times N$ is decided . The test image of size $A \times B$ is fed to the neural network. Let Φ_i is the vector of neural weights of size $M \times N$ between the input image and the hidden layer, then, the output of the hidden neurons Y_i , can be written as [33]:

$$y_i = f\left[\sum_{y=1}^M \sum_{x=1}^N \Phi_i(x, y)\gamma(x, y) + b_i\right] \quad 6.1$$

where f is the activation function and the bias is of hidden neuron denoted by b_i . The above equation is the output of sub-image γ . So for the entire image, the output will take the form [33]:

$$y_{i,Global} = f\left[\sum_{y=-N/2}^{N/2} \sum_{x=-N/2}^{N/2} \Phi_i(x, y)\lambda(b+x, a+y) + B_i\right] \quad 6.2$$

This above equation shows the cross-correlation. Hence it follows that [31],

$$y_{i,Global} = f(\Phi_i \otimes \chi + B_i) \quad 6.3$$

Here, $Y_{i,Global}$ is the activity of the i^{th} hidden unit for the entire Left Ventricle image,

In Fourier domain [32],

$$\chi \otimes \Phi_i = F^{-1}(F(\chi) \cdot \hat{F}(\Phi_i)) \quad 6.4$$

This cross correlation makes the computation faster as compared to the conventional neural networks.

The final output of the network can be found out to be [33] :

$$P = f(W_j^o \sum_{j=1} f(W_j^h \sum_{i=1} f(\chi \otimes \Phi_i' + B_i') + B_j^N) + B^o) \quad 6.5$$

Here, the final output is P . W^o , W^h , Φ_i are the weights of the output layer, hidden layer and the input layer. As it is a 3 layer or in other words, a multilayer perceptron, equation (3) is substituted into the activity of neuron of each layer. The final output is in the form of a matrix. Hence, by evaluating this cross correlation, a speed up ratio can be obtained compared to conventional neural networks.

The behavior of the neural networks can be accelerated during the search process [42]. The speed up of the detection process can be achieved by normalization in the frequency domain which in turn can be achieved by either normalizing the subimages of the input image or the weight matrix [43]. But normalization of an image through normalization of weights is faster than normalization of each subimage. Besides, normalization of weights can be done offline. So, normalization of weights is a better choice to get a speed up ratio. By using weight normalization, the speed up ratio for image normalization S can be calculated as [43] :

$$S = O\left(\frac{(N-n+1)^2}{q}\right) \quad 6.6$$

where, q is the number of neurons in the hidden layer, $N \times N$ is the size of the image and $n \times n$ is the size of the subimage.

6.4 Proposed Method

The large data content in diagnostic images causes problems in training the neural networks. So, some preprocessing at the very beginning has been done to

reduce the data size. SPECT image data have been acquired from the Medical Imaging Research Laboratory (MIRL), Dept. of Radiology, University of Utah, USA and from the internet [44-61]. The color images are converted into corresponding gray level images.

Artificial neural networks learn by example. The number of examples needed for network training depends on the size of the network. A large network that is fed with many input variables needs many examples to be trained properly. Images, especially in radiology, in nuclear medicine and magnetic resonance imaging, contain large numbers of pixels. A commonly used image matrix in a scintigram is 256×256 , i.e., 65,536 pixels. If all these pixel values are fed to a neural network, thousands of examples would be needed [34]. A substantial data reduction must, therefore, be performed, with out loss of relevant information, before training the network. The size of the SPECT images varied from 72×77 to 87×95 . So, the images after gray level conversion have been preprocessed to remove the unwanted background (as shedding off the unwanted information saves some execution time) by rejecting pixel values outside the region of interest in the main image. This is done using an edge detection technique that determines the boundary of the LV. The minimum and maximum x- and y- coordinates of this boundary decide the rectangle

that houses the LV. This minimum and maximum (x,y) points are used to reduce the images to a standard size of 50×40 pixels.

The reduced image is then processed through a fast neural network to find out if any lesion is present within the boundary region. A lesion, we define, as a window having a size of 3×3 , 2×3 , 3×2 pixel or more with a defined intensity level. This window is then multiplied in frequency domain with the input image. The weight matrix has been normalized. The output layer consists of five neurons; one to indicate the presence or absence of the lesion, two neurons to give the x and y position of the lesion (x_{start} and y_{start}) and two more neurons to give the distant in the x and y direction (x_{dist} and y_{dist}). These values, x_{start} , y_{start} , x_{dist} and y_{dist} are need during the post processing to localize the lesion. The activation function used in

all the neurons is a logsigmoid function but for the output, a threshold is used to give a binary output of 0 or 1 to indicate the presence or absence of the lesion.

The output of the FNN may consist of positive and false detection. As in medical imaging, any false detection is to be avoided, therefore, Error Back Propagation Neural Network (EBPNN) is designed. The output of the Fast Neural Network is fed as the input to the EBPNN. Sigmoid function is used as an activation function. The network consists of one input layer, one hidden layer and one output layer. It has one neuron in the input layer apart from a bias. The hidden layer contains three neurons and the output layer contains one neuron that encoded whether Coronary Artery Diseases (CAD) is present or not. During the training process, the connection weights between the neurons are adjusted using the back-propagation algorithm. The sigmoid activation function is used. The learning rate is fixed initially at 0.2. During the training, it is decreased between epochs. The momentum is set to 0.5. The network weights are initiated with random numbers using the rand instruction of MATLAB. Training is terminated for an error value of 0.0001. The code has been developed using MATLAB.

In post processing, the x_{start} , y_{start} , x_{dist} and y_{dist} are used to approximate the size and location of the lesion by drawing a rectangle starting at (x_{start}, y_{start}) with its length as $x = x_{dist} + 4$ and $y = y_{dist} + 4$. This rectangle is then superimposed on the original input image to get the final image. Thus, these four outputs highlight the lesion. In this way, post processing helps to visualize the lesion within the image.

6.5 Results

Images for this work are collected from MIRL, Dept. of Radiology, UTAH, USA and downloaded from the internet [45 – 62]. 450 slices of emission images of SPECT for the left ventricle of different patients have been considered for the purpose. Out of these 450 images, 300 are without lesion and rests are with lesion. Testing of the neural networks has been done with 345 images: 248 are without

lesion [61] and 97 are with lesion. The network has been tested with 105 images, of which 69 are with out lesion and 36 are with lesion. Some of the images are presented below out of which some images have lesion. Fig. 6.2 shows the original images. Fig 6.3 (a) and (b) show the grey level resized images. And the final output is shown in fig. 6.6.

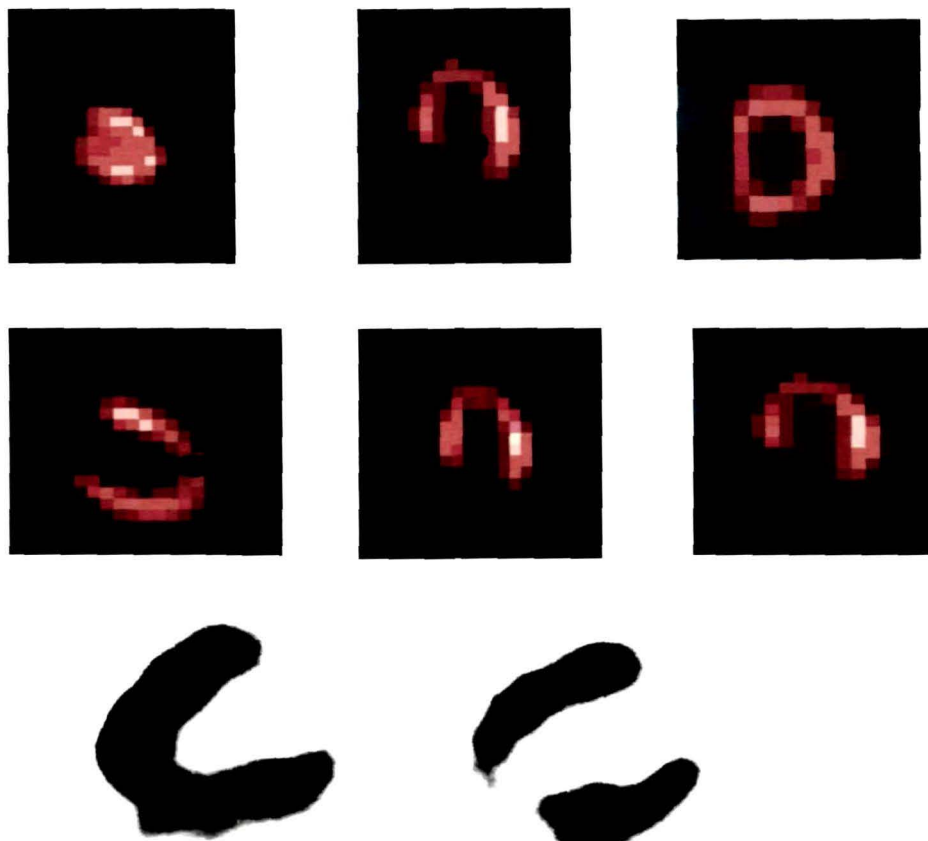


Figure 6.2(a): Some of the original images that have been considered for our work.

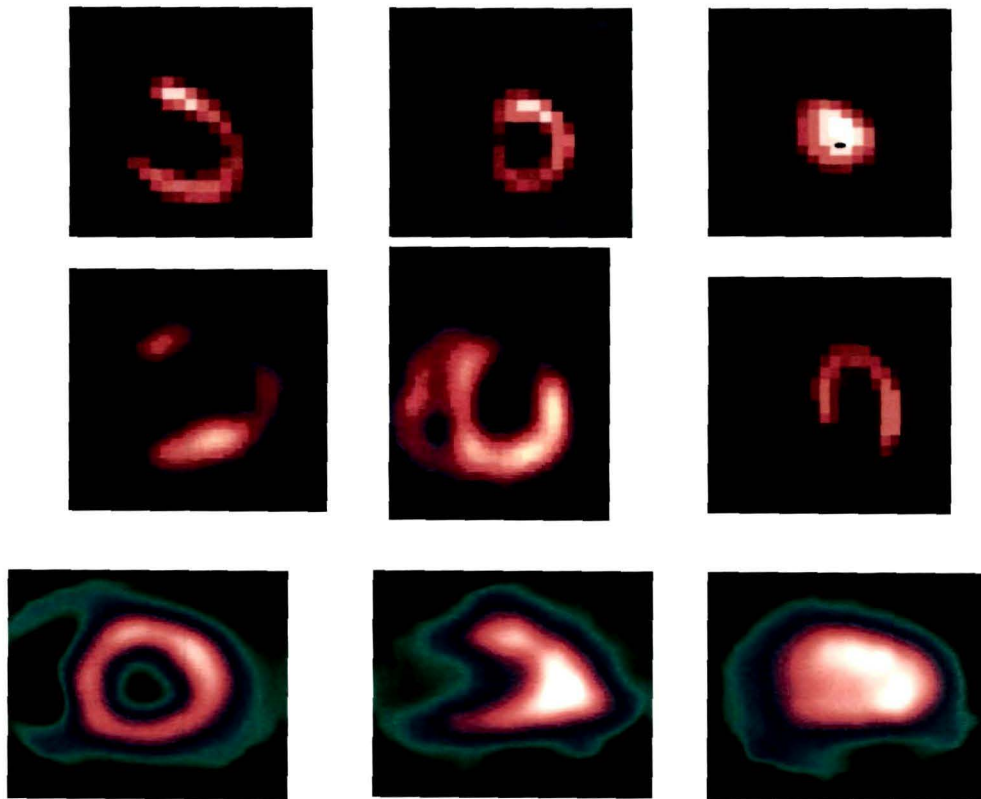
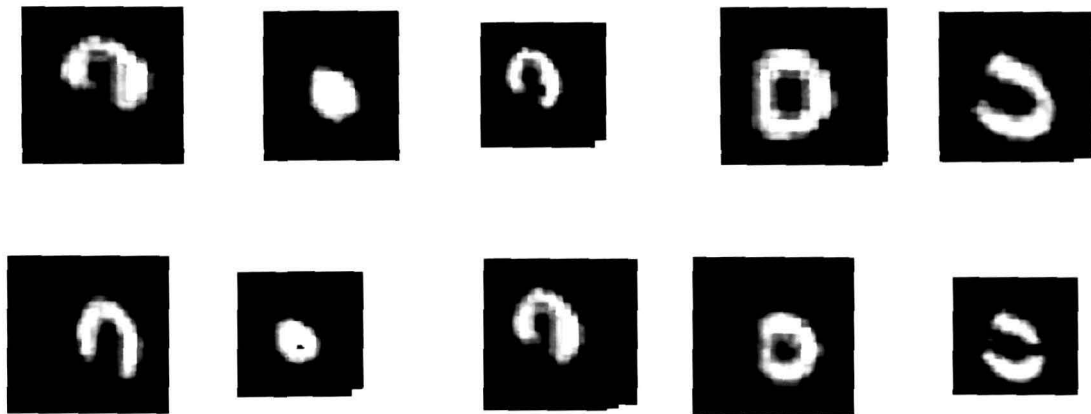
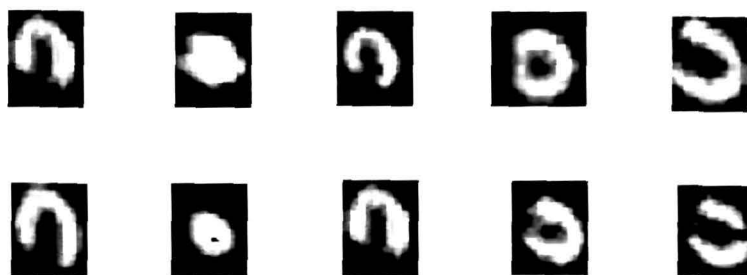


Figure 6.2(b): Some of the original images considered for the work.



(a)



(b)

Figure 6.3: Images resized after converting them to their grey level; (a) grey level conversion using MATLAB, (b) resized to 50x40 image matrix.

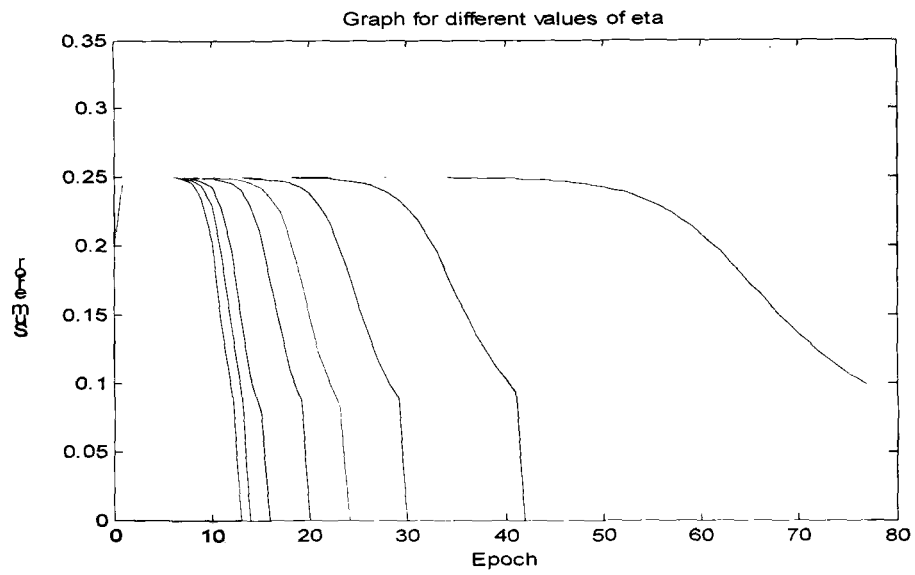


Figure 6.4: Graph for different values of Eta

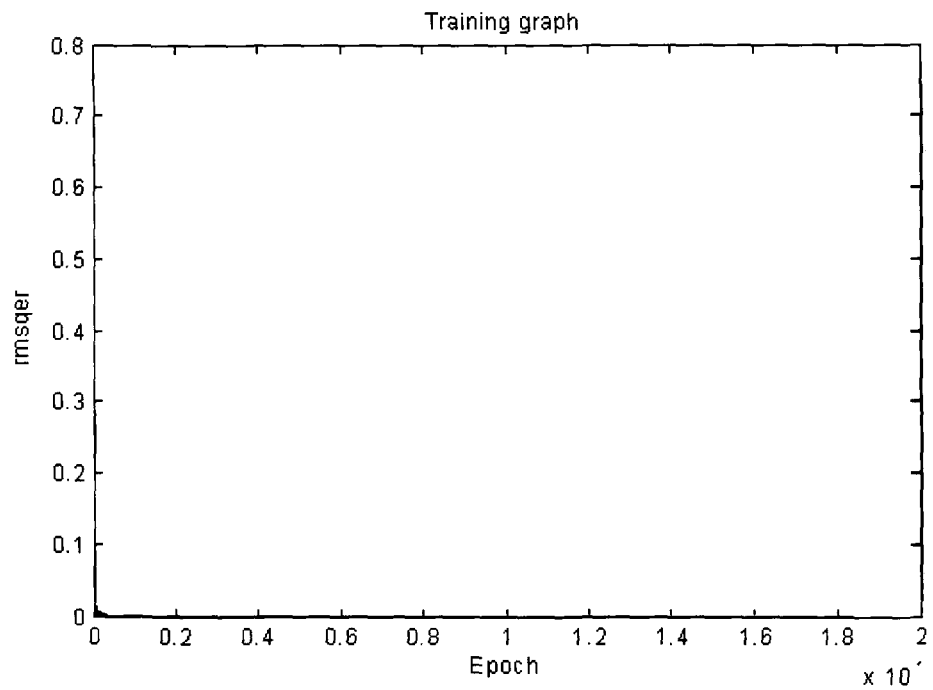


Figure 6.5: Graph showing the convergence of the network.

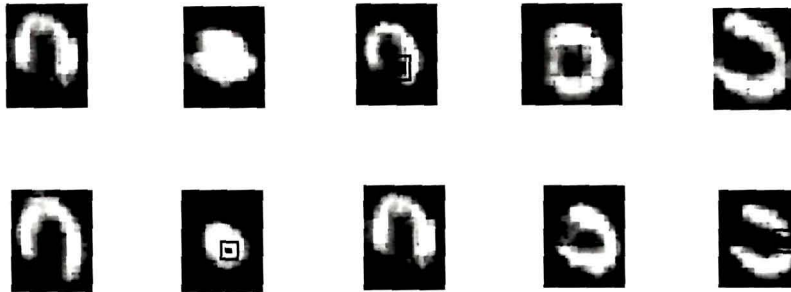


Figure 6.6: Images after the post processing.

Speedup Ratio

Fast Neural Network takes less computation as compared to that of conventional Neural network as seen in the figure 6.7.

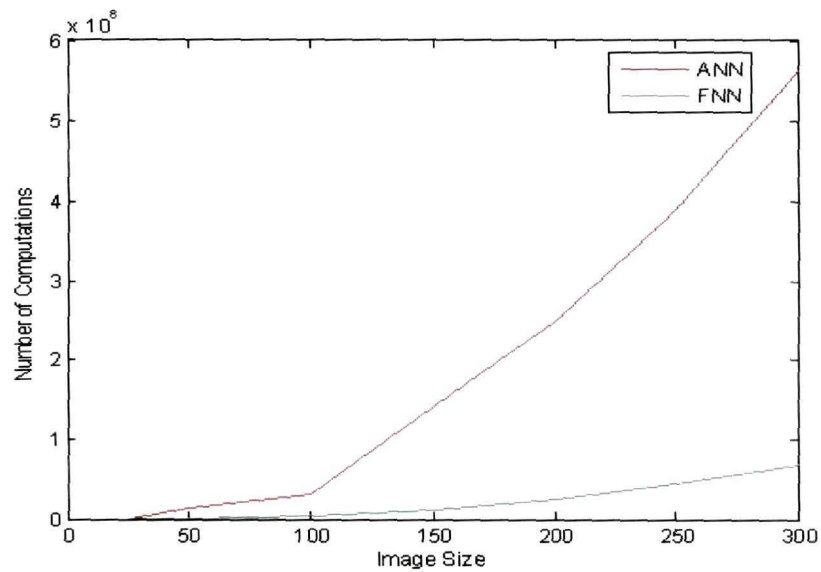


Figure 6.7: Comparison between Artificial Neural Network and Fast Neural Network.

In the testing phase, the network gives 4 cases of false alarms, hence the accuracy of the network has been found to be 96.2%. Of these 4 cases, there is one false positive which indicates that the rate of false positive detection is 0.95% and the detection rate of false negative is 2.87%.

6.6 Conclusion

Here, a Fast Neural Network based method of artifact detection combined with a classical network (to take care of false detection) is designed. This approach improves speed and increases the efficiency and accuracy of the detection method. In this work, some manual pre processing of the images have been done in order to standardize the images to a uniform reduced size. However, a smart algorithm can be designed to automatically standardize the images before giving them as input of the first neural network. The output results in terms of detection, false detection etc. shows the potentiality of the proposed method.

6.7 References

- [1]. Underwood SR, Shaw LJ, Anagnostopoulos C, *et. al.* “Myocardial perfusion scintigraphy and cost effectiveness of diagnosis and management of coronary heart disease”, *Heart*, 90 (suppl 5) :v34–v36, 2004.
- [2]. Beller GA, Mario S. Verani, MD, “First annual memorial lecture: clinical value of myocardial perfusion imaging in coronary artery disease” *J Nucl Cardiol.* vol. 10, pp. 529–542, 2003.
- [3]. Tobias Funk, Dennis L. Kirch,; John E. Koss, Elias Botvinick, Bruce H. Hasegawa, “A Novel Approach to Multipinhole SPECT for Myocardial Perfusion Imaging”, *the Journal of Nuclear medicine*, vol. 47, no. 4, pp-595-602, 2006.
- [4]. Luechinger R, Zeijlemaker VA, Pedersen EM, *et al.* “In vivo heating of pacemaker leads during magnetic resonance imaging”, *Eur Heart J.* vol. 26, pp. 325–327, 2005.

- [5]. Rozner MA, Burton AW, Kumar A. "Pacemaker complication during magnetic resonance imaging" *J Am Coll Cardiol.*, vol. 45, pp. 161–162, 2005.
- [6]. Garber AM, Solomon NA., "Cost-effectiveness of alternative test strategies for the diagnosis of coronary artery disease", *Ann Intern Med.*, vol. 130, pp. 719–728, 1999.
- [7]. Klocke FJ, Baird MG, Lorell BH, et al. ACC/AHA/ASNC guidelines for the clinical use of cardiac radionuclide imaging: executive summary—a report of the American College of Cardiology/American Heart Association Task Force on Practice Guidelines (ACC/AHA/ASNC Committee to Revise the 1995 Guidelines for the Clinical Use of Cardiac Radionuclide Imaging). *Circulation.* 108: pp. 1404–1418, 2003.
- [8]. Sorensen ES, Zeng GL, and Gullberg GT, "Comparison of SPECT vs. planar imaging for lesion detection" *Conference Record of the 2002 IEEE Nuclear Science Symposium and Medical Imaging Conference, Norfolk, VA*, vol. 3, pp. 1731-1735, Nov. 13-16, 2002.
- [9]. Miller AS. Blott BH. Harnes TK. "Review of neural network applications in medical imaging and signal processing. *Mea Biol Eng Compiti* 1992:30:449-464.
- [10]. Datz FL. Rosenberg C. Gabor FV. et al. "The use of computer-assisted diagnosis in cardiac perfusion nuclear medicine studies: a review" *J Digit Imaging*, vol. 6, pp. 67-80, 1993.
- [11]. S.A. Karkanis, D.K. Iakovidis, D.E. Maroulis, G.D. Magoulas, N.G. Theofanous "Tumor Recognition in Endoscopic Video Images using artificial neural network architecture" *Proceedings of the 26th Euromicro Conference*, vol 2, pp. 423 – 429, 2000.
- [12]. Karkanis, S.A.; Iakovidis, D.K.; Karras, D.A.; Maroulis, D.E. "Detection of lesions in endoscopic video using textural descriptors on wavelet domain supported by artificial neural network architectures" *Proceedings of International Conference on Image Processing*, vol. 2, pp. 833 – 836, 7-10 Oct 2001

- [13]. Zaidi, Habib, Koral, Kenneth, "Scatter modeling and compensation in emission tomography", *European Journal of Nuclear Medicine and Molecular Imaging*, vol. 31, no. 5, pp. 761-782, May 2004.
- [14]. Cross SS, Harrison RF. Kennedy RL. "Introduction to neural networks", *Lancet*; vol. 346, pp. 1075-1079, 1995.
- [15]. Baxt WG. "Application of artificial neural networks to clinical medicine", *Lancet*, vol. 346, pp. 1135-1138, 1995.
- [16]. A. S. Miller, B. H. Blott, and T. K. Hames "Review of Neural Network applications in medical imaging and signal processing", *Journal of Medical and biological Engineering and Computing*, vol. 30, no. 5, pp. 449-464, September 1992.
- [17]. Scott JA, Palmer EL. "Neural network analysis of ventilation-perfusion lung scans", *Radiolog.*, vol.186, pp.661-664, 1993.
- [18]. Fujita H. Katafuchi T. Uehara T. Nishimura T. "Application of artificial neural network to computer-aided diagnosis of coronary artery disease in myocardial SPECT bull's-eye images", *J Nuclear Medicine*, vol. 33, pp. 272-276, 1992.
- [19]. Heden B. Edenbrandt L. Wesley K. Haisty JR. Pahlm "Artificial neural networks for the electrocardiographic diagnosis of healed myocardial infarction", *Im J Cardiol*, vol. 74, pp. 5-8, 1994.
- [20]. Tourassi GD, Floyd CE. Sostman HD. Coleman RE. "Artificial neural network for diagnosis of acute pulmonary embolism: effect of case and observer selection", *Radiologi-* vol. 194, pp. 889-893, 1995.
- [21]. David Hamilton, Peter J Riley, U J Miola, A A. Amro, "A feed forward neural network for classification of bull's-eye myocardial perfusion images", *European Journal of Nuclear Medicine and Molecular Imaging*, vol. 22, no. 2, Feb. 1995.
- [22]. Takeshi Hara, Hiroshi Fujita, Yongbum Lee, Hitoshi Yoshimura, Shoji Kido "Automated Lesion Detection Methods for 2D and 3D Chest X-Ray Images", *Proceedings of the 10th International Conference on Image Analysis and Processing*, pp. 768, 1999.

- [23]. Metin Akay, "Noninvasive diagnosis of coronary artery disease using a neural network algorithm", *Journal of biological Cybernetics*, vol. 67, no. 4, pp.361 – 367, August 1992.
- [24]. Constantin Tranulis, Louis-Gilles Durand, Lotfi Senhadji, and Philippe Pibarot "Estimation of pulmonary arterial pressure by a neural network analysis using features based on time-frequency representations of the second heart sound", *Journal of Medical and Biological engineering and Computing*, vol. 40, no. 2, pp. 205–212, March 2002.
- [25]. Zehang Sun, George Bebis, Ronald Miller, "Object detection using feature subset selection" *Journal of Elsevier on Pattern Recognition*, vol. 37, pp. 2165 – 2176, 2004.
- [26]. Christopher Garcia and Manolis Delakis, "A neural architecture for fast and robust face detection" *IEEE Transactions on Pattern Analysis and Machine Intelligence*, vol. 26, no. 11, pp. 1408-1423, Nov. 2004.
- [27]. Hazem M. El Barky, "Human face detection using new high speed modular neural networks", *Int. Conference on Artificial Neural Networks, Poland*, vol. 3696, pp. 543-550, 2005.
- [28]. Fei Zuo and Peter H N de With, "Fast human face detection using successive face detectors with incremental detection capability" *Proc. Of Electronic Imaging Visual Communications and Image Processing*, vol. 5022, pp. 831-841, 2003.
- [29]. S Ben-Yacoub, B. Fasel and J Leutten, "Fast Face Detection using MLP and FFT", *Proc. Second International Conference on Audio and Video-based Biometric Person Authentication (AVBPA'99)*, Washington, DC, USA, March, pp. 31–36, 1999.
- [30]. B. Fasel, S Ben-Yacoub, J Leutten, "Fast Multi-Scale Face Detection," *IDIAP-Com*, pp. 98-04, 1998.
- [31]. H. M. El-Bakry, "Fast Sub-Image Detection Using Neural Networks and Cross Correlation in Frequency Domain," *Proc. of IS 2004: 14th Annual Canadian Conference on Intelligent Systems, Ottawa, Ontario, 6-8 June, 2004*.

- [32]. Hazem M. El-Bakry "Fast Neural Network for pattern detection usign 2D-FFT" EURASIP Journal on Applied Signal Processing, Issue 13, pp. 2054-2060, 2005.
- [33]. K A Ishak, S A Ahmed, A Hussain and B Y Majlis, "A fast and robust face detection using neural networks", Proceedings of the International Symposium on Information and Communicaiton Technologies, Multimedia University, Putrajaya, Malayasia, vol. 2, pp. 5-8, 2004.
- [34]. Dan Lindahl, John Palmer, Mattias Ohlsson, Carsten Peterson, Anders Lundin and Lars Edenbrandt, "Automated Interpretation of Myocardial SPECT Perfusion Images Using Artificial Neural Networks" the Journal of Nuclear Medicine, vol. 38, no. 12, December 1997.
- [35]. H. M. El-Bakry, "Human iris detection using fast cooperative modular neural networks and image decomposition," Machine Graphics & Vision Journal, vol. 11, no. 4, pp. 498–512, 2002.
- [36]. H. M. El-Bakry, "Automatic human face recognition using modular neural networks," Machine Graphics & Vision Journal, vol. 10, no. 1, pp. 47–73, 2001.
- [37]. S. Baluja, H. A. Rowley, and T. Kanade, "Neural network based face detection," IEEE Trans. Pattern Anal. Machine Intell., vol. 20, no. 1, pp. 23–38, 1998.
- [38]. S. Srisuk and W. Kurutach, "A new robust face detection in color images," Proc. 5th IEEE International Conference on Automatic Face and Gesture Recognition (AFGR '02), Washington, DC, USA, pp. 291– 296, May 2002.
- [39]. Y. Zhu, S. Schwartz, and M. Orchard, "Fast face detection using subspace discriminate wavelet features," Proc. IEEE Conference on Computer Vision and Pattern Recognition , HiltonHead Island, SC, USA, vol. 1, pp. 636–642, June 2000.
- [40]. B. Fasel, "Fast multi-scale face detection," IDIAP-Com 98-04, IDIAP, Eurecom, Sofia-Antipolis, France, 1998.
- [41]. S. Ben-Yacoub, "Fast object detection using MLP and FFT," IDIAP-RR 11, IDIAP, Martigny, Switzerland, 1997.

-
- [42]. R. Feraud, O. Bernier, J. E. Viallet, and M. Collobert, "A fast and accurate face detector for indexation of face images," Proc. 4th IEEE International Conference on Automatic Face and Gesture Recognition, France, pp. 77–82, March 2000.
- [43]. HazemM. El-Bakry, Qiangfu Zhao, "Fast Pattern Detection Using Normalized Neural Networks and Cross-Correlation in the Frequency Domain" EURASIP Journal on Applied Signal Processing vol.13, pp.2054–2060, 2005.
- [44]. **S Devi, M Dutta, "Detection of cold lesions in SPECT images of cardiac", National Conference on Trends in Advanced Computing, pp. 216-219, 2007.**
- [45]. <http://brighamrad.harvard.edu/Cases/jpnm/hcache/1073/unknown.html>
- [46]. www.inviasolutions.com
- [47]. www.auntminnie.com
- [48]. www.brighamrad.harvard.edu
- [49]. <http://www.medx-inc.com/nuquest.html>
- [50]. www.fsnm.org
- [51]. www.csmc.edu
- [52]. www.biocardiology.com
- [53]. www.emory.edu
- [54]. www.maxxgeneralimaging.org
- [55]. www.uhrad.com
- [56]. www.mimvista.com
- [57]. <http://www.bocaradiology.com/Procedures/cardiac/index.htm>
- [58]. http://www.pmod.com/technologies/gallery/cardiology/P3D/P3D_case_1.html
- [59]. <http://www.biomedcentral.com/1471-2385/6/5/figure/F3>
- [60]. http://www.medical.philips.com/main/products/nuclearmedicine/products/rightview_spect/index.asp
- [61]. <http://www.globalintermed.com/gamma5.htm>
- [62]. <http://brighamrad.harvard.edu/Cases/jpnm/images/1073/PreSestamibiBarrow.GIF>

Chapter 7

PSNR Enhancement using Bacterial Foraging (BFG) Optimization Technique

- 7.1 Introduction to breast cancer detection
- 7.2 Limitations of the present techniques
 - 7.2.1 Effect of noise
 - 7.2.2 Denoising: Present status
 - 7.2.3 Performance Metrics
- 7.3 Proposed BFG optimization
 - 7.3.1 Results of proposed method
 - 7.3.2 Result with Lena test image & performance evaluation
 - 7.3.2 With Mammogram Images, SPECT Images
 - 7.3.1 Discussion on the result
- 7.4 Proposed Median-BFG hybrid method
 - 7.4.1 Median-BFG hybrid method (MED-BFO)
 - 7.4.2 Result of the Median-BFG hybrid code
 - 7.4.3 Result with Lena test image & performance evaluation
 - 7.4.4 Result with Bridge test image
 - 7.4.5 With Mammogram image
- 7.5 References

7. PSNR Enhancement using Bacterial Foraging (BFG) Optimization Technique

7.1 Introduction to breast cancer detection

Breast cancer is a cancer of the glandular breast tissue. Worldwide, breast cancer is the fifth most common cause of cancer death (after lung cancer, stomach cancer, liver cancer, and colon cancer). In 2005, breast cancer caused 502,000 deaths (7% of cancer deaths; almost 1% of all deaths) worldwide. Among women worldwide, breast cancer is the most common cancer and the most common cause of cancer death [1]. Because the breast is composed of identical tissues in males and females, breast cancer also occurs in males, though it is less common[2].

One of the most commonly recommended screening methods for breast cancer is X-ray mammography. Mammography has been estimated to reduce breast cancer-related mortality by 20-30% [3]. A Mammogram is an X-ray photograph of the breast. A digital mammogram is created when a conventional mammogram is digitized, through the use of a specific

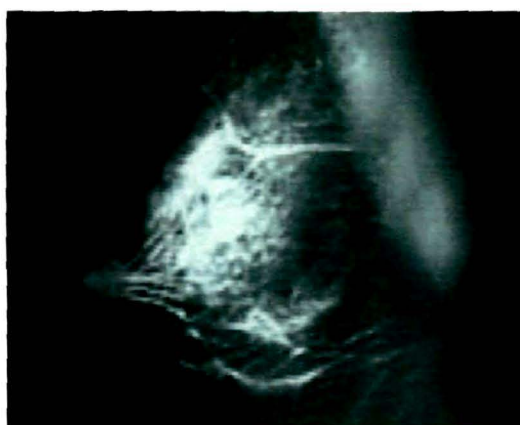


Figure 7.1: A mammogram image

mammogram digitizer or a camera. Alternately, digital mammography, also called full-field digital mammography (FFDM), is a mammography system in

which the x-ray film is replaced by solid-state detectors that convert x-rays into electrical signals. These detectors are similar to those found in digital cameras. The electrical signals are used to produce images of the breast that can be seen on a computer screen or printed on special film similar to conventional mammograms. Although breasts have been X-rayed for more than 70 years, but modern mammography has existed since 1969. It was during this time that the first X-ray machine was used just for breast imaging. Since then, the technology has advanced a great deal. The modern day's technique uses a special machine only for breast X-rays to produce images that are of high quality but have a low radiation

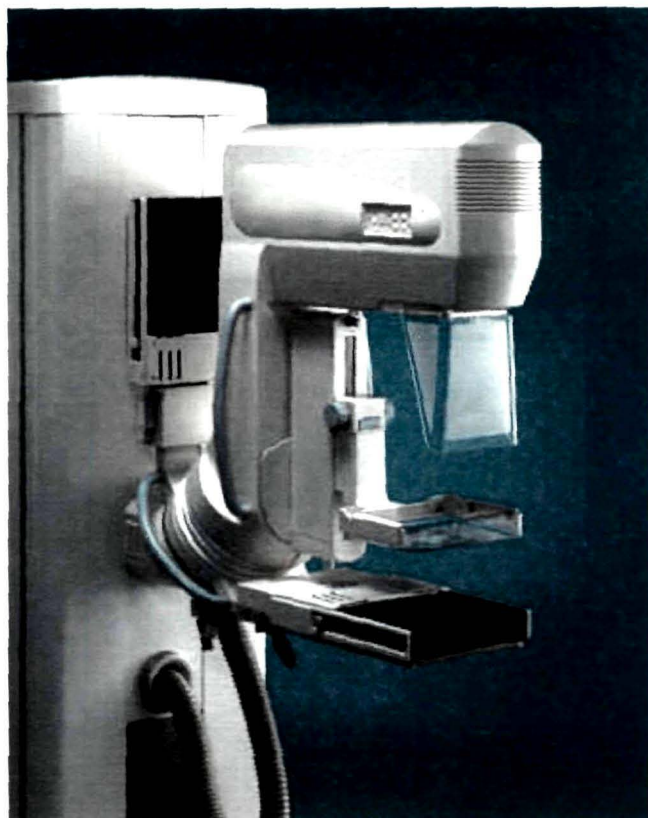


Figure7.2 A mammography equipment

dose (usually about 0.1 to 0.2 red doses per picture.). But still diagnosing breast cancer tumor or cancer tissues using X-ray mammogram is not only a time consuming task but also a difficult job even for highly skilled radiologists. This is

because proper detection of malignant or benign masses demands an improvement in the image

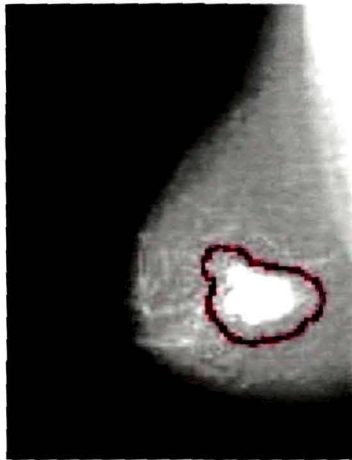


Figure7.3. A Mammogram image showing a mass.

contrast, enhancement in the fine details of parenchymal tissues structures, suspicious areas, macro-calcification, micro-calcification clusters and optimal suppression of noise.

CAD Systems (Computer Aided Diagnosis) help radiologists to evaluate X-ray images to detect breast cancer in an early stage. It is used in addition to the human evaluation. False positives are a major problem of mammographic breast cancer screening. Data reported in the UK Million Woman Study indicates that if 134 mammograms are performed, 20 women will be called back for suspicious findings, and four biopsies will be necessary, to diagnose one cancer. These rates are higher in the U.S. than in the UK [4]. The contribution of mammography to the early diagnosis of cancer cannot be overstated, but it comes at a huge financial and psychological cost to the women found to have a nodule. In general, digital mammography and computer-aided mammography have increased the sensitivity of mammograms, but at the cost of more numerous false positive results.

Mammography is still the modality of choice for screening of early breast cancer [5], since it is relatively fast, reasonably accurate, and widely available in developed countries.

Hence, in this section of the thesis work, an attempt has been made to enhance the mammography images so as to make the detection of the breast masses more error free.

7.2 Limitations of the present techniques

Interpretations of mammograms can be difficult because a normal breast can appear differently for each woman. Also, the appearance of an image may be compromised if there is powder or salve on the breasts or if one has undergone breast surgery. Relevance of diagnosis mainly depends on mammographic image quality, among others are: adequate optical density range, good resolution and sharpness.

To add to an efficient segmentation of features and accurate detection procedure it is easier is to enhance them beforehand [5]. Image enhancement is usually made by either suppressing noise or increasing image contrast. Several studies have been devoted to contrast enhancement on mammographic images, while few studies were concerned with noise reduction [6, 7, 8, 9].

A mammogram contains low signal to noise ratio (low contrast) & noisy images. Added to this, a mammography image may be corrupted by impulse noise due to transmission errors, malfunctioning pixel elements in the camera / scanner sensors, faulty memory locations, and timing errors in digital to analog conversion. Researches are on to improve mammography by enhancing mammogram image quality, develop statistical techniques for computer assisted interpretation of images; enable long-distance, electronic image transmission technology (tele-mammography / tele-radiology) for clinical consultations, and improve image guided techniques to assist with breast biopsies.

7.2.1 Effect of noise

In the medical viewing task, the observer has to locate pathology embedded within a complex background of anatomical structure or clutter. This job of

diagnosing cancer tissues from X-ray mammograms is greatly affected by low contrast and noisy images. Hence, the goal of enhancement lies in improving the quality of image signal. It can be accomplished by removing noise, enhancing contrast and enhancing edges [55]. Noise reduces the visibility of some structures and objects, especially those that have relatively low contrast. In medical imaging the objective is to eliminate the noise, if not to reduce it to a clinically acceptable level.

7.2.2 Denoising: Present Status

To suit the medical analysis, their Peak Signal to Noise Ratio (PSNR) seeks for a method that can yield a better image quality. After reviewing literatures on different filters and soft computing techniques available, a Bacterial Foraging Optimization Technique has been used in this thesis to filter the noise thereby enhancing the mammography image.

There are two noise models that mainly represent most of the noises[10]: Gaussian noise and impulse noise. Gaussian noise, additive in nature, is characterized by superimposing values from a zero-mean Gaussian distribution to each pixels of the image. This noise is usually found during image acquisition. Impulse noise is characterized by perturbing some of the image's pixels values with random numbers. So, the most noticeable and the least acceptable pixels in the noisy image are those whose intensities are much different from their neighbors.

Literature survey shows the existence of various filters; some perform very well for a Gaussian noise whereas the others are good for impulse noise only.

Classical linear digital image filters, such as Gaussian filter or averaging low pass filters, smoothens noise efficiently but blur the edges significantly and destroys lines, edges and other fine details of the image. As a solution to this problem, non linear methods are used, most notably the anisotropic diffusion technique of Perona and Malik [11]. Another method is the bilateral filter studied

by Tomasi and Manducci [12] based on the original idea of Overton and Weymouth [13]. These methods use the local measures of an image to quantitatively detect edges and to smooth them less than the rest of the image. These noise removal methods cannot remove impulse noise adequately. So, a separate class of non linear filters has been designed specially to handle the impulse noise. Among these filters, many are extensions of the median filter [14-15], or the rank statistics [16-18]. These filters detect the noisy pixels and replace them with their estimated values. The drawback of these filters is the fact that when they are applied to Gaussian method, the filters are not effective and in most of the cases leave grainy images. Wavelet theory has also been used for image denoising. In wavelet domain, each noise wavelet coefficient is modified according to a certain threshold. But this threshold needs to be properly chosen. Soft thresholding, due to its effectiveness and simplicity, has been used in the literature [19, 20]. Alternative approaches are suggested in the papers [21-30]. In paper [31], VisuShrink uses a universal threshold, Birge-Massart [32] uses a penalization method to select the value of the threshold, BayesShrink [33, 34].

Most basic impulse detectors are based on two state methods to find pixels that are significant outliers when compared to its neighbors. Some denoising methods like two-state SD-ROM [35,36] and CSAM [37] filters are easily customizable, but they suffer from a more complex criterion of judging whether a pixel is an impulse. Study shows that a separate class of non-linear filters have been developed for the removal of impulse noise; some of them being the extension of the median filter [38-15,16], others use rank statistics [16-18]. The median filter yields excellent results for image corrupted by impulse noise because of its computational efficiency [39]. The different types of median filters have been used e.g. the adaptive median filter [40-42], the multistate median filter [43], the median filter based on homogeneity information [44], switching median filter[45], progressive switching median filter[46], directional and difference based switching median filter[47].

The draw back of median filters is that the noisy pixels are replaced by some median value without taking into account local features such as the possible

presence of edges. When the noise level is high, the details of edge are not recovered satisfactory. For successful preserving the edges details preserving median based filters are used [48]. For highly corrupted images co-efficient approach [49] and two stage algorithm i.e. median type noise detector and detail preserving algorithm [50] is used. For image restoration rank conditioned rank selection filters [51] are used.

In an attempt to explore the use of soft computing method, for the job, different techniques like Genetic Algorithm, Particle Swarm Optimization, Bacterial Foraging Optimization. (BFO) have been studied and the BFO has been investigated for its use as a signal enhancer thus improving PSNR.

7.2.3 Performance Metrics

The performance of this optimization technique is evaluated based on Peak Signal to Noise Ratio (PSNR) and Mean Absolute Error (MAE) [53], Structural Contents Image Fidelity, Normalized Correlation Quality. Let $\hat{f}_{i,j}$ and $f_{i,j}$ denote the pixel values of the restored image and the original image respectively. Then,

1. Peak Signal to Noise Ratio (PSNR) given by [39]:

$$PSNR(\hat{f}) = 10 \log_{10} \left(\frac{\sum_{i,j=1}^{m,n} 255^2}{\sum_{i,j=1}^{m,n} (\hat{f}_{i,j} - f_{i,j})^2} \right) \text{ db} \quad 7.1$$

where $(\hat{f}_{i,j} - f_{i,j})^2$ is the Mean Square Error.

2. Mean Absolute Error: It is defined by the following formula :

$$MAE = \frac{1}{MN} \sum_{i,j}^{M,N} |\hat{f}_{i,j} - f_{i,j}| \quad 7.2$$

3. **Structural Content (SC) & Normalized Correlation Quality(NK) :** SC and NK are the indicators of similarity between two digital images, in terms of correlation function. They are expressed by the following formulas:

$$SC = \frac{\sum_{j=1}^M \sum_{k=1}^N f_{i,j}^2}{\sum_{j=1}^M \sum_{k=1}^N \hat{f}_{i,j}^2} \quad 7.3$$

$$NK = \frac{\sum_{j=1}^M \sum_{k=1}^N [f_{i,j} \hat{f}_{i,j}]}{\sum_{j=1}^M \sum_{k=1}^N [f_{i,j}^2]} \quad 7.4$$

4. Image Fidelity : Image fidelity refers to the ability of a process to render an image accurately, without any visible distortion or information loss [56].

$$IF = 1 - \frac{\sum_{j=1}^M \sum_{k=1}^N [f_{i,j} - \hat{f}_{i,j}]}{\sum_{j=1}^M \sum_{k=1}^N [f_{i,j}^2]} \quad 7.5$$

7.3 Proposed Bacterial Foraging for Optimization

Let $f(i,j)$ represent an input image, and $f_n(i,j)$, the image after being corrupted by noise. Both these images are placed in the search space. The gray level values of each pixel of the output image are continuously compared with that of the input image. This comparison continues for the entire pixels, until the error is equal to or less than 0.00001. If the minimization of error proceeds in right direction, swarming or the running speed is increased. This in turn increases the convergence speed. If the minimization error increases, the bacterium tumbles and searches the right path. This process continues for the entire pixels (or the bacteria). During reproduction, the pixels leading towards the right direction will split into two. These new bacteria are placed in the same location. The elimination and dispersal phase helps during chemotactic processes by moving the pixels to the nearest required values away from the noisy image. The cost function that has been used here for the optimization process is:

$$J = \frac{1}{MN} \sum_{m=0}^{M-1} \sum_{n=0}^{N-1} [f_n(i, j) - f(i, j)]^2 \quad 73$$

where, $M \times N$ is the size of the original image $f(x, y)$ and its noisy image $f_n(x, y)$.

The block diagram of the proposed method is

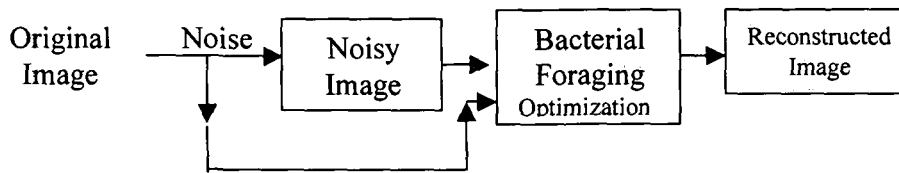


Figure.7.4. Block diagram of the proposed BFO method.

For the Lena image and the mammogram, 64,000 bacteria have been used for searching the total region. The swimming length N_s has been taken as 4. Two reproduction cycles and elimination and dispersal cycles have been considered. The probability of elimination and dispersal has been taken to be 0.25.

The algorithm starts with the true image being converted into a noisy image. Salt and pepper noise of different noise densities have been added to corrupt the true image. A few preprocessing steps are used to bring all the images into the same format, class and size.

7.3.1 Results of the proposed methods

The proposed methods have been extensively tested with different images. To evaluate this method, the developed code was tested with the standard Lena test image (512x512). The original Lena image has been corrupted with impulse noise (salt and pepper noise) with different noise probability density. Then these corrupted Lena images have been denoised using the BFO algorithm. After the image has been denoised, its Peak Signal to Noise Ratio (PSNR) has been calculated. The PSNR is then compared with the published values as reported in different papers [43-47] for the same images to see the accuracy of the method i.e., for validation..

Parameters used in the BFO algorithm are:

- i) Number of bacteria used for searching the total region (S) = 6400.
- ii) Swimming length $N_s = 4$.
- iii) The number of iterations taken in a Chemotactic loop N_c ($N_c > N_s$) = 10.
- iv) The number of reproduction $N_{re} = 2$.
- v) The number of elimination and dispersal $N_{ed} = 2$.

vi) Probability of elimination and dispersal $P_{ed} = 0.25$

Table 7.1 gives a comparison of the proposed method with the other methods [59, 60]. Other methods report a PSNR of 26.21db to 31.36 db for the case of impulse noise, this proposed method gives PSNR of 57.24db for denoising the Lena image with a noise density of 40%.

Table 7.1: Comparison of proposed BFO Technique with other existing methods with a noise density of 40%.

Method	Lena image; PSNR
3x3 Median Filter[43]	26.21 db
5x5 Median Filter[43]	27.61 db
Median Filter with Adaptive Length[44]	27.75 db
Sun and Neuvo Switching Scheme[45]	27.97 db
Rank Conditioned Rank Selection Filter[46]	27.72 db
SD-ROM without training[47]	28.30db
SD-ROM with training[47]	29.19 db
Trilateral filter[43]	31.36 db
Proposed method of BFO	57.24 db

Table 7.2: Values of different performance metrics of proposed method (applied on Lena Image).

Sl.No.	Noise Density	PSNR(db)	Time(sec)	Structural Contents (SC)	Image Fidelity (IF)	Normalized Correlation Quality (NK)
1	0.1	63.4241	443.781	0.9091	0.6981	0.9910
2	0.2	60.1131	440.968	0.8168	0.5739	0.9958
3	0.3	58.7326	430.719	0.7807	0.5172	0.9668
4	0.4	57.4023	432.953	0.7268	0.4223	0.9520
5	0.5	56.3698	552.218	1.4943	0.5997	0.6344

Output of the BFG

Original Lena image



(a)



(b)



(c)

Figure7.5. (a) : Lena (512x512) image cropped into 80x80 size (b) Corrupted with 40 % noise, (c) Output Image after using the proposed

7.3.2 Results with Lena test image

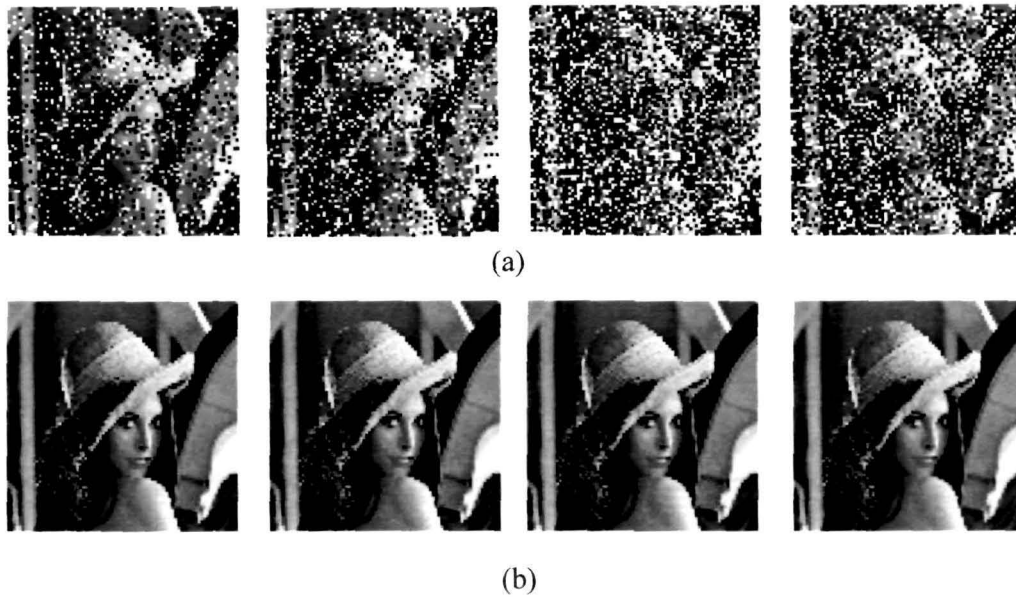


Figure 7.6. (a) Lena image corrupted with noise density of 20%, 30%, 40% and 50% respectively (b) denoised image from (a).

7.3.3 Results with Mammogram Images, SPECT Images



Figure 7.7 Mammogram image showing a mass.

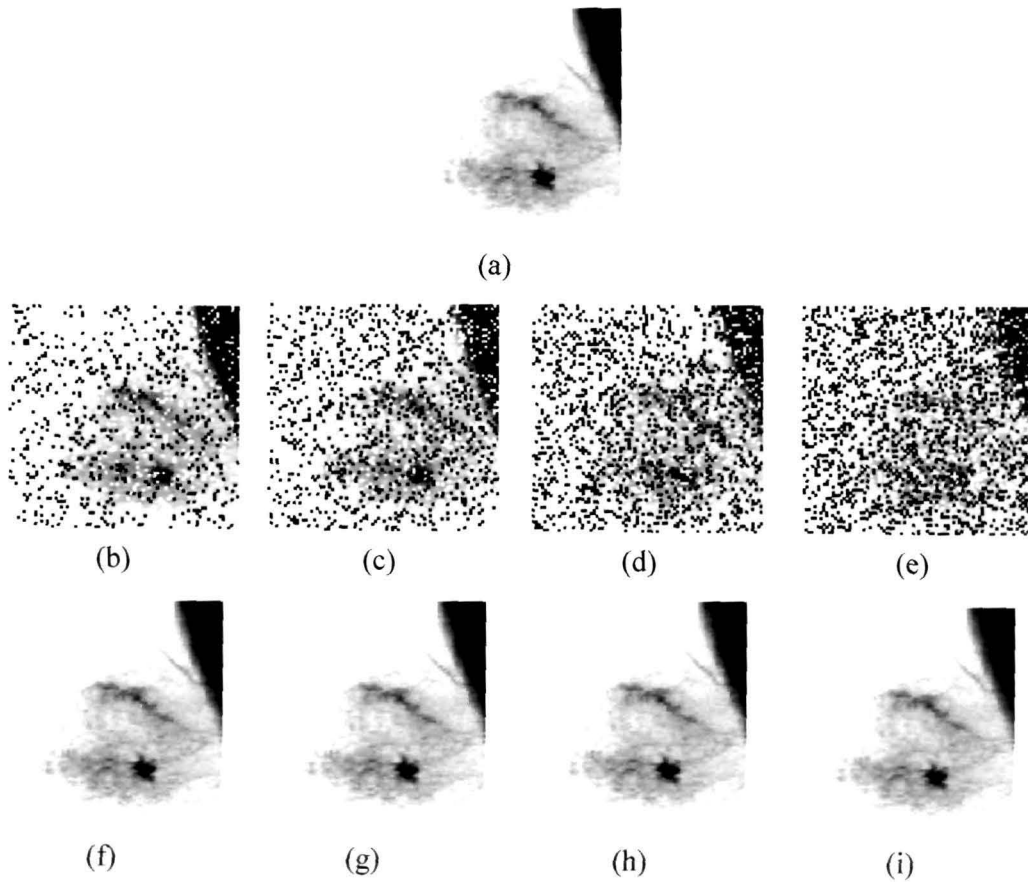


Figure 7.8. (a) : Original mammogram image cropped into 80x80 pixels, (b) Corrupted with 20 % noise, (c) with 30% noise, (d) with 40% noise, (e) with 50% noise, (f) – (i) Output Image after using BFO on (b) - (e) respectively.

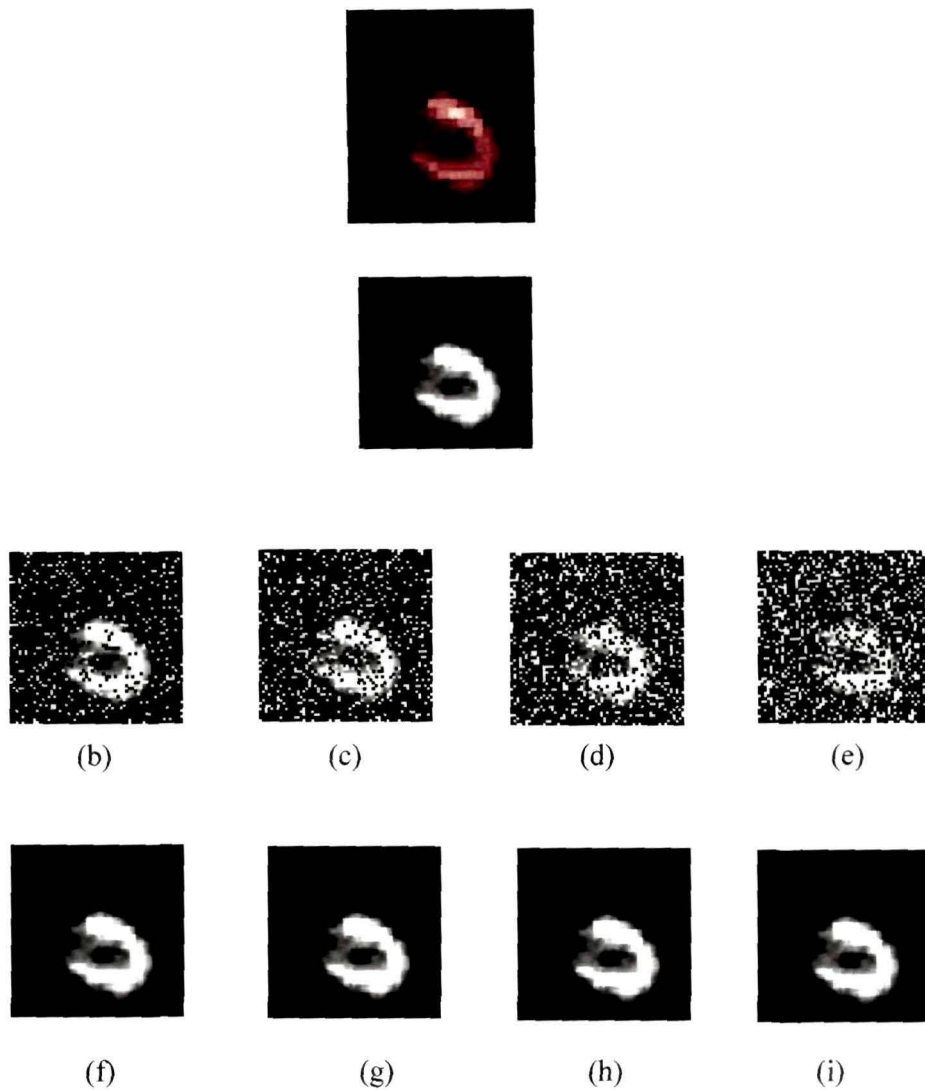


Figure 7.9. (a) : Original SPECT image cropped into 60x60 pixels, (b) Corrupted with 20 % noise, (c) with 30% noise, (d) with 40% noise, (e) with 50% noise, (f) – (i) Output Image after using BFO on (b) - (e).

The algorithm has also been applied on a SPECT cardiac image and fig. 7.9 shows the results. For the SPECT image 3,600 bacteria have been considered.

7.3.4 Discussion on the results

Table 7.3: Result of denoising using BFO Technique.

Image	PSNR & Time Taken for Iterations			
	P=20%	P=30%	P=40%	P=50%
Lena	60.45db; 100.59 Sec	58.62 db; 99.08 Sec	57.24 db; 298.69 Sec	56.18 db; 84.56 Sec
Mammography	59.24 db; 100.29 Sec	57.39 db; 246.45 Sec	56.28 db; 131.81 Sec	55.28 db; 133.76 Sec
SPECT Image	58.50 db; 107.97 Sec	57.01 db; 163.33 Sec	55.27 db; 86.86 Sec	54.73 db; 115.20 Sec

Table 7.3 gives the PSNR value and the time taken by the BFO algorithm to denoise different images corrupted with different noise densities.

7.4 Proposed Median-BFG hybrid method

7.4.1 Median-BFG hybrid method (MED-BFO)

In this proposed method, the bacterial foraging optimization technique is used with median filter to remove salt and pepper noise from corrupted image. In the first stage, the median filter is applied to remove the noise and to keep the uncorrupted information as far as possible. In the second stage, bacterial foraging optimization technique is used to compensate for the sensitive regions for image quality enhancement. This method removes salt and pepper noise with a high noise density. With an image corrupted with synthetic noise as high as 90%, this

method has been found to give a good peak signal to noise ratio and less mean absolute error.

Median filter:

Median filters [52], are non linear digital filter or order-statistics filter. A median filter considers each pixel in the image in turn and looks at its nearby neighbors to decide whether or not is representative of its surroundings. Instead of simply replacing the pixel value with the *mean* of neighboring pixel values, it replaces it with the *median* of those values. The median is calculated by first sorting all the pixel values from the surrounding neighborhood into numerical order and then replacing the pixel being considered with the middle pixel value. If the neighborhood under consideration contains an even number of pixels, the average of the two middle pixel values is used. It provides very good noise-reduction capabilities, with considerably less blurring. Median filters are particularly very effective in the presence of impulse noise. This is because of the characteristics of impulse noise as white and black dots appear on an image. The principal function of median filter is to force points with distinct gray levels to be more like their neighbors. It replaces the value of a pixel by the median of the gray levels in the neighborhood of that pixel:

$$\hat{f}(x, y) = \underset{(s, t) \in S_{xy}}{\text{median}}\{g(s, t)\} \quad 7.4$$

where, $\hat{f}(x, y)$ is the restored image after denoising; $g(s, t)$ is the corrupted image in the area defined by S_{xy} and S_{xy} represent the set of coordinates in a rectangular subimage window of size $m \times n$ centered at point (x, y) .

The block diagram of the whole method is given below :

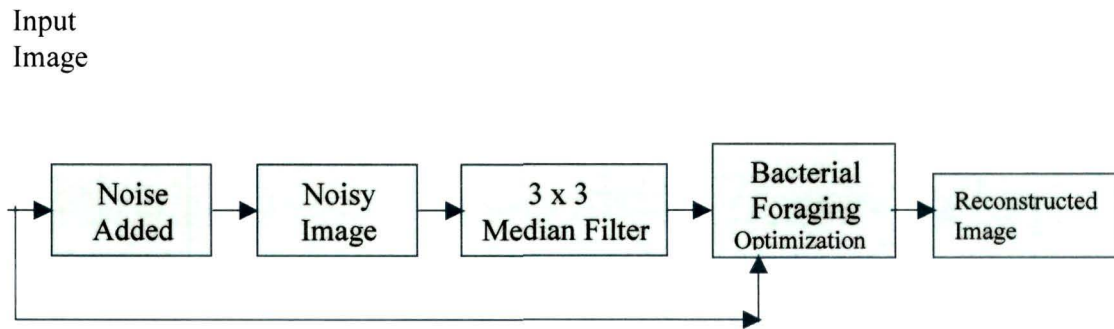


Figure 7:10: Proposed Median-BFG filter

This present approach is basically a two-steps procedure. In the first step, the original input image corrupted with a “Salt & Pepper” noise of varied densities is applied to the median filter. The window size of median filter is chosen as 3x3. Both the original image and median filter output image are passed as search space variables to the bacterial foraging optimization technique.

In the second step, both the images are placed randomly in the search space then the searching technique starts. The number of bacteria chosen depends on the number of input pixels of the image. If the optimization proceeds in right direction, then the swarming (running speed) increases. Otherwise, a tumble takes place to proceed in the right direction.

The following parameters are selected for Bacterial Foraging Optimization during simulations.

- i) Number of bacteria used for searching the total stages the total region (S)
 = 262144 (For Lena image)
 = 78995 (For Mammography image)
- ii) Swimming length $N_s = 2$.
- iii) The number of iterations taken in a Chemotactic loop $N_c (N_c > N_s) = 3$.
- iv) The number of reproduction $N_{re} = 2$.
- v) The number of elimination and dispersal $N_{ed} = 2$.
- vi) Probability of elimination and dispersal $P_{ed} = 0.25$.

The mean square error given by equation [5] between the original image and the noisy image is used as a cost function to optimize the signal to noise ratio.

$$Error = \frac{1}{MN} \left[\sum_{i=1}^M \sum_{j=1}^N \hat{f}(x, y) - f(x, y) \right]^2 \quad 7.5$$

where, $M \times N$ is the size of both the original image $f(x, y)$ and its restored image $\hat{f}(x, y)$.

7.4.2 Results of the Median-BFG code

The performance analysis of the Bacterial Foraging optimization with median filter has been done by testing it with the same standard Lena image (512x512) and Mammography image (305x259) cropped into 80x80 images as shown fig. 7.14 (a) and fig. 7.15(a). The proposed method restores the images and also calculates Peak signal to Noise ratio (PSNR) and Mean Absolute Error (MAE) in each case. In order to test the efficiency of the method, the images have been corrupted with noise densities from 10% to 90% with increments of 10%. In all the cases the proposed method is found to give a better PSNR and less MAE as compared to other methods. Fig 7.14 shows results of the Lena image corrupt with noise densities 10% to 50%. The table 7.4 brings out a comparison among the results of proposed method and other existing method for Lena image (corrupted with noise density 70%). Table 7.5 tabulates the result of the median-BFO method as applied on the Lena image corrupted with noise of different densities.

7.4.3 Results with Lena test image & performance evaluation



Figure 7.11. (a) Original 512 X 512 Lena Image cropped into 80X80 size, (b) Original Image of (a) corrupted with noise density of 10%, 20 %, 30%,40%, and 50% respectively, (c) Image after median filtering of mask 3x3, (d) Restored image using proposed MED-BFO technique.

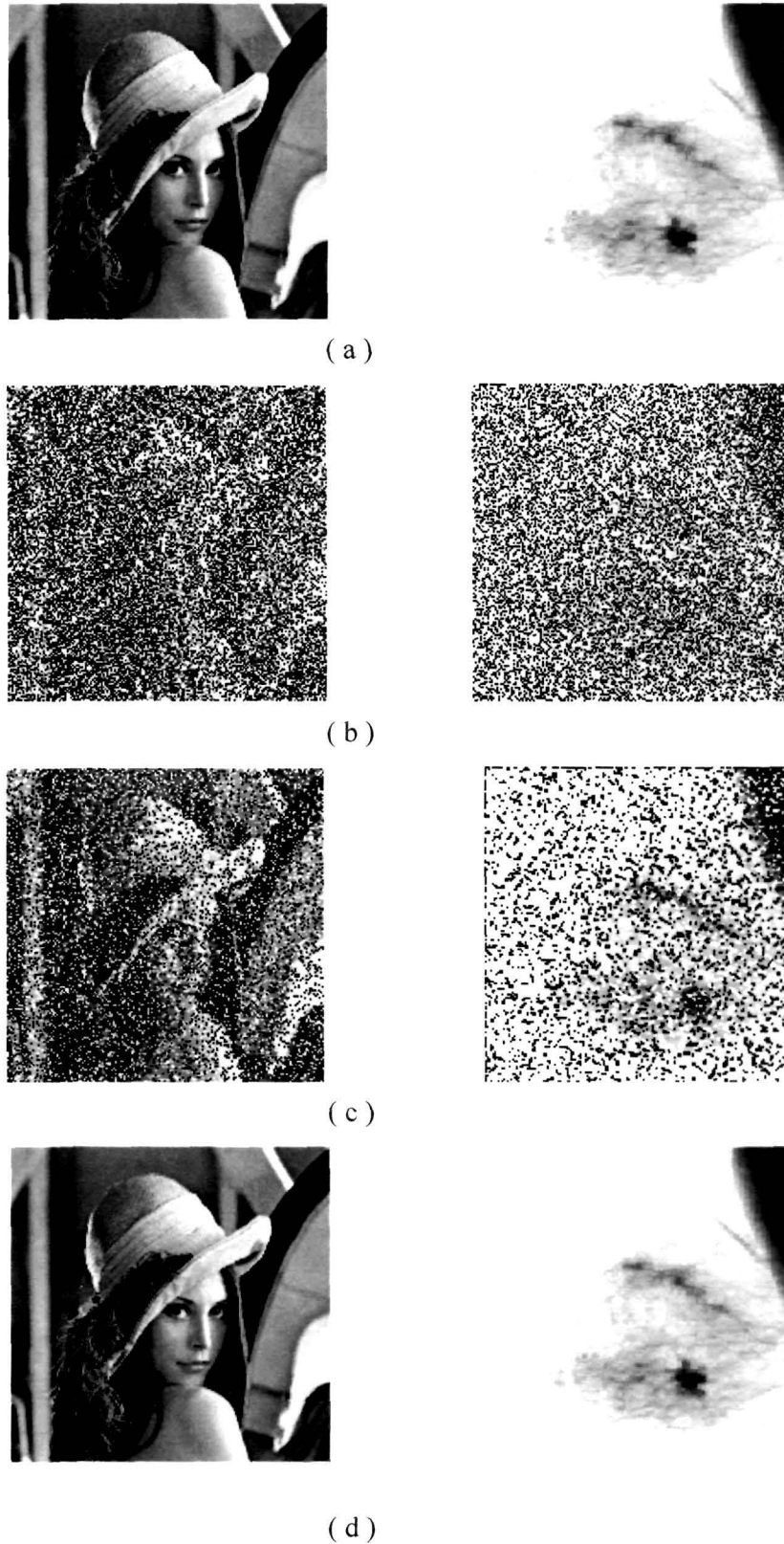


Figure 7.12: (a) Lena and Mammography images, (b) Images with 70% noise density, (c) Median filter output, (d) Restored images using BFG&MF.

Table 7.4: Comparison of proposed method and other existing methods with noise density of 70% on Lena image.

Method	PSNR 70%
MED Filter [19]	23.2 db
PSM Filter [19]	19.5 db
MSM Filter [19]	19.0 db
DDBSM Filter [19]	17.5 db
NASM Filter [19]	21.8 db
ISM filter [19]	23.4 db
Proposed Method	45.91 db

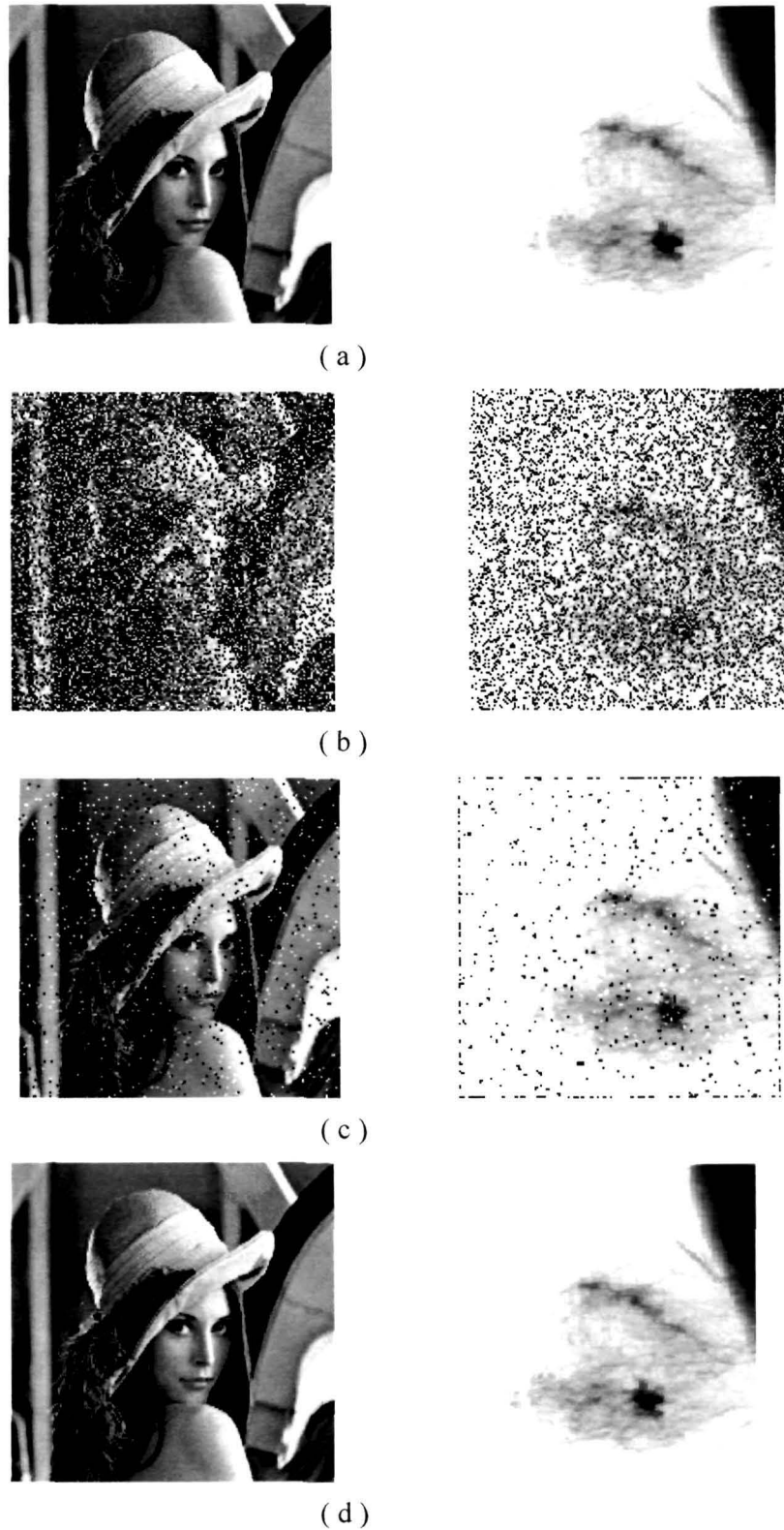


Figure 7.13: (a) Lena and Mammography images, (b) Images with 40% noise density, (c) Median filter output, (d) Restored images using BFG&MF.

Table 7.5: Comparison of Proposed method with other existing methods for noise density of 40% on Lena image.

Method	PSNR 40%
3 x3 Median Filter [38]	26.21 db
5x5 Median Filter [38]	27.61 db
Median Filter with Adaptive Length [42]	27.75 db
Sun and Neuvo Switching Scheme [48]	27.97 db
SD-ROM without training [49]	28.30 db
SD-ROM with training [49]	29.19 db
Trilateral Filter [38]	31.36 db
Proposed Method (MF & BFG)	54.90 db

Table 7.6: Result of Median-BFO method as applied on Lena image (512x512) corrupted with different noise densities.

Noise Density	PSNR (in db)	MAE	Time taken for iterations (in sec.)
10%	68.19	0.0127	2710.77
20%	64.34	0.0159	2736.34
30%	59.39	0.0230	2702.95
40%	54.90	0.0384	2696.62
50%	51.24	0.0681	2708.33
60%	47.23	0.0983	2696.46
70%	45.91	0.1894	2653.54
80%	44.24	0.2354	2651.96
90%	42.53	0.3856	2654.76

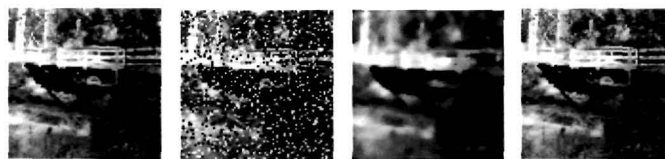
7.4.4 Results with Bridge test image

The algorithm was also tested with a standard Bridge image of the size 256x256. The Bridge image (fig. 7.14a) was corrupted with salt and pepper noise of various noise densities (fig. 7.14b) and then the noisy image is passed in one

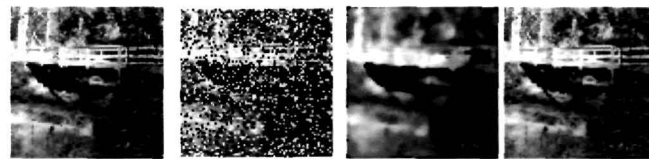
case through a Median filter (fig. 7.14c), and in the second case through the **Median-BFO** algorithm(fig. 7.14d). The images in figure 7.14 shows the input and output images in each cases.



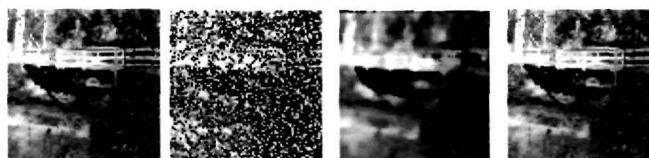
10%



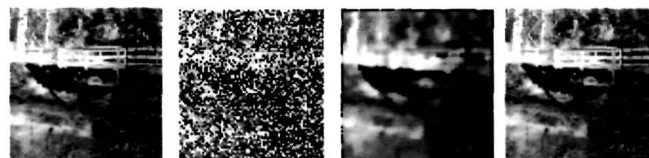
20%



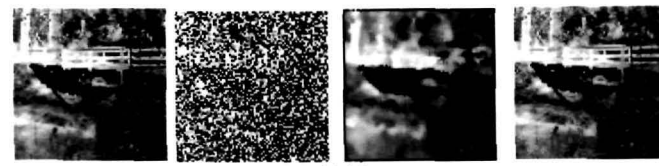
30%



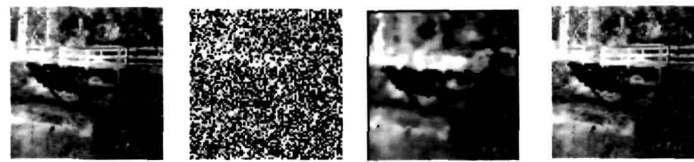
40%



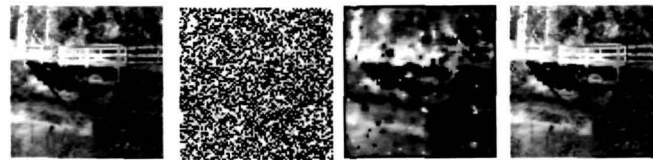
50%



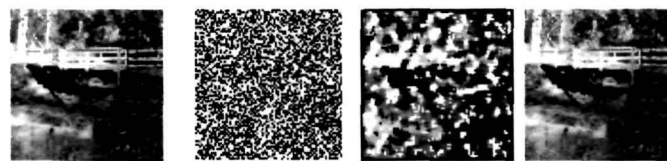
60%



70%



80%



90%

(a)

(b)

(c)

(d)

Figure 7.14: From left to right, respectively, (a) Original Bridge Image (b) Image corrupted with noise (top to bottom: noise of densities ranging from 10% to 90 %) (c) denoising result after using Median Filter (d) denoising result after using developed method.

The Mean Absolute Error, Peak Signal to Noise Ratio, and the time taken for execution are observed and recorded in table 7.7 below.

Table 7.7: Result of Median-BFO method as applied Bridge test image corrupted with different noise densities.

Noise Density	MAE	PSNR (in db)	Time taken for iterations (sec)
10%	0.0685	68.16	938.93
20%	0.0718	67.37	948.16
30%	0.0742	66.95	938.45
40%	0.0845	65.38	956.85
50%	0.0957	64.98	934.78
60%	0.1028	62.56	936.85
70%	0.1125	61.59	932.78
80%	0.1267	59.18	939.78
90%	0.1358	57.45	937.89

7.4.5 Results with Mammogram Image

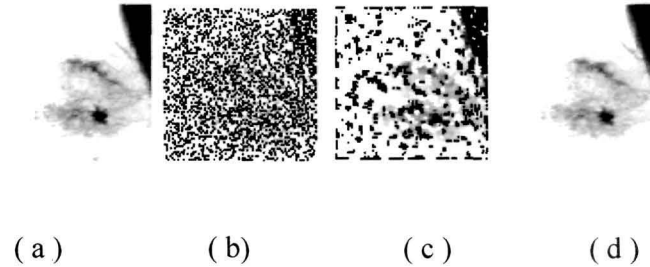


Figure 7.15: (a) Original Mammography (305X259) image cropped into 80x80 size; (b) corrupted with noise density of 40%; (c) Median filter output image corresponding to (c); (d) Restored image using MED-BFO.

Table 7.8: Result of Median-BFO method as applied on mammogram image (305X259) corrupted with different noise densities.

Noise Density	PSNR (in db)	MAE	Time taken for iterations (in sec.)
10%	69.09	0.0042	444.88
20%	63.57	0.0062	446.58
30%	57.62	0.0135	449.75
40%	53.64	0.0284	432.99
50%	49.64	0.0591	446.31
60%	47.17	0.1088	453.04
70%	44.82	0.1820	448.45
80%	43.02	0.2731	447.09
90%	41.52	0.3834	445.06

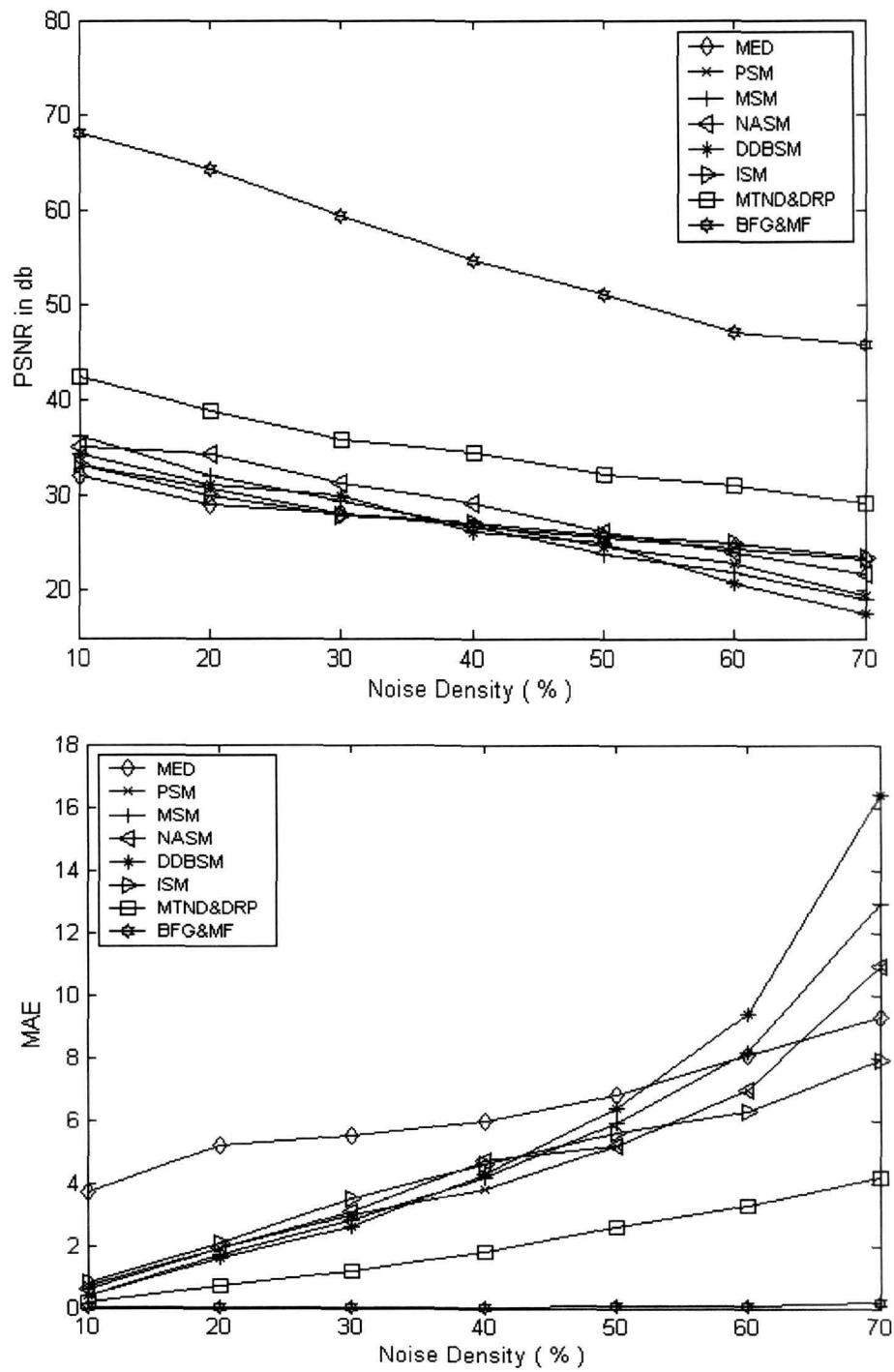


Figure 7.16: (a) & (b) Comparison results in PNSR and MAE for the Lena Image at noise density with various algorithms and developed method

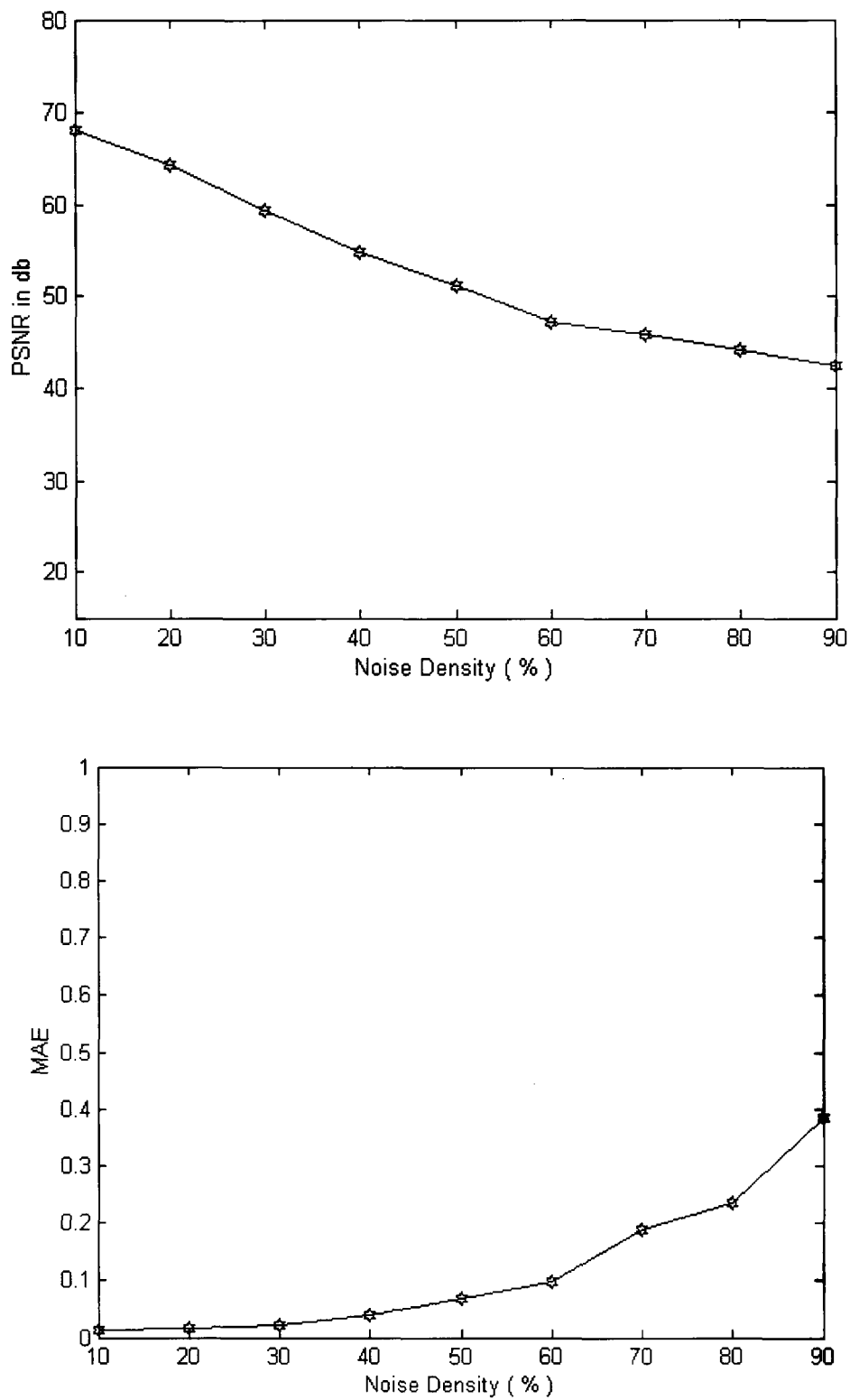


Figure 7.17 : (a) & (b) PSNR & MAE of Lena restored image for noise densities 10% to 90%.

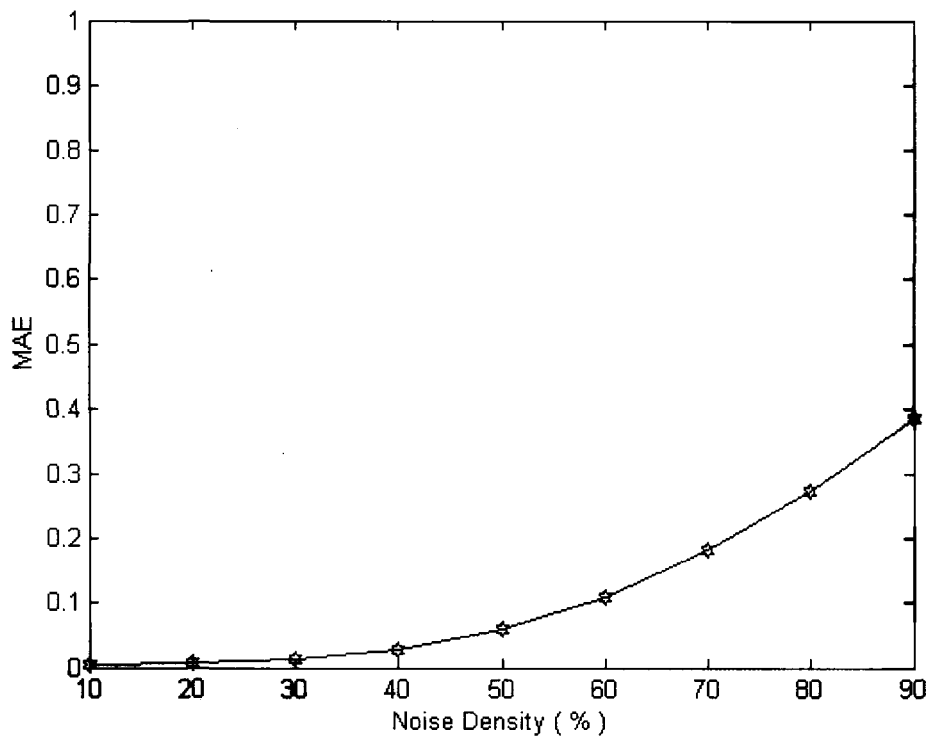
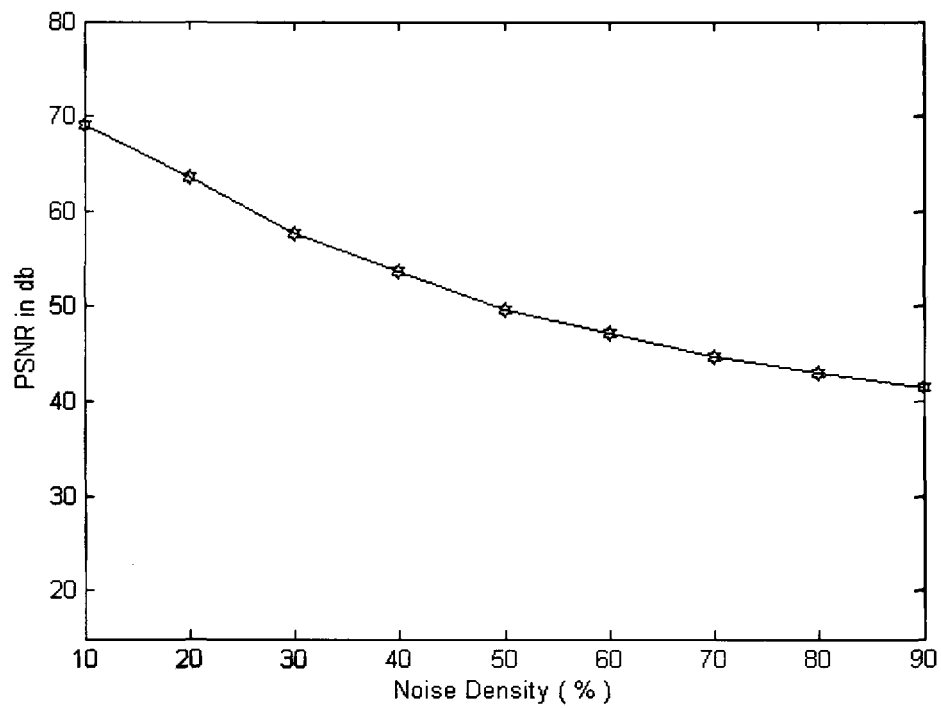


Figure 7.18: (a) & (b) PSNR & MAE of Mammography restored image for noise densities 10% to 90%.

Table 7.9: Comparison of the proposed method with other existing methods for Lena image in terms of computational time (in seconds).

Method	Noise	Density
	70%	90%
Adaptive Median Filter [57]	23	311
Variational Method for Impulse Noise Cleaning [58]	6865	>12000
MTND& DPR[58]	2009	6917
Proposed Method (BFG&MF)	2653	2654

7.5 References

- [1]. World Health Organization (February 2006). Fact sheet No. 297: Cancer
- [2]. Male Breast Cancer Treatment - National Cancer Institute. *National Cancer Institute*, Retrieved on 2006-10-16, 2006.
- [3]. Elwood J, Cox B, Richardson A. "The effectiveness of breast cancer screening by mammography in younger women.". *Online J Curr Clin Trials Doc No 32*: PMID 8305999.
- [4]. Smith-Bindman R, Ballard-Barbash R, Miglioretti DL, Patnick J, Kerlikowske K "Comparing the performance of mammography screening in the USA and the UK", *Journal of medical screening*, vol. 12, no.1, pp. 50-4, 2005.
- [5]. M. Adel, D. Zuwala, M. Rasigni and S. Bourenane "Noise reduction on mammographic phantom images", *Electronic Letters on Computer Vision and Image Analysis*, vol. 5, no. 4, pp.64-74, 2006.
- [6]. F. Aghadasi, R.K. Ward, B. Palcic, "Noise filtering for mammographic images", *Proceeding of the 14th Annual International Conference of the IEEE Engineering in Medicine and Biology Society*, pp. 1877-1878, 1992.

- [7]. V. Guis, M. Adel, M. Rasigni, G. Rasigni, B. Seradour, P. Heid, "Adaptive neighborhood contrast enhancement in mammographic phantom images", *Opt. Eng.*, vol. 42, no. 2, pp. 357-366, 2003.
- [8]. J. Martens, "Adaptive contrast enhancement through residue-image processing", *Signal Processing*, vol. 44, pp.1-18, 1995.
- [9]. W. Qian, L.P. Clarke, M. Kallergi, R.A. Clark, "Tree-Structured Nonlinear Filters in Digital Mammography", *IEEE Trans. Med. Imaging*, vol. 13, no. 1, pp. 25-36, 1994.
- [10]. Roman Garnett, Timothy Huegerich, Charles Chui, Wenjie He, "A Universal Noise Removal Algorithm with an Impulse Detector", *Journal of IP (N 4)*, Issue 11, pp 1747-1754, November 2005.
- [11]. P Perona and J Malik, "Scale-space and edge detection using anisotropic diffusion", *IEEE Trans. Pattern Anal. Machine Intell*, vol. 12, pp. 629-639, 1990.
- [12]. C.Tomasi, R. Manduchi, "Bilateral Filtering for gray and color images", *Proceedings IEEE International Conference Computer Vision*, pp.839-846, 1998.
- [13]. K J Overton and T E Weymouth, "A noise reducing preprocessing algorithm", *Proceedings of IEEE Computer Science Conference on Pattern Recognition and Image Processing*, Chicago, pp. 498-507, 1979.
- [14]. H Lin and A N Willson Jr., "Median filters with adaptive length", *IEEE Trans. Circuits syst.*, vol.35, pp. 675-690, June 1988.
- [15]. T Sun and Y Neuvo, "Detail-preserving median based filters in image processing", *Patt. Recogn. Lett.*, vol. 15, pp. 341-347, Apr. 1994.
- [16]. A C Bovik, T S Huang and D C Munson, "A generalization of median filtering using linear combinations of order statistics" *IEEE Trans. ASSP*. vol. 31, pp. 1342-1350, Dec. 1983.
- [17]. R C Hardie, K E Barner, "Rank conditioned rank selection filters for signal restoration", *IEEE Trans. Image Processing*, vol. 3, pp. 192-206, Mar. 1994.
- [18]. G Pok, J Liu and A S Nair, "Selective removal of impulse noise based on homogeneity level information", *IEEE Trans. Image Processing*, vol. 12, pp. 85-92, Jan. 2003.

- [19]. Fu Chenzhao; Liu Jian; Li Yanming; Liu Jie; Wang Guogang, "Application of soft-threshold wavelet de-noising method in the diagnosis of transformer during impulse test", Proceedings of International Symposium on Electrical Insulating Materials, pp. 845 – 848, 2001.
- [20]. D. L. Donoho, "De-noising by Soft-Thresholding", IEEE Trans. Inform. Theory, vol. 41, pp. 613–627, May 1995.
- [21]. Gabriel Cristobal, Monica Chagoyen, Boris Escalante-Ramirez, Juan R Lopez, "Wavelet-based denoising methods: A comparative study with applications in microscopy", Proc. SPIE's International Symposium on Optical Science, Engineering and Instrumentation, Wavelet Applications in Signal and Image Processing IV, vol. 2825, 1996.
- [22]. David L Donoho, "Ideal spatial adaptation by wavelet shrinkage", *Biometrika*, vol. 81, no. 3, pp. 425-455, August 1994.
- [23]. David L. Donoho and Iain M. Johnstone, "Adapting to Unknown Smoothness via Wavelet Shrinkage," *Journal of American Statistical Association*, vol. 90, no. 432, pp. 1200-1224, December 1995.
- [24]. G. P. Nason, "Wavelet Shrinkage Using Cross-Validation" *Journal of the Royal Statistical Society. Series B (Methodological)*, vol. 58, no. 2, pp. 463-479, 1996.
- [25]. N. Fieguth, P "A Gabor based technique for image denoising" Nezamoddini-Kachouie Canadian Conference on Electrical and Computer Engineering, 1-4 May pp. 980 – 983, 2005.
- [26]. J. Portilla, V. Strela, M. Wainwright, and E. Simoncelli, "Adaptive wiener Denoising using a Gaussian Scale Mixture Model," Proc. Int. Conf. Image Process. 2001.
- [27]. J. Liu and P. Moulin, "Image Denoising Based on Scale-Space Mixture Modeling of Wavelet Coefficients, " Proc. IEEE Int. Conf. Image Process., Kobe, Japan, Oct. 1999.
- [28]. R. Coifman and D. Donoho, "Time-Invariant Wavelet Denoising in Wavelet and Statistics, A. Antoniadis and G. Oppenheim, Eds. New York: Springer-Verlag, vol. 103, Lecture Notes in Statistics, pp. 125–150, 1995.

- [29]. M. K. Mihcak, I. Kozintsev, K. Ramchandran, and P. Moulin, "Low Complexity Image Denoising Based on Statistical Modeling of Wavelet Coefficients" *IEEE Signal Processing Lett.*, vol. 6, pp. 300–303, Dec.1999.
- [30]. F. Abramovich and Y. Benjamini, "Adaptive thresholding of wavelet coefficients" *Comput. Statist. Data Anal.*, vol. 22, pp. 351–361, 1996.
- [31]. D. L. Donoho and I. M. Johnstone, "Ideal Spatial Adaptation by Wavelet Shrinkage," *Biometrika*, vol. 81, no. 3, pp. 425–455, 1994.
- [32]. S. Grace Chang, Bin Yu and Martin Vetterli, "Adaptive Wavelet Thresholding for Image Denoising and Compression," *IEEE Trans. Image Processing*, vol. 9, no. 9, pp. 1532-1546, Sept 2000.
- [33]. Birgé, L. and P. Massart, "From Model Selection to Adaptive Estimation," in D. Pollard (ed), *Festchrift for L. Le Cam*, Springer, pp. 55-88, 1997.
- [34]. Mohiy Hadhoud, Mohamed Amin, Walid Dabbour "Detection of Breast Cancer Tumor Algorithm using Mathematical Morphology and Wavelet Analysis", *GVIP 05 Conference, CICC, Cairo, Egypt, 19-21 December 2005*.
- [35]. E Abreu, M Leightstone, S Mitra and K Arakawa, "A new efficient approach for the removal of impulse noise from highly corrupted images", *IEEE Trans. Image Processing*, vol. 5, pp. 1012-1025, June 1996.
- [36]. Y Dong, Raymond H Chang and Shufang Xu, "A detection statistics for random-valued impulse noise" *IEEE Transactions on Image Processing*, vol. 16, no. 4, April 2007.
- [37]. G Pok, J C Liu and A S Nair, "Selective Removal of impulse noise based on homogeneity level information", *IEEE Trans. Image Processing*, vol. 12, no. 1, pp.-85-92, Jan. 2003.
- [38]. Garnett, R.; Huegerich, T.; Chui, C.; Wenjie He "A universal noise removal algorithm with an impulse detector" *Image Processing, IEEE Transactions on* vol. 14, Issue 11, pp. 1747 – 1754, Nov. 2005.
- [39]. T.S. Huang, G.L. Yang, and G.Y. Tang, "Fast two-dimensional median filtering algorithm ," *IEEE trans. Acoustics, speech, Signal Process.*, vol. ASSP-1, no. 1, pp. 13-18, Jan. 1979.

- [40]. T.A. Nodes and N.C. Gallagher, Jr., "The output distribution of median type filters," *IEEE Trans. Commun.*, vol. COM-32, no. 5, pp. 532-541, May 1984.
- [41]. H. Lin and A N Willson, Jr., "Median Filters with adaptive length", *IEEE Trans. Circuits System*, vol. 35, pp. 675-690, June 1998.
- [42]. H. Hwang and R.A. Haddad, "Adaptive median filters: New algorithms and results," *IEEE Trans. Image Processing*, vol. 4, no. 4, pp. 499-502, Apr. 1995.
- [43]. T. Chen and H.R. Wu. "Space variant median filters for the restoration of impulse noise corrupted images," *IEEE trans. Circuits Syst. II, Analog Digit. Signal Process.*, vol. 48, pp. 784-789, Aug.2001.
- [44]. H. L. Eng. and K.K. Ma, "Noise adaptive soft-switching median filter," *IEEE Trans. Image Process.*, vol. 10, no.2, pp. 242-251, Feb.2001.
- [45]. S. Zhang and M.A. Karim, "A new impulse detector for switching median filters," *IEEE Signal Process. Lett.*, vol. 9, no.11, pp. 360-363, Nov. 2002.
- [46]. Z. Wang and D. Zhang, "Progressive switching median filter for the removal of impulse noise from highly corrupted images," *IEEE trans. Circuits System II., Analog Digit. Signal Process.*, vol.46, no. 1, pp. 78-80, Jan.1999.
- [47]. Y. Hashimoto, Y. Kajikawa, and Y. Nomura, "Directional difference based switching median filters," *Electro. Commun. Japan*. vol. 85, pp. 22-23, 2002.
- [48]. T. Sun and Y Neuvo, "Detail preserving median based filters in image processing", *Pattern Recognition. Letter*, vol. 15, pp. 341-347, Apr. 1994.
- [49]. E. Abreu, M Lightstone, S Mitra, K Arakawa, "A new co-efficient approach for the removal of impulse noise from highly corrupted images", *IEEE Transactions Image processing*, vol. 5, pp. 1012-1025, June 1996.
- [50]. Raymond H. Chan. Chung-Wa Ho, and Mila Nikolova, "Salt-and-Pepper Noise Removal by Median-type Noise Detector and Detail-Preserving Regularization," *IEEE transaction on Image Processing* vol. 14, no. 10, October 2005.

- [51]. R. C. Hradie and K.E. Barner, "Rank conditioned rank selection filters for signal restoration", IEEE Trans. Image Processing, vol. 2, no. 2, pp. 192-206. Mar 1994.
- [52]. Rafael C. Gonzalez and Richard E. Woods, Digital Image Processing, second edition, Addison Wesley, 2005.
- [53]. Raymond H. Chan. Chung-Wa Ho, and Mila Nikolova, "Salt-and-Pepper Noise Removal by Median-type Noise Detector and Detail-Preserving Regularization," IEEE transaction on Image Processing vol. 14, no. 10, October 2005
- [54]. MATLAB, the Language of Technical Computing, <http://www.mathworks.com/>
- [55]. Mohiy Hadhoud, Mohamed Amin, Walid Dabbour "Detection of Breast Cancer Tumor Algorithm using Mathematical Morphology and Wavelet Analysis", GVIP 05 Conference, , CICC, Cairo, Egypt, 19-21 December 2005.
- [56]. Y H Dandawate, M A Joshi, A V. Chitre, "Color Image Compression using Enhanced Vector Quantizer designed with Self Organizing Feature Maps", Int. Conference of Information Processing, pp. 80-85, 2007.
- [57]. H. Hwang and R.A. Haddad, "Adaptive median filters: New algorithms and results," IEEE Trans. Image Processing, vol. 4, no. 4, pp. 499-502, Apr. 1995.
- [58]. Raymond H. Chan. Chung-Wa Ho, and Mila Nikolova, "Salt-and-Pepper Noise Removal by Median-type Noise Detector and Detail-Preserving Regularization", IEEE transaction on Image Processing, vol. 14, No.10, pp.1479-1485, October 2005.
- [59]. Swapna Devi, Malay Dutta, S S Pattnaik, G V R S Sastry, Ch. Vidya Sagar, P K Patra, "Bacterial Foraging Optimization for a better Peak Signal to Noise Ratio in image" International Conference on Modeling and Simulation at Coimbatore, 2007.
- [60]. Swapna Devi, Malay Dutta, G V R S Sastry, S S Pattnaik, P K Patra, Ch. Vidya Sagar, "Image Denoising using Bacterial Foraging Optimization Technique" International Conference on Information Processing, Bangalore, pp. 73-79, 2007.

Chapter 8

Noise Removal from a single image

- 8.1 Introduction to breast cancer detection
- 8.2 Proposed method
- 8.3 Results
- 8.4 Conclusion
- 8.5 References

8. Noise Removal from a single image

8.1 Introduction

The main two limitations in image accuracy are blur and noise [1]. Blur is intrinsic to image acquisition systems and the second main perturbation of image is noise. In the previous chapter, it is seen how noise can be removed efficiently from a noisy image. In most of the algorithms, an estimate of noise level of the images is required to remove the noise [2 - 7]. And this estimation of a noise level from a single image appears to be a very difficult task as recognizing whether local image variation are due to the noise, color, texture or some variation in lightening [8]. So, in absence of a sophisticated prior model for an image, denoising the image is a challenge. In this section, an attempt has been made to denoise a given image without any *apriori* knowledge about it.

8.2 Proposed Median-BFO filter from a single image.

In all the methods (BFO and MED-BFO) as proposed in the previous chapter, the cost function has been taken as the difference of the original image and the noisy image. As long as the original image is known, these methods are fine. But, as it happens in most of the practical cases, the original image is not known. Under the circumstances, the following method (fig. 8.1) is proposed for effective noise removal.

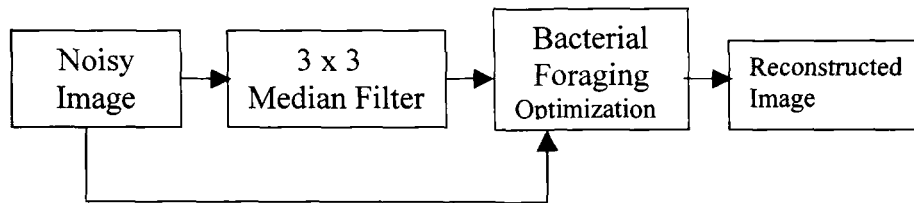


Figure 8.1: Proposed Median-BFG filter

In this proposed method, first, the noisy image is cleaned through a median filter of 3x3. Now, the difference between the noisy image and the output of the median filter acts as a objective function. This objective function is then fed to the Bacterial Foraging Optimization block to get an almost noise free image. Here, in this method the original image is not used in the whole process of denoising.

8.3 Results

The results of this proposed method are shown in the following figures and graphs. Fig. 8.2 (a) shows the original image of the test Lena cropped into 80x80 for quick computation, its noise corrupted images (noise densities ranging from 10% to 50% has been added to get the noisy images) are shown in (b). These images have then been separately considered for denoising using this proposed algorithm. Output of the median filter is shown in (c) and the final output, i.e., the output of the BFO is shown in (d). Table 8.1 list the values of PSNR, Structural Contents, Image Fidelity, Normalized Correlation Quality and the time taken to execute the algorithm for the Lena image corrupt with different noise densities.

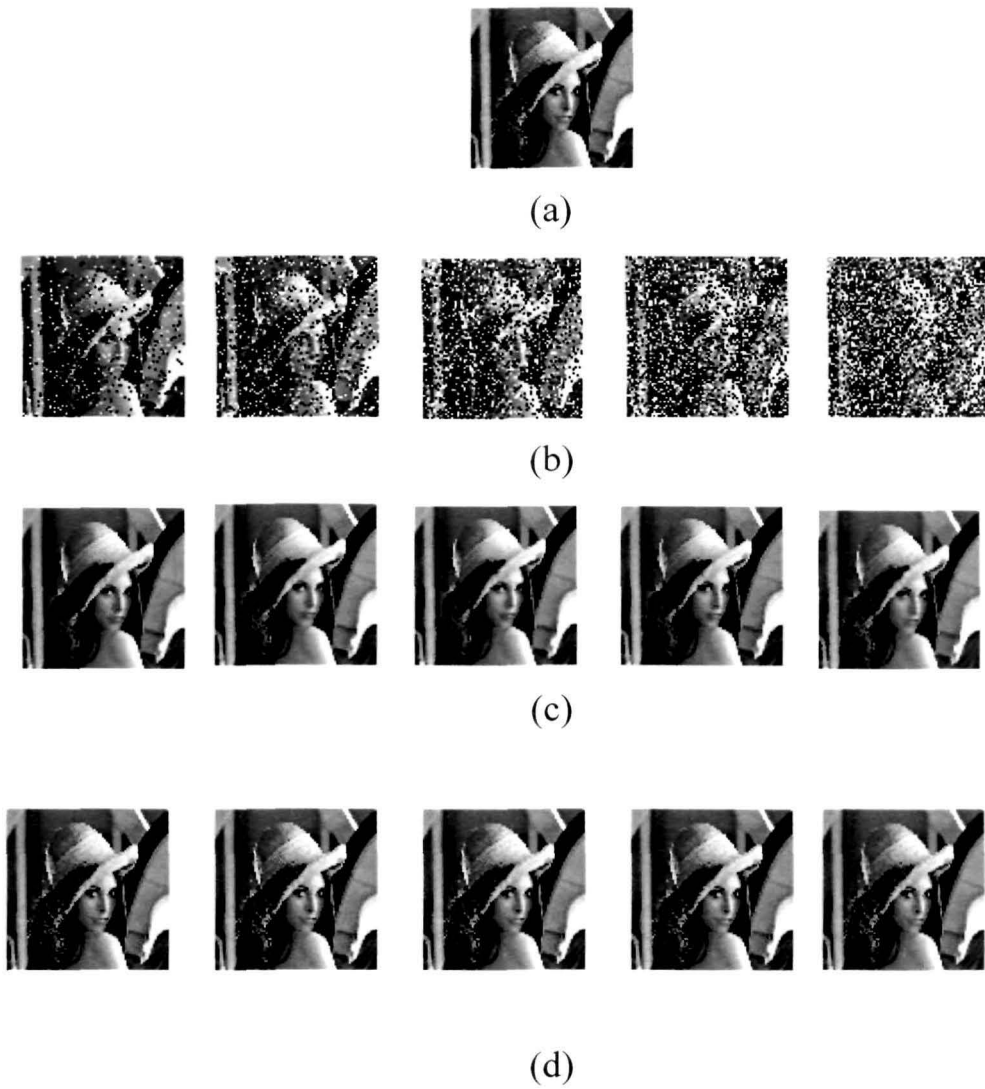


Figure 8.2: (a) Original 512 X 512 Lena Image cropped into 80X80 size
(b) Original image is corrupted with noise density of 10%- 50% resp.
(c) Image after median filtering of mask 3X3.
(d) Restored image corresponding to (c).

Table 8.1 : Results of the proposed method as applied on 512x512 Lena image

Sr.No.	Noise Density	PSNR (db)	Time (sec)	Structural Contents (SC)	Image Fidelity (IF)	Normalized Correlation Quality (NK)
1	10%	61.9167	1295.4	1.1000	0.7466	0.7446
2	20%	59.3694	442.09	1.2242	0.7004	0.7004
3	30%	58.1447	439.79	1.2809	0.6586	0.6586
4	40%	56.9415	438.42	1.3755	0.6259	0.6259
5	50%	55.9950	440.59	1.4987	0.5980	0.5980

The 512x512 original Lena image and its noisy counterpart are each divided into blocks of 16x16 each. For each of these blocks, their mean and variance is calculated. The following figure (fig.8.3 and 8.4) show the plot of the mean and variance of the noisy image and original image respectively.

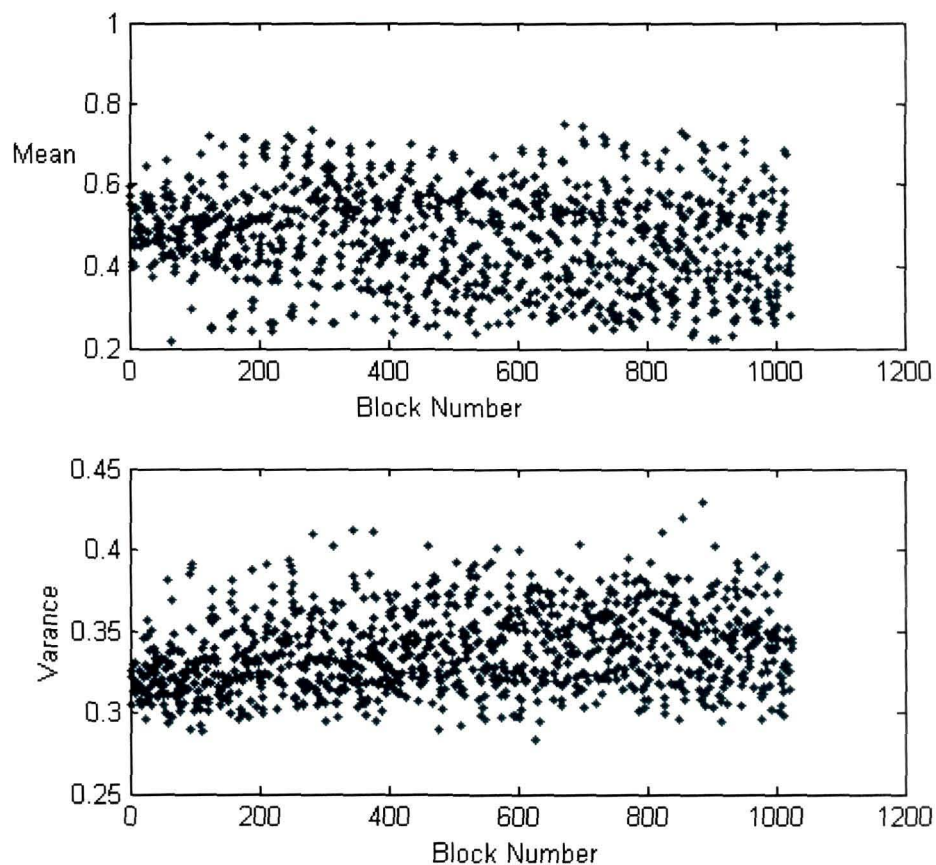


Figure 8.3 Mean and Variance of Noisy Lena Image

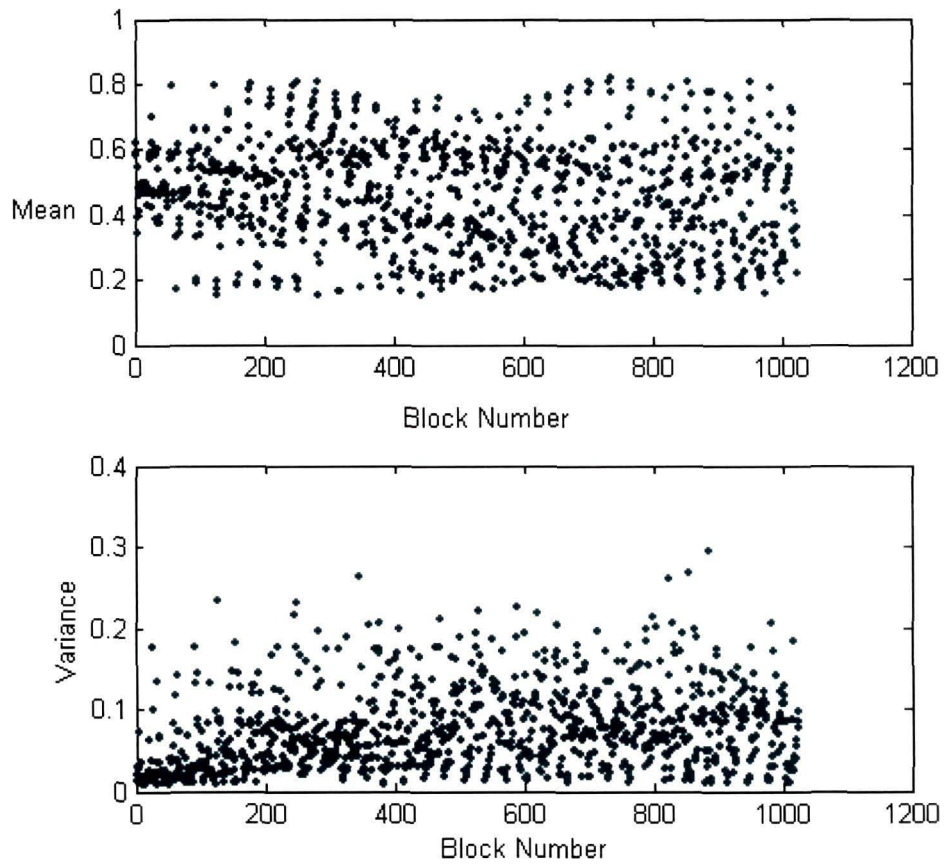
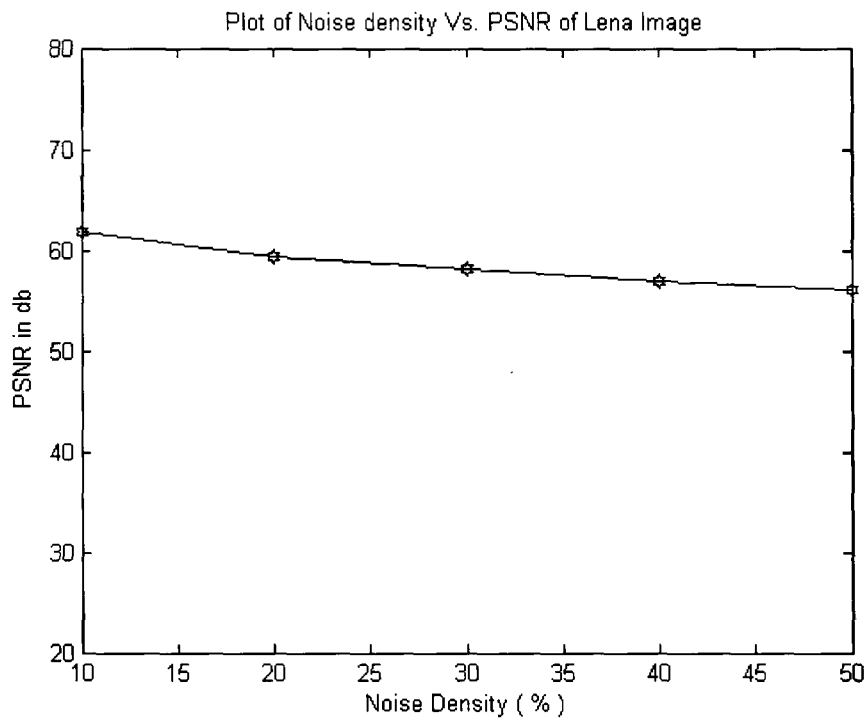
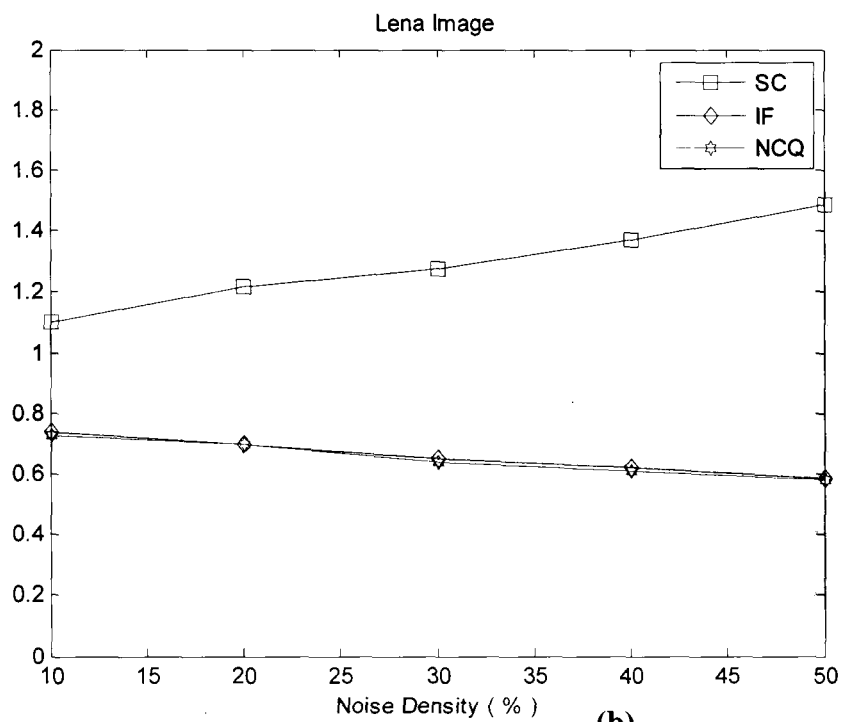


Figure 8.4. Mean and Variance of restored Image



(a)



(b)

Figure 8.5. (a) Plot of PSNR against the noise density and (b) plots SC, IF, NCQ against the noise density (for Lena image).

Now, the proposed method is applied on a mammography image. Table 8.2 shows the PSNR, SC, IF, NK, and time for the image corrupt with different noise density.

Table 8.2. Results of the proposed method as applied on mammography (80x80) image

Sl.No.	Noise Density	PSNR (db)	Time (sec)	Structural Contents (SC)	Image Fidelity (IF)	Normalized Correlation Quality (NK)
1	0.1	62.1237	457.8	1.0	0.75	0.75
2	0.2	60.5637	443.20	1.12	0.72	0.71
3	0.3	59.1437	440.85	1.23	0.68	0.68
4	0.4	57.5236	498.85	1.32	0.63	0.63
5	0.5	56.8529	455.85	1.45	0.62	0.61

In figure 8.5, a mammography image is shown, it is then corrupted with noise of various densities ranging from 10% to 50% (b), passed through the median filter (c) and the final output of the BFO is shown in (d). In both the cases, it is observed that the PSNR value decreases as compared to the method proposed in the previous chapter. This is due to the fact that in the previous method, the objective function was based on the original image but in this present proposed method, the objective function is derived only from the noisy image.

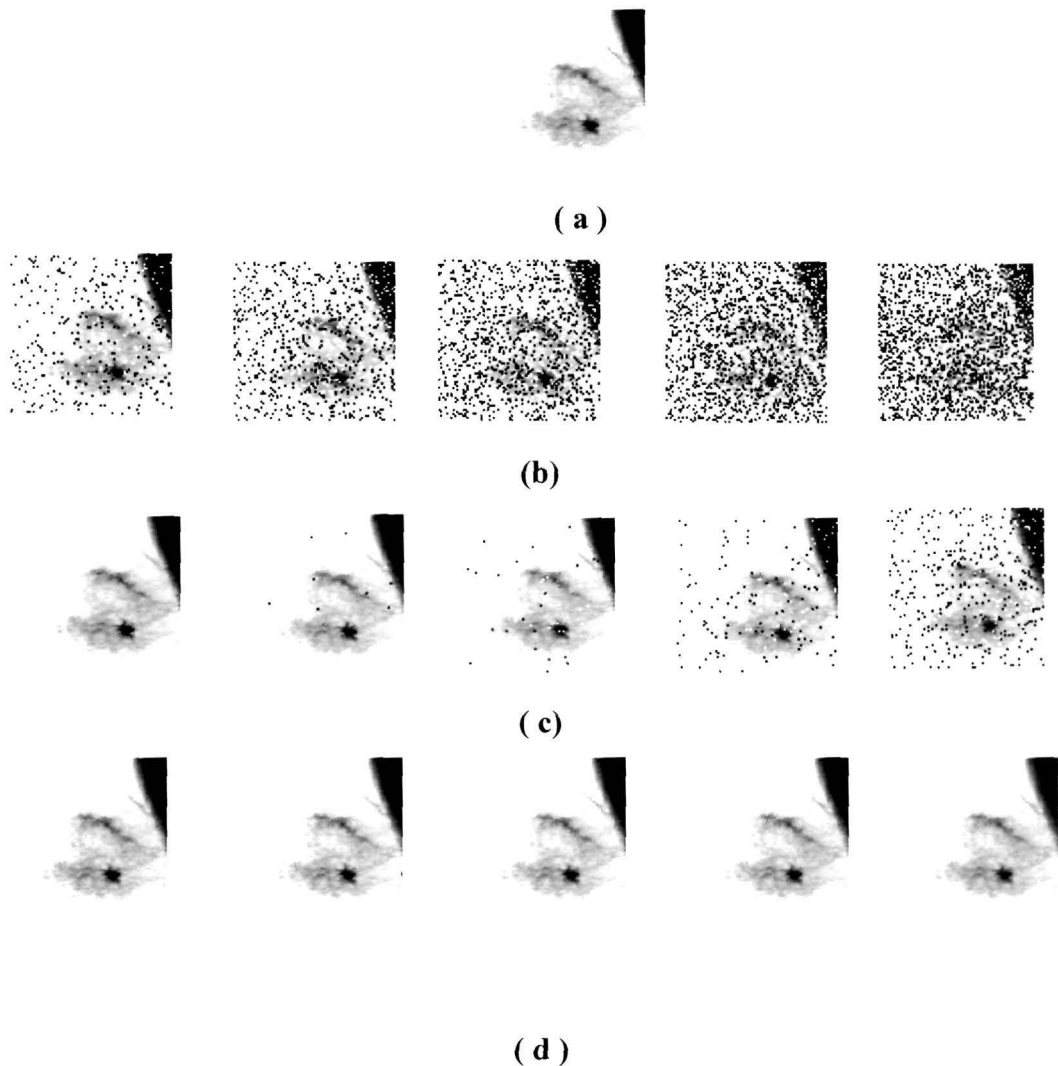


Figure 8.6: (a) Original 305x259 mammography image cropped to 80x80 size, (b) Original image corrupted with noise density of 10%- 50% resp. (c) Image after median filtering of mask 3X3. (d) Restored image corresponding to (c).

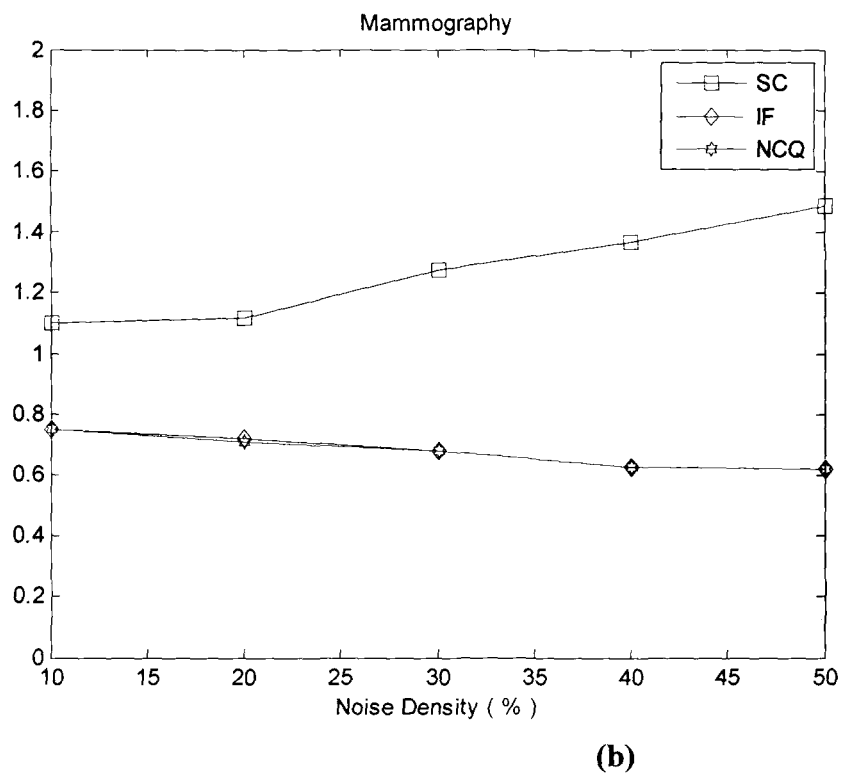
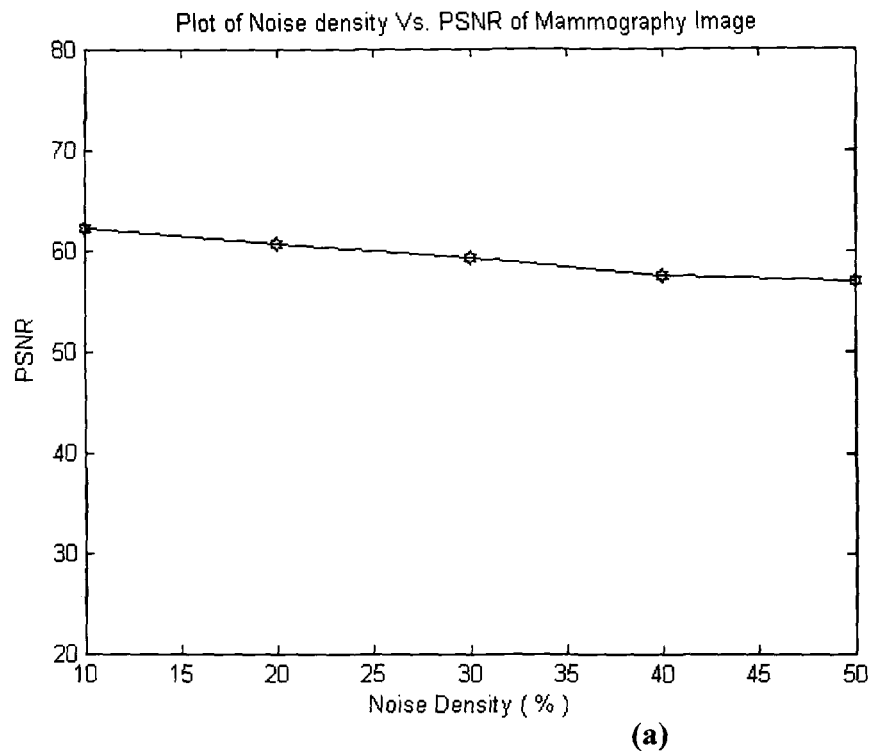


Figure 8.7. (a) Plot of PSNR against the noise density and (b) plots SC, IF, NCQ against the noise density (mammography).

8.4 Conclusion

This work addresses the fundamental issue of noise removal in a more realistic and reliable way. Real-world images have been denoised here. Though the PSNR obtained by this method is slightly less than that of the methods mentioned in the earlier chapter, but the approach of automatically inferring the denoised image from an unknown noise level makes it more useful for its application in medical images.

8.5 References

- [1]. A Buades, B Coll, J M Morel, “A review of image denoising algorithms, with a new one”, *Journal of Multiscale Model. Simul.*, vol. 4, no. 2, pp. 490-530, 2005.
- [2]. S. Baker and I. Matthews, “Lucas-Kanade 20 years on: a unifying framework” *Int'l Journal on Computer Vision*, vol. 56, no. 3, pp.221–255, 2004.
- [3]. W. T. Freeman, E. C. Pasztor, and O. T. Carmichael. Learning low-level vision. *Int'l Journal on Computer Vision*, vol. 40, no. 1, pp.25–47, 2000.
- [4]. P. Perona and J. Malik. Scale-space and edge detection using anisotropic diffusion. *IEEE Trans. on Pattern Analysis and Machine Intelligence*, vol. 12, no. 7, pp. 629–639, 1990.
- [5]. J. Portilla, V. Strela, M. J. Wainwright, and E. P. Simoncelli, “Image denoising using scale mixtures of Gaussians in the wavelet domain”, *IEEE Transactions on Image Processing*, vol. 12, no.11, pp. 1338–1351, Nov 2003.
- [6]. R. Zhang, P. Tsai, J. Cryer, and M. Shah. “Shape from shading: A survey”, *IEEE Trans. on Pattern Analysis and Machine Intelligence*, vol. 21, no. 8, pp.690–706, 1999.
- [7]. D. Lowe, “Object recognition from local scale-invariant features”, *Proc. IEEE Int'l Conf. Computer Vision*, pp. 1150–1157, 1999.

- [8]. Ce Liu William T. Freeman, Richard Szeliski Sing Bing Kang, “Noise Estimation from a Single Image”, IEEE Conference on Computer Vision and Pattern Recognition, 2006.

Chapter 9

Conclusion

- 9.1 Conclusion
- 9.2 Future Scope

9.1 Conclusion

Error free detection and diagnosis is a big challenge to the success of medical science and technology. The advancement of computational software, hardware, image techniques, intelligent-smart system etc, is paving path for accurate automatic detection and diagnosis. The works carried out under the problem statements of this thesis aim at providing certain degree of achievements and solutions to march forward in the direction of automatic detection and diagnosis of diseases that will help the urban and more so the rural population where expertise is scanty. The thesis has addressed five major issues viz., (i) automatic detection and diagnosis of arrhythmias (ii) denoising of medical images (iii) faster detection and localization of lesion in the cardiac images (iv) PSNR (image) enhancement to detect and accurately diagnosis (v) detection in absence of original image from mammography and from SPECT images. The developed methods have been validated using the standard images used by researchers for validation.

With rise of heart related problems, the solution for arrhythmias is considered as a potential problem in this thesis. Arrhythmias- abnormalities in the rhythm of the heart's pumping mechanism can lead to interrupted blood flow, oxygen starvation of the heart muscle and complete shut down of the heart - the so called cardiac arrest. There are various types and forms of arrhythmias, the detection and diagnosis of these depends mainly on experience and expertise of doctors. In multi functional disorder situations, the detection and diagnosis further gets complicated due to nonlinear behavior of the heart activities, thus, making possible for erroneous detection and diagnosis. Therefore, in chapter 4 of this thesis artificial neural networks have been developed to detect and diagnoses the arrhythmias from the ECG trace or data. Original potentials data have been used to develop train and test the network. The back propagation algorithm based neural network designed in the said chapter can take data from ECG trace by converting image into graphs as proposed in thesis or directly from ECG data file. The developed network has been tested with various

patient data after training the network with 539 nos. of patient data. The network at the present moment is capable of detecting and diagnosing 16 arrhythmias with error vary from 3 to 4%. The computational time is considerably low making it possible as a potential tool to detect and diagnoses more arrhythmias from the single network in future. The result achieved in the chapter 4 is more accurate and more in arrhythmias numbers compared to so far published results.

The imperfections of an image acquisition systems and transmission channels often corrupt image with noise. It is further added with malfunctioning pixel elements in the camera sensors, faulty memory locations, and timing errors. The noise significantly reduces the quality of the images making it difficult for detection and diagnosis task. There are various types of noises. Salt and pepper noise which is due to above stated facts needs to be eliminated or reduced to an acceptable limit for error free detection and diagnosis of diseases. Therefore, the work of chapter 5 of this thesis is dedicated to the development of an artificial neural network using gradient descent algorithm to remove impulse noise or salt and pepper noise. In the proposed method, images are pre-processed before feeding them to artificial neural networks. The pre-processed image is fed to a neural network. The network is trained with 200 images added with varied noise densities (10% to 60%). The developed trained network is tested with 100 images of varied noise densities. The results of 5 such cases have been presented in chapter 5 of the thesis. The results have been compared with that of other methods published in various literatures. The presented method gives a better PSNR thus showing a better noise removal. The performance of the network in terms of PSNR decreases with increase in noise density which is true for other published methods. But the PSNR of the present method is higher and thus, the method is more efficient in removing the noise. The algorithm is simple to implement and the computational time is considerably small thus making the proposed approach more attractive for medical applications.

In chapter 6 of the thesis, emphasis has been on accurate detection and localization of lesion in SPECT cardiac images while reducing computational time. Among all form of illness, coronary artery disease (CAD) is the single greatest cause of morbidity and mortality in the world. Early detection of any lesions in cardiac is an effective method to reduce the number of death caused by coronary artery diseases. The present imaging methods viz., CT, PET, MRI & SPECT etc. suffer from prolonged study times because of relatively low detection efficiency. Therefore, in this thesis attempt has been made to develop computer aided detection and localization of lesion using a fast neural network in conjunction with back propagation neural network. The approach is in two steps viz., (i) to speed up the detection and (ii) to accurately detect and localized the lesion. Large data processing in a neural networks increases the training time. Therefore, in the proposed method, a preprocessing algorithm is run on the data received from MIRL, University Utah, USA and down loaded from various internet sites. 345 images out of which 248 without lesion are used for training the network and 105 images out of which 69 without lesions are used for testing. The fast neural network has reduced the computational time by more than 5 folds while the back propagation neural network has ensured reduction and elimination of false detection. In the proposed method, an accuracy of approximately 97% is achieved with the detection rate of false positive as 0.95 % and false negative as 2.87%. The cascaded neural networks proposed in the chapter 6 seems to be potential CAD (Computer aided) tool for detection and localization of lesion due to drastic reduction in computational time while achieving high degree of accuracy.

Medical imaging suffers from false detection or no detection leading to wrong diagnosis specially when the foreign object is very small in size or inflammation is high leading to almost difficult for imaging. Diseases like breast cancer can be made non-fatal if the detection is possible in early stage i.e. when the cancerous tissue size or cyst size is less than 2 cm. So is the case in SPECT imaging

for heart/cardiac related alignments. Imaging techniques such as mammography, SPECT etc have their own limitations in the said situation. Therefore, in chapter 7 of the thesis, efforts have been made to use the potential of evolutionary optimization technique viz. Bacterial Foraging to enhance the PSNR values while reducing MAE for detection even small foreign object. In the proposed method, bacterial foraging optimization technique has been cascaded with the median filter to enhance the PSNR considerably making it possible to even detect a very small object. The method has been validated with standard Lena images (512 x 512) and then has been used in mammography and SPECT images. In the proposed method, the bacterial foraging optimization technique has been used to minimize the error that arises between the output of a median filter and the original image. PSNR more than 50 dB is achieved with noise density of 70% which is quite high in comparison to published results in various literatures where the PSNR value is below 40 dB for the same percentage of noise density. The results achieved for mammography and SPECT images are quite promising and will make the proposed technique to go a long way in detection and diagnosis of medical imaging.

The search for original image to minimize the error is a challenging problem in any image restoration and enhancement techniques or methods. In the absence of an original image, many algorithms or methods fail to restore the image or enhance the image. Therefore, in chapter 8, a novel technique of using bacterial foraging is proposed to restore image with enhanced PSNR from a noisy image. In the proposed method, bacterial foraging optimization technique is applied to minimize the error that arises due to difference between the output of median filter and that of noisy image. Image quality measures such as PSNR, MAE, Image Fidelity, Structural Content, Normalized Correction Quality etc. have been studied. The method is applied to standard Lena images for validation. Noise density levels are varied from 10% to 90% to evaluate the performance in less to high critical noise conditions. More than 50 dB PSNR is obtained which shows potentiality of the suggested method. However, PSNR less by 5dB is observed when compared to the

results obtained using original image. Thus, the proposed method will go a long way in development of blind detection technique which is very much pertinent to medical imaging detection and diagnosis. The outcomes of the thesis in terms of automatic detection, localization, noise removal, enhancement, diagnosis etc will act as potential tools for CAD supported detection and diagnosis techniques on which many researchers and industries world wide are working in the present time. The simple, novel and accurate methods present in this thesis will go a long way in drawing the attention of researchers and industries for potential applications in medical science specially in automated detection and diagnosis technique.

9.2 Future Scope

Hybrid model of bacterial foraging with fast neural network, integration of Fuzzy intelligence to neuro-bacterial foraging models may help to reduce computational time while improving the accuracy. Therefore, the out comes of this thesis pave a way to future development by integrating Fuzzy, Neural computing & evolutionary optimization technique to develop an efficient, cost effective and accurate automatic detection and diagnosis system for medical use. The soft-computing approach in conjunction with FPGA can provide hardware efficient detection devices for medical applications.

Publications out of the thesis work

Papers published :

- [1]. “Image Denoising using Bacterial Foraging Optimization Technique” International Journal on Information Processing, Issue –2, Jan 2008.
- [2]. “A novel approach of denoising images using Particle Swarm Optimization”, International Journal on Information Sciences of world scientific publishing company, USA, pp. 995-1001, 2007 (eISBN 987-981-270-967-7). (Same paper has been presented in Jt. Conference on Information Sciences, Salt Lake City, USA, July 15-22, 2007.
- [3]. “Image Denoising using Bacterial Foraging Optimization Technique” International Conference on Information Processing, Bangalore, 2007 **(adjudged as the Best Paper Award)**.
- [4]. “Bacterial Foraging Optimization Technique to Calculate Resonant Frequency of Rectangular Microstrip Antenna” Accepted for publication in International Journal of RF and Microwave Computer –Aided Engineering, March 2008.
- [5]. “Denoising using Particle Swarm Optimization Technique” International Conference on Information Processing, Bangalore, 2007.
- [6]. “Bacterial Foraging Optimization for a better Peak Signal to Noise Ratio in image” International Conference on Modeling and Simulation at Coimbatore, 2007
- [7]. “Neuro-Computing Approach to remove noise from SPECT images”, All India Seminar on Bio-Medical and Bio-Informatics, 24-25th March, 2007, Agra.
- [8]. “Detection of cold lesions in SPECT images of cardiac”, National Conference on Trends in Advanced Computing, 22-23 March 2007, Tezpur University, Assam.
- [9]. “Bacteria Foraging : A soft Computing Approach to Engineering Applications” National Conference on Mechatronics, NITTTR, 8-9 March, 2007.

- [10]. "Particle Swarm Optimization and Genetic Algorithm: A Review", National Conference on Mechatronics, 8-9th March, 2007, Chandigarh.
- [11]. "De-noising of Impulse Noise in an Image by Artificial Neural Netowrk" National Conference on Mechatronics, NITTTR, 8-9 March, 2007.
- [12]. "Pattern Recognition Using Radial Basis Function" National Conference on Mechatronics, 8-9th March, 2007, Chandigarh.
- [13]. "Detection of Cold lesions in SPECT Images of Cardiac" accepted In International Conference on Information Systems, Technology and Management at IMT, Gaziabad, March 2007.
- [14]. "MATLAB Based Techniques For Detection Of Arrhythmia", accepted in international conference on artificial Intelligence and applications (AIA 2006) in Austria, 2006.
- [15]. "Segmentation based computer aided analysis of Electrocardiograph for arrhythmias" National conference on Emerging Trends in Computer and Electronics Engineering for Rural Development, Chhatrapati Shivaji Institute of Technology, Durg, 4-5th March 2006, pp.15-160.
- [16]. "Computer Aided Analysis of ECG for Arrhythmias", National Seminar on CAD/CAM, NITTTR, Chandigarh, 22-24th March 2006.
- [17]. "A state of art model for Diagnosis of patients using neuro-computing technique" National Seminar on ICT Enabled Education, 17-18 Nov. 2004.

Papers submitted:

1. "Bacterial Foraging Optimization Technique Cascaded with Median Filter to Remove impulse Noise", sent to International Journal of Hybrid Intelligent Systems, 2008.
2. "Denoisign of Video frames using Bacterial Foraging Optimization Technique" International Journal of Visual Communication and Image Representation, Elsevier.

3. “A New and Novel Approach to use Bacterial Foraging with Adaptive and Median Filter for PSNR Enhancement”, submitted to IEEE Trans. of Image Processing.